Recognition of unrelated extracellular pathogen-derived protease inhibitors in Solanaceae

Shivani Malik

Department of Biology
Mathematical, Physical and Life Sciences Division
Somerville College
University of Oxford

Supervised by Professor Renier A.L. van der Hoorn



Thesis submitted for the degree of Doctor of Philosophy

Hilary Term 2025

Recognition of unrelated extracellular pathogen-derived protease inhibitors in Solanaceae

Shivani Malik; DPhil Thesis, Michaelmas Term 2015 to Hilary Term 2025,
University of Oxford



Solanum pennellii



Capsicum galapagoense



Solanum bulbocastanum



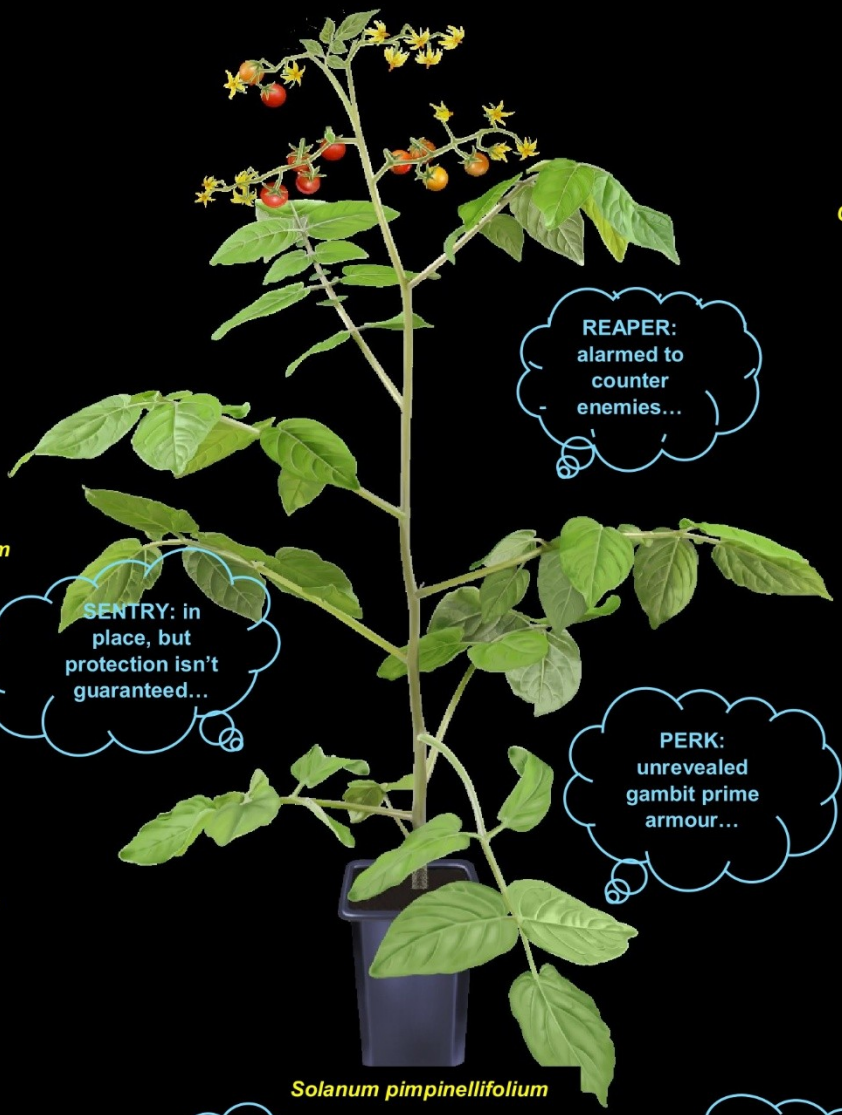
Petunia integrifolia



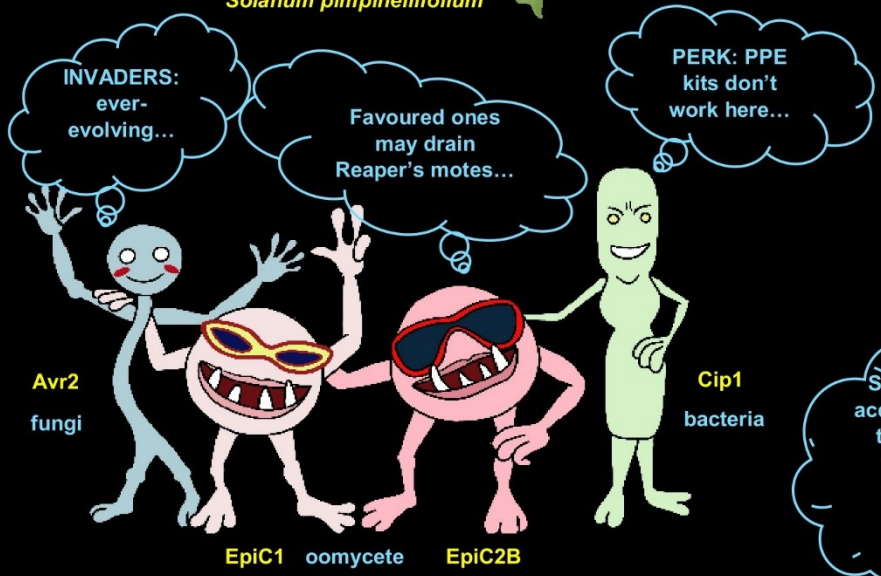
Solanum dasyphyllum



Nicotiana tabacum



Solanum pimpinellifolium



Painting Credits: ShivaniMalik© at ThePlantChemeticsLab and Biswa; Created from specimens in this study; My callout inspirations: Destiny 2

Dedicated with deepest gratitude,

To Professors Renier A.L. van der Hoorn, Jonathan D.G. Jones, Amar Kumar, John P. Carr, Sophien Kamoun, and Frederick M. Ausubel. Their remarkable research achievements first inspired my curiosity in understanding the diversity and mechanisms of host immunity against pathogens and I am honoured to have received their guidance/feedback in different ways. To my parents, my brothers and to all my mentors and friends.

"My DPhil journey, so to say has been the most transformative phase of my life thus far! I am deeply grateful for the immense intellectual, social and personal growth I have experienced."

-Shivani Malik

June, 2025

'Teamwork is the ability to work together toward a common vision. The ability to direct individual accomplishments toward organizational objectives. It is the fuel that allows common people to attain uncommon results."

-Andrew Carnegie

Table of contents

Abstract	1
Declaration	3
Acknowledgments	4
Abbreviations	6
List of figures	8
List of tables	11
List of supplementary figures and tables	12
List of input data analysis files attached as supplementary	14
List of appendix figures	16
Chapter 1: Introduction	17
1.1 Plant diseases threaten global food security	17
1.2 The immune system of plants	18
1.2.1 Gene-for-gene and inverse models of interaction	18
1.2.2 Mutual potentiation between PTI and ETI	20
1.2.3 Role of RLPs, RLKs and H-NLRs in effector recognition	20
1.3 *Cladosporium fulvum*	21
1.3.1 *C. fulvum* resistance gene family in tomato	22
1.3.2 Cf-mediated perception of Avr effectors of *C. fulvum*	23
1.4 Other apoplastic cysteine proteases	24
1.5 Guard versus decoy model of Cf-2/Rcr3-mediated Avr2 recognition	24
1.6 Inhibition of extracellular host proteases by *Phytophthora infestans* secreted effectors	25
1.7 *Pseudomonas syringae*-derived Cip1 inhibits apoplastic proteases	26
1.8 Harnessing diversity in Solanaceae wild crop relatives for novel pathogen recognition specificities	27
1.9 Aims and outline of this thesis	28
Chapter 2: Materials and methods	32
2.1 General materials	32
2.2 General methods	34
2.3 Plant materials and growth conditions	35
2.4 Pathogen-derived inhibitors used in this study	37
2.5 Screening for hypersensitivity cell-death response phenotype	43

2.6 Genotyping by PCR of *Cf* and cysteine protease genes 45
2.7 Virus-induced gene silencing (VIGS) in wild *Solanum* species 50
2.8 Bioinformatics analysis of diversity and evolution of Cf-like proteins beyond phylogenetic boundaries 54
2.9 Appendix: transient expression analysis in *N. benthamiana* 56
*Data Availability 58

Chapter 3: Hypersensitive response profiling of 302 populations across Solanaceae reveal heterogeneity in protease inhibitor recognition 67
3.1 Introduction 68
3.2 Results 71
3.2.1 Collection of Solanaceae germplasms selected for HR assay in this study 71
3.2.2 Selection, construction, over-expression and purification of candidate protease inhibitor mutants 75
3.2.3 Mutant inhibitor proteins do not inhibit Rcr3 77
3.2.4 Wild-type inhibitors trigger differential HR, whereas their mutants are not recognised clearly in control plant lines and test representative wild tomato and wild potato 77
3.2.5 *Solanum pimpinellifolium* recognise Avr2 throughout distribution range with heterogeneity in HR in plants of same or different populations 80
3.2.6 Inhibitor recognition in *S. pimpinellifolium* 82
3.2.7 Inhibitor recognition in wild tomato 86
3.2.8 Inhibitor recognition in wild potato 90
3.2.9 Inhibitor recognition in other Solanaceous plants 93
3.2.10 Recognition frequencies differ between geographic regions 93
3.2.11 Inhibitor recognition varies by altitude 96
3.2.12 Distribution of responsive populations candidates for further studies 98
3.3 Discussion 102

Chapter 4: Genotyping tomato *Cf-2* family and apoplastic proteases show variability associated with inhibitor recognition 109
4.1 Introduction 110
4.2 Results 114
4.2.1 Genotyping highly homologous *Cf-2* gene family, *Cf-9* and *9DC* in control plant line 114

4.2.2 *Cf-2/Hcr2s*, *Cf-9* and *9DC* show variation among individuals of same population and their presence does not specifically correlate with inhibitor recognition 117
4.2.3 Variation in *Cf* gene frequencies and their relatedness to inhibitor recognition across natural distribution ranges of S*. pimpinellifolium* 121
4.2.4 *Hcr2* family is conserved in wild tomato and show intra-population and inter-specific variations 125
4.2.5 *Cf-2-like* genes are found throughout diploid wild potato species from different origin centres 126
4.2.6 Sequencing apoplastic cysteine proteases for relatedness with HR-associated recognition of unrelated inhibitors 128
4.2.7 Effect of natural variation in *Rcr3* on recognition of inhibitors and evidence of positive selection revealing species-wide and Solanaceae-wide hotspots in Rcr3 131
4.2.8 Natural diversity in *Pip1* gene and their consequences in relation to observed variations in inhibitor recognition and evolutionary selection pressures 143
4.2.9 Natural variation and sites under positive selection identified in *C14* 147
4.3 Discussion 152
Appendix figures 163

Chapter 5: Functional characterisation of *Cf-2*-homologs and likely co-receptors using virus-induced gene silencing and phylogenetic analysis of Cf-like RLPs 167
5.1 Introduction 168
5.2 Results 175
5.2.1 Silencing *Cf-2* compromise HR against Avr2, but does not affect recognition of Cip1 and EpiCs in *S. pimpinellifolium* 175
5.2.2 Silencing of *Cf-2/Hcr2s* in wild potato do not influence EpiC2B perception 181
5.2.3 Silencing of *Rcr3*, *Pip1* and *C14* in *S. pimpinellifolium* differentially diminish HR induced by unrelated inhibitors 185
5.2.4 Recognition of unrelated inhibitors is dependent on *SOBIR1* in wild tomato and potato 189
5.2.5 Cf-like RLPs are widely distributed across Solanaceae and most abundantly in genus *Solanum* 189
5.2.6 Phylogenetic analysis indicate that Cf-2/Hcr2 have recently evolved in Solanaceae 195

5.3 Discussion 196

Chapter 6: Thesis conclusion and future perspectives 210

6.1 Recognition of unrelated inhibitors shows natural variation and is conserved in tomato and potato 211

6.2 *Cf-2* is present in wild relatives beyond *S. pimpinellifolium* and *Hcr2* number/type variations exist 212

6.3 *Rcr3*, *Pip1* and *C14* natural variation analysis revealed hotspots of positive selection in tomato and potato 214

6.4 *Cf-2/Hcr2* silencing effectively compromise Avr2 recognition but not inevitably of EpiCs and Cip1 216

6.5 Silencing *Rcr3*, *Pip1*, *C14* and *SOBIR1* reduces HR severity 216

6.6 *In-silico* analysis identified that Cf-2 originated in tomato, whereas Hcrs are distributed across Solanaceae 217

6.7 Proposed molecular perception of Avr2, EpiCs and Cip1 in tomato and potato 218

6.8 Future directions 221

Bibliography 224

DPhil publications 247

Conference presentations/abstracts submitted 247

Recognition of unrelated extracellular pathogen-derived protease inhibitors in Solanaceae

Shivani Malik, Somerville College, Department of Biology, University of Oxford

Thesis submitted for the degree of Doctor of Philosophy

Michaelmas 2015 to Hilary Term 2025

Abstract

Extracellular immune proteases Rcr3, Pip1 and C14 of tomato are convergent targets of Avr2, EpiCs and Cip1 secreted by *Cladosporium fulvum*, *Phytophthora infestans*, and *Pseudomonas syringae*, respectively. Avr2-Rcr3 interaction is sensed by a cell-surface localised Receptor-like protein, encoded by resistance gene *Cf-2* in wild tomato *S. pimpinellifolium*, triggering a hypersensitivity cell-death response (HR). Stealthy EpiCs and Cip1 weakly interact with Rcr3, thus escape recognition in plants carrying *Rcr3* and *Cf-2*.

We investigated 302 natural solanaceae populations for HR upon infiltration of purified Avr2, EpiC1, EpiC2B and Cip1. We found that these protease inhibitors induce HR in wild tomato and potato, but not in other solanaceae species. Avr2 is most frequently recognised in wild tomato whereas EpiC2B is the most frequently recognised in wild potato, consistent with *C. fulvum* coevolving with tomato and *P. infestans* with potato. Intra/inter-population variations in HR were observed across geographical origins. We further show that homologs of *Cf-2* (*Hcr2s*) exist species-wide in tomato and potato. Avr2 recognition does occur in the absence of *Cf-2*, but is weak. Allelic variation analysis revealed that *Rcr3* and *C14* are under diversifying selection within *S. pimpinellifolium* and *Pip1* in wild tomato.

Virus-induced gene silencing in *S. pimpinellifolium* and wild potato indicate that EpiCs/Cip1 recognition is independent of *Cf-2*. *Pip1* and *C14* silencing reduced recognition of EpiCs/Cip1 more than *Rcr3*. Silencing Receptor-like kinase *SOBIR1*, reduces the recognition of inhibitors, indicating that inhibitor recognition require a Receptor-like protein. We identified 491 Cf-RLPs by bioinformatics, all limited to Solanaceae and expanded within *Solanum*. Our analysis indicate that Cf-9 is older than Cf-2 in tomato, but Hcr2s exist in potato, eggplant and pepper. Overall, recognition frequency of unrelated inhibitors, variation and role of extracellular immunity components that likely underpin inhibitor perception are reported in this thesis. Our work demonstrates that utilizing wild populations for novel resistance sources can guide bioengineering of targeted crop protection against pathogens.

Declaration

I present my original doctoral research work and writing in this thesis, completed under the guidance of my supervisor, Prof Renier A.L. van der Hoorn. This work has not been submitted, in part or in whole, for any other degree or professional application/qualification, except for appendix 4 (chapter 4). Appendix 4 is not presented as primary thesis result, but contributed to a publication [Kourelis, J., Malik, S., Mattinson, O., Krauter, S., Kahlon, P.S., Paulus, J.K., and van der Hoorn, R.A.L. Evolution of a guarded decoy protease and its receptor in solanaceous plants. *Nat Commun* **11**, 4393 (2020)].

Information derived from published research is acknowledged and listed in bibliography. Sources of chemicals/reagents/equipment and licensed/free/open source analysis software or computational platforms are described in chapter 2. Plasmids used from other sources were already available in lab collection and are referenced in Table 2.8.

Colleague/collaboration contributions and sources of biological seed samples are explicitly credited in each chapter and are detailed below:

1. Tomato seeds were donated by Tomato Genetic Resource Centre (TGRC), University of California Davis, USA and potato/eggplant/pepper seeds were gifted by Centre for Genetic Resources (CGN), Wageningen University and Research, the Netherlands.
2. Plasmids pJK153, pJK155, pJK157 and pJK159 used for expression and purification of pathogen inhibitors in chapters 3 and 5 were provided by Dr Jiorgos Kourelis.
3. Mutant inhibitor plasmids, Avr2 and EpiC2B in chapters 3 and 5 were generated using parent plasmids (pJK019 and pJK017) constructed by Dr Jiorgos Kourelis. Mutant inhibitor plasmids EpiC1 and Cip1 were constructed using template vector pFGH027 and pFGH026, provided by Dr Friederike Grosse-Holz.
4. Level 2 golden gate vector assembly components (pJK082 and pJK120) in chapter 3 and pTRV2 background vector (pJK037) used for assembly of silencing fragments in chapter 5 were all provided by Dr Jiorgos Kourelis.
5. *Cf-2::eGfp* plasmid used as template for *Cf-2* silencing fragment in chapter 5 was gifted by Dr Matthieu Joosten at the University of Wageningen.
6. My investigations in published article contributed to main results (figures 5a and 5b in the publication and appendix 4.2 in this thesis), whereas results that were generated during this publication, but remain unpublished are included as appendix.

Acknowledgements

My Supervisor, **Prof Renier A.L. van der Hoorn**, has my deepest thanks for giving me an incredible DPhil opportunity at Oxford, project guidance and for his exceptional support to my research work (including some silly experimental ideas and a very long timeline!). I was initially somewhat inarticulate, but he recognised uniqueness in our collaboration and his inspiration and reliability has expanded my professional confidence and vision. To **Professors Nick J. Kruger** and **Emily Flashman** (Directors of Graduate Studies), thank you sincerely for reassuring support on academic progression. Many thanks to my second Supervisor, **Prof Lee J. Sweetlove**, for being an open-minded source of advice on academic matters. I am grateful to **Prof Gail Preston** and **Dr Steve Kelly** for their suggestions of improvement during my internal examinations. I am truly thankful to the **Plant Chemetics Lab**, **Department of Biology** (Plant Sciences) and **Mathematical, Physical and Life Sciences Division** (MPLS) for providing necessary research facilities, upskill opportunities and for a stimulating research environment. I am grateful to **Somerville College**, **Oxford-India Centre for Sustainable Development** (OICSD) and the **University of Oxford** for three years award of Oxford-Indira Gandhi Scholarship, an additional OICSD-Covid-19 grant for Michaelmas term-2020 and for their academic support over these years.

To **Baroness Royall of Blaisdon-Jan Royall** (Principal) and **Ms Sara Kalim** (Director of Development), a very special thank you from the bottom of my heart, for their encouragement and support. I am extremely thankful to **Dr Siddharth Arora** at OICSD, who has been an exceptional support as an elder brother at Oxford, I will never forget it; to my college supervisor **Prof Philip S. Poole**, and **Dr Alfred Gathorne Hardy**, a warm thank you for our thoughtful formal dinner and brown bag lunch discussions. Over these years, I have received extensive administrative support, my particular thanks to **Ms Gem Toes-Crichton**, **Dr Roni McGowan** and **Ms Heather Green** at my department and **Ms Saphire Richards** at my college. I have deep appreciation for my colleagues at the Plant Chemetics Lab, huge thank you to: the genius I have learned a lot from, **Dr Jiorgos Kourelis**, for extending valuable assistance in my project development and sparking my interests in bioengineering; **Dr Balakumaran Chandrasekar** for supervising my introductory ABPP experiments and adaptation at Oxford; **Dr Daniel Krahn** for probe chemistry knowledge and helping me monitor late running protein filtrations; **Dr Judith K. Paulus** for guiding protein purification protocols and those delicious Christmas bakes I never managed to find elsewhere; **Dr Daniela Sueldo** and **Dr Luisa Madeira**, for their motivating presence in the team; **Dr Friederike Grosse-Holz** whose discipline at work was commendable and ideal;

Dr Marcel Bach-Pages for being a cheering hard-working bench neighbour; **Drs Kyoko Morimoto**, **Pierre Buscaill** and **Philippe-Varennes-Jutras**, for being so amazing seniors; **Drs Maria Fonte-Farre**, **Awais Zahid**, **Emma Thomas**, **Felix Homma**, **Ziad Soufi** and **Ane Kjersti Vie** for delightful times at work. Many thanks to **Ms Ursula Pyzio**, **Ms Sarah Rodgers**, **Ms Caroline O' Brien** and **Mr Timothy Wroe**, for excellent technical support.

To **Drs Parvinderdeep Singh Kahlon**, **Zhe Ji (Luke)** and **Ursula Flores-Perez**, I am immensely grateful for our uncountable joyous moments at the department, meaningful friendships and celebrations at Oxford; to **Drs Vaanathi Uma Sundaresan, Vinoy Ramachandran**, **Chirayu Thakkar**, **Naganand Saravanan**, **Markus Schepers**, **Mr Narendra Killada**, **Ms Brookes Dambachar** and **Danteshwari Chalasani,** my special thanks to all for being supportive and motivating friends. My loving thanks to **Mrs Rahina Gul** and **Mr Rizwan Mir**, for delicious food parcels, but most importantly for their care and affection. To **Prof Nrisingha Dey,** for shaping my interest in research during my internship at the Institute of Life Sciences, Odisha. **To Professors P. Chitralekha**, **Sanjiv Mallick**, **Amar Kumar**, **Arun Jagannath** and **Priyavrat Arya** at the University of Delhi, I am deeply thankful for their instrumental roles in my academic journey. I must also thank **Prof Faisal Devji** at St. Antony's, for reinforcing my leadership years at the Oxford-India Society, **Ms Ranjita Rajan** for entrusting my academic advisory collaboration with the Karta Initiative and **Ms Rowena Mitchell** for outreach partnership with Biochemical Society at Oxford.

I am eternally grateful to my mother, **Mrs Sudesh Malik**, for being the most inspirational figure in my life and to **Mr Ramkishan Malik**, my cherished late father. No words are enough to thank my closest companions and confidants of boundless positive energy, my elder brother, **Mr Vinay Malik** and younger brother, **CA Vikrant Malik**. I have had my share of personal and academic moments of descent, but the unwavering support and love of my mom and brothers have kept the inquisitive me inexpressibly firm, both emotionally and financially. My heartfelt gratitude to **Gurudev Sri Sri Ravi Shankar Ji**, I treasure his guidance of my journey within. I also want to acknowledge my paternal and maternal grandparents for being examples of disciplined visionaries with utmost simplicity in their ways of life. To all my Uncles and Aunts. To **Mr Rohit Chahal**, for his exceptional nurturing generosity in our limited association, which unnoticeably favoured my metamorphosis. To **Mr Abhishek Parihar**, for adding a significant fitness dimension in my life during writing.

Finally, thank you very much in advance to my **Examiners**, **Prof Gail Preston** at the University of Oxford and **Dr Jason Rudd** at Rothamsted Research, for kindly accepting the invitation to examine my DPhil thesis. I hope they will find it worthwhile of their time.

Abbreviations

AA: Amino Acid

Avr: Avirulence gene

ACIK1: AVR9/Cf-9-Induced Kinase1

Avr2: Avriulence Protein 2 of *C. fulvum*

bp: Base Pair

BAK1: Brassinosteroid Insensitive 1-Associated Kinase1

BUSTED: Branch-site Unrestricted Statistical Test for Episodic Diversification

Cip1: C14-Inhibiing Protein

CPKs: Ca2+ dependent protein kinases

CGN: Centre for Genetic Resources Netherlands

C14: Chagasin-like 14 Cysteine Protease

C. fulvum: *Cladosporium fulvum*

Cf-2: *Cladosporium fulvum Disease Resistance Gene 2*

Cf-9: *Cladosporium fulvum Disease Resistance Gene 9*

CC: Coiled coil

C-ABPP: Competitive-Activity Based Protein Profiling

CBB: Coomassie brilliant blue

DNA: Deoxyribonucleic Acid

DPI/dpi: Days Post-Infiltration

ETI: Effector-Triggered Immunity

ETS: Effector-Triggered Susceptibility

EDS1: Enhanced Disease Susceptibility 1

EIX: Ethylene-Inducing Xylanase

FEL: Fixed-Effects Likelihood

FUBAR: Fast, Unconstrained Bayesian AppRoximation

Hcr2: *Homolog of Cf-2* gene

Hcr9: *Homolog of Cf-9* gene

HR: Hypersensitive response

kDa: Kilo-dalton

LRR: Leucine Rich Repeat

MAMP: Microbe Associated Molecular Patterns

ML500: Maximum-likelihood with 500 Bootstrap Replications

MEME: Mixed Effects Model of Evolution

MAPKs: Mitogen-Activated Protein Kinases

MUSCLE: MUltiple Sequence Comparison by Log-Expectation

MSA: Multiple Sequence Alignment

NRC: NLR required for cell death

Nt: Nucleotide

NLR: Nucleotide-Binding Leucine Rich Repeat

PLCP: Papain-like Cysteine Protease

PRR: Pattern Recognition Receptor

PTI: Pattern-Triggered Immunity

P. infestans: *Phytophthora infestans*

EpiC1: *Phytophthora infestans* cystatin-like effector protein 1

EpiC2B: *Phytophthora infestans* cystatin-like effector protein 2

Pip1: *Phytophthora*-inhibited protease 1

PCR: Polymerase Chain Reaction

***Pst*DC3000:** *Pseudomonas syringae pv*. tomato DC3000

qPCR: Quantitative PCR

Rcr3: Required For *C. fulvum* Resistance 3

RLCK: Receptor-like Cytoplasmic Kinase

RLK: Receptor-like kinase

RLP: Receptor-like Protein

R-gene: Resistance gene

RNA: Ribonucleic Acid

MM: *S. lycoperiscum* Money Maker

SDS-PAGE: Sodium Dodecyl Sulphate Poly-Acylamide Gel Electrophoresis

SP: Signal peptide

LeEix2: *Solanum lycopersicum* RLP recognising EIX elicitor

SERK3: Somatic Embryogenesis Receptor Kinase3

SOBIR1: Suppressor of BIR1-1

TRV: *Tobacco Rattle Virus*

TGRC: Tomato Genetics Resource Centre

TM: Transmembrane domain

VAP1: Venom Allergen-like Protein 1

Ve: *Verticillium* Wilt Disease Resistance Protein

VIGS: Virus-Induced Gene Silencing

List of figures

Figure 1.1: Illustration showing PTI-ETI intersection, particularly in extracellular immunity against four important pathogens of solanaceae crops.

Figure 2.1: Map showing collection sites of populations and species tested in this study.

Figure 3.1: Phylogenetic trees generated to show relationships among species tested in this study.

Figure 3.2: Over-expression, purification, and activity profiling of recombinant inhibitors.

Figure 3.3: Screening of populations for response against four unrelated protein inhibitors.

Figure 3.4: *Solanum pimpinellifolium* populations show variation in recognition of unrelated inhibitors and their mutants that target convergent apoplastic cysteine proteases with differential affinities.

Figure 3.5: Wild tomato species show inter-specific and intra-specific differences in recognition against four inhibitors and their mutants tested in this study.

Figure 3.6: Inhibitor associated HR is induced in wild potato populations, but not in species beyond potato.

Figure 3.7: Estimated relative frequencies of inhibitor recognition reveal geographic disparity.

Figure 3.8: Altitude distribution of recognition frequencies against wild type and mutant inhibitors.

Figure 3.9: Distribution of responsive populations identified in *S. pimpinellifolium*, wild tomato and wild potato across latitude/longitude, altitude and geographical regions.

Figure 4.1: Schematic illustration showing intron-less *Cf-2* gene cluster on chromosome 6.

Figure 4.2: Allelic regions and PCR of *Cf-9* gene cluster on chromosome 1.

Figure 4.3: Occurrence of *Cf-2*, *Hcr2's*, *Cf-9* and *9DC* in relation to responsiveness towards each inhibitor in *S. pimpinellifolium* populations from Region A (Ecuador) and Region B (North).

Figure 4.4: Association of *Cf-2*, *Hcr2's*, *Cf-9* and *9DC* to inhibitor recognitions in *S. pimpinellifolium* populations from Region C (Centre) and Region D (South).

Figure 4.5: Variation in *Cf* gene frequencies across *S. pimpinellifolium* natural geographical distribution ranges.

Figure 4.6: *Cf-2* amplification in *S. habrochaites* and *S. pennellii* correlate with strong HR phenotype against Avr2. EpiC1, EpiC2B and Cip1 recognitions do not fully associate with presence of *Cf-2*, *Cf-9* or *9DC* in *S. habrochaites*, *S. pennellii* and *S. corneliomuelleri.*

Figure 4.7: *Cf-2-like* fragments are present in genotyped wild potato populations.

Figure 4.8: Detection and sequencing scheme of cysteine proteases Schematic *Rcr3*, *Pip1* and *C14*.

Figure 4.9: Phylogenetic tree of *Rcr3* gene family in Solanaceae.

Figure 4.10: *Rcr3* is under diversifying selection in *S. pimpinellifolium.*

Figure 4.11: *Rcr3* is under diversifying selection in wild tomato.

Figure 4.12: Clade-wide signature of diversifying selection not detected on *Rcr3* in wild potato.

Figure 4.13: Evolutionary analysis in Solanaceae suggests *Pip1* is under diversifying selection in wild tomato, but not in *S. pimpinellifolium* and wild potato.

Figure 4.14: *C14* is under diversifying selection in *S. pimpinellifolium* while no other branch-specific episodes of positive selection were identified in this study.

Figure 5.1: Phylogenetic relationships derived to guide silencing of *Cf-2* and *Hcr2* genes.

Figure 5.2: *TRV*-based virus-induced gene silencing (VIGS) assay in wild species of tomato and potato.

Figure 5.3: Silencing with *Cf-2* fragment reduce Avr2-induced HR in wild tomato *Sp*LA0369.

Figure 5.4: Avr2 recognition is reduced upon Hcr2 silencing whilst EpiC1, EpiC2B and Cip1 recognition remains unaffected in wild tomato *Sp*LA0753.

Figure 5.5: EpiC2B recognition is not affected in *Hcr2* silenced wild potato *Si*CGN17720.

Figure 5.6: EpiC2B perception is not affected upon *Hcr2* silencing in wild potato *Sb*CGN22732.

Figure 5.7: Silencing Rcr3, Pip1 and C14 variably reduce recognition of inhibitors in *S. pimpinellifolium.*

Figure 5.8: Effect of *Rcr3*, *Pip1* and *C14* silencing on HR-triggered by inhibitors in wild potato.

Figure 5.9: *SOBIR1* silencing reduces inhibitor recognition in wild tomato and wild potato.

Figure 5.10: A detailed computational approach that identified Cf-like Receptor-like proteins (RLPs) in Solanaceae. Ve and EIX were included in this approach for outgroup clustering.

Figure 5.11: Distribution of Cf-like RLPs in Solanaceae.

Figure 5.12: Hcr2s are most recently evolved Cf-like proteins.

Figure 5.13: Summary of Cf-2/Hcr2 RLP evolution in Solanaceae.

Figure 6.1: Proposed co-evolutionary dynamics of pathogen-derived inhibitors, Avr2, Cip1 and EpiCs with host protease targets Rcr3, Pip1 and C14 and recognition by Hcr2 receptors.

Figure 6.2: Perception model of unrelated pathogen-derived inhibitors Avr2, Cip1 and EpiCs.

List of tables

Table 1.1: LRR-RLPs identified to confer extracellular recognition in Solanaceae.

Table 2.1: List of *Solanum pimpinellifolium* populations tested in this study.

Table 2.2: List of wild tomato species populations tested in this study.

Table 2.3: List of control plant lines used in this study.

Table 2.4: List of wild potato populations tested in this study.

Table 2.5: List of other Solanaceae species (eggplant, pepper, petunia, and tobacco) in this study.

Table 2.6: List of primers used for PCR, sequencing and qPCR.

Table 2.7: List of plasmids generated in this study.

Table 2.8: List of sourced plasmids used in this study.

List of supplementary figures and tables

Supplementary 3.1: No HR response phenotypes observed against inhibitor infiltrations in eggplant (both cultivated and wild populations shown), pepper, petunia and tobacco populations.

Supplementary 3.2: Different symptoms observed in a few tomato and eggplant populations.

Supplementary 4.1: Graphs showing the posterior distribution through discretized rate grid generated using Fast Unconstrained Bayesian Approximation (FUBAR) test to detect site-selection in (a) *Rcr3*, (b) *Pip1* and (c) *C14* in *S. pimpinellifolium,* wild tomato and wild potato.

Supplementary 4.2: Fixed-effects likelihood test for statistical significance was estimated on the basis of 500-site level parametric bootstrap replicates for combined selection signatures on sequences generated in this study for (a) *Rcr3*, (b) *Pip1*, and (c) *C14.*

Supplementary 4.3: Branch-site Unrestricted Statistical Test for Episodic Diversification (BUSTED) to detect episodes of positive selection in *Rcr3* family in Solanaceae.

Supplementary 4.4: Branch-site Unrestricted Statistical Test for Episodic Diversification (BUSTED) to detect episodes of positive selection in *Pip1* family in Solanaceae.

Supplementary 4.5: Branch-site Unrestricted Statistical Test for Episodic Diversification (BUSTED) to detect episodes of positive selection in *C14* family in Solanaceae.

Supplementary 5.1(a): VIGS fragments used to silence *Cf-2* and *Hcr2s* in wild tomato and potato.

Supplementary 5.1(b): Target efficiency of four different VIGS fragments designed in this study to member genes of *Cf-2* clan.

Supplementary 5.1(c): Target efficiency of four different VIGS fragments designed in this study to member genes of *Cf5* clan.

Supplementary 5.1(d): Target efficiency of four different VIGS fragments designed in this study to member genes of *Full-length Hcr2s* clan.

Supplementary 5.1(e): Target efficiency of four different VIGS fragments designed in this study to member genes of Truncated *Hcr2s* clan.

Supplementary 5.1(f): Target efficiency of four different VIGS fragments designed in this study to cross-targets *Hcr2s* in tomato and potato.

Supplementary 5.2: Agarose DNA gel showing PCR of *Cf-2* (clan 1) VIGS nucleotide fragment.

Supplementary 5.3: VIGS fragments used to silence cysteine proteases and *SOBIR1* in wild tomato and potato.

List of input data analysis files attached as supplementary

Supplementary 2.1: Tables 2.1 to 2.5 excel files for populations screened

Supplementary 3.3: R code and three input data files (.csv format) used for complex heatmap representation of HR phenotype scoring in *S pimpinellifolium* (shown as figure 3.4)

Supplementary 3.4: R code and three input data files (.csv format) used for complex heatmap representation of HR phenotype scoring in wild tomato (shown as figure 3.5)

Supplementary 3.5: R code and three input data files (.csv format) used for complex heatmap representation of HR phenotype scoring in wild potato and other Solanaceae species (shown as figure 3.6)

Supplementary 3.6: R code and two input data files (excel sheets) for regional recognition frequency and altitude recognition frequency (shown as figures 3.7 and 3.8)

Supplementary 3.7: Two R code and three input data files (.csv format) for population response mapping across latitude/longitude/elevation regions (shown as figure 3.9)

Supplementary 4.6: Raw data file (excel sheet) used to estimate frequency of *Cf* genes in *S. pimpinellifolium* across distribution range (shown as figure 4.5)

Supplementary 4.7: MUSCLE alignment (fasta file), maximum-likelihood 500 bootstrap replication phylogenetic tree (newick file) and iTOL annotation datasets (four excel files + one fasta file) for *Rcr3* phylogeny across Solanaceae (shown as figure 4.9)

Supplementary 4.8: *Rcr3* nucleotide and translated protein sequences (two fasta files) generated in this study and pruned alignment dataset (one fasta file) displayed in figures 4.10, 4.11 and 4.12

Supplementary 4.9: *Pip1* nucleotide and translated protein sequences (two fasta files) generated in this study. MUSCLE alignment (fasta file), maximum-likelihood 500 bootstrap replication phylogenetic tree (newick file) and iTOL annotation datasets (four excel files + one fasta file) for *Pip1* phylogeny (shown as figure 4.13) are also included

Supplementary 4.10: *C14* nucleotide and translated protein sequences (two fasta files) generated in this study. MUSCLE alignment (fasta file), maximum-likelihood 500 bootstrap replication phylogenetic tree (newick file) and iTOL annotation datasets (four excel files + one fasta file) for *C14* phylogeny (shown as figure 4.14) are also included

Supplementary 5.4: Maximum-likelihood 500 bootstrap replication tree (newick file), *Hcr2* gene sequences (fasta file) and iTOL annotations complied in one excel sheet (data shown as figure 5.1)

Supplementary 5.5: NEEDLE pair-wise alignment used to estimate efficiency of each VIGS fragment (clan 1, 2, 3 or 4) to target genes in same or different clans and cross targets are shown (20 fasta files; data summarised in supplementary figures 5.1(b) to 5.1(f))

Supplementary 5.6: Efficiency of *Rcr3* VIGS fragment to silence variants in closely and distantly related species within Solanaceae family estimated using NEEDLE pair-wise alignment (fasta file)

Supplementary 5.7: Efficiency of *Pip1* VIGS fragment to silence variants in closely and distantly related species within Solanaceae family estimated using NEEDLE pair-wise alignment (fasta file)

Supplementary 5.8: Efficiency of *C14* VIGS fragment to silence variants in closely and distantly related species within Solanaceae family estimated using NEEDLE pair-wise alignment (fasta file)

Supplementary 5.9: Efficiency of *SOBIR1* VIGS fragment to silence variants in closely and distantly related species within Solanaceae family estimated using NEEDLE pair-wise alignment (fasta file)

Supplementary 5.10: Cf-like proteins (fasta file) extracted in this study (figure 5.10 and 5.11), maximum-likelihood 500 bootstrap replication tree (newick file) and iTOL annotations organised as an excel file are attached (data shown as figure 5.12)

List of appendix figures

Appendix 4.1: αRcr3 western blot showing natural *Rcr3* variants tested.

Appendix 4.2: Active Rcr3 variant exist in other Solanaceae species and some of them have the ability to trigger HR in the presence of transiently co-expressed *Avr2* and *Cf-2* in *N. benthamiana.*

Appendix 4.3: *Cip1* and *EpiCs* do not trigger HR when transiently co-expressed with *Cf-2* and tomato or potato *Rcr3.*

Chapter 1

Introduction

1.1 Plant diseases threaten global food security

Global food insecurity is an issue greater than ever with an estimated 9.2% of the population still suffering hunger adversity (State of Food Security and Nutrition in the World Report, 2023). Moreover, climate change projections predict the decrease in productivity of economically important crops, including tomato by 2050 (Cammarano et al., 2022) and given the prediction of nearly ten billion people on earth by 2050 (United Nations Report 2017), the acceleration of sustainable crop improvement innovations to sustain the crisis is thus important. A major challenge in this direction is to increase plant disease resistance to reduce yield losses that are threatened by fungal, bacterial, viral and oomycete plant pathogens found worldwide (European Plant Protection Organisation database 2025).

Tomato, potato, eggplant and pepper, are major crops of the economically important family, Solanaceae (FAOSTAT 2023) and have been conventionally bred for biotic and abiotic resistance traits. The emergence of new strains of pathogens and severity of infections in greenhouse and field environments challenge the production of tomato and potato. However, the extensive availability of natural resources, advancements in genomic research, biotechnological gene editing and artificial intelligence driven methods offer an opportunity to innovate environment-friendly climate resilient crops and yield enhancement strategies to meet the increasing food demands (Gerakari et al., 2025).

1.2 The immune system of plants

Plants and their pathogens are engaged in a co-evolutionary arms race battle, where the outcome of plant's interaction with invading pathogen is governed by plant's ability to respond to counter-strategies in pathogens (Ali et al., 2024). The leaf apoplast or the extracellular space is a critical battleground, where effector protein repertoire secreted by pathogens function as virulence factors to target host immune proteins and suppress pathogen detection by the host (Erickson and Schuster, 2024). Perception of effectors can trigger host immune signalling that prevents the pathogen from establishing a successful infection. Hallmarks of plant innate immunity against pathogens are described as a zig-zag-zig framework that incorporates Pattern-triggered immunity (PTI) and Effector-triggered immunity (ETI) (Jones and Dangl, 2006). PTI is conceptually cell-surface immunity, activated by detection of extracellular and conserved pathogen-/microbial-/herbivore-/damage-associated molecular patterns (PAMPs/MAMPs/HAMPs/DAMPs) by pattern-recognition receptors (PRRs) at the cell-surface (Ngou et al., 2022). Cell-surface immune receptors are generally either Receptor-like kinase (RLK) proteins or Receptor-like proteins (RLPs) (Bentham et al., 2020).

1.2.1 Gene-for-gene and inverse models of interaction

Effector-triggered susceptibility (ETS) ensue when pathogen secreted effectors, encoded by dominant *Avirulence* (*Avr*) genes, suppress and evade PTI. In turn, the classical gene-for-gene model (Flor, 1954) typically applies to plant-biotrophic/hemibiotrophic pathogens, where ETI is triggered in plants when effectors are usually recognised by corresponding dominant *Resistance* (*R*) genes encoded nucleotide-binding (NB)-leucine rich repeat (LRR) receptors (NLRs) resulting in a type of programmed cell death (PCD) called hypersensitive response (HR). Recognition of extracellular effectors mediated by cell-surface receptors

can also trigger ETI (Jones et al., 1994). NLRs are reportedly complex and sub-functionalised, for instance functioning as NLR networks or NLR pairs, where one NLR acts as a sensor (S) and another as a helper (H) to achieve a durable resistance (Feehan et al., 2020). Based on their N-terminal, NLRs can further be classified into CC (Coiled-coil) or TIR (Toll-interleukin-1 receptor) types (Jones and Dangl, 2006). Many new terms have lately been introduced to original conception of plant immunity, for instance extracellularly-triggered (ExIT) and intracellularly-triggered immunity (InTI), distinguished based on location of pathogen-secreted effector recognition (van der Burgh and Joosten 2019). In this thesis, we focus on host-mediated extracellular recognition of unrelated pathogen secreted protease inhibitors.

Accumulating evidences suggest a mirror concept of gene-for-gene model of plant interaction with specialist necrotrophic fungal pathogens, which feed on dead host tissues and release specific necrotrphic effectors (NEs) to hijack biotrophic host-mediated HR and induce host susceptibility. In a compatible inverse gene-for-gene interaction, host-specific NEs are recognised by specific dominant susceptibility genes, leading to activation of PCD and necrosis instead of resistance in host (Friesen and Faris, 2010). Well-known examples are pathogenic fungi, wheat Septoria nodorum blotch causing *Parastagonospora nodorum* (formerly *Stagonospora nodorum*) and wheat tan-spot disease causing *Pyrenophora tritici-repentis*. A small secreted NE, called ToxA first identified in P. tritici-repentis and referred to as SnToxA in P. nodorum, are recognised in dominant susceptibility gene Tsn1 harbouring wheat genotypes. Tsn1 protein has serine/threonine kinase and NB-LRR domains and mediates susceptibilty to pathogens (Friesen and Faris, 2021).

1.2.2 Mutual potentiation between PTI and ETI

Overlaps between PTI and ETI since original proposition in 2011 (Qi et al., 2011) are increasingly emerging. Even though PTI and ETI deploy distinct class of receptors, they

both mutually potentiate to confer a robust immune response (Ngou et al., 2021, Yuan et al., 2021). As an example, EDS1 (Enhanced disease susceptibility 1), PAD4 (Phytoalexin-deficient 4) and ADR1 (Activated disease resistance 1) are common intracellular ETI components in *Arabidopsis* (Hu et al., 2005). EDS1 associates with PAD4 physically and the EDS1/PAD4 further requires ADR1, a helper(H)-NLR to mediate RLP23 mediated basal defence upon perception of Notch-like protein (NLP) secreted by fungal pathogen *Botrytis cinerea* (Wu et al., 2019, Dongus and Parker, 2021). Several downstream immunity outputs like ROS (Reactive oxygen species) production, calcium influx, MAPK (Mitogen-Activated Protein Kinase), role of transcription factors, expression and accumulation of PR (Pathogenesis-related) proteins are common to both PTI and ETI (Yuan et al., 2021). **Figure 1.1** illustrates PTI-ETI intersection, particularly in context of extracellular immunity against unrelated inhibitors that are a focus of this thesis.

1.2.3 Role of RLPs, RLKs and H-NLRs in effector recognition

RLPs constitute a group of R proteins carrying an extracellular LRR domain and a short transmembrane domain (TM). RLPs do not have an intracellular kinase domain, hence they lack a capacity to transduce the signal and require RLKs like BAK1 (Brassinosteroid Insensitive 1-Associated Kinase1)/SERK3 (Somatic Embryogenesis Receptor Kinase 3) and SOBIR1 (Suppressor of BIR1-1) for downstream signalling (Liebrand et al., 2013, Postma et al., 2016, van der Burgh et al., 2019). PAMPs (interchangeably termed extracellular immunogenic patterns or ExIPs) and effectors at the cell-surface can be perceived directly or indirectly (van der Hoorn and Kamoun, 2008) by corresponding RLPs or RLKs, activating frontline ExTI (Huang and Joosten, 2025) (**Table 1.1** list LRR-RLPs identified to confer extracellular recognition in Solanaceae). In Solanaceae, a subclade of H-NLRs, called NRCs (NLR required for HR-associated cell death), is largely expanded and form a diversified central network required to mediate NLR- or RLP-dependent recognition of different pathogens (Lida et al., 2021, Kourelis et al., 2022). For instance, NRC2 and

NRC3 (Wu et al., 2017) directly interact with Prf/Pto complex, a S-NLR and an intracellular serine/threonine kinase respectively (Pedley and Martin, 2003). Upon recognition of AvrPto/AvrPtoB effectors secreted by *Pseudomonas syringae* strain DC3000, NRC2/NRC3 dissociate from Prf/Pto complex, triggering a downstream cell-death response and MAPK signalling (Zhang et al., 2024). The extracellularly-triggered immune signalling in plant-pathogen dynamics however, have been overlooked due to common focus on cytosolic effectors and experimental challenges posed by the transient nature of these interactions (Erickson and Schuster, 2024, Mooney and van der Hoorn, 2024).

1.3 *Cladosporium fulvum*

C. fulvum (currently called *Fulvia fulva*) (Videira et al., 2017), an ascomycete hemibiotrophic fungal pathogen of tomato, is known to cause leaf mould, a devastating disease responsible for severe losses (Thomma et al., 2005, de Wit, 2024). Under high disease pressure, leaf mould caused losses can be over 50% (Zhao et al. 2022). *C. fulvum* unlike other pathogens does not produce structures like haustoria to invade the host, hence its encounter with the host in extracellular space importantly defines the outcome. *C. fulvum* secretes at least 75 effectors or small protein inhibitors (<300 amino acids long), encoded by *Avr* (*Avirulence*) or *Ecp* (*Extracellular Protein*) genes, to promote colonisation of host extracellular space or the apoplast (Lauge et al., 2000, Luderer et al., 2002, Mesarich et al., 2018). *Avr* gene products known at present are not produced by all isolates of *C. fulvum* and are race-specific, where Avr2, Avr4, Avr4E and Avr9 are well studied (van der Hoorn et al., 2000, Luderer et al., 2002) and can trigger HR in tomato. Contrastingly, *Ecp's* genes are present in all known isolates, however, isolated *Ecp* genes have lower sequence variations in comparison to *Avr* genes (van der Ackerveken et al., 1993, Lauge et al., 2000, Krujit, 2005, Mesarich et al., 2018). *C. fulvum*-tomato is a model plant-pathogen interaction. Recognition of Avr and Ecp proteins in several wild relatives of tomato occurs in a gene-for-gene

interaction manner, where cognate plant *C. fulvum* resistance (Cf) proteins and their homologs mediating resistance to similar Avr have been reported (Jones et al., 1996, Dixon et al., 1998, van der Hoorn et al., 2001). New *C. fulvum* races are continuously being identified and isolated across different parts of the world (Li et al., 2015), therefore mining new *C. fulvum* resistance is crucial.

1.3.1 *C. fulvum* resistance gene family in tomato

C. fulvum resistance genes in tomato, called *Cf* genes, are localised at the cell surface and all encode receptor-like proteins (RLPs) (Dixon et al., 1998 and Thomas et al., 1998). The first gene isolated against *C. fulvum* was *Cf-9* (Jones et al., 1994). *Cf* genes cloned so far are classified into two groups: the *Hcr9* gene family (*Homologous to C. fulvum resistance gene Cf-9*) (Parniske et al.,1999) and the *Hcr2* gene family (*Homologous to C. fulvum resistance gene Cf-2*) (Dixon et al., 1998). *Hcr9s* are primarily located on chromosome 1 while *Hcr2s* reside on chromosome 6. *Cf-2* isolated from the *Hcr2* locus and *Cf-9* were both introgressed from wild tomato relative *Solanum pimpinellifolium*. In *S. lycopersicum* Money Maker (MM)-*Cf0*, two *Cf-2* homologs, *Hcr2-0A* and *Hcr2-0B* were identified from chromosome 6 (Dixon et al.,1996, Dixon et al., 1998). Other wild relatives of tomato have also been sources of *Cf* genes, for example, *Cf-4* was introgressed from *Solanum habrochaites* and recognises Avr4. Cf-4 is also an Hcr9 and highly similar to Cf-9 (Thomas et al., 1997), consisting variable number of LRR domains, 25 and 27, respectively and sharing several features required crucially for inhibitor perception (van der Hoorn et al., 2001a, Wulff et al., 2001). Further, the discovery of functional *Cf* genes is ongoing, where *Cf-16* in this direction has most recently been mapped to chromosome 6 (Zhang et al., 2023).

1.3.2 Cf-mediated perception of Avr effectors of *C. fulvum*

A molecular mechanism of *Cf-2*-mediated perception of Avr2 has been proposed. An unlinked papain-like cysteine protease (PLCP), *Rcr3* from *S. pimpinellifolium* (*Rcr3*^{pim}), was found to be required for *Cf-2* function (Dixon et al., 2000), whereas its homolog in *S. lycopersicum* (*Rcr3*^{lyc}) was identified to be autonecrotic (Krüger et al., 2002). PLCPs, broadly categorised into four subfamilies are 20 to 25 KDa endopeptidases, play crucial roles in several plant-pathogen interactions (Shindo and van der Hoorn, 2008, MEROPS database). PLCPs have a Cys-His-Asn catalytic triad containing the catalytic cysteine residue in the substrate binding groove and are secreted as pro-proteases with an auto-inhibitory pro-domain, which is proteolytically removed for maturation and activation of protease (Shindo and van der Hoorn, 2008). Rcr3 requires subtilase P69B (Paulus et al., 2020) in the apoplast for activation specifically to mediate Cf-2-dependent perception of Avr2 (Krüger et al., 2002). *Rcr3* homologs from most *Solanum* species can be inhibited by Avr2 (Kourelis et al., 2020).

Further, LRR-RLPs usually constitutively associate with SOBIR1 via GxxxGxxxG dimerization motif present in the transmembrane domain of Cf proteins and SOBIR1 (Bi et al., 2016). The LRR-RLP/SOBIR1 complex actively recruits BAK1 to induce downstream signalling followed upon ligand perception (Albert et al., 2015, Postma et al., 2016). The amounts of SOBIR1/SOBIR-like that associate with Cf proteins likely trigger different intensities of HR upon Avr recognition. As an example, HR triggered by Cf-9-mediated recognition of Avr9 is more intense than Cf-2-dependent HR induced by Avr2 (Brading et al., 2000). Upon Avr4 perception together with SOBIR1, Cf-4 reportedly undergoes SERK3-dependent endocytosis (Postma et al., 2016). The activated phosphorylation cascade upon RLP/RLK association further activates RLCKs (Receptor-like cytoplasmic kinases), which lack an extracellular domain (Kourelis, 2023). Requirement of NRC3 in Cf-2, Cf-4, Cf5 and Cf-9 mediated recognitions (Kourelis et al., 2022) and NRC-dependent HR mediated by

RLPs, LeEIX2 and Ve1 in tomato (Gabriels et al., 2007, Fradin et al., 2009) have been demonstrated. Role of EDS1 in full immunity conferred by Cf-4 and Ve1 (conferring recognition of *Verticillium* effector) is also indicated (Kourelis et al., 2022, Zönnchen et al., 2022).

Based on RNA-Seq analysis, over a hundred transcription factors (TFs) representing thirty-seven families that are key regulators of pathways of plant-pathogen interaction, signal transduction, circadian rhythm and MAPK signalling, were recently reported as differentially regulated during different stages of immune response particularly mediated by *Cf-13* and *Cf-19* genes upon *C. fulvum* infection (Zhao et al., 2019, Zhang et al., 2020, Jiang et al., 2022 and Tong et al., 2024). EREB is a speculated TF that interacts with WRKY80 to likely mediate cross-talks with MAPK signalling pathway. Further, using VIGS, EREB silencing decreased the WRKY80 expression that also lead to decreased *Cf-19* mediated resistance (Tong et al., 2024).

1.4 Other apoplastic cysteine proteases

Pip1 is another PLCP that is paralogous to *Rcr3* and both Rcr3 and Pip1 are inhibited by Avr2 (Shabab et al., 2008, Ilyas et al., 2015). C14, a PLCP unrelated to Rcr3 and Pip1 carries a C-terminal granulin domain and also contributes to basal defence against different pathogens (Kaschani et al., 2010). Studies exploring natural variation and evolutionary selection pressures on *Rcr3*, *Pip1* and *C14* suggested that while Rcr3 and Pip1 are diversifying in tomato, C14 is under diversifying selection in potato (Shabab et al., 2008, Kaschani et al., 2010). Therefore, Rcr3, Pip1 and C14 play crucial yet distinct defence roles in recognition of various pathogens.

1.5 Guard versus decoy model of Cf-2/Rcr3-mediated Avr2 recognition

The gene-for-gene model was further expanded when guard hypothesis was proposed (Dangl and Jones, 2001), suggesting that R-protein physically associate and “guard” the activity of a “guardee” which is a defense protein in host. Multiple pathogen effectors target the guardee which can be guarded by more than one R-protein in a resistant host. In first prediction, the guard model speculate that R-protein constitutively interacts with the guardee and an effector-mediated modification in guardee leads to the release and activation of R-protein. In a second prediction of guard model, an effector is indicated to interact with the guardee that leads to conformational change enhancing affinity of effector-guardee complex for binding with R-protein and its activation (Dangl and Jones, 2001). An extension of guard model called the decoy model proposes that certain effector targets in host serve as decoy to mimic host target and induce an immune response upon effector recognition mediated by R-proteins (van der Hoorn and Kamoun, 2008).

Based on the guard hypothesis, Cf-2/Rcr3 is a salient example of indirect recognition mechanism, where resistance protein Cf-2 recognise the complex of Rcr3 and pathogen-derived inhibitor Avr2 (van der Hoorn and Kamoun, 2008). Since Avr2 also inhibits Pip1 in tomato (Shabab et al., 2008), decoy model predicts that Rcr3 only functions in the presence of Cf-2 receptor and does not function in immunity in the absence of *Cf-2* (Ilyas et al., 2015 and Kourelis and van der Hoorn, 2018). So far, Cf-2/Rcr3 dependent perception of Avr2 and recognition of *Fusarium oxysporum* secreted Avr3 by I-3-RLK (Catanzariti et al., 2015), are some examples of indirect extracellular perception in tomato, however, physical interactions remains to be shown. *Cf-2* was suggested to have a dual recognition ability when a nematode inhibitor, Vap1 of *Globodera rostochiensis*, was shown to be recognised by Cf-2/Rcr3 (Lozzano et al., 2012). However, this could not be established in research

assays of our group. Further, *Cf*-genes appear to be limited to Solanaceae (Kourelis et al., 2020), while LRR-RLPs like *Ve1* are conserved beyond Solanaceae (Fradin et al., 2011).

Proteomic experiments and transcript level estimation in *S. pimpinellifolium*, *S. pennellii* and cultivated *S. lycopersicum* (MM and Heinz), implied that *Pip1* is ~10-fold more abundant than *Rcr3* (Koenig et al., 2013, Ilyas et al., 2015). Interestingly, *Cf-2/Rcr3* perception studies support hypothesis of indirect perception, where in the absence of *Cf-2*, *Rcr3* was demonstrated to contribute to basal defence against *P. infestans*, supporting the guard hypothesis of indirect perception. On the other hand, the insignificant contribution of *Rcr3* against *C. fulvum* in the absence of *Cf-2*, supports the decoy hypothesis of indirect perception (Ilyas et al., 2015). Therefore, further research into evolution of functional *Cf-2/Rcr3* across Solanaceae was triggered.

1.6 Inhibition of extracellular host proteases by *Phytophthora infestans* secreted effectors

The oomycete pathogen *P. infestans*, which causes late blight, became significant since major outbreak in the 1845 that led to the catastrophic Irish potato famine (Wang et al., 2024) and continues to threaten production of tomato and potato worldwide (Coomber et al., 2024). *P. infestans* is a hemibiotroph that adopts biotrophy in initial infection stage to derive nutrients from the host living cells and eventually becomes necrotrophic to obtain nutrients from dead cells (Kamoun et al., 2015). To overcome recognition and resistance by host, *P. infestans* secrete a large number of effectors that could function extracellularly or intracellularly (Du et al., 2021). While over 500 effectors have been predicted in *P. infestans* genome, only 12 are characterised (Varshney and Tuberosa, 2013, Coomber et al., 2024). Many *P. infestans* effectors are cytosolic, known to be translocated by host and contain an RxLR (Arginine-any-Leucine-Arginine) motif (Wawra et al., 2017, Schornack et

al., 2010). *P. infestans* secreted extracellular effectors are structurally different from cytosolic effectors, but target several common host components (Bozkurt et al., 2011). Cystatin-like inhibitors EpiC1 and EpiC2B of *P. infestans*, inhibit Rcr3, Pip1 and C14 with variable affinities, but remain stealthy as they escape recognition and triggering of HR in tomato (Tian et al., 2007, Song et al., 2009, Kaschani et al., 2010). Further, C14 silencing in *N. benthamiana* enhanced susceptibility to *P. infestans* (Kaschani et al., 2010). Kazal-like serine protease inhibitors, EPI1 and EPI10, inhibit secreted tomato subtilase P69B in the apoplast (Tian et al., 2005, Paulus et al., 2020). P69B also participates in cleavage of *P. infestans* secreted cysteine rich small protein PC2 (Wang et al., 2021) and maturation by cleavage of Rcr3 involved in *C. fulvum* recognition (Paulus et al., 2020, Homma et al. 2023). Interestingly, P69 family members are conserved and can have different functions as P69D is inhibited by bacterial wilt causal pathogen, *Ralstonia solanacearum* but not to other pathogens (Zhang et al., 2024). A higher evolution rate and enhanced genome plasticity are driving the emergence of novel strains of *P. infestans* to overcome the defence surveillance by host plant (Dong et al., 2015, Dong and Zhou, 2022).

1.7 *Pseudomonas syringae*-derived Cip1 inhibits apoplastic proteases

Approximately 64 pathovars of *Gammaproteobacteria* species, *P. syringae*, have been identified and are known to cause disease in a diversity of plant species (Bundalovic-Torma et al., 2022). Bacterial speck caused by *P. syringae* pv. tomato was first identified in 1987 in Chile (Latorre and Lolas 1988) and is also a significant pathogen of tomato (de Wit, 2024). *P. syringae* pv. tomato DC3000 (*Pto*DC3000) is the most intensively studied and type-III (T3) secretion system (T3SS) injected T3 effectors into the host are commonly characterised (Lindberg et al., 2012). A screen of non-annotated apoplastic effectors from *Pto*DC3000 identified a chagasin-like protein, Cip1 that can significantly supress C14 and

Pip1 and weakly inhibit Rcr3 (Shindo et al., 2016). Mutant *cip1* showed significantly retarded *Pto*DC3000 growth on tomato, but transformation with *Cip1* restored bacterial growth on host, suggesting that extracellular Cip1 effector has a role in bacterial virulence. However, similar to *P. infestans* secreted EpiCs, Cip1 is also stealthy as it does not trigger HR (Shindo et al., 2016).

1.8 Harnessing diversity in Solanaceae wild crop relatives for novel pathogen recognition specificities

Germplasm screening has historically been an approach to identify novel resistance sources against fungal, oomycete and bacterial pathogens. Several previous studies screening, tomato-*C. fulvum*, tomato-*P. syringae*, potato-*P. infestans* and non-Solanaceaous crops, wheat-*Puccinia graminis*, flax-*Melampsora lini* and lettuce-*Bremia lactucae* often have revealed the largest pool of germplasms contain resistance against fungi and comparably fewer against oomycete and bacteria. *S. pimpinellifolium* populations have recently also been screened for resistance against *P. syringae* derived effectors, AvrPto and AvrPtoB (Pedley and Martin, 2003) that are recognised by NLR, Pto/Prf (Hassan et al., 2024). Wild ancestors of Solanaceae crop species inhabit diverse habitats and are rich sources of *R*-genes against *C. fulvum*, *P. infestans* and *P. syringae*. The established and extending understanding of plant immunity over the last 25 years, including convergent evolution of several immunity components, gives a collective context to explore the potential of nature-guided bioengineering of host targets for broad-spectrum resistance in crops.

Interaction of effectors with host apoplastic proteases and ligand binding by extracellular domains of RLPs are crucial for cytosolic signal transduction leading to successful recognition of pathogens in the apoplast. De novo engineering of such indirect mode of immunity by modifying the substrate specificity of host decoy proteins to expand their

recognition potential of new effectors has previously been demonstrated (Kim et al., 2016). Therefore, chimera generation of these proteases acting as co-receptors and RLPs as well as transfer of functionally validated chimeras can overcome species specific limitations of pathogen recognition (Schwessinger et al., 2015). In this direction, our group recently generated many chimeric fragments of the decoy protease, Rcr3, by domain swapping tomato *Rcr3*, whose inhibition by Avr2 can trigger Cf-2-mediated recognition, and eggplant *Rcr3*, which gets inhibited by Avr2 but does not activate Cf-2-immunity (Kourelis et al., 2020, Kourelis et al., 2024). *N. benthamiana* Rcr3 does not get inhibited by Avr2, hence Cf-2-mediated immunity is not triggered. However, when G194 residue in *N. benthamiana Rcr3* is swapped with N194 along with three key residues, *Nb*Rcr3 is inhibited by Avr2 and a robust Cf-2-dependent HR is visible (Kourelis et al., 2020). The analysis of HR transiently induced by these chimeras when expressed in combination with *Cf-2* and *Avr2* in *N. benthamiana* lead to the identification of a proline residue that can sufficiently trigger Cf-2-dependent HR by interaction of eggplant Rcr3 and Avr2 (Kourelis et al., 2024).

Further, when chimeric proteases derived from *Rcr3* and *Pip1* fragments were probed using mutagenesis, substituting 16 Rcr3 residues into Pip1 were sufficient to achieve Rcr3 type efficacy of Pip1 in triggering Cf-2-mediated immunity (Kourelis et al., 2024, Laflamme, 2024). These findings along with structural modelling tools (Schuster et al., 2024) will guide future efforts into investigating physical interaction between Avr2/Rcr3 and Cf-2, translating into bioengineering of new protease or co-receptor/receptor pairs with novel recognition specificities against several pathogens that target extracellular host proteins.

1.9 Aims and outline of this thesis:

This thesis aims to understand the recognition of unrelated pathogen-derived protease inhibitors, Avr2, EpiC1, EpiC2B and Cip1 in Solanaceae. The extent of Avr9 recognition in

Cf-9 source species *S. pimpinellifolium* and other wild tomato relatives has been extensively investigated (van der Hoorn et al., 2001, Krujit et al., 2005, Kahlon et al., 2020). However, the frequency of Avr2 recognition in *S. pimpinellifolium* and other wild relatives of tomato has not been analysed. Since *C. fulvum* specifically infects tomato, we hypothesised that Avr2 is a frequently recognised inhibitor in wild tomato, whereas, wild potato being the natural host of *P. infestans*, frequently recognises EpiCs. **In Chapter 3**, we report results from an extensive HR screening towards our aims: **(1)** whether recognition frequencies of these unrelated inhibitors varies across geographic origin ranges of wild relatives of tomato; **(2)** whether these inhibitor recognitions are conserved in distantly related wild tomato species, wild potato species and in fartherly evolved species in Solanaceae. A comprehensive analysis answers the question of Avr2 recognition distribution in the source species of *Cf-2*, *S. pimpinellifolium* and whether other distantly related wild tomato, wild potato and other Solanaceae species recognise Avr2 and show variation in relation to unrelated inhibitor recognitions.

Given the fact that Rcr3, Pip1 and C14 are variably inhibited by Avr2, EpiCs and Cip1, but only Avr2-Rcr3 interaction in the presence of *Cf-2* triggers HR, we were curious to analyse the frequency of *Cf-2* in wild populations and how this correlates with recognition frequencies of different inhibitors. We further hypothesised that natural variation in cysteine proteases underlie differences in their interaction with distinct inhibitors and HR phenotype variations in plants. Insights into the *Hcr9* gene clusters were a hallmark discovery, which showed that on the short arm of chromosome 1, *Hcr9* family members are present at least at five different loci (Parniske et al., 1997). However, not all *Hcr9s* are involved in pathogen recognitions. Therefore, identifying occurrence of *Cf-2* gene in natural populations and segregation of different *Cf*-genes was our interest. **Chapter 4** reports our next aims: **(3)** the frequency of *Cf-2* and genetic profiling variation in number of *Hcr2s*; **(4)** the extent of polymorphism that naturally exist in *Rcr3*, *Pip1* and *C14* in wild tomato and other species.

Only Avr2, but not EpiCs or Cip1 can induce HR in *Cf-2/Rcr3* Money Maker-tomato lines. Therefore, in **Chapter 5**, we hypothesised that while Cf-2 primarily may have evolved to confer Avr2 recognition, Cf-2-variants or Cf-2-like RLPs exist in Solanaceae that can confer recognition of EpiCs and Cip1. In this direction: **(5)** the role of these immune proteases and *Cf-2/Hcr2*s in recognition of Avr2, EpiC1, EpiC2B and Cip1 in native populations was first examined using *TRV*-based virus-induced gene silencing. Since Cf-RLP-mediated recognitions are dependent on RLKs and we did not observe a correlation with Cf-2 and recognition of EpiCs and Cip1, our next aim was to study **(6)** whether downstream signalling of all four inhibitors, similarly to other Cf receptors (Postma et al., 2016 and van der Burgh et al., 2019), converge on a common receptor-like kinase-SOBIR1. The evolutionary analysis of *Rcr3* suggested that it evolved much earlier than *Cf-2* in Solanaceae (Kourelis et al., 2020). Therefore, we next developed an *in-silico* pipeline to identify **(7)** the diversity of Cf-like RLPs and their phylogenetic evolution. All materials and methods used in this thesis are described in detail in **Chapter 2**. Finally, **Chapter 6** discussed the overall conclusion of this thesis and future perspectives.

LRR-RLP Gene	Species	Chromosome	Pathogen/ Stressor	Ligand/ Elicitor	Co-receptor(s)/ Components	PTI-ETI Intersection	Function	Reference(s)
Cf2	*S. pimpinellifolium*	6	*Cladosporium fulvum*	Avr2	Rcr3/Pip1/ SOBIR1/BAK1	-	ETI	Jones et a., 1994 & Dixon et al., 1996
Cf4	*S. habrochaites*	1	*Cladosporium fulvum*	Avr4	SOBIR1/BAK1/ SERK3	NRC/EDS1/ RLCK	ETI	Thomas et al., 1997 & Kourelis et al., 2022
Cf5	*S. esculentum var. cerasiforme*	6	*Cladosporium fulvum*	Avr5	-	-	ETI	Dixon et al., 1996
Cf9	*S. pimpinellifolium*	1	*Cladosporium fulvum*	Avr9	SOBIR1/BAK1	ACIK1	ETI	Jones et al., 1994
CuRe1	*S. lycopersicum*	-	*Cuscuta reflexa*	Crip21	-	-	PTI	Hegenauer et al., 2016
EIX2	*S. lycopersicum*	7	*Trichoderma viride*	EIX	-	NRC4a	PTI	Ron and Avni, 2004
EIX2	*N. benthamiana*	7	*Verticillium dahliae*	EIX3	-	-	PTI	Yin et al., 2021
ELR	*S. microdontum*	12	*Phytophthora infestans*	INF1	SOBIR1/BAK1	-	Enhanced late blight resistance	Du et al., 2015
I	*S. lycopersicum Heinz 1706*	11	*Fusarium oxysporum f sp. lycopersici*	Avr1	SOBIR1/BAK1/ SERK3	EDS1	ETI	Hu et al., 2005 & Catanzariti et al., 2017
RE02	*N. benthamiana*	-	*Valsa mali*	VmE02	SOBIR1/BAK1	-	PTI	Saur et al., 2016
REL	*N. benthamiana*	-	*Phytophthora sp.*	ELI	SOBIR1/BAK1	NRC	Required for ELI-triggered response	Gabriels et al., 2006 & Chen et al., 2023
REli	*N. benthamiana*	-	*Pythium periplocum*	Eli2	SOBIR1/BAK1	-	PTI	Yang et al., 2023
Ve1	*S. lycopersicum*	9	*Verticillium dahliae*	Ave1	SOBIR1/BAK1	NRC/EDS1	ETI	Kawchuk et al., 2001 & Fradin et al., 2009
XEG1	*N. benthamiana*	-	*Phytophthora sojae*	XEG1	SOBIR1/BAK1/ SERK3	-	PTI	Wang et al., 2018

Table 1.1 LRR-RLPs identified to confer extracellular recognition in Solanaceae.

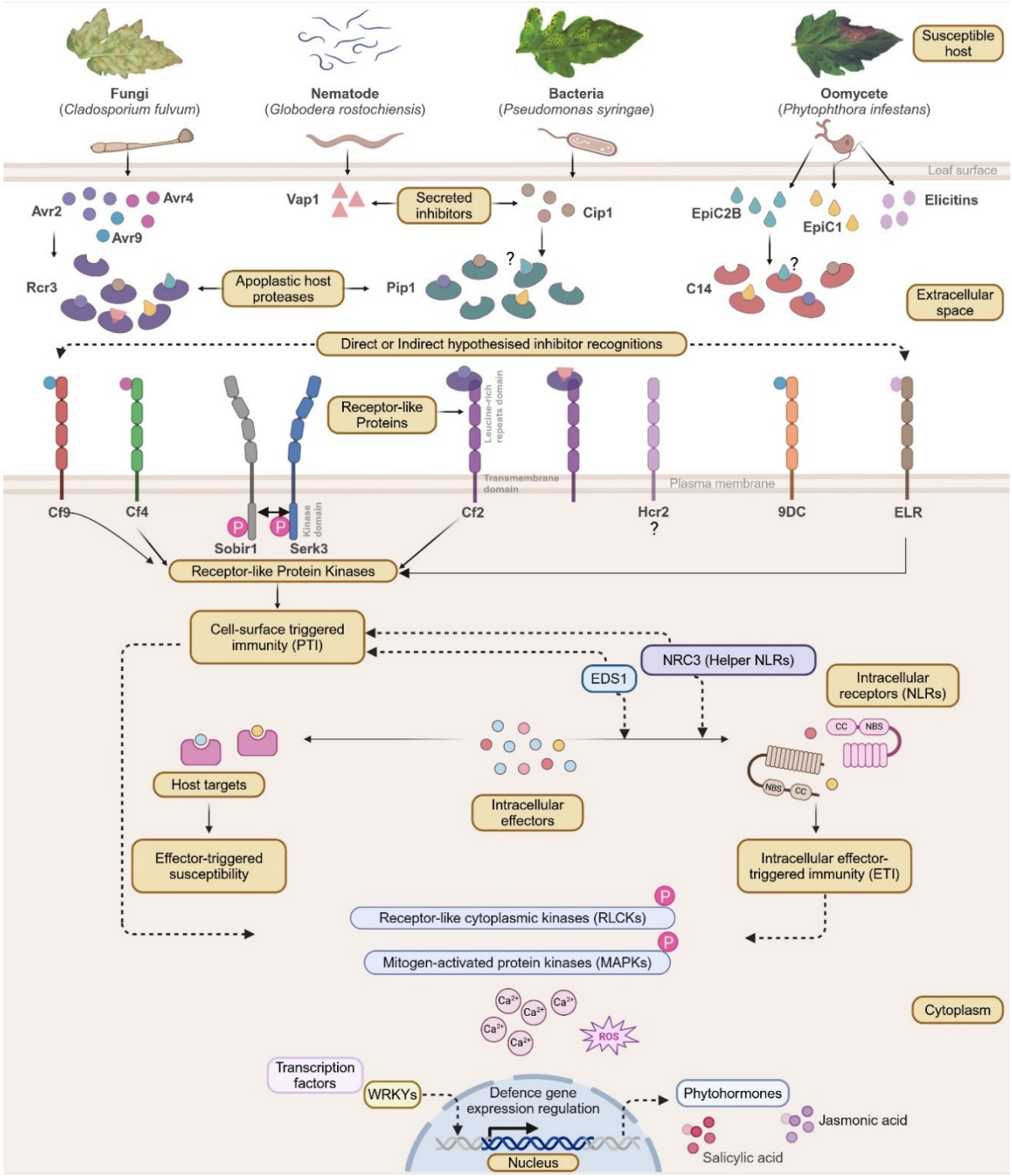


Figure 1.1: Illustration showing PTI-ETI intersection, particularly in extracellular immunity against important pathogens of Solanaceae crops.

Chapter 2

Materials and methods

2.1 General materials

2.1.1 Chemicals

All general chemicals, including antibiotics, media and buffer components were purchased from Sigma-Aldrich, Merck UK (www.sigmaaldrich.com/united-kingdom) and Fisher Scientific, UK (www.fishersci.co.uk). Chemicals and media were prepared using double distilled water purified by Milli-Q® Ultrapure system, Merck Millipore (www.merckmillipore.com). Antibiotics were used at given working concentrations: kanamycin (50 µg/ml and 100 µg/ml), gentamycin (25µg/ml), rifampcin (25 µg/ml, dissolved in methanol) and spectinomycin (50 µg/ml).

2.1.2 Enzymes, probes and antibodies

Restriction enzymes were from Thermo Fisher Scientific (www.thermofisher.com) while Q5-High fidelity PCR enzyme and components were from New England Biolabs®, UK (www.neb.uk.com). Enzymes were used as required units in a reaction. E-64 inhibitor was purchased from Sigma-Aldrich, Merck UK. Fluorescent epoxide probe MV201 (Richau *et al*., 2012) was used from original stocks in our lab. MV201 was dissolved in DMSO to a working concentration of 1 mM. Antibody α-Rcr3 (Rooney *et al*., 2005) was used at dilution 1: 5000 and HRP-conjugated secondary α-Rabbit antibody (Sigma-Aldrich, Merck UK) was used at 1: 10000.

2.1.3 Primers

Primers were designed using Primer3 v2.4 (Untergasser *et al*., 2012). Modified and non-modified desalt (DST) purified custom oligonucleotides for genomic DNA PCR, QPCR and Sequencing were ordered from Sigma-Aldrich, UK. Primers were diluted to a stock concentration of 100 µM using Milli-Q water. All primers are listed in **Table 2.6**.

2.1.4 Gel equipment and scanner

Wide-Mini Sub Cell horizontal gel electrophoresis unit was used to run DNA agarose gels. Criterion™ vertical midi-format gel electrophoresis unit was used to run SDS-PAGE protein gels. PowerPac™ Basic Power Supply units were supplies for current source. All these systems were from Bio-Rad, UK (www.bio-rad.com/en-uk). Pre-stained kaleidoscope (10-250 kD, Bio-Rad UK) was used as a protein standard and Gene Ruler 1 kb Plus DNA ladder (Thermo Fisher Scientific, UK) was used as a standard for DNA gels. Manual gel documentation system used for DNA gel scanning was compatible for image analysis and processing by GeneSnap software v7.12 (Syngene, Synoptcis Group UK; www.syngene.com). Coomassie brilliant blue (CBB) stained protein gels were scanned using Epson V600 (www.epson.co.uk).

2.1.5 Polymerase chain reaction (PCR) thermocycler

All genomic DNA and plasmid construction PCRs and enzymatic reactions were performed in an Applied Biosystems MiniAmp® plus thermal cycler veriflex block (96 well, 0.2 mL).

2.2 General methods

2.2.1 Sterilisation and centrifugation

Autoclaving for general sterilisation was done at 121°C for 20 minutes under 105 kPa. Antibiotics and heat-intolerant chemicals were sterilised using 0.2 µM syringe filters. Centrifugation, unless specified otherwise, was carried out using a benchtop Eppendorf MiniSpin™, non-refrigerated centrifuge (www.eppendorf.co.uk).

2.2.2 Competent cells of *Escherichia coli* and *Agrobacterium tumefaciens*

Competent cells from original sources were maintained as per their required conditions. *E. coli* DH10ß cells (Invitrogen, Thermo Fisher Scientific) were used for construction of Level 0 plasmids and *E. coli* Rossetta2 (DE3) pLysS cells (Merck UK) were used to transform with Level 2 vectors for protein expression and purification. Binary expression vectors for transient assays and gene silencing were transformed into *A. tumefaciens* strain GV3101 pMP90.

2.2.3 Growth media and gels

LB media containing 10 g/L tryptone, 5 g/L yeast extract and 10 g/L NaCl with specific antibiotic(s) was used for bacterial growth. 10 g/L agar was added additionally to prepare solid media. All agarose and SDS-PAGE gels were freshly prepared and used.

2.2.4 Storage of stocks

Purified plasmids, DNA and RNA samples in nuclease-free water were stored at -20°C. Bacterial strains were maintained as glycerol stocks at -80°C. Buffers, antibiotics, enzymes and primers were maintained at -20°C to 4°C as specified by the manufacturer. Light-sensitive chemicals and probes were stored in dark where required.

2.3 Plant materials and growth conditions

2.3.1 Seed sterilisation

For improved germination, all *Solanum* and *Capsicum* seeds were soaked in half-strength 2.7% sodium hypochlorite bleach for 25 minutes (45 minutes for *S. cheesmaniae, S. ochranthum, S. galapagense, S. sitiens, S. juglandifolium,* and *S. lycopersicoides*). Seeds were rinsed thoroughly with water and germinated on a 2M Whatman® filter paper bed in a sterilised petri plate. The petri plates were incubated in dark at 22 to 25°C for 7-10 days.

2.3.2 Plant growth and maintenance

Germinated seeds were transferred to pots with a soil composition having 3 parts multipurpose compost (Levington® Advance M2 75 Lt), 1 part of vermiculite (Westland Gro-Sure) and 0.1 g/10L Exemptor® insecticide dust by Bayer. The plants were maintained in a controlled green house with supplemental full-spectrum lights that generate minimal heat but mimic efficient sunlight (16h light/8h dark, 55% humidity at 22°-25°C). To maintain healthy plants, Miracle-Gro® all-purpose concentrated liquid food was fed diluted as per instruction in water once every 15 days. Tomato plants were not allowed to flower and thus

were pruned to transplant between 4 to 5 weeks of age for maintaining continuous growth for propagation.

2.3.3 Collection of seeds used in this study

To represent a comprehensive analysis across the Solanaceae family, I investigated a total of 302 populations or accessions with 112 populations representing *Solanum pimpinellifolium*; 71 populations representing 18 other wild tomato species; 50 populations representing 12 wild potato species; 22 populations representing ten cultivated and wild eggplant species; 26 populations representing five cultivated and wild pepper species; eight populations representing four hybrid and wild petunia species; 13 populations representing ten cultivated and wild tobacco species. Populations from each species are derived from in and around centres of origin, hence we expected these representatives to contain natural variation in disease resistance. Wild tomato populations, unless specified otherwise, were donated by Tomato Genetic Resource Centre (TGCR), University of California Davis, USA and are listed in **Tables 2.1** and **2.2**. Accessions of potato, eggplant and pepper listed in **Tables 2.4** and **2.5** were generously provided by The Centre for Genetic Resources (CGN), Wageningen University and Research, the Netherlands. Petunia and tobacco accessions were ordered from commercial sources with details listed in **Tables 2.5**. Resistance controls of near isogenic lines of *Solanum lycopersicum* cultivar Money Maker, *Solanum tuberosum* and *Nicotiana benthamiana* were from original source lines maintained in our lab.

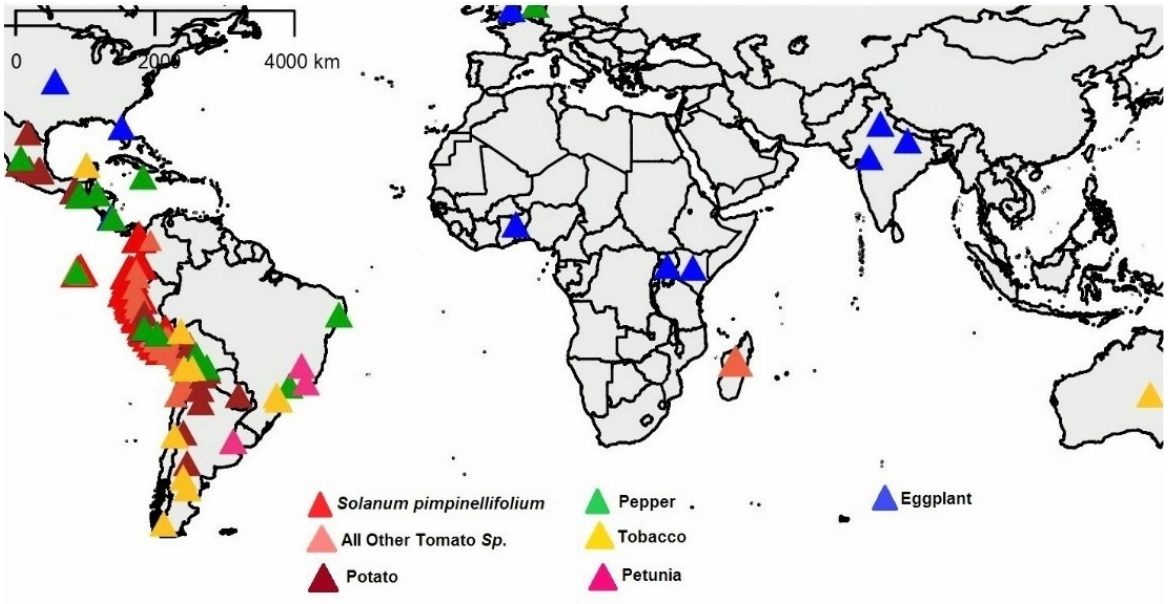


Figure 2.1 Map showing collection sites of populations and species tested in this study.

2.3.4 Taxonomic sampling for in-group/outgroup analysis

Based on taxonomic classification and phylogeny of *Solanum* sect. by Bombarely *et al.,* (2016), Rodriguez *et al*., (2009) and Peralta *et al*., (2008), I recreated a species tree in **Figure 3.1** to define in-group, more close and distant outgroup species complexes in this study. S. *lycopersicoides* and S. *sitiens* were analysed as outgroup species to all wild tomato. *Solanum* sect. Petota acted as outgroup to entire tomato complex. *S. palustre* (syn. *S. brevidens*) was chosen to represent an outgroup species in potato. *S. dasyphyllum* was outgroup for eggplant (Aubriot *et al.*, 2018). *C. tovarii* was a selected outgroup species to pepper (Garcia *et al.*, 2016). *N. tomentosiformis* was taken as a representative outgroup species for tobacco while *P. integrifolia* was considered as outgroup to petunia in this study. Further, median time scales of evolution of each species adjusted in relation to *S. lycopersicum* in this study were computed using TimeTree and they were used to indicate evolution of recognition specificities against inhibitors.

2.4 Pathogen-derived inhibitors used in this study

2.4.1 Golden gate cloning based inhibitor plasmids

Partially domesticated cloning components and vectors were used from the original Golden Gate Modular Cloning (MoClo) Plant Parts kit (www.addgene.org; Weber *et al*., 2011 and Engler *et al*., 2014). Cloning and assembly protocol is based on published references (The Sainsbury Laboratory, Norwich UK, http://synbio.tsl.ac.uk/?p=92), and Kourelis *et al*., 2020). **Table 2.8** list all level 0 and level 2 plasmids that have been sourced from elsewhere in this study. pJK153 (pL1VE-R1-PU-T7_S-OmpA-His-TEV_C-AVR2_T-T7) (Kourelis *et al*., 2020) was used for expression and purification of *Cladosporium fulvum* encoded inhibitor *Avr2* (Genbank accession AJ421629.1). Expression plasmids pJK155 and pJK157 were respectively used for *Phytophthora infestans* inhibitors *EpiC1* (Genbank accession AY935250) and *EpiC2B* (Genbank accession AY935252). pJK159 was used for inhibitor *Cip1* (Genbank accession AE016853) from *Pseudomonas syringae* (*Pst DC3000*). pJK153, pJK155, pJK157 and pJK159 were cloned by Dr Jiorgos Kourelis as described for pJK153 by Kourelis *et al*., 2020.

2.4.2 Golden gate based site-directed mutagenesis of inhibitor mutant plasmids

Previously reported least inhibitory mutant versions of four inhibitors (referenced and detailed below) tested in this study, were generated to represent appropriate controls while selecting positive resistance phenotypes from screening of plants. Level 0 and level 2 plasmids generated in this study are listed in **Table 2.7**.

2.4.2.1 Construction of level 0 modules

pSM001 (pL0M-C-Avr2Δ6), lacking six C-terminal residues required for Avr2's inhibition of tomato Rcr3 (Van't Klooster *et al*., 2011) was constructed by using primer pair SM_AVR2_C53X_F and _R to PCR on pJK019 (pL0M-C-Avr2). A conserved motif QxVxG is known to be crucial for EpiCs to inhibit Pip1 and Rcr3 in tomato (Tian et al., 2007). This motif was thus substituted to NxLxA to generate EpiC mutants in this study. Primer pair SM_EPIC1_2B_MUT_F and _R were used to PCR on template plasmids pFGH027 and pJK017 for construction of pSM002 (pL0M-C-EpiC1_QxVxG>NxLxA) and pSM003 (pL0M-C-EpiC2B_QxVxG>NxLxA). For construction of Cip1 mutant in this study (pSM004), two threonine residues from a conserved NPTTG motif were deleted. This deletion efficiently diminishes the inhibitory activity of Cip1 as reported by Shindo *et al*., 2016. pSM004 (pL0M-C-Cip1ΔTT) was generated by PCR on pFGH026 using primers SM_CIP1_DTT_F and _R. PCR conditions are described below, and the linear products were later circularized in a one-pot *Bpi*I reaction. Level 0 PCR reaction of 25 µl using NEB Q5®-high fidelity DNA polymerase was set up as per manufacturer's instructions.

Level 0 PCR run program included: step **1** at 98°C for 30 secs, step **2** at 98°C for 10 secs, step **3** at 60°C for 20 secs, step **4** at 72°C for 2 mins and 30 secs. Then four cycles were repeated from step **2** and continued to step **5** at 98°C for 10 secs, step **6** at 72°C for 20 secs, step **7** at 72°C for 2 mins and 30 secs. 24 cycles from step **5** were repeated and PCR was continued to step **8** at 72°C for 3 mins and at step **9** was hold at 4°C. A one-pot golden gate (digestion-ligation) reaction was then set up with following components: PCR product from above reaction (1 µl), 10 units/µl thermo fast digest *Bpi*I (0.25 µl), fast digest buffer (0.5 µl), 400 units/µl NEB T4 DNA ligase (0.25 µl), 10 mM ATP (0.5 µl) and Milli-Q water (2.5 µl). Reaction conditions for one-pot reaction (set up in a PCR thermocycler) were: step **1** at 37°C for 10 mins, followed by step **2** at 16°C for 10 mins. Three cycles from step **1** were

repeated and the reaction continued with step **3** at 37°C for 10 mins, and step **4** at 65°C for 20 mins. The reaction was on hold at 4°C.

Transformation of *E. coli*

In a PCR tube containing 5 µl *Bpi*I reaction product, 50 µl competent cells of *E. coli* DH10ß were added and the mixture was left on ice for 30 minutes. *E.coli* cells were heat shocked at 42°C for 45 seconds and incubated on ice for 2 minutes. 100 µl LB media was added to recover cells at 37°C for 60 minutes. Cells were re-suspended and incubated overnight at 37°C (not more than 16 hours) on LB agar plates containing selection marker kanamycin[50] or spectinomycin[50]. Next day, a few colonies of *E.coli* per plasmid of interest were grown overnight in 5 mL LB media with appropriate antibiotic at 37°C for 13 hours. Plasmids were further isolated as described in next section.

Plasmid isolation

Plasmids were isolated using QIAprep® Spin Miniprep Kit by Qiagen (www.qiagen.com), following the exact steps in manufacturer's protocol. Level 0 plasmids were verified by sequencing primers (listed in **Table 2.6**) and used further for assembly of Level 2 plasmids.

2.4.2.2 Construction of level 2 modules:

The plasmid products from level 0 were then tagged and assembled into level 2 vectors using required components in a *Bsa*I reaction. Level 2 plasmid pSM101 (pET28b-T7::OmpA-HIS-TEV-Avr2_C53X) was generated by combining with promoter fragment pJP001 (pL0M-PU-T7-LacO-T7), backbone pJK082 (pL1VE-R (pET28b)), N-terminal 6X-His tag pJK120 (pL0M-S-OmpA-His6-TEV) and terminator fragment pJP002 (pL0M-T-T7 terminator). Similarly pSM102 (pET28b-T7::OmpA-HIS-TEV-EpiC1_QxVxG>NxLxA),

pSM103 (pET28b-T7::OmpA-HIS-TEV-EpiC2B_QxVxG>NxLxA) and pSM104 (pET28b-T7::OmpA-HIS-TEV-Cip1ΔTT) were constructed. A 5 µl *BsaI* reaction with following components was used: 20 units/µl *Bsa*I (0.25 µl), NEB Cut Smart Buffer (0.5 µl), 400 units/µl NEB T4 DNA Ligase (0.25 µl), 10 mM ATP (0.5 µl), pL0M (pSM00- plasmid template; 0.25 µl), pJK082 (0.25 µl), pJP001 (0.25 µl), pJK120 (pJK253 for pSM-005/006) (0.25 µl), pJP002 (0.25 µl) and Milli-Q water (2.5 µl). Reaction conditions for *Bsa*I level 2 module (set up in a PCR thermocycler) were: step **1** at 40°C for 10 mins, step **2** at 16°C for 10 mins; pEC15259 (0.25 µl added to pSM005/006) and two cycles from step **1** were repeated. Then step **3** at 50°C for 10 mins was continued, followed by step **4** at 80°C for 20 mins. The reaction was finally on hold at 4°C. *Bsa*I reaction products were individually transformed by heat-shock into *E. coli* DH10ß. Plasmids were isolated as per QIAprep® protocol mentioned above. The eluted plasmids were verified by sequencing using primers for level 2 modules (listed in **Table 2.6**) and transformed into *E.coli* Rossetta strain for use in expression and purification of inhibitors and their mutants.

2.4.3 Affinity chromatography based purification of recombinant proteins

E. coli Rossetta cultures expressing inhibitor (Avr2, EpiC1, EpiC2B or Cip1) or inhibitor mutant of interest were incubated in LB containing 50 µg/Ml kanamycin overnight at 37°C. On the next day, this culture with OD_{600}≈0.6 was diluted at 1:100 in TB media [24 g/L tryptone, 48 g/L yeast extract, 0.4% glycerol and 0.2 M potassium phosphate buffer (173.2 g/L K_2HPO_4 and 26.8 g/L KH_2PO_4), pH 7.6] and incubated at 37°C, 220 rpm for 4 hours until OD_{600}≈0.6. Protein over-expression was then induced overnight by adding 0.8 mM Isopropyl β-D-1-thiogalactopyranosidase (IPTG). Next morning, bacterial culture supernatant containing 6X-histidine tagged protein of interest was centrifuged at 6,000 g for 25 minutes in a 4°C high-speed centrifuge with a JA-14 rotor by Beckman Coulter Life Sciences (www.beckman.com). The supernatant was filtered using a 0.22 µM or 0.5 µM Millipore vacuum filter unit (www.merckmillipore.com). For purification under native conditions, the

filtered supernatant was loaded onto Qiagen Ni-NTA Superflow® agarose resin. Two strengths of imidazole purification buffer [PB0 (50 mM Tris-HCl and 150 mM NaCl, pH 7.6) and PB50 (50 mM Tris-HCl, 150 mM NaCl and 50 mM imidazole, pH 7.6)] were used to purify the protein of interest. The proteins were finally eluted in PB250 (50 mM Tris-HCl, 150 mM NaCl and 250 mM imidazole, pH 7.6), concentrated using 3 kD filters (Amicon® ultra-0.5 mL by Merck) and stored at -80°C.

2.4.4 Protein quantification

Purified proteins were quantified using Qubit™ Protein Assay Kit by Invitrogen™. The concentrated assay reagent was accordingly mixed with provided dilution buffer and added to 2 µl of each purified inhibitor or mutant protein. Diluted BSA samples in kit were used as reference and protein concentrations were estimated using a Qubit® Fluorometer. To also check the purity of proteins, 5 µl of each purified protein was mixed with 4X gel loading buffer (50 mM Tris-HCl pH 6.7, 2% SDS, 10% glycerol, 100 mM DTT and bromophenol blue) and denatured at 95°C for 5 minutes. These samples were then separated on a 15% SDS-PAGE gel at 200 volts for 50 minutes and stained with CBB® G-250. The addition of two methyl groups and a slightly green tint differentiates the colloidal Coomassie dye G-250 from R-250 version. G-250 also has high sensitivity and eliminates the need for elaborate destaining. For staining solution preparation, 50 mg dye is dissolved in 25 mL of 95% ethanol. 50 mL of 85% phosphoric acid is then added while stirring continuously. Once the dye particles dissolve, Mill-Q water is used for dilution up to 500 mL.

2.4.5 Competitive-activity based protein profiling (C-ABPP)

C-ABPP was performed to determine the specificity of each inhibitor and its mutant towards Rcr3. Apoplastic fluid (AF) isolated from *Nicotiana benthamiana* over-expressing Rcr3

(pJK284) was pre-incubated with 4 µM of purified proteins from bacteria containing either pJK153 (Avr2), pJK155 (EpiC1), pJK157 (EpiC2B), pJK159 (Cip1), pSM101 (Avr2 mutant), pSM102 (EpiC1 mutant), pSM103 (Epic2B mutant) or pSM104 (Cip1 mutant) in a 50 µL reaction, containing 3 mM DTT and 50 mM sodium acetate pH 5.5 buffer for 40 minutes. Next, 1 µM labelling probe MV201 diluted in DMSO was added, and the reaction was kept at RT for 3.5 hours (Kourelis *et al.*, 2020). A reaction with no inhibitor protein and another incubated with 1 mM E-64 were used as negative and positive controls respectively. Samples were centrifuged for 10 minutes at maximum speed. The pellets were dissolved in 2X gel-loading buffer, heated at 95°C, and proteins were seperated on 15% SDS-PAGE gel. Amersham™ Typhoon™ scanner (GE Healthcare) at Cy3 settings was used to scan the gel for fluorescence.

2.5 Screening for hypersensitivity cell-death response phenotype

To analyse the geographic pattern and frequency of recognition of Avr2, Epic1, Epic2B and Cip1, I performed an HR assay by infiltrating each inhibitor protein versus its mutant protein generated in this study. Before performing HR assays, leaf cuttings from each individual plant after ~ 3 weeks old stage were maintained for re-screening, to constitute three independent experiments for HR. 2-3 centimetres leaf sections were clonally propagated on soil after treatment with Doff® hormone rooting powder containing 0.43% w/w 1-NAA. Water sprayed autoclave bags were used over the plant trays to create a humid chamber for initial growth of leaf cuttings. Plants were thereafter maintained under growth conditions as mentioned earlier in this chapter.

2.5.1 Infiltration of inhibitors and their mutants

All tomato plants were infiltrated when four-weeks old. All potato, eggplant, pepper, petunia, and tobacco plants were tested after four to five weeks, depending on their growth rate and availability of fully expanded leaves for testing. Eight individual plants from each tomato population, and four plants for each of remaining populations were tested by syringe-infiltrating an inhibitor protein and its mutant in opposite halves on same leaflet. Three leaflets on a same leaf in tomato and three individual leaves representing three independent tests per plant were infiltrated for each inhibitor of interest. Purified Avr2, Cip1 and their mutant proteins were infiltrated at a concentration of 2 µM, whereas Epic1, Epic2B and their mutant proteins were infiltrated at 6 µM.

2.5.2 Scoring of resistance phenotypes

Severity of HR symptoms was monitored from 2 days post infiltration (dpi) to 7 dpi. In cases of no HR symptoms, response phenotype was monitored until 21 dpi. Scoring was done as: (-): numeric score **0**, indicating no damage at infiltration site or no HR symptom at all; (+): numeric score **1**, indicating slight HR in or around the borderline of infiltration site to avoid counting by damage; (++): numeric score **2**, indicating well developed HR in the infiltration site; (+++): numeric score **3**, indicating HR developing outside the infiltration zone and (++++): numeric score **4**, indicating HR strongly often spreading beyond infiltrated zone. A scoring scheme is shown in **Figure 3.3(b)**.

2.5.3 HR phenotype analysis using R

Analysis was done using R-Studio desktop for Windows versions 1.4.1106 and 2023.03.0-386, along with R versions 3.3.0+ and 4.2.3. HR responsive populations were clustered in

multivariate Complex Heatmaps created using circlize (Gu *et al*., 2014), Complexheatmaps (Gu *et al.*, 2022), RColorBrewer (Neuwirth, 2022), and Viridis (Garnier *et al*., 2023) packages. Regional and altitude recognition frequency were analysed using ggplot2 (Wickham, 2016), dplyr, tidyr and forcats (Wickham *et al*., 2023). Finally, mapping of responsive populations along latitude/longitude and elevation points was done using packages: raster (Hijmans *et al*., 2023), sp (Pebesma and Bivand, 2005), maps, mapplots (Gerritsen, 2018), mapdata (R version by Brownrigg, 2022), ggplot2, and RPMG (Lees and Anderson, 2019). The maps were then layered using InkScape 1.2.2 (December 2022). R scripts, and input data files are attached as **Supplementary 3.3 to 3.7**.

2.6 Genotyping by PCR of *Cf* and cysteine protease genes

To investigate a link between HR phenotype and presence/absence or nucleotide variations of the *Cf-2/Rcr3* system, I used a genomic DNA PCR approach. Four individual plants from each of forty responsive vs non-/weakly-responsive populations of *S. pimpinellifolium* across different geographical ranges were selected for genotyping of *Cf-2/Hcr2's*. Similarly, four plants from each of six populations of wild tomato and six populations of wild potato were genotyped. Further, to assess indication on segregation of other *Cf* genes in responsive plants, *Cf-9* and *9DC* (van der Hoorn *et al*., 2001a) were genotyped in a few of these populations. *Act* gene was used as positive control. PCR primers and products are listed in **Table 2.6**. Control and differing representatives from PCR were sequenced with primer detailed in **Table 2.6**.

To uncover any allelic specificities underlying patterns of variation in resistance responses, I sequenced cysteine protease-encoding genes possibly included in inhibitor recognition. A total of 86 sequences were obtained for *Rcr3*, including 38 from *S. pimpinellifolium*, 24 from wild tomato and 24 from wild potato. For *Pip1* and *C14* sequencing, 14 individuals were

sequenced for *S. pimpinellifolium*, ten individuals for wild tomato and ten for wild potato. Primer pairs for PCR and sequencing are listed in **Table 2.6** and illustrated in **Figure 4.8**. Samples were sequenced either at Eurofins or SourceBio.

2.6.1 DNA isolation

Total cellular DNA samples were extracted using Qiagen® DNeasy Plant Mini Kit according to manufacturer's instructions: for each sample, 50 to 70 mg of leaf tissue was ground in liquid nitrogen using sterilised pestle and mortar. The powdered sample was transferred to a 1.5 mL micro-centrifuge tube and mixed with 400 µl buffer AP and 4 µl RNase A. The mixture was vortexed and incubated for 10 minutes at 65°C. 130 µl of buffer P3 was added and the mixture was kept on ice for 5 minutes. The lysate was centrifuged at a high speed for 5 minutes and loaded onto a QIA shredder column placed in a 2 mL collection tube. The columns were centrifuged for 2 minutes, supernatant was collected and pipette mixed with 1.5 volumes of wash buffer AW1 (composition unknown in readymade supply). 650 µl of the resultant mixture was transferred onto a mini spin column and this was centrifuged for 1 minute at 8,000 rpm. The flow through was discarded and column was placed into a new 2 mL tube. 500 µl of buffer AW2 was added to the tube and centrifuged. The spin column was transferred to a new 1.5 mL tube and incubated with 50 to 100 µl nuclease free water for 5 minutes at room temperature. DNA was eluted by spinning this column for 1 minute at 8,000 rpm. DNA samples were then separated on 1% agarose gel in TAE buffer (1 mM EDTA, 40 mM Tris and 20 mM acetic acid, pH 8.2). 0.4 µg/mL ethidium bromide was added to the buffer for DNA detection on gel. Samples were used for genotyping by PCR and stored at -20ºC.

2.6.2 PCR reaction and conditions

All reaction components were assembled on ice, mixed with a quick spin and transferred immediately to a 98°C preheated thermocycler. *Aspartate carbamoyl transferase* (*Act*) gene was used as an endogenous control (Overduin *et al*., 1993). The PCR reaction mixture of 25 µl included 5 µl Q5 reaction buffer (1x), 10 mM dNTPs mix, 10 µM forward primer, 10 µM reverse primer, 1 µl template DNA, 0.25 µl Q5® DNA Polymerase (0.02 U/µl) and nuclease-free water.

The presence of *Homologs of Cladosporium fulvum Resistance 2 (Hcr2's)* (Caicedo and Schaal, 2004) and *Cf-2* was detected by amplifying CDS using primers SM_CF-2/CF5_F and _R (**Table 2.6**). PCR program was as follows: step **1** for initial denaturation at 98°C for 30 secs, step **2** with five cycles at 98°C for 10 secs, 62°C for 25 secs and 72°C for 90 secs. Four cycles from step **2** were then repeated and reaction was proceeded to step **3** with 25 cycles at 98°C for 10 secs, 65°C for 25 secs and 72°C for 90 secs. 24 cycles from step **3** were repeated and final extension was performed at 72°C for 3 mins. The reaction was on hold at 4°C and PCR products were separated on 1% agarose gel at 120 volts for 1.5 hours.

Primers used for amplification of *Cf-9*, *9DC*, *Rcr3*, *Pip1* and *C14* are listed in **Table 2.6**. The PCR reaction conditions for *Rcr3*, *Pip1* and *C14* were as follows: step **1** for initial denaturation at 98°C for 30 secs, followed by step **2** with 25 cycles at 98°C for 10 secs, 60°C to 65°C for 25 secs and 72°C for 60 secs. Then final extension at 72°C for 2 mins was performed, and reaction was on hold at 4°C. PCR products were separated on 1.5% agarose gels at 180 volts for 45 minutes.

2.6.3 PCR purification

Selective PCR products were purified using QIAquick® PCR Purification Kit (Qiagen). All centrifugation steps were carried out at 12,000 g for 1 minute at room temperature. To a PCR reaction, 5 volumes of purification buffer was added, this mixture was loaded onto a QIAquick binding column and centrifuged. 750 µl of wash buffer was added, the tube was centrifuged and the flow through was discarded. To remove residual buffer, the column was centrifuged again. The column was then placed in a 1.5 mL micro-centrifuge tube and PCR product was eluted using 50 µl nuclease free water.

2.6.4 Sanger sequencing and analysis

For sequencing, a 10 µl reaction mix contained ~10 ng/µl purified PCR product and 5 µl of sequencing primer (5 µM). Sanger sequencing was done using pre-paid Mix2seq kits (Eurofins Genomics, Europe) or SourceBio. Sequenced contigs were edited, back translated, and assembled using Geneious^{2} Prime 2023.0 for windows. Sequencing samples were selected to represent statistically significant numbers as well to reflect species diversity across centres of origin, within and among taxonomic complexes defined in this study (**Figure 3.1**).

2.6.5 Bioinformatics to predict selection forces on apoplastic proteases

Sequences were aligned using MUSCLE and Maximum-likelihood 500 (ML500) bootstrap replication trees were constructed in MEGA12 (Kumar *et al*., 2024). To study directional selection pressures within a group and overall, upon specific cysteine protease clade, I used HyPhy (Hypothesis Testing Using Phylogenies; https://hyphy.org/about/) 2.5.33 (Kosakovsky-Pond *et al*., 2020) and results were visualized using interactive network

DataMonkey 2.0 (Weaver *et al*., 2018). dN/dS analysis was used to compute relative abundance of observed non-synonymous to synonymous substitutions by pairwise distance codon matrices for assessment within *S. pimpinellifolium*. Similarly, substitution matrices were generated to evaluate pairwise distances within wild tomato and wild potato. At least four species are required to perform tests of neutrality and predict a selection pressure on gene of interest, so appropriate samples were used as inputs to obtain a statistically significant confidence value and infer comparative selection pressures indicative of evolution of host ranges.

For detecting site-specific selection on *Rcr3*, *Pip1* or *C14* within a group, for example, *S. pimpinellifolium*, wild tomato or wild potato, MEME (Mixed Effects Model of Evolution) (Murrell *et al*., 2012) method of episodic selection and FUBAR (Fast, Unconstrained Bayesian AppRoximation) (Murrell *et al*., 2013) method of pervasive selection were used. In-frame alignment of codons was used as input for specific groups. MEME hypothesise that individual sites are subject to diversifying selection. Using a mixed-effects ML approach, MEME aims to identify sites under positive selection in a few sequences related in any branch. MEME represent output probabilities of selection on each site. FUBAR uses a Bayesian algorithm to predict posterior probabilities (pp) instead of p-values that indicate selection pressure (pp ≥0.9 suggest strong positive selection on a site). When site-specific signatures of positive selection are relatively weak, then FUBAR offers a powerful approach. Assumption of constant pressure of selection on each site, FUBAR like MEME infers dN/dS substitution rates on each site.

Next, codon alignments from all groups were combined for each gene. For example, *Rcr3* sequences generated from *S. pimpinellifolium*, wild tomato and wild potato were then combined to estimate the overall type of natural selection acting on *Rcr3*. I used a Fixed-Effects Likelihood (FEL) (Kosakovsky-Pond *et al*., 2005) approach that employs ML to compute dN/dS per site in a gene. FEL is more time consuming than FUBAR and assumes

the selection forces are constant throughout a phylogeny range. Further, to correlate the output of FEL and specific FUBAR tests, I used BUSTED (Branch-site Unrestricted Statistical Test for Episodic Diversification) (Murrell *et al*., 2015) to identify gene-wide selection. Episode of positive selection on even a single branch across phylogeny can be revealed by BUSTED. Compared to MEME, FEL and FUBAR, BUSTED generate Evidence Ratios (ER) that represent log-likelihood values of positive selection on a branch. ERs are rather descriptive than statistically significant estimates such as MEME, FEL and FUBAR.

Heatmap visualisation to understand the distribution pattern of each inhibitor recognition, and binary datasets for presence of *Cf-2*, *Cf-9* or *9DC* and alignment sections of *Rcr3*, *Pip1* and *C14* variation were generated using different dataset features in iTOL v6 (https://itol.embl.de/). Sequences from this study and iTOL trees are attached as supplementary files for Chapter 4.

2.7 Virus-induced gene silencing (VIGS) in wild *Solanum* species

VIGS was used to assess role of candidate genes for their potential to confer resistance against each of the four inhibitors. Based on sequence similarity, four clans were defined for *Hcr2*'s on a *Cf-2/Hcr2* in tomato/potato ML500 generated tree in this study (**Figure 5.1**). Genes were silenced of clan 1(*Cf-2)*, clan 2 (*Cf5-like homologs*), clan 3 (*Full-length Hcr2s*), and clan 4 (containing truncated sequences lacking a transmembrane domain or a signal peptide). Apoplastic proteases *Rcr3*, *Pip1* and *C14* were also silenced. For VIGS, I selected *S. pimpinellifolium* populations that were (a) responsive to Avr2 only (b) responsive to all inhibitors Avr2, EpiC1, EpiC2B and Cip1, and diploid potato accessions that were (a) responsive to EpiC2B and at least one more inhibitor, and (b) responsive strongly to EpiC2B only. I further silenced tomato Receptor-like kinase (RLK) *SOBIR1*, to investigate

downstream signalling effects in one responsive population of *S. pimpinellifolium* and *S. bulbocastanum.*

2.7.1 Design and golden-gate based construction of TRV2 plasmids

Silencing constructs were designed to share sufficient identity to expect silencing in tomato and potato. All VIGS fragments are listed in **Supplementary 5.1**. Alignment of *Cf/Hcr2* VIGS fragments to expected clan and cross targets in tomato and alignment to potential targets in potato are shown in **Supplementary 5.2**. Silencing potential of cysteine protease and Receptor-like Kinase-*SOBIR1* VIGS fragments in tomato and potato are shown as alignment to targets in **Supplementary 5.3 and 5.4**, respectively. *Tobacco Rattle Virus (TRV*) bipartite genome is split into TRV1 and TRV2 RNA molecules. TRV2 is modified to carry a silencing fragment of host gene of interest. After introduction into the plant using *Agrobacterium*-mediated transformation, TRV2 replicates to produce double-stranded RNA, which further gets processed by plant's RNA silencing machinery into small-interfering RNAs (siRNAs). RNA-induced silencing complex then degrades the mRNA of endogenous gene of interest in plant and silencing is achieved (Liu et al., 2002). Fragments were assembled into a domesticated TRV2-based vector pJK037 (pL1V2-TRV2) (Kourelis *et al*., 2020) using an *Eco*RI*/Bam*HI restriction golden gate cloning. pTRV2 vector originally described by Liu *et al*., 2002a was the template for partial domestication of pJK037. Target regions were designed using Sol Genomics Network (SGN)-VIGS tool algorithm (Fernandez-Pozo *et al*., 2015) and suggested 300 bp fragments with minimum off-targets were selected for cloning. All vectors constructed or sourced are detailed in **Table 2.7 and 2.8**. Silencing fragment were ordered as 300 bp GeneArt™ Strings™ DNA fragments (Thermo Fisher Scientific, UK), except that *Cf-2*-clan1 VIGS fragment was amplified using primers listed in **Table 2.6** from plasmid (*Cf-2::eGFP*, kindly provided by Matthieu Joosten).

A one-pot ligation reaction for all VIGS constructs was used for final assembly into the level 2 plasmid. A 5 µl reaction with following components was set up: NEB cut smart buffer (0.5 µl), *Eco*RI (0.25 µl), *Bam*HI (0.25 µl), pJK037 (0.25 µl; backbone for pL2-TRV2), gene string fragment or PCR product (0.5 µl) and Milli-Q water. The reaction in a PCR thermocycler was incubated at 37°C for 1 hour, followed by 80°C for 20 mins. The reaction mix was stored at 4°C or proceed to next step, where 10 mM ATP and 0.25 µl of T4 DNA ligase were added. The reaction mixture was incubated at 16°C for 1 hour. Each resultant vector was further transformed into *E. coli* DH10ß followed by plasmid isolation. Sequenced plasmids were transformed by heat shock into Agrobacterium strain GV3101.

2.7.2 Agroinfiltration for VIGS

The VIGS assay was performed as described previously by (Liu *et al*., 2002b; Senthil-Kumar and Kiran-Kumar, 2011). Agrobacterium GV3101 carrying pTRV2 derivatives of interest and pTRV1 (Liu *et al.*, 2002) were cultured overnight at 28°C with appropriate antibiotics. Overnight grown cells were harvested and re-suspended in 50 mM MES infiltration buffer with 200 µM acetosyringone to OD_{600}≈1, pH 5.6. Bacteria were incubated at 28°C, 220 rpm for approximately 2 hours. Each pTRV2 culture was mixed with pTRV1 in 1:1 ratio and OD_{600} was adjusted to 0.5 using infiltration buffer. These bacterial mixtures were then syringe-infiltrated into leaves.

For VIGS in tomato, six to eight days-old plantlet propagates from specific mother plant were used. Cuttings are not truly young plants, however after observation of high polymorphism in resistance, it was essential that I choose to study clonal individuals of tomato. In addition, published studies have shown unsuccessful attempts of silencing in cultivated potato species grown from leaves or tubers. However wild species *S. bulbocastanum* was shown to display good silencing efficiency in plants grown from seeds

or tubers (Brigneti *et al*., 2004). Since variation in response among individuals of same potato population were rare in this study, I used seed grown potatoes for VIGS. Potato plants were silenced when 15 to 20 days old (four-leaves stage), depending upon germination. TRV carrying a fragment of tomato *Phytoene Desaturase* (PDS; accession Sopim03g123760) gene was used as a positive control to observe silencing. pTRV2-*GFP* was used as a negative control while *N. benthamiana* was used as a positive control to test efficiency of tomato *PDS* construct (~88% nucleotide similarity). Six individual plants in three sets of experiments were infiltrated for each construct and plants were monitored for pTRV2-related HR until seven days after infiltration of TRV vectors. *Solanum* species have been reported to take three-weeks or longer before full silencing is established, hence for HR assay on silenced plants, inhibitors were infiltrated four-weeks after silencing. HR assays were carried out as described previously in section 2.5 of this chapter.

2.7.3 RNA isolation

Leaf samples were harvested 4-weeks after silencing and before inhibitor infiltration. Total RNA samples were extracted from 50 mg leaf as per instructions of Qiagen RNEasy Kit. Optical density for sample concentration at A_{260}/A_{280} was measured in a Nanodrop spectrophotometer (Thermo Fisher Scientific).

2.7.4 Quantitative PCR (qPCR)

To assess the extent of gene silencing, I designed a SYBR® Green-ROX based one-step QPCR assay using total RNA as template for a high-throughput sensitive and less expensive analysis. Three biological replicates of each silenced construct were included in this experiment and reactions were set up with three technical replicates. Power SYBR® Green 1-step Kit was purchased from Applied Biosystems™. Negative reaction Control with

wells containing water instead of RNA template was used to check for specific amplification of the targets. Tomato *actin* (*act*) was used as an endogenous control, to normalise relative transcript abundance of target genes to be quantified. *TRV::GFP*-infiltrated plants were used as reference controls. The tubes containing components were placed on ice and after the reagents were thawed, they were gently mixed before assembling the PCR master mix. *Act* is generally one of the most stable housekeeping reference gene in tomato varieties such as Money maker under biotic stress, therefore, a single housekeeping control was considered appropriate (Bai et al., 2022).

A 20 µl reaction for qPCR consisted 10µl of 2x Power SYBR® Green RT-PCR mix, 150 nM of forward and reverse primers, 0.16 µl of 125x RT enzyme mix, 60 to 100 ng RNA template and RNase-free water. The reactions were pipetted in MicroAmp™ Fast Optical 96-Well reaction plate (Lot: 4346906) and sealed using Applied Biosystems™ MicroAmp™ optical adhesive film (Lot: 4311971). The reaction plate was centrifuged at 12,000 g for 60 seconds and loaded onto Applied Biosystems StepOne™ Real-Time PCR System (Lot: 4376374).

Singleplex PCR run was designed using Advanced Setup and an experiment file was created with labelling of each well. The experiment was set up using thermal-cycling conditions (Ramp Speed: Standard) with following steps; reverse transcription stage hold at 48°C for 30 mins, activation of AmpliTaq Gold® DNA polymerase (ultra-pure) stage hold at 95°C for 10 mins, 40 cycles to denature at 95°C for 15 secs and anneal/extend at 60°C for 1 min. After RT-PCR, a dissociation curve run was performed to detect non-specific amplification using melting curve conditions of denaturing at 95°C for 15 secs, annealing at 60°C for 15 secs. This was followed by denaturing at 95°C for 15 secs. Derived Ct_{mean} values were used for ΔΔCt or relative quantification analysis using Graphpad Prism 9 software.

2.8 Bioinformatics analysis of diversity and evolution of Cf-like proteins beyond phylogenetic boundaries

For *in-silico* analysis, I scanned a total of 116 completed and draft genomes belonging to kingdom Viridiplantae or green plants. Cf-2.2 protein sequence (NCBI accession AAX19020) was used as a query for Hidden Markov Model prediction/analysis using HMMER v3.3.2 (http://hmmer.org/). I performed a phmmerscan to search homolog protein sequences against up to release no. 54 of *Ensembl*Plants having cut off values 10^{-2}, hit 0.03, customised visualization with secondary or known IDs and hit positions, gap penalties open=0.02 and extend=0.4. Release 54 was updated by July 2022 and had newly added assemblies from various crop cultivars, hence, shows more appropriately annotated sequences that may not be included in archive releases. *Ensembl*Plants Release no. 56 is available since February 2023, (https://plants.ensembl.org/index.html). However, this study has not missed any new Solanaceae annotations that were covered in retrieval from Sol Genomics Database until January 2025.

To allow moderate inclusion of more distantly related organisms with sequences closely related to query Cf-2.2, a substitution scoring matrix was developed using BLOSUM62. I used a threshold of 10^{-2} to screen for enriched sequences from the resulting proteins that had homology with any LRR-domains of Cf-2. I then filtered high-quality sequences that were discovered to be limited to Solanales. Additional selection and enrichment revealed that only the Solanaceae family consisted of annotated and non-annotated proteins. There are not many representative wild genomes of Solanaceae or other assemblies of cultivated tomato accessions in *Ensembl*Plants. Therefore, I downloaded Sol Genomics Network FTP genome or protein annotations (https://solgenomics.net/genomes/sequenced_accessions) and performed a blast with 10^{-4}e using Cf-2.2 protein and corresponding gene sequence. Further, NCBI protein search using representative sequences from HMM profiling was used

as a query to blast with 10^{-4}e so to included sequences that were missed in HMMER scan. This comprehensive list of 1456 sequences now included all annotated and non-annotated Cf-like RLPs retrieved from cultivated and wild representative genomes and were still restricted to Solanaceae.

The search also included well-annotated RLPs known to share close homology to Cf-2, namely Cf-9/-homologs (Hcr9's), Ve- and EIX-homologs. These proteins were selected to represent outgroup clusters in our pipeline. However, no additional search using Cf-9, Hcr9's, Ve and EIX proteins were performed as described with Cf-2.2. Duplicated sequences were then removed and a total of 970 sequences were retained. I then predicted the structural architecture of each of these non-redundant sequences searching Pfam v35.0, Phobius and SignalP via HMMscan interface. Proteins with tyrosine-kinase, kinase domains, UbiA prenyltransferase family signatures or only unusual domains such as Malectin-like and thaumatin domain containing proteins (searched vis IUPred) were further removed. Finally, a set of 491 unique homologous sequences were used for MUSCLE alignment and a ML500 phylogeny reconstruction using MEGA12. Phylogenetic tree was further detailed using iTol v6. A pipeline with extraction of sequences at each step has been detailed in **Figure 5.10**. Protein sequences retrieved, annotations, and iTOL tree in newick format are attached as **Supplementary 5.5**. HMMER-based pipelines have previously been used for genome-wide evolutionary analysis of NLR genes in Solanaceae (Seo et al., 2016).

2.9 Appendix: transient expression analysis in *N. benthamiana*

2.9.1 Binary plasmid construction of *Rcr3* sequences from different species

The appendix 2.9 section describe methods already published in Kourelis *et al*., 2020. With an aim to link natural variation at the *Rcr3* locus in Solanaceae to functional diversity against

C. fulvum (Avr2), fifteen variant *Rcr3* sequences from multiple species were cloned by using *EcoRI* and *BamHI* based Golden Gate cloning (Kourelis *et al.*, 2020). Background of reference expression vectors used are listed in **Table 2.8**.

2.9.2 Over-expression of different *Rcr3* in *N. benthamiana* leaves

A. tumefaciens strain GV3101 carrying various binary plasmids (Kourelis *et al*., 2020) were cultured in LB containing 25 µg/mL rifampicin, 50 µg/mL kanamycin and 50 µg/mL gentamicin. Overnight grown *A. tumefaciens* cells were harvested by centrifugation at 2500 *g* for 10 minutes at 20°C and re-suspended in 10 mL of infiltration buffer (10 mM MES, 10 mM $MgCl_2$, pH 5.6), and 100 µM acetosyringone. OD_{600} was adjusted to 1 using infiltration buffer. The re-suspended cell mixtures were incubated at 28°C for 2 hours and infiltrated into leaves of five-week-old *N. benthamiana.* Three leaves of each plant were infiltrated with specific vector for over-expression of individual protein. Plants were maintained in controlled growth chambers. Fresh leaves were dried using tissue towels and apoplastic fluids (AFs) were isolated 4 dpi by using ice-cold water and vacuum in an exicator centrifuged at 3,500 g for 10 minutes at 4°C. Isolated AFs were collected in tubes and used for reactions or stored at -80 °C (Joosten, 2012).

2.9.3 Competitive-activity based protein profiling (C-ABPP)

C-ABPP assays were performed to determine each variant's active state and ability to interact with Avr2 and Avr2 mutant. AFs were labeled for 3.5 hours in a 50 µL reaction using 1 µM fluorescent DCG-04 (MV201) (Richau et al., 2012) diluted in DMSO with 3 mM DTT and 50 mM sodium acetate labeling buffer (pH 5.5). Competitive-ABPP assays were performed by pre-incubating AFs with 3 µM affinity purified Avr2 (or its inactive mutant) in labelling buffer and DTT, followed by labelling for 3.5 hours. The samples were precipitated

using 5 volumes of ice-cold 100% acetone, centrifuged for 15 minutes at 4°C, maximum speed. Pellets were air dried and dissolved in 30 µL 2X Gel Loading Buffer (GLB). The samples were heated at 95°C and proteins were separated on 15% SDS-PAGE gels. Fluorescently labelled proteins were imaged using an Amersham™ Typhoon™ scanner (GE Healthcare) at Cy3 settings. A negative control without inhibitor and a positive control with 100 mM E-64 were included in inhibition assay.

2.9.4 Western blotting

1X GLB was added to AF samples, and these were heated at 95°C for 5 minutes. The samples were separated on a 15% SDS-PAGE gel, run at 180 Volts for 90 minutes. Proteins were transferred to a 0.2 µM nitrocellulose membrane (GE Healthcare) using a trans-blot system (Bio-Rad). The membrane was blocked with skimmed milk (5% in 1X Tris-Buffered Saline 0.1 Tween®20/TBST) overnight at 4°C and incubated with primary antibody, αRcr3 (Paulus *et al*., 2020) 1:5000 of antibody in 5% skimmed milk in 1X TBST for 90 minutes at room temperature (RT). 1X TBST was used to wash the membrane three times for ten minutes each. The membrane was incubated for 90 minutes at room temperature with HRP conjugated secondary anti-rabbit (A069, Sigma-Aldrich UK) (1:10000 in 5% skim milk in 1X TBST). used 1X TBST to wash the membrane three times for ten minutes each. The blots were developed using Clarity™ Western ECL Substrate (Bio-Rad), and the ImageQuant™ LAS 4000 (GE Healthcare) was used to detect the chemiluminescence.

2.9.5 Transient hypersensitivity cell-death response assays

Transient co-expression HR assays were performed to assess each Rcr3 protease variant's capability to trigger a defence response against Avr2. *A. tumefaciens* strain GV3101 containing binary expression vector for *Rcr3, Cf-2 or Avr2*, were grown overnight in LB

culture containing 25 µg/mL rifampicin, 50 µg/mL kanamycin and 50 µg/mL gentamicin at 28°C, 220 rpm. Bacterial cultures with OD_{600} ≈ 0.5 were then mixed in combinations (for example, *Cf-2, Avr2, and Rcr3pim or Avr2* and centrifuged at 2500 g for 10 mins at 20°C. The pellets were re-suspended in 5 mL of 10 mM MES and 10 mM $MgCl_2$ infiltration buffer pH 5.6. Using infiltration buffer OD_{600} was adjusted to 0.5 and samples were incubated at 28°C, for 2 hours. The desired combination of constructs was infiltrated in 5-week-old *N. benthamiana* plants. HR was observed from 1 to 7dpi using criteria mentioned previously in this chapter.

*Data availability

All data files in this study are submitted as supplementary and can be retrieved via Oxford University Archives (OUA) Network after release online at https://ora.ox.ac.uk/. Illustrations in this thesis were created using BioRender (https://biorender.com/) and Inkscape (https://inkscape.org/). Alternatively, all data files can be available upon request to thesis supervisor at renier.vanderhoorn@biology.ox.ac.uk.

***Ethics statement:** rare, protected or endangered species used in this study are from propagated seed collections of donors.
Samples were legally obtained under appropriate agreements. Nagoya Protocol legislations were not applicable at the time of procurement from the USA, the Netherlands and within the UK.
Imported samples were custom cleared with requirements of Phytosanitary certifications.
For screening, seeds were grown and maintained under greenhouse environment as instructed.

Table 2.1 *Solanum pimpinellifolium* populations (TGRC, Davis)

Population	Region	Zone	Microclimate	Location	Latitude	Longitude	Asl metres	Country	Mating	Any source note
LA1547	A	Ecuador	Mediterranean climate	Carchi	0.58333	-77.93333	3000	Ecuador	Autogamous-SC	Resistance to *Cladosporium fulvum*
LA2093	A	Ecuador	Hot Desert	El Oro	-3.62806	-79.88806	300	Ecuador	Autogamous-SC	
LA2857	A	Ecuador	Subtropical variations	Galapagos Is	-0.95	-90.96667	5	Ecuador	Autogamous-SC	
LA3123	A	Ecuador	Subtropical variations	Galapagos Is	-0.61667	-90.38333	600	Ecuador	Autogamous-SC	
LA0413	A	Ecuador	Humid Tropical Climate	Guayas	-2.33333	-80.26667	80	Ecuador	Autogamous-SC	
LA0417	A	Ecuador	Humid Tropical Climate	Guayas	-2.73333	-79.91667	30	Ecuador	Autogamous-SC	
LA0420	A	Ecuador	Humid Tropical Climate	Guayas	-1.06	-79.65	100	Ecuador	Autogamous-SC	
LA2097	A	Ecuador	Warm temperate	Loja	-4.39389	-79.91806	400	Ecuador	Autogamous-SC	
LA2102	A	Ecuador	Warm temperate	Loja	-4.40167	-79.4675	1000	Ecuador	Autogamous-SC	
LA2112	A	Ecuador	Warm temperate	Loja	-3.95	-79.43333	1800	Ecuador	Autogamous-SC	Suggests drought resistance
LA0412	A	Ecuador	Humid Tropical Climate	Los Rios	-1.1	-79.48333	250	Ecuador	Autogamous-SC	Homozygous for all tested isozyme markers (00L2653)
LA1428	A	Ecuador	Humid Tropical Climate	Manabi	-0.81667	-80.21667	98	Ecuador	Autogamous-SC	
LA1429	A	Ecuador	Humid Tropical Climate	Manabi	-0.81667	-80.21667	98	Ecuador	Autogamous-SC	
LA2853	A	Ecuador	Humid Tropical Climate	Manabi	-1.05	-80.45	66	Ecuador	Autogamous-SC	
LA2854	A	Ecuador	Humid Tropical Climate	Manabi	-1.35	-80.58333	80	Ecuador	Autogamous-SC	
LA2933	A	Ecuador	Humid Tropical Climate	Manabi	-1.44167	-80.5625	375	Ecuador	Autogamous-SC	
LA1263	A	Ecuador	Mediterranean climate	Pichincha	-2.06667	-79.81667	50	Ecuador	Autogamous-SC	
LA1382	B	North	Amazon Tropical lowland	Amazonas	-6.23169	-77.86903	1883	Peru	Facultative-SC	
LA2186	B	North	Amazon Tropical lowland	Amazonas	5.89167	-78.16667	550	Peru	Autogamous-SC	
LA2187	B	North	Amazon Tropical lowland	Amazonas	-5.925	-78.05	650	Peru	Autogamous-SC	
LA2188	B	North	Amazon Tropical lowland	Amazonas	-5.98333	-78.18333	700	Peru	Autogamous-SC	
LA0391	B	North	Andean Mountain Range	Cajamarca	-7.24417	-78.68167	1200	Peru	Autogamous-SC	
LA0398	B	North	Andean Mountain Range	Cajamarca	-6.58139	-79.23611	1000	Peru	Autogamous-SC	
LA2147	B	North	Andean Mountain Range	Cajamarca	-7.2	-78.98333	550	Peru	Autogamous-SC	
LA2149	B	North	Andean Mountain Range	Cajamarca	-7.21806	-78.78778	850	Peru	Autogamous-SC	
LA2181	B	North	Andean Mountain Range	Cajamarca	-5.77583	-78.78306	850	Peru	Autogamous-SC	
LA2547	B	North	Andean Mountain Range	Cajamarca	-7.18333	-79.01667	550	Peru	Autogamous-SC	
LA2549	B	North	Andean Mountain Range	Cajamarca	-7.21639	-78.78694	870	Peru	Autogamous-SC	

LA0114	B	North	North Coast	La Libertad	-7.4	-79.56667	30	Peru	Facultative-SC	
LA0121	B	North	North Coast	La Libertad	-8.18444	-78.99556	80	Peru	Autogamous-SC	Resistance to potato cyst nematode (*Globodera rostochiensis*)
LA0122	B	North	North Coast	La Libertad	-8.01	-78.72	200	Peru	Autogamous-SC	
LA0381	B	North	North Coast	La Libertad	-7.2	-79.05	300	Peru	Autogamous-SC	
LA0722	B	North	North Coast	La Libertad	-8.11667	-79.03333	350	Peru	Autogamous-SC	
LA1344	B	North	North Coast	La Libertad	-8.08611	-78.88806	400	Peru	Autogamous-SC	
LA1348	B	North	North Coast	La Libertad	-7.45	-79.5	55	Peru	Facultative-SC	
LA1577	B	North	North Coast	La Libertad	-7.81	-79.18	55	Peru	Facultative outcrosser	Reclassified as FO
LA1578	B	North	North Coast	La Libertad	-7.33333	-79.58333	55	Peru	Facultative-SC	probably relatively inbred
LA1589	B	North	North Coast	La Libertad	-8.39	-78.74	51	Peru	Autogamous-SC	
LA1591	B	North	North Coast	La Libertad	-7.71667	-79.11667	45	Peru	Facultative-SC	
LA1592	B	North	North Coast	La Libertad	-8.17083	-79.00417	15	Peru	Facultative-SC	
LA1631	B	North	North Coast	La Libertad	-8.16667	-79	50	Peru	Autogamous-SC	
LA2974	B	North	North Coast	La Libertad	-8.13333	-78.99444	30	Peru	Autogamous-SC	
LA1470	B	North	Hot Coastal Desert	Lambayeque	-6.06667	-79.73333	252	Peru	Autogamous-SC	
LA1471	B	North	Hot Coastal Desert	Lambayeque	-6.31667	-79.75	80	Peru	Facultative-SC	
LA1584	B	North	Hot Coastal Desert	Lambayeque	-6.37	-79.79	70	Peru	Facultative-SC	
LA2534	B	North	Hot Coastal Desert	Lambayeque	-6.725	-79.75	30	Peru	Autogamous-SC	Mixed collection *S. habrochaites*
LA2535	B	North	Hot Coastal Desert	Lambayeque	-6.74167	-79.64167	50	Peru	Facultative-SC	
LA2536	B	North	Hot Coastal Desert	Lambayeque	-6.74167	-79.59167	50	Peru	Facultative-SC	
LA1617	B	North	North Coast	Tumbes	-3.56667	-80.46667	57	Peru	Facultative-SC	
LA1618	B	North	North Coast	Tumbes	-3.56667	-80.46667	57	Peru	Autogamous-SC	
LA2656	B	North	North Coast	Tumbes	-3.8	-80.7	70	Peru	Facultative-SC	
LA0400	B	North	Semi-arid Desert	Piura	-5.26083	-79.96417	800	Peru	Facultative-SC	
LA1478	B	North	Semi-arid Desert	Piura	-5.21667	-80.08333	100	Peru	Facultative-SC	Resistant to powdery mildew (*Leveillula taurica*)
LA1683	B	North	Semi-arid Desert	Piura	-4.87	-81.11	10	Peru	Facultative-SC	Resistance to *Cladosporium fulvum*
LA1688	B	North	Semi-arid Desert	Piura	-4.88333	-80.375	50	Peru	Facultative-SC	
LA1690	B	North	Semi-arid Desert	Piura	-5.17639	-80.6175	36	Peru	Facultative-SC	
LA0373	C	Centre	Centre coast	Ancash	-9.93694	-78.21833	60	Peru	Autogamous-SC	
LA0375	C	Centre	Centre coast	Ancash	-9.94	-78.21	100	Peru	Autogamous-SC	
LA0442	C	Centre	Centre coast	Ancash	-9.48167	-78.25917	100	Peru	Facultative-SC	
LA1342	C	Centre	Centre coast	Ancash	-9.46028	-78.32944	25	Peru	Autogamous-SC	
LA1597	C	Centre	Centre coast	Ancash	-9.47	-78.34	200	Peru	Autogamous-SC	
LA1598	C	Centre	Centre coast	Ancash	-9.93	-78.19	75	Peru	Autogamous-SC	
LA1599	C	Centre	Centre coast	Ancash	-10.06722	-78.12639	30	Peru	Autogamous-SC	
LA1659	C	Centre	Centre coast	Ancash	-9.54667	-77.85861	1350	Peru	Autogamous-SC	
LA1660	C	Centre	Centre coast	Ancash	-9.53333	-77.96667	1000	Peru	Facultative-SC	
LA2401	C	Centre	Centre coast	Ancash	-9.50833	-78.22778	100	Peru	Autogamous-SC	
LA2576	C	Centre	Centre coast	Ancash	-9.55	-77.89167	1450	Peru	Autogamous-SC	
LA2578	C	Centre	Centre coast	Ancash	-9.525	-77.925	980	Peru	Autogamous-SC	
LA0100	C	Centre	Centre coast	Lima	-11.95	-76.71667	300	Peru	Autogamous-SC	
LA0369	C	Centre	Centre coast	Lima	-11.95	-76.71667	300	Peru	Autogamous-SC	
LA0753	C	Centre	Centre coast	Lima	-12.25	-76.89583	20	Peru	Autogamous-SC	
LA1269	C	Centre	Centre coast	Lima	-11.475	-77.10833	400	Peru	Autogamous-SC	Reported to be resistant to late blight and bacterial wilt
LA1279	C	Centre	Centre coast	Lima	-12.13333	-76.81667	200	Peru	Autogamous-SC	
LA1280	C	Centre	Centre coast	Lima	-12.03333	-76.71667	600	Peru	Autogamous-SC	
LA1370	C	Centre	Centre coast	Lima	-11.86722	-76.64472	1430	Peru	Autogamous-SC	
LA1514	C	Centre	Centre coast	Lima	-11.04528	-77.11889	800	Peru	Autogamous-SC	Mixed collection *S. pennellii*
LA1520	C	Centre	Centre coast	Lima	-11.04528	-77.11889	800	Peru	Autogamous-SC	
LA1521	C	Centre	Centre coast	Lima	-12.76472	-76.50528	150	Peru	Autogamous-SC	
LA1561	C	Centre	Centre coast	Lima	-11.1	-77.41667	252	Peru	Autogamous-SC	
LA1572	C	Centre	Centre coast	Lima	-11.96667	-76.78333	200	Peru	Autogamous-SC	
LA1602	C	Centre	Centre coast	Lima	-11.78333	-76.98333	470	Peru	Autogamous-SC	
LA1611	C	Centre	Centre coast	Lima	-12.6	-76.61667	80	Peru	Autogamous-SC	
LA1614	C	Centre	Centre coast	Lima	-11.11667	-77.36667	450	Peru	Autogamous-SC	
LA1629	C	Centre	Centre coast	Lima	-12.11667	-77.03333	sea level	Peru	Autogamous-SC	
LA1651	C	Centre	Centre coast	Lima	-12.08528	-76.94611	240	Peru	Autogamous-SC	
LA1661	C	Centre	Centre coast	Lima	-12.76667	-76.5	200	Peru	Autogamous-SC	
LA1992	C	Centre	Centre coast	Lima	-12.06667	-76.75	500	Peru	Autogamous-SC	
LA2533	C	Centre	Centre coast	Lima	-11.3	-77.36	400	Peru	Autogamous-SC	Resistant to *Phytophthora infestans*, races 0 and 1
LA2718	C	Centre	Centre coast	Lima	-12.47556	-76.70528	100	Peru	Autogamous-SC	
LA2914A	C	Centre	Centre coast	Lima	-12.13333	-77.01667	150	Peru	Autogamous-SC	
LA2934	C	Centre	Centre coast	Lima	-11.85444	-77.0375	250	Peru	Autogamous-SC	Resistant to *Pseudomonas syringae*
LA2966	C	Centre	Centre coast	Lima	-12.08333	-76.95	250	Peru	Autogamous-SC	
LA2982	C	Centre	Centre coast	Lima	-12.53194	-76.76278	5	Peru	Autogamous-SC	
LA2983	C	Centre	Centre coast	Lima	-12.53194	-76.76278	5	Peru	Autogamous-SC	
LA4138	C	Centre	Centre coast	Lima	-12.09667	-76.95139	36	Peru	Autogamous-SC	
LA1301	D	South	South coast	Ica	-13.73333	-75.91667	800	Peru	Autogamous-SC	
LA1332	D	South	South coast	Ica	-14.83333	-74.95	700	Peru	Autogamous-SC	
LA1374	D	South	South coast	Ica	-14.68333	-75.15833	300	Peru	Autogamous-SC	
LA1606	D	South	South coast	Ica	-13.46667	-76.2	10	Peru	Facultative-SC	
LA1630	D	South	South coast	Ica	-13.5	-76.18333	sea level	Peru	Autogamous-SC	
LA1634	D	South	South coast	Ica	-14.63333	-75.06667	700	Peru	Autogamous-SC	
LA1635	D	South	South coast	Ica	-14.63333	-75.06667	700	Peru	Autogamous-SC	
LA1637	D	South	South coast	Ica	-13.36667	-75.83333	700	Peru	Autogamous-SC	
LA1679	D	South	South coast	Ica	-13.46667	-76.18333	270	Peru	Autogamous-SC	
LA1729	D	South	South coast	Ica	-13.29694	-75.64056	1200	Peru	Autogamous-SC	
LA1925	D	South	South coast	Ica	-14.83778	-74.94556	550	Peru	Autogamous-SC	
LA2831	D	South	South coast	Ica	-14.83333	-74.98333	500	Peru	Autogamous-SC	
LA2836	D	South	South coast	Ica	-14.78333	-74.85	1100	Peru	Autogamous-SC	
LA1335	D	South	Coastal Desert	Arequipa	-16.4	-73.22083	50	Peru	Autogamous-SC	
LA1933	D	South	Coastal Desert	Arequipa	-15.45639	-74.44583	140	Peru	Autogamous-SC	
LA1950	D	South	Coastal Desert	Arequipa	-16.38861	-73.25806	20	Peru	Autogamous-SC	
LA2628	D	South	Subtropical highland	Cusco	-12.735	-72.616	950	Peru	Autogamous-SC	

Table 2.2 Wild tomato populations (TGRC, Davis)

Population	Region	Zone	Microclimate	Location	Latitude	Longitude	Asl metres	Country	Species	Mating	Any source note
LA2788	A	Ecuador	Andes Mountains	Antioquia	5.57944	-75.77861	1900	Colombia	*S. juglandifolium*	Allogamous-SI	
LA1041	A	Ecuador	Subtropical variations	Galapagos Isl	-0.66944	-90.26528	230	Ecuador	*S. cheesmaniae*	Autogamous-SC	
LA1043	A	Ecuador	Subtropical variations	Galapagos Isl	-0.88694	-91.00444	60	Ecuador	*S. cheesmaniae*	Autogamous-SC	
LA1404	A	Ecuador	Subtropical variations	Galapagos Isl	-0.36667	-91.61667	300	Ecuador	*S. cheesmaniae*	Autogamous-SC	
LA0438	A	Ecuador	Subtropical variations	Galapagos Isl	-0.9775	-91.02111	30	Ecuador	*S. galapagense*	Autogamous-SC	
LA0528	A	Ecuador	Subtropical variations	Galapagos Isl	-0.75	-90.31667	31	Ecuador	*S. galapagense*	Autogamous-SC	LA0528 seed lots split into 2 accessions (see LA0528B)
LA0532	A	Ecuador	Subtropical variations	Galapagos Isl	-0.6	-90.68333	5	Ecuador	*S. galapagense*	Autogamous-SC	
LA1508	A	Ecuador	Subtropical variations	Galapagos Isl	-1.21611	-90.42306	5	Ecuador	*S. galapagense*	Autogamous-SC	
LA2113	A	Ecuador	Warm temperate	Loja	-4	-79.29	1300	Ecuador	*S. neorickii*	Autogamous-SC	

LA2120	A	Ecuador		Zamora-Ch.	-3.96667	-79.05	2000	Ecuador	*S. juglandifolium*	Allogamous-SI	
LA3322	A	Ecuador	Mediterranean climate	Pichincha	-0.27972	-78.69722	2706	Ecuador	*S. juglandifolium*	Allogamous-SI	
1180J	A	Ecuador			-1.831239	-78.183403	1117	Ecuador	*S. quitoense*		Chiltern Seeds UK variety
1180M	A	Ecuador			-34.603722	-58.381592	29	S. America	*S. sisymbriifolium*		Chiltern Seeds UK variety
LA2202	B	North	Amazon Tropical lowland	Amazonas	-6.11583	-77.8975	1500	Peru	*S. neorickii*	Autogamous-SC	
LA2157	B	North	Andean Mountain Range	Cajamarca	-6.50583	-78.80889	1600	Peru	*S. arcanum*	Facultative-SC	Resistant to *Meloidogyne spp* (heat stable), *Clavibacter michiganensis* , and *Alternaria solani*
LA2172	B	North	Andean Mountain Range	Cajamarca	-6.01667	-78.93333	750	Peru	*S. arcanum*	Allogamous-SI	Resistant to *Oidium neolycopersici* and *Meloidogyne spp.*
LA1353	B	North	Andean Mountain Range	Cajamarca	-7.36667	-78.8	2650	Peru	*S. habrochaites*	Allogamous-SI	Resistant to late blight
LA2160	B	North	Andean Mountain Range	Cajamarca	-6.4	-78.85	2400	Peru	*S. ochranthum*	Allogamous-SI	
LA2166	B	North	Andean Mountain Range	Cajamarca	-6.33861	-79.02222	2300	Peru	*S. ochranthum*	Allogamous-SI	
LA2162	B	North	Andean Mountain Range	Cajamarca	-6.36667	-78.75	2400	Peru	*S. ochranthum*	Allogamous-SI	
LA1346	B	North	North Coast	La Libertad	-7.96667	-78.63333	1800	Peru	*S. arcanum*	Allogamous-SI	Associated Biota: *S. habrochaites*
LA1657	C	Centre	Centre Coast	Ancash	-9.46667	-78.13333	700	Peru	*S. pennellii*	Allogamous-SI	
LA1626	C	Centre	Centre Coast	Ancash	-8.50833	-77.36667	1700	Peru	*S. arcanum*	Allogamous-SI	
LA2917	C	Centre	Centre Coast	Ancash	-9.3	-77.01667	2430	Peru	*S. arcanum*		Probably a northern race of peruvanium, of '*S. arcanum* ' type
LA1360	C	Centre	Centre Coast	Ancash	-9.54583	-77.92917	1490	Peru	*S. huaylasense*	Allogamous-SI	
LA1365	C	Centre	Centre Coast	Ancash	-10.15	-77.41667	2450	Peru	*S. huaylasense*	Allogamous-SI	
LA2561	C	Centre	Centre Coast	Ancash	-8.81667	-77.86667	1580	Peru	*S. huaylasense*	Allogamous-SI	
LA1775	C	Centre	Centre Coast	Ancash	-9.51667	-77.88333	1200	Peru	*S. habrochaites*	Allogamous-SI	Resistant to late blight
LA1777	C	Centre	Centre Coast	Ancash	-9.55	-77.66667	3216	Peru	*S. habrochaites*	Allogamous-SI	
LA1317	C	Centre	Centre Coast	Ayacucho	-13.41667	-73.84167	2610	Peru	*S. chmielewskii*	Facultative-SC	
LA2613	C	Centre	Centre Coast	Huanuco	-10.25833	-76.15	2400	Peru	*S. neorickii*	Autogamous-SC	
LA0247	C	Centre	Centre Coast	Huanuco	-9.78333	-76.58333	2100	Peru	*S. neorickii*	Autogamous-SC	
LA1523	C	Centre	Centre Coast	Lima	-11.36667	-77.325	400	Peru	*S. pennellii*	Allogamous-SI	
LA1272	C	Centre	Centre Coast	Lima	-11.52	-77	1000	Peru	*S. pennellii*	Allogamous-SI	
LA1517	C	Centre	Centre Coast	Lima	-11.35	-77.33333	236	Peru	*S. peruvianum*	Allogamous-SI	
LA1278	C	Centre	Centre Coast	Lima	-11.64167	-76.95833	800	Peru	*S. peruvianum*	Allogamous-SI	Salt tolerance
LA1295	C	Centre	Centre Coast	Lima	-11.88333	-76.44167	2100	Peru	*S. habrochaites*	Allogamous-SI	
LA2724	C	Centre	Centre Coast	Lima	-12.45472	-75.88528	2850	Peru	*S. cornelomulleri*	Allogamous-SI	
LA1283	C	Centre	Centre Coast	Lima	-12.11667	-76.46667	2000	Peru	*S. cornelomulleri*	Allogamous-SI	
LA1649	D	South	South Coast	Ica	-14.63833	-74.99056	580	Peru	*S. pennellii*	Allogamous-SI	
LA0750	D	South	South Coast	Ica	-14.77528	-75.03417	550	Peru	*S. pennellii*	Allogamous-SI	
LA1302	D	South	South Coast	Ica	-13.63333	-75.71667	700	Peru	*S. pennellii*	Allogamous-SI	
LA1926	D	South	South Coast	Ica	-14.58333	-74.975	1200	Peru	*S. pennellii*	Allogamous-SI	Salt tolerance
LA1929	D	South	South Coast	Ica	-14.55	-75.06667	1100	Peru	*S. peruvianum*	Allogamous-SI	
LA0445	D	South	South Coast	Ica	-13.45	-76.13333	80	Peru	*S. peruvianum*	Allogamous-SI	
LA1325	D	South	Humid and Dry	Apurimac	-13.56361	-72.57556	1900	Peru	*S. chmielewskii*	Facultative-SC	
LA1319	D	South	Humid and Dry	Apurimac	-13.61167	-72.86389	1810	Peru	*S. neorickii*	Autogamous-SC	
LA1938	D	South	Coastal Desert	Arequipa	-15.68333	-73.83333	1400	Peru	*S. chilense*	Allogamous-SI	Resistant to viruses *PBNV* , *TSWV* , *ToMoV* and *TYLCV*
LA1932	D	South	Coastal Desert	Arequipa	-15.41667	-74.7	1100	Peru	*S. chilense*	Allogamous-SI	Resistant to viruses *PBNV* , *ToMoV* , *TYLCV* , and *CMV* , including satellite strains
LA1937	D	South	Coastal Desert	Arequipa	-15.6	-73.77	2500	Peru	*S. cornelomulleri*	Allogamous-SI	
LA0451	D	South	Coastal Desert	Arequipa	-16.28333	-71.66667	3200	Peru	*S. cornelomulleri*	Allogamous-SI	
LA0716	D	South	Coastal Desert	Arequipa	-16.225	-73.61667	50	Peru	*S. pennellii*	Facultative-SC	Resistance to *Xanthomonas campestris pv. vesicatoria* T3, *Alternaria alternata* , and *Fusarium*
LA1941	D	South	Coastal Desert	Arequipa	-15.83333	-73.575	1100	Peru	*S. pennellii*	Mixed-SI and SC	
LA1954	D	South	Coastal Desert	Arequipa	-17.01667	-72.08333	50	Peru	*S. peruvianum*	Allogamous-SI	
LA1513	D	South	Coastal Desert	Arequipa	-15.78333	-73.63333	600	Peru	*S. peruvianum*	Allogamous-SI	
LA0446	D	South	Coastal Desert	Arequipa	-15.80833	-74.38333	150	Peru	*S. peruvianum*	Allogamous-SI	
LA2663	D	South	Subtropical highland	Cusco	-13.69556	-71.99417	2500	Peru	*S. chmielewskii*	Facultative-SC	
LA2695	D	South	Subtropical highland	Cusco	-13.95722	-71.76167	2300	Peru	*S. chmielewskii*	Facultative-SC	Uppermost of the *S. chmielewskii* collections
LA1960	D	South	Cold Desert	Moquegua	-17.08333	-70.86667	1850	Peru	*S. chilense*	Allogamous-SI	Resistant to *PBNV*
LA1969	D	South	Pacific shores	Tacna	-17.55278	-70.02833	3250	Peru	*S. chilense*	Allogamous-SI	Resistant to *Tomato YellowLeafCurl* disease
LA0458	D	South	Pacific shores	Tacna	-17.96667	-70.18333	800	Peru	*S. chilense*	Allogamous-SI	Source of resistance to *CMV* and *Leveillula taurica*
LA2387	D	South	Pacific shores	Tacna	-17.36667	-70.31667	2800	Peru	*S. lycopersicoides*	Allogamous-SI	
LA4339	E	Chile	Suntropical-Cold Desert	Antofagasta	-25.5375	-70.47222	514	Chile	*S. chilense*		This is the southernmost known population of *S. chilense*
LA2876	E	Chile	Suntropical-Cold Desert	Antofagasta	-22.31667	-68.96667	2800	Chile	*S. sitiens*	Allogamous-SI	Drought tolerance
LA4105	E	Chile	Suntropical-Cold Desert	Antofagasta	-24.21056	-69.24139	2590	Chile	*S. sitiens*	Allogamous-SI	
LA4110	E	Chile	Suntropical-Cold Desert	Antofagasta	-23.0925	-69.04	2600	Chile	*S. sitiens*	Allogamous-SI	
LA4113	E	Chile	Suntropical-Cold Desert	Antofagasta	-22.23472	-68.76222	2680	Chile	*S. sitiens*	Allogamous-SI	
LA2778	E	Chile	Coastal Desert	Arica & Pari.	-18.38333	-69.55	2900	Chile	*S. chilense*	Allogamous-SI	
LA2730	E	Chile	Coastal Desert	Tarapaca	-19.35	-69.51667	1700	Chile	*S. lycopersicoides*	Allogamous-SI	
LA2957B	E	Chile	Coastal Desert	Tarapaca	-19.35	-69.51667	1850	Chile	*S. peruvianum*	Allogamous-SI	Mixed collection of mostly *S. chilense*
1179F	E	Chile	Tropical		-18.766947	-46.869106	194	Madagascar	*S. pyracanthum*		Chiltern Seeds UK variety

Table 2.3 *Solanum lycopersicum* 'Money Maker' control lines

Cf-2/Rcr3pim	Resistant to *C. fulvum* strains carrying Avr2 (Jones *et al* ., 1993)
Cf-2/rcr3-3pim	Have premature stop codon in *Rcr3* (Rooney *et al* ., 2005)
Cf0/Rcr3pim	Generated by Ilyas *et al* ., 2015
Cf0/Rcr3lyc	No resistance to *C. fulvum* strains carrying *Avr2* (Jones *et al* ., 1993)
Cf-9	Resistant to *C. fulvum* strains carrying Avr9; no resistance to Avr2 (Tigchelaar *et al* ., 1984 and Hammond-Kosack *et al* ., 1998)

Table 2.4 Wild potato populations (CGN, Netherlands)

Population	Region	Country	Latitude	Longitude	Asl metres	Species	Chr	Any source note
CGN17687	A	Mexico	19.360533	-99.226707	2250	*S. bulbocastanum*	2n=24	Moderately resistant to late blight
CGN24973	A	Mexico	19.483	-98.9	2200	*S. bulbocastanum*		
CGN17765	A	Mexico	19.7007809	-101.18443	2950	*S. verrucosum*	2n=24	Susceptible to late blight
CGN17767	A	Mexico	19.7007809	-101.18443	2950	*S. verrucosum*	2n=24	Susceptible to late blight
CGN17770	A	Mexico	20.659698	-103.34961	3250	*S. verrucosum*	2n=24	Resistant to late blight
CGN17774	A	Mexico	19.432608	-99.133209	2300	*S. verrucosum*	2n=24	Susceptible to late blight
CGN20567	A	Mexico	26.909979	-101.43076	3300	*S. verrucosum*	2n=24	Susceptible to late blight
CGN22374	A	Mexico	19.432608	-99.133209	2300	*S. verrucosum*	2n=24	Moderately resistant to late blight
CGN17809	A	Mexico	19.388454	-99.19467	2300	*S. demissum*	2n=72	Resistant to late blight
CGN17812	A	Mexico	19.432608	-99.133209	2300	*S. demissum*	2n=72	Resistant to late blight
CGN17813	A	Mexico	19.432608	-99.133209	2300	*S. demissum*	2n=72	Resistant to late blight
CGN17816	A	Mexico	19.432608	-99.133209	3000	*S. demissum*	2n=72	Resistant to late blight
CGN17818	A	Mexico	19.432608	-99.133209	2900	*S. demissum*	2n=72	Resistant to late blight
CGN23782	A	Mexico	15.16318	-91.95608	3200	*S. demissum*		
CGN17605	A	Mexico	19.432241	-99.177254	2900	*S. stoloniferum*	2n=48	Moderately resistant to late blight
CGN18332	A	Mexico	19.432608	-99.133209	2300	*S. stoloniferum*	2n=48	Resistant to late blight
CGN18333	A	Mexico	19.12384	-98.76649	3200	*S. stoloniferum*	2n=48	Resistant to late blight
CGN23519	A	Mexico	19.432608	-99.133209	2300	*S. stoloniferum*		
CGN21363	A	Guatemala	15.1027803	-90.318062	1430	*S. bulbocastanum*	2n=24	
CGN22732	A	Guatemala	15.3191795	-91.472412	1900	*S. bulbocastanum*		
CGN20571	A	Guatemala	15.3191795	-91.472412	3500	*S. demissum*	2n=72	Susceptible to late blight
CGN20679	A	Guatemala	15.3191795	-91.472412	3400	*S. demissum*	2n=72	
CGN20665	B	Peru	-12.132571	-77.02787	138	*S. acaule*	2n=48	Susceptible to late blight

CGN23044	B	Peru	-12.043181	-77.028236	138	*S. chacoense*		
CGN24123	B	Peru	-9.133	-77.017	3750	*S. orophilum*		
CGN23985	B	Peru	-9.133	-77.017	3450	*S. orophilum*		
CGN18286	B	Chile	-32.89067	-68.846136	654	*S. palustre*	2n=24	Susceptible to late blight
CGN20623	B	Bolivia	-18.806667	-65.5116	3960	*S. acaule*	2n=24	Weakly resistant to late blight
CGN18197	B	Bolivia	-17.413977	-66.165321	3300	*S. acaule*	2n=48	Susceptible to late blight
CGN24850	B	Bolivia	-18.333	-65	2400	*S. chacoense*		
CGN17720	B	Bolivia	-21.521383	-64.728096	1420	*S. infundibuliforme*	2n=24	Susceptible to late blight
CGN18195	B	Bolivia	-15.467	-67.533	3700	*S. infundibuliforme*	2n=24	Susceptible to late blight
CGN23061	B	Bolivia	-15.467	-67.533	3800	*S. infundibuliforme*		
CGN24372	B	Bolivia	-17.413977	-66.165321	3800	*S. gourlayi*		
CGN24574	B	Bolivia	-20.55	-63.8	3900	*S. gourlayi*		
CGN17933	C	Argentina	-24.18434	-65.302177	3940	*S. acaule*	2n=48	Susceptible to late blight
CGN17674	C	Argentina	-24.7859	-65.411659	3200	*S. acaule*	2n=48	Susceptible to late blight
CGN22359	C	Argentina	-26.824141	-65.222603	2950	*S. acaule*	2n=48	Moderately resistant to late blight
CGN25180	C	Argentina	-24.7859	-65.411659	1000	*S. chacoense*		
CGN18041	C	Argentina	-24.18434	-65.302177	3650	*S. infundibuliforme*	2n=24	Susceptible to late blight
CGN17755	C	Argentina	-34.603722	-58.381592	3200	*S. venturii*	2n=24	Susceptible to late blight
CGN17761	C	Argentina	-34.603722	-58.381592	3200	*S. venturii*	2n=24	Susceptible to late blight
CGN18000	C	Argentina	-34.603722	-58.381592	3200	*S. venturii*	2n=24	Resistant to late blight
CGN17992	C	Argentina	-24.18434	-65.302177	3200	*S. vernei*	2n=24	Slightly susceptible to late blight
CGN17993	C	Argentina	-24.18434	-65.302177	3200	*S. vernei*	2n=24	Slightly susceptible to late blight
CGN21315	C	Argentina	-24.18434	-65.302177	2850	*S. vernei*	2n=24	Slightly susceptible to late blight
CGN21332	C	Argentina	-24.18434	-65.302177	3200	*S. gourlayi*	2n=48	Susceptible to late blight
CGN24384	C	Argentina	-24.18434	-65.302177	3100	*S. gourlayi*		
CGN17983	C	Argentina	-38.95161	-68.0591	704	*S. palustre*	2n=24	
CGN18338	C	Paraguay	-25.383	-57.267	200	*S. chacoense*	2n=24	Susceptible to late blight

Table 2.5 Other Solanaceae species in this study

Population	Country	Latitude	Longitude	Species	Type
Eggplant (CGN, Netherlands)					
CGN23305	USA	27.9944	-81.7603	*S. melongena*	Breeder's variety
CGN23599	Togo	8.619543	0.824782	*S. melongena*	Land variety
CGN23664	Togo	8.619543	0.824782	*S. melongena*	Land variety
CGN17495	Netherlands	52.37022	4.895168	*S. melongena*	Breeder's variety
CGN18769	Netherlands	52.37022	4.895168	*S. melongena*	Breeder's variety
CGN18573	UK	51.50987	-0.11809	*S. melongena*	Breeder's variety
CGN18495 (PI-286099)	USA	37.09024	-95.7129	*S. melongena*	Research material
CGN17522	India	25.31668	82.91667	*S. melongena*	Land variety
CGN17473	USA	37.09024	-95.7129	*S. melongena*	Breeder's variety
CGN17526 (PI-121359)	India	21.98	74.866	*S. melongena*	Land variety
CGN17492 (No. 967)	Netherlands	52.37022	4.895168	*S. melongena*	Breeder's variety
CGN17484	India	28.6448	77.21672	*S. melongena*	Breeder's variety
CGN23848 (S.0871)	Uganda	0.347596	32.58252	*S. anguivi*	Wild
CGN23600	Togo	8.619543	0.824782	*S. dasyphyllum*	Wild
CGN23851	Kenya	-0.02356	37.90619	*S. incanum*	Wild
CGN23687	Togo	8.619543	0.824782	*S. macrocarpon*	Wild
CGN23587	Netherlands	52.37022	4.895168	*S. nigrum*	Wild
CGN21367	Costa Rica	9.934739	-84.0875	*S. nigrescens*	Wild
CGN22915	India	28.6448	77.21672		Wild
CGN21369	Costa Rica	9.934739	-84.0875	*S. viarum*	Wild
JS2075	UK	51.50987	-0.11809	*S. burbankii*	Jungle Seeds Co.
JS3209	Peru	-12.1326	-77.0279	*S. torvum*	Jungle Seeds Co.
Pepper (CGN, Netherlands)					
CGN21474 (CAP-497)	Unknown	52.37022	4.895168	*C. annum*	Wild
CGN21526 (2363)	Mexico	19.43261	-99.1332	*C. annum*	Wild
CGN16975 (AC 1979)	Jamaica	18.10958	-77.2975	*C. annum*	Wild
CGN20787 (507)	Guatemala	14.305	-90.785	*C. annum*	Wild
CGN20808 (AC 2017)	Bolivia	-16.9707	-64.2696	*C. annum*	Wild
CGN23200 (7112A)	Costa Rica	9.90467	-83.6835	*C. annum*	Wild
CGN16976 (AC 2255)	Honduras	14.76166	-86.9216	*C. annum*	Wild
CGN16974 (AC 1534)	Mexico	19.18095	-96.1429	*C. annum*	Wild

CGN22777 (7116)	Costa Rica	9.90467	-83.6835	*C. annum*	Wild
CGN22783 (CB-4)	Mexico	21.86286	-102.911	*C. annum*	Wild
CGN22866 (CB-8)	Guatemala	14.62843	-90.5227	*C. annum*	Wild
CGN22873 (C-36)	Mexico	19.18095	-96.1429	*C. annum*	Wild
CGN22773 (7101)	Guatemala	14.62843	-90.5227	*C. annum*	Wild
Tepin (JS1173)	Mexico	19.43261	-99.1332	*C. annum*	Jungle Seeds Co.
CGN17025 (NO. 1553)	Bolivia	-17.414	-66.1653	*C. annum*	Wild
CGN21467 (AC 1230)	Brazil	-23.5338	-46.6253	*C. annum*	Wild
CGN23205 (SA 326)	Bolivia	-19.7999	-63.9546	*C. annum*	Wild
CGN23278 (PI-337524)	Argentina	-34.6037	-58.3816	*C. baccatum*	Wild
CGN20805 (SA 222)	Brazil	-9.37139	-36.2408	*C. baccatum*	Wild
CGN22794 (SA 221)	Brazil	-9.37139	-36.2408	*C. baccatum*	Wild
CGN23210 (SA 137)	Peru	-12.0464	-77.0428	*C. baccatum*	Wild
CGN22775 (7104)	Guatemala	14.3	-90.75	*C. baccatum*	Wild
CGN22790 (AC 1249)	Mexico	19.43261	-99.1332	*C. frutescens*	Wild
CGN22792 (SA 252)	Peru	-12.0464	-77.0428	*C. frutescens*	Wild
CGN22208 (AC 1501)	Ecuador	-0.77726	-91.1426	*C. galapagoense*	Rare wild
CGN22876 (PI-606708)	Peru	-13.1588	-74.2232	*C. tovarii*	Wild
Petunia					
BM79 'Mini Max Pink'	USA	-34.6037	-58.3816	*P. integrifolia*	Seedman Co.
BM76 'Mini Max Coral'	USA	-34.6037	-58.3816	*P. integrifolia*	Seedman Co.
BM77 'Midnight Blue'	USA	-34.6037	-58.3816	*P. integrifolia*	Seedman Co.
BM78 'Midnight Violet'	USA	-34.6037	-58.3816	*P. integrifolia*	Seedman Co.
3433	Chile	-33.4475	-70.6737	*P. integrifolia*	Seedman Co.
977p	S. America	-19.5578	-44.0814	*P. grandiflora*	Wild (Chiltern Seeds Co.)
PWS1	Brazil	-22.9064	-43.1822	*P. exserta*	Extremely rare wild (PWS)
PWS2	S. America	-19.5578	-44.0814	*P. axillaris*	Rare wild (Plant World Seeds)
Tobacco					
898F	Brazil	-26.3045	-48.8434	*N. affinis*	Chiltern Seeds Co.
897C	S. America	-41.8101	-68.9063	*N. alata*	Chiltern Seeds Co.
W235	S. America	-44	-68	*N. alata*	Seedman Co.
899X	Australia	-25.2744	133.7751	*N. excelsior*	Chiltern Seeds Co.
JS1286	S. America	-51	-73	*N. glauca*	Wild (Jungle Seeds)
899Q	Peru	-12.6719	-69.3555	*N. glutinosa*	Rare wild (Chiltern Seeds)
899F	S. America	-33.4475	-70.6737	*N. langsdorffii*	Chiltern Seeds Co.
899M	Brazil	-25.4411	-49.2769	*N. mutabilis*	Chiltern Seeds Co.
PWS3	Mexico	20.40042	-89.1349	*N. rustica*	Wild (PWS)
JS713	S. America	-44	-68	*N. sylvestris*	Jungle Seeds Co.
900A	S. America	-20	-67		Chiltern Seeds Co.
JS1277	America	-20	-67	*N. tabacum*	Jungle Seeds Co.
GV1	Bolivia	-20.133	-68.75	*N. tomentosiformis*	Wild (Georgia vines, USA)

Table 2.6 List of primers used for PCR, sequencing and qPCR

Primers used for gDNA PCR (5' to 3' direction)			**Product**	**Reference**
SM_AVR2_C53X_F	F	TTGAAGACAACCCGGGCTTTCGCTGGCTGAC	2410bp	This study
SM_AVR2_C53X_R	R	TTGAAGACAACGGGTTGCTGGGCAGCGT		
SM_EPIC1_2B_MUT_F	F	TTGAAGACAACTGTCGGCGGAGAACTACAAGTTCCACG	2569bp	This study
SM_EPIC1_2B_MUT_R	R	TTGAAGACAAACAGGACGTTAGTCTCGAGACTGTCGAC		

SM_CIP1_DTT_F	F	TTGAAGACAATGCTGAGCTTTGAGACCACG AAG	2581bp	This study
SM_CIP1_DTT_R	R	TTGAAGACAAAGCAAAGGTGATTACCCTGC AC		
SM_CF-2/CF5_F	F	GCAACTGCCCTCTTGAAATGGA	<2892bp	This study
SM_CF-2/CF5_R	R	CTTGAGGGATGCATCCTTGGAG		
F_RCR3/072	F	AGCTCCATGGCTATGAAAGTTGATTTGATG	1109bp	Hörger *et al.*, 2012
R_RCR3/073	R	AGCTCTCGAGCTATGCTATGTTTGGATAAG AAGAC		
SM_VIGS-Cf-2_F	F	AAGAATTCCAGATTTCAGGAACAATACCAC	300bp	This study
SM_VIGS-Cf-2_R	R	TTGGATCCGCCATTAAGAGCATTCTCAC		
CS5	F	TTTCCAACTTACAATCCCTTC	378bp	van der Hoorn *et al.*, 2001a
CS1	R	GCCGTTCAGTTGGGTGTT		
DS1	F	GAGAGCTCAACCTTTACGAA	507bp	van der Hoorn *et al.*, 2001a
CS1	R	GCCGTTCAGTTGGGTGTT		
ACT1	F	GGTTATCTTATGGCTACTCTG	778bp	Overduin *et al.*, 1993
ACT2	R	GCGCCATCCGAATGTAGAG		
SM_C14_1	F	CAGGGAGTTGTTGGGCATTC	1298bp & ~923bp	This study
SM_C14_2	R	AGAACTGCTCTTCTTTCCTC		
SM_PIP1_1	F	ACCGCTTCAAAACATTCAAGGAAA	1232bp	This study
SM_PIP1_2	R	ACAGTAGGGAACGAAGCAACC		
Specific primers used for DNA sequencing (5' to 3' direction)				
pL0M (0015)	F	CGTTATCCCCTGATTCTGTGGATAAC		Lvl-0 (MoClo) kit
pL0M (0016)	R	GTCTCATGAGCGGATACATATTTGAATG		
R145_F_RCR3_SEQ	F	ACTGGATTAAACATACCTAATTCATATC		Hörger *et al.*, 2012
SM_C14_1	F	CAGGGAGTTGTTGGGCATTC		This study
SM_PIP1_1	F	ACCGCTTCAAAACATTCAAGGAAA		This study
F_93	F	TGTTCAGGCGGTTCTTGTGTGTCA		(MoClo) kit
R_94	R	TGTTCAGGCGGTTCTTGTGTGTCA		
Primers used for QPCR				
SM_Rcr3q1	F	CAAGCCGTAACTAAACAGCC		This study
SM_Rcr3q2	R	TTCATAAACCCATTCTCGCC		
SM_Pip1q1	F	GGGGGCATTACCACAGAGAC		This study
SM_Pip1q2	R	CCACAATGGCCACCATCAAC		
SM_C14q1	F	GGCTGTTGCACATCAACCTG		This study
SM_C14q2	R	AAGTGGCTCCTTCAAGTGGG		
SM_Cf_clan2q1	F	TGGAGGGAGCAATACCACAA		This study
SM_Cf_clan2q2	R	GACCGAGGGATTTCATCTGCT		
SM_Trun_cladeq1	F	TTGGTTCACTAGCCAAGCTTCA		This study
SM_Trun_cladeq2	R	ATCAGTGAACATCCAATGGCCAAAA		
R266_Cf-2q1	F	GATCTCATTGCGATCCGTATA		Ilyas *et al.*, 2015
R268_Cf-2q2	R	ATAGCCCATCAGAGCTGCTTTCC		
SM_SlSobir1q1	F	TCCCTCCAAAACAACAAACTC		This study

SM_SlSobirq2	R	CAAGAAGTTCAGGTTCCCAG	
Tomato Actin_q1	F	ATGAAGCTCAATCCAAGAGGGGTATC	Ilyas *et al*., 2015
Tomato Actin_q2	R	CTCCTGCTCATAGTCAAGAGCCAC	
SM_tPDSq1	F	TGAGAGTCCAAGGTAGTTCAG	This study
SM_tPDSq2	R	TGATGATAAAAATGCAGCCTCC	

Table 2.7 List of plasmids generated in this study

Plasmid	Derivative/Gene	Source Organism	Selection	Assembly vector	Restriction sites
pL0M (Golden Gate Cloning Level 0)					
pSM001	pL0M-C-AVR2_C53X	*C. fulvum*	Kan[50]	pJK019	*Bsa*I/*Bpi*I
pSM002	pL0M-C-EPIC1 QxVxG>NxLxA	*P. infestans*	Spec[50]	pFGH027	*Bsa*I/*Bpi*I
pSM003	pL0M-C-EPIC2B QxVxG>NxLxA	*P. infestans*	Kan[50]	pJK017	*Bsa*I/*Bpi*I
pSM004	pL0M-C-CIP1ΔTT	*P. syringae*	Spec[50]	pFGH026	*Bsa*I/*Bpi*I
pSM005	C-terminally His-tagged EPIC1 QxVxG>NxLxA	*P. infestans*	Spec[50]	pFGH084	*Bsa*I/*Bpi*I
pSM006	C-terminally His-tagged EPIC2B QxVxG>NxLxA	*P. infestans*	Kan[50]	pJK255	*Bsa*I/*Bpi*I
pL1M or pL2M (Golden Gate Cloning Level 2 or expression/binary vectors)					
pSM101	pL1VE-R1-PU-T7_S-OmpA-His-TEV_C-AVR2_C53X_T-T7	*E. coli* DH10ß	Kan[50]	pSM001	*Bsa*I/*Bpi*I
pSM102	pL1VE-R1-PU-T7_S-OmpA-His-TEV_C-EPIC1 QxVxG>NxLxA_T-T7	*E. coli* DH10ß	Kan[50]	pSM002	*Bsa*I/*Bpi*I
pSM103	pL1VE-R1-PU-T7_S-OmpA-His-TEV_C-EPIC2B QxVxG>NxLxA_T-T7	*E. coli* DH10ß	Kan[50]	pSM003	*Bsa*I/*Bpi*I
pSM104	pL1VE-R1-PU-T7_S-OmpA-His-TEV_CIP1ΔTT_T-T7	*E. coli* DH10ß	Kan[50]	pSM004	*Bsa*I/*Bpi*I
pSM105	pL1VE-R1-PU-T7_S-His-TEV_C-EPIC1QxVxG>NxLxA_T-T7	*E. coli* DH10ß	Kan[50]	pSM005	*Bsa*I/*Bpi*I
pSM106	pL1VE-R1-PU-T7_S-His-TEV_C-EPIC2BQxVxG>NxLxA_T-T7	*E. coli* DH10ß	Kan[50]	pSM006	*Bsa*I/*Bpi*I
pSM107	pL2M-TRV2-RCR3	*S. pimpinellifolium* (JQ927269)	Kan[50], Gent[25], Rif[25]	pJK037 (pL1V2-TRV2)	*Eco*RI/*Bam*HI

pSM108	pL2M-TRV2-Clan 4	*S. pimpinellifolium* (AY793367)	Kan^{50}, Gent^{25}, Rif^{25}	pJK037	*Eco*RI/*Bam*HI
pSM109	pL2M-TRV2-Clan 2	*S. pimpinellifolium* (AF053995)	Kan^{50}, Gent^{25}, Rif^{25}	pJK037	*Eco*RI/*Bam*HI
pSM110	pL2M-TRV2-Clan 3	*S. pimpinellifolium* (AY793352)	Kan^{50}, Gent^{25}, Rif^{25}	pJK037	*Eco*RI/*Bam*HI
pSM111	pL2M-TRV2-Clan 1	S. *pimpinellifolium* (AY793348.1)	Kan^{50}, Gent^{25}, Rif^{25}	(PCR on pBIN-Ks-35s::*Cf-2.2*-gwy-eGFP; Sol 2738) pJK037	*Eco*RI/*Bam*HI
pSM112	pL2M-TRV2-PDS	*S. pimpinellifolium* (Sopim03g123760)	Kan^{50}, Gent^{25}, Rif^{25}	pJK037	*Eco*RI/*Bam*HI
pSM113	pL2M-TRV2-PIP1	*S. lycopersicum* (778273)	Kan^{50}, Gent^{25}, Rif^{25}	pJK037	*Eco*RI/*Bam*HI
pSM120	pL2M-TRV2-C14	*S. lycopersicum* (Solyc12g088670.0.1)	Kan^{50}, Gent^{25}, Rif^{25}	pJK037	*Eco*RI/*Bam*HI
pSM122	pL2M-TRV2-SOBIR1	*S. pimpinellifolium* (Sopim06g071810.0.1)	Kan^{50}, Gent^{25}, Rif^{25}	pJK037	*Eco*RI/*Bam*HI

Table 2.8 List of sourced plasmids used in this study (from Kourelis J., 2018 and Kourelis *et al*., 2020 unless specified otherwise)

Name/ID	Background Description
EC15259	pL0M-C2-6xHis-15259 (Ben Miller, UEA)
pFGH026	pL0M-C-Cip1deltaTT
pFGH027	pL0M-C-Epic1QxVxG Grosse- Holz *et al.*, 2018
pFGH084	pL0M-C1-EPIC1 delta SP
pJK017	pL0M-C-EPIC2B (AY935252) delta SP
pJK019	pL0M-C-AJ421629 - avr2 CDS delta SP
pJK024	pL2M-P19-2x35S::Cf-2
pJK037	pL1V2-TRV2 (AF406991) - ccdB annotated
pJK050	pL2M-F1-PU-35S-TMV_SC-P19_T-35S (P19)
pJK082	pL1VE-R (pET28b)
pJK120	pL0M-S-OmpA-His6-TEV
pJK153	pL1VE-R1-PU-T7_S-OmpA-His-TEV_C-AVR2_T-T7
pJK155	pL1VE-R1-PU-T7_S-OmpA-His-TEV_C-EPIC1_T-T7
pJK157	pL1VE-R1-PU-T7_S-OmpA-His-TEV_C-EPIC2B_T-T7
pJK159	pL1VE-R1-PU-T7_S-OmpA-His-TEV_C-CIP1_T-T7

pJK175	pL2M-F1-P19-F2-35S::RCR3lyc-His
pJK225	pL2M-P19-2x35S::AVR2
pJK253	pL0M-S-OmpA
pJK255	pL0M-C1-EPIC2B (AY935252) delta SP
pJK284	pL2M-P19-2x35S::RCR3pim
pJK285-12	pL2M-P19-2x35S::RCR3tuba
pJK285-17	pL2M-P19-2x35S::RCR3tub1
pJK285-18	pL2M-P19-2x35S::RCR3tbs1(KF536710)(tub8)
pJK285-19	pL2M-P19-2x35S::RCR3slf(KF536706)(sto1)
pJK285-20	pL2M-P19-2x35S::RCR3sto2
pJK285-21	pL2M-P19-2x35S::RCR3dms1(KF536707)(dms1)
pJK285-22	pL2M-P19-2x35S::RCR3dms3(KF536708)(dms3)
pJK285-23	pL2M-P19-2x35S::RCR3vcs(KF536709)(ver)
pJK419-01	pL2M-P19-2x35S::NtRCR3
pJK419-02	pL2M-P19-2x35S::CapanaRCR3
pJK419-03	pL2M-P19-2x35S::SmeRCR3
pJK419-04	pL2M-P19-2x35S::PeinfRCR3
pJK419-05	pL2M-P19-2x35S::NSylRCR3a_(Nsyl_KD935601.1)
pJK488	pL2M-P19-2x35S::Pip1
pJK590#07_SP	pL2M-P19-2x35S::C14_DA
pJP001	pL0M-PU-T7-LacO-T7
pJP002	pL0M-T-T7 terminator
Cf-2::EGFP	Matthieu Joosten

Chapter 3

Hypersensitive response profiling of 302 populations across Solanaceae reveal heterogeneity in protease inhibitor recognition

Shivani Malik[1], Jiorgos Kourelis[1,2] and Renier A.L. van der Hoorn[1*]

[1]Plant Chemetics Laboratory, Department of Plant Sciences, University of Oxford, South Parks Road, OX1 3RB Oxford, UK. [2]Current address: Department of Life Sciences, Imperial College, SW7 2AZ, London, UK. *Correspondence: renier.vanderhoorn@biology.ox.ac.uk

Author Contributions:

Research design: SM and RvdH; Seed collection procurement: SM; Experimental investigations: SM; Cloning: L0 and L2 cloning for wild-type inhibitor plasmids, binary vector *Rcr3*, and domesticated assembly components of L2 inhibitor mutants: JK; Site-directed mutagenesis of L0 and assembly of L2 mutant inhibitor plasmids: SM; Data analysis, Figures, and writing: SM with critical inputs from RvdH; Funding acquisition: RvdH.

Acknowledgement:

We thank Tomato Genetics Resource Centre (TGRC), Davis and Centre for Genetic Resources (CGN), Netherlands, for seed donations; Friederike Grosse-Holz for L0 pFGH026 and pFGH027 used for cloning L0 pSM004 and pSM002; Judith K. Paulus and Selva Kumari for protein purification protocols; Ursula Pyzio and Timothy Wroe for greenhouse assistance; Sarah Rodgers and Caroline O' Brien for technical support; SM was supported by Oxford-Indira Gandhi Scholarship.

3.1 Introduction

Solanaceae is the most studied plant family and has over 102 genera. It is a broadly diverse family, which has *Solanum* as the largest genus consisting of several crops of increasing economic significance such as tomato, potato and eggplant (PBI *Solanum* Project 2014, FAOSTAT, 2021). Despite being distributed in highly variable ecosystems around the world, Solanaceae species have uncommonly conserved genomes and surprisingly high specialized local adaptations showing phenotypic variations (Sol Genomics 2022). However, crop yields in Solanaceae are significantly reduced under native and greenhouse conditions due to notable destructive pathogens, such as *Cladosporium fulvum*, *Phytophthora infestans* and *Pseudomonas syringae*.

The ascomycete hemibiotrophic fungal pathogen *C. fulvum* causes leaf mould infection in tomato (Thomma et al., 2005). The gram negative bacterial pathogen, *P. syringae* pv. *tomato* DC3000 and the oomycete pathogen *P. infestans*, cause bacterial speck and late blight disease, respectively, in a wide range of species. These three pathogens live in the apoplast and secrete many proteins and other molecules to manipulate the host. Resistance (*R*) genes that recognise these pathogens trigger a complex locally executed cell death or hypersensitive response (HR) upon pathogen entry into the host plant. (van der Hoorn and Kamoun, 2008, Chen et al., 2015).

HR is an effective race-specific pathogen recognition process found ubiquitously in the plant kingdom and manifests variations in different interactions in related or distant host species (Mesarich et al., 2018, Balint-Kurti, 2019). Visible HR phenotypes triggered by direct or indirect recognition of pathogen-secreted proteins are thus a reliable approach to screen germplasms for identification of plants carrying *R* genes. In cases of pathogen restrictions of host range, HR-based assays may pose a limitation and the reliability of HR phenotype

assays in different pathogen interactions with same host may vary. However, specific HR-associated recognition of *C. fulvum* and *P. infestans* secreted proteins in several distantly evolved non-host species has been shown (Vleeshouwers et al., 2000, Lauge et al., 2000, De Kock et al., 2004, Kahlon et al., 2020).

Recognition of Avr2, a small cysteine rich protease inhibitor secreted by *C. fulvum* trigger a visible rapid hypersensitive response (HR) in plants carrying *Cf-2* resistance gene, encoding a cell surface receptor-like protein (RLP) consisting extracellular leucine-rich repeat domains (Dixon et al., 1996, Luderer et al., 2002). Tomato and *C. fulvum* interaction is a model for *Resistance* gene for *Avirulence* gene interaction (Flor, 1971), where resistance against Avr2 is indirectly mediated by its inhibition of papain-like cysteine protease, Rcr3 in the host apoplast and eventually the recognition of Avr2-Rcr3 interaction by Cf-2 (Kruger et al., 2002, Rooney et al., 2005). In addition to Rcr3, its paralog Pip1 is also targeted by Avr2 (Song et al., 2009). Various cysteine proteases in tomato and potato are convergent targets of multiple inhibitors from distinct pathogens.

EpiC1 and EpiC2B are cystatin-like inhibitors secreted by *P. infestans* that have also been shown to interact and inhibit Rcr3 and Pip1 (Tian et al., 2007, Song et al., 2009). However, EpiC1 and EpiC2B more strongly inhibit a different cysteine protease, C14, compared to Rcr3 and Pip1 (Kaschani et al., 2010). Likewise, Cip1 is a chagasin-like inhibitor secreted by *P. syringae Pst* DC3000 that is known to preferably target C14 and Pip1 (Shindo et al., 2016). In contrast to Avr2, EpiC1, EpiC2B and Cip1 are stealthy inhibitors as they do not induce Cf-2-mediated HR, possibly because they are weak Rcr3 inhibitors. The *Cf-2/Rcr3* perception system has been introgressed into cultivated tomato *S. lycopersicum*, from its closest wild relative, *S. pimpinellifolium* (Dixon et al., 1996, Kruger et al., 2002). A survey for identification of *Cf-2* homologs in *S. pimpinellifolium* uncovered that *Cf-2* gene family is complex and heterogeneous (Schaal and Caicedo, 2004). An evolutionary study of Rcr3

revealed natural variants with different sensitivities to Avr2 (Hörger et al., 2012, Kourelis et al., 2020) and EpiC/Cip1 (referred as Rip1 in reference) inhibitors (Hörger, 2011).

Furthermore, the emergence of pathogen races, including of *C. fulvum*, continuously adapting and evolving to overcome plant resistance under native and greenhouse environments worldwide (Derivnina et al., 2016, Bernal-Cabrera et al., 2021) highlight the need to identify sources of durable resistance. Previous studies have shown recognition frequency of Av9 of *C. fulvum* throughout populations of *S. pimpinellifolium* (van der Hoorn et al., 2001, Krujit et al., 2005) and in other wild tomato species *S. chilense* (Kahlon et al., 2020). Natural response variation in wild tomato species against *P. syringae* (Kraus et al., 2016, Roberts et al., 2019) and *P. infestans* (Arafa et al., 2017, Kahlon et al., 2021) have also been evaluated in several studies. In the present study, we evaluated 302 Solanaceae populations to infer natural variation in recognition of four distinct pathogen-derived inhibitors (Avr2, Cip1, EpiC1 and EpiC2B). This is the first report of extensive screening of Avr2 recognition in *S. piminellifolium* and several relatives across Solanaceae. We hypothesised that EpiCs and Cip1 are recognised in plants where these inhibitors would form a stronger complex with a co-receptor cysteine protease that is recognised by a Cf-2 variant or a related receptor-like protein. Here, we first report that EpiC1, EpiC2B and Cip1 can trigger HR.

We were seeking to answer the following questions: How frequent is Avr2 recognition in *S. pimpinellifolium* populations? Are EpiCs and Cip1 also recognised in natural populations of *S. pimpineliifolium*? Does the recognition of any or all of these proteins occur in other wild tomato species? Do these inhibitors induce HR in species distantly related to tomato, including potato, eggplant, pepper, tobacco and petunia? Does the estimated frequency of inhibitors vary among inhibitors in different species across geographic climatic variations and altitudes? Our results have answered these questions and identified source populations/species with potential recognition of three important pathogens of the

Solanaceae family. This will eventually help in the accelerated development of broad spectrum resistance in crops against multiple pathogens.

3.2 Results

3.2.1 Collection of Solanaceae germplasms selected for HR assay in this study

A phylogenetic tree (**Figure 3.1**) based on genomic data was reconstructed to classify species of interest (Peralta et al., 2008, Rodriguez et al., 2009, Bombarley et al., 2016., Garcia et al., 2016, Aubriot et al., 2018, Huang et al., 2019,) that were selected on basis of their availability from germplasm depositories. The species were further evaluated for their phylogenetic closeness and median evolutionary time scales with respect to the domesticated tomato, *S. lycopersicum* using TimeTree (Kumar et al., 2022). We screened a diversity of wild tomato species obtained from TGRC. Initial screening focused on the closest wild relative of *S. lycopersicum*, constituting a collection of 112 populations of *S. pimpinellifolium*. *S. pimpinellifolium* inhabit humid environments at elevations up to 500 metres, exceptionally up to 3000 metres, natively distributed from Ecuador to shared origins of domesticated *S. lycopersicum*, South of Peru.

Next, we included two closely related tomato species endemic to Galapagos Islands, *S. cheesmaniae* (n = 3) and *S. galapagense* (n = 4), which both occur along coastal ranges with distribution from sea level to over 1300 metres and form a group closely related *S. pimpinellifolium*. We also included *S. arcanum* (n = 5), *S. chmielewskii* (n = 4) and *S. neorickii* (n = 5), which spread in different Andean valley climatic variations, but ranging up to 3000 metres. *S. arcanum* inhabits coastal Andean valleys of Northern Peru, while *S. chmielewskii* and *S. neorickii* inhabit dry Andean valleys of Southern Peru. We included *S. hualysense* (n = 3), which exclusively occurs in Northern Peru along riverside rocky slopes,

from 1700 to 3000 metres and *S. peruvianum* (n = 8) which occurs in Centre of Peru to North of Chile, exceptionally in coastal deserts of up to 600 metres. We included *S. chilense* (n = 7) which is another representative species inhabiting up to 3000 metres with ranges in west Andean slope in Southern Peru to coastal deserts of Northern Chile and *S. corneliomuelleri* (n = 4), which inhabits Central Peru to South of Peru, along the western Andes slopes with elevations of 1000 to 3000 metres. We included *S. habrochaites* (n = 4), which occurs in Central Ecuador to Central Peru and rarely Northern Peru, comprising dry Andean forests and loma formations in Peru, represent the origin regions, growing from 400 to 3600 metres. We included *S. pennellii* (n = 9), which has distribution ranges from North of Peru to North of Chile, occurring in dry hilly rocks to sandy areas up to ~2800 metres. We also included two species occurring up to elevations of over 3000 metres and representing close outgroups to wild tomatoes: *S. juglandifolium* (n = 3), which is distributed from Colombia to Ecuador South and *S. ochranthum* (n = 3), which is distributed from Colombia to South of Peru. Another two outgroup wild tomato species included were *S. sitiens* (n = 4), originating from Northern Chile and *S. lycopersicoides* (n = 2), distributed from Peru to Northern Chile and both inhabiting Andean hills over 2000 metres (Peralta et al., 2008).

We also included wild potato species, which are distributed natively from South-west of the United States toward central regions of great species richness, including central Mexico, Guatemala and Andean highlands and to Southern regions, including central Chile, Bolivia and Argentina (Hijmans and Spooner, 2001, Vincent et al., 2013). Tuber-bearing landraces and wild relatives of potato consists a complex diversity of gene pool. Nearly 70% of wild potatoes are diploid while the remaining are polyploids (mostly 2n = 4x = 48 or 2n = 6x = 72) (Cai et al., 2012). We obtained wild potato accessions from CGN, Netherlands. *S. bulbocastanum* (n = 4), a diploid from Central America to Mexico in North is one of the most widely used for breeding (Castañeda-Álva-rez et al., 2015) and is the most distantly evolved *tuberosum* tested in this study. From the diploid pool, we included *S. verrucosum* (n = 6),

which is distribute in the North across 2300 to 3300 metres altitude, *S. chacoense* (n = 4), which occurs in Peru and South at 138 to 1000 metres high, *S. infundibuliforme* (n = 4) spreading from Bolivia and Argentina across 1420 to 3800 metres elevation, *S. venturii* (n = 3) and *S. vernei* (n = 3), both of which occur in South region at ~3200 metres. From polyploid pool, *S. demissum* (n = 8) (ploidy 2n = 72) was a significant species specifically representing elevation variations 2300 to 3500 metres in the North region. *S. stoloniferum* (n = 4) (ploidy 2n = 48) originating from 2300 to 3200 metres, from Mexico was included. *S. bulbocastanum*, *S. chacoense* and *S. demissum* are known to potentially resist multiple pathogens and most of our populations are known to confer moderate to strong resistance to late blight (**Table 2.4**). We also included *S. acaule* (n = 6) (ploidy 2n = 24 and 2n = 48) and *S. gourlayi* (n = 2) with highest altitude ranges in South were also evaluated. *Etuberosum* represented by *S. palustre* (n = 2) (ploidy 2n = 24) that is endemic to central Chile and Argentina was selected as outgroup for potato.

Further in genus *Solanum*, we tested 13 land varieties and nine wild varieties of eggplant, representing cultivated *S. melongena* to outgroup *S. dasyphyllum*. We also tested 26 cultivated and wild varieties of pepper, 13 tobacco varieties and eight petunia varieties. Except for country of origin of our populations (**Table 2.5**), no other information was available for these accessions.

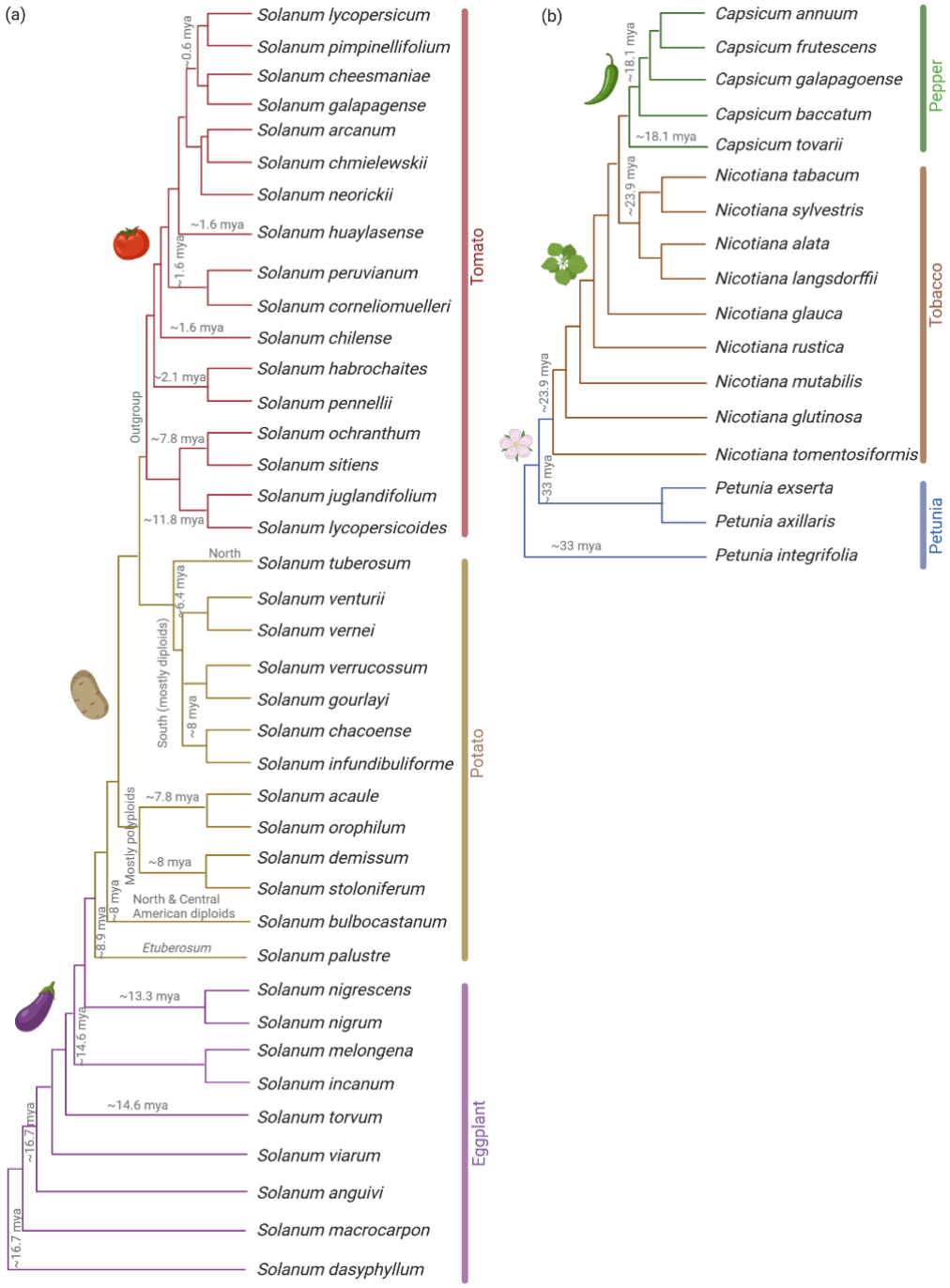


Figure 3.1 Phylogenetic trees generated to show relationships among species tested in this study.

These trees were reconstructed to select Solanaceae-wide taxonomic samples for HR screening against inhibitors. Tested species were classified as closely or distantly related to *S. lycopersicum*. **(a)** Hierarchy of *Solanum* species show *S. pimpinellifolium* as the closest wild relative of cultivated tomato, *S. lycopersicum*. *S. pimpinellifolium* is also the source of *Cf-2/Rcr3*, hence the largest pool was screened for this species in this study. *Solanum* species outside tomato included potato and eggplant. Potato species are grouped based on ploidy levels of origin. **(b)** Genus' beyond *Solanum* extended this study to more anciently originated species. Estimated median evolutionary timescales from multiple studies using TimeTree are indicated.

3.2.2 Selection, construction, over-expression and purification of candidate protease inhibitor mutants

To identify valid recognition of candidate inhibitors in our HR screening, we designed experimental controls of corresponding mutant inhibitors by selecting previously identified residues that are essential for inhibitory activity in Avr2 (Van't Klooster et al., 2011), Cip1 (Shindo et al., 2016), EpiC1 and EpiC2B (Tian et al., 2007, Ilyas, 2014). It should be noted that several different inhibitor variants were already screened in reference studies, therefore in this thesis, only least or inactive inhibitor variants were domesticated into cloning and used. Employing a golden-gate based site-directed mutagenesis approach (Weber er al., 2011, Engler et al., 2014), we modified wild-type Avr2, EpiC1, EpiC2B and Cip1 plasmids (**Figure 3.2(a)**) to generate mutant inhibitors.

Avr2 mutant inhibitor was generated by deletion of the six C-terminal residues CFGLCG while deletion of two conserved threonine residues in a conserved NPTTG motif produced Cip1 mutant inhibitor. For construction of EpiC1 and EpiC2B mutant inhibitors, we substituted the central QxVxG motif into NxLxA (**Figure 3.2(b)**). Based on reported studies, all constructed mutants were expected to be soluble proteins, displaying low or no binding affinity towards tomato cysteine proteases. Wild-type and mutant inhibitor proteins were over-expressed in *E. coli* and successfully purified using Ni-NTA affinity chromatography (**Figure 3.2(c)**). Purified proteins were analysed using SDS-PAGE gel electrophoresis and were detected at an apparent molecular weight that is close to the predicted molecular weight (**Figure 3.2(d)**).

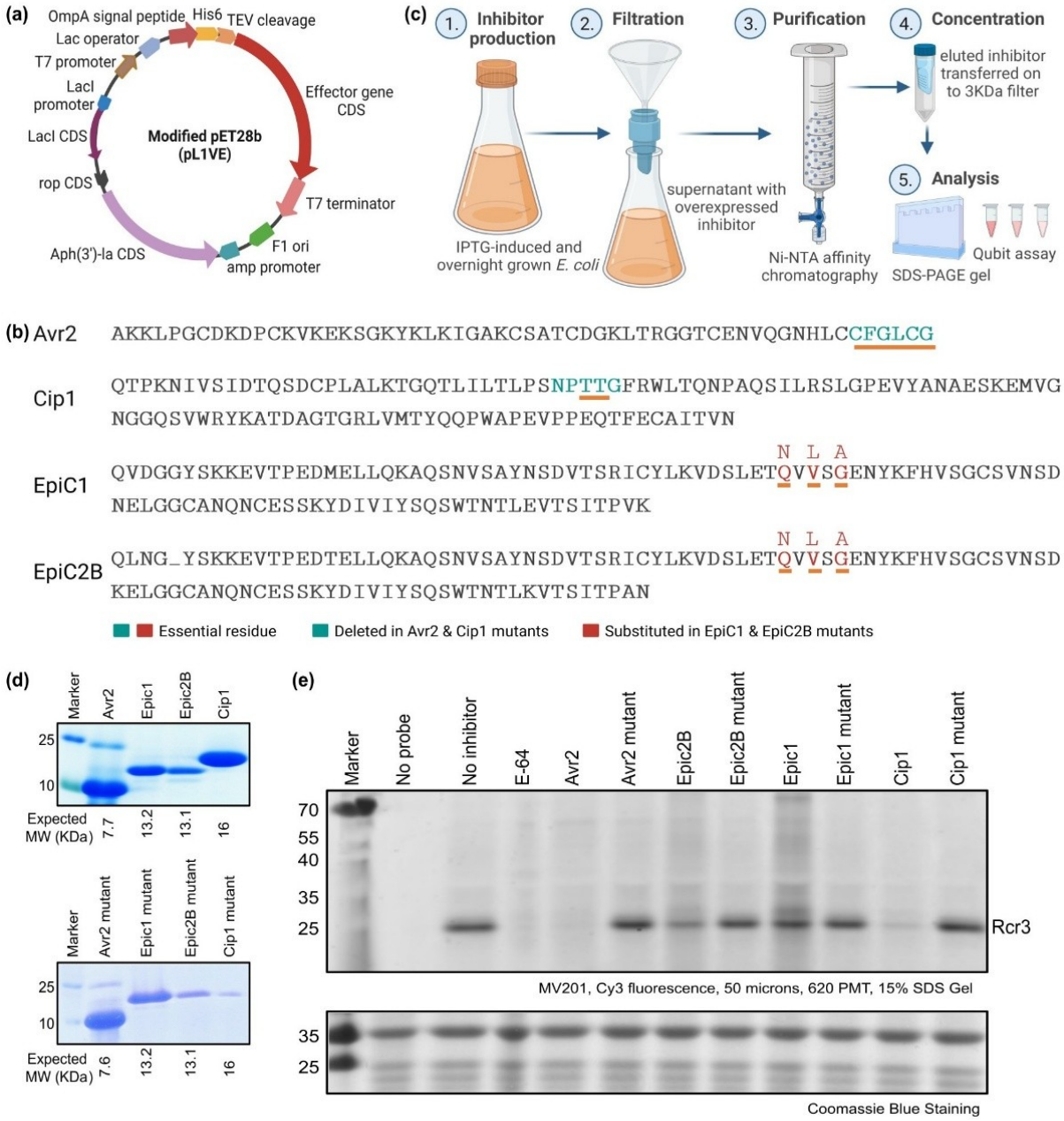


Figure 3.2 Over-expression, purification and activity profiling of recombinant inhibitors.
(a) A modified pET28b golden-gate compatible vector was used for expression of wild-type and mutant inhibitors. **(b)** Mature inhibitor proteins highlighting essential residues that were deleted in Avr2 and Cip1, and substituted in EpiC1 and EpiC2B are undefined in red. **(c)** Illustration of recombinant 6X-His tagged inhibitor expression and Ni-NTA based purification. **(d)** Purified inhibitor proteins were separated on a 15% SDS-PAGE gel and stained with Coomassie blue G-250. **(e)** Competitive activity-based protein profiling was used to test specificity of wild-type and mutant inhibitors against Rcr3, a well-studied tomato papain-like cysteine protease. Apoplastic fluid from *N. benthamiana* leaves containing transiently expressed Rcr3 were pre-incubated with 4 µM of specific inhibitor in labelling buffer. 1 µM MV201 was used to label for 3.5 hrs at room temperature. A no probe reaction, a no inhibitor reaction and a general protease inhibitor (E-64) reaction were used as controls.

3.2.3 Mutant inhibitor proteins do not inhibit Rcr3

To assess the strength of Rcr3 inhibition by purified mutant inhibitors versus wild-type inhibitors, competitive activity-based protein profiling (C-ABPP) fluorescent labelling with MV201 (Richau *et al*., 2012) was performed. Apoplastic fluids from leaves of *Nicotiana benthamiana* transiently expressing Rcr3 were pre-incubated with 4 µM of wild-type or mutant inhibitor in individual reactions for 30 min and further labelled with MV201 for 3.5 hrs at room temperature. A broad range PLCP inhibitor lacking specificity determinants, E-64 (Greenbaum et al., 2002) was included as a positive control and a no inhibitor reaction as a negative control. Consistent with previous studies, this experiment shows strong inhibition of Rcr3 by Avr2 (Rooney et al., 2005, Shabab et al., 2008, van Esse et al., 2008) and Cip1 (Shindo et al., 2016) (**Figure 3.2(e)**). Avr2 and Cip1 mutants were unable to inhibit Rcr3. Further, our C-ABPP result indicate very weak Rcr3 inhibition by EpiC2B and EpiC1, but mutant inhibitors of EpiC1 and EpiC2B, both do not inhibit Rcr3 in our assay (**Figure 3.2(e)**). Already published studies have demonstrated that EpiC1 and EpiC2B inhibit Rcr3 with reduced affinity in contrast to Avr2 (Tian et al., 2007, Song et al., 2009, Kaschani et al., 2010). Therefore, these protease inhibitors and their respective mutants can be used for HR screening in the next section of our study.

3.2.4 Wild-type inhibitors trigger differential HR, whereas their mutants are not recognised clearly in control plant lines and test representative wild tomato and wild potato

As positive and negative control lines for HR screening of our range of populations (**Figure 3.3(a)**), we infiltrated three leaflets of a leaf in eight individual plants of *Cf-2/Rcr3* and *Cf0/Rcr3*, with purified wild-type inhibitor on one leaflet half and mutant inhibitor on the other half. Protein purification buffer was infiltrated as a control to score mechanical damage in

same leaflet. HR severity was monitored up to seven days, post-infiltration and phenotypes were scored in five groups as described in **Figure 3.3(b)**. Similar to previous findings, we observed robust HR upon Avr2 infiltration in *Cf-2/Rcr3*, whereas mutant Avr2 triggered significantly weaker HR (Van't Klooster et al., 2011). However, EpiC1, EpiC2B and Cip1 and their mutants did not induce HR in either control line (**Figure 3.3(c)**), consistent with previous studies (Song et al., 2009; Shindo et al., 2016). We randomly selected a representative population of *S. pimpinellifolium* (LA2401) to identify variation in recognition of four candidate inhibitors. LA2401 displayed the most severe HR symptoms against Avr2 (score = 4), followed by recognition of EpiC2B (score = 3), Cip1 (score = 2) and EpiC1 (score = 1). Further, Avr2 mutant was weakly recognised (score = 1), although no other mutant inhibitor induced HR in LA2401 (**Figure 3.3(c)**).

A representative population of *S. chacoense* (CGN18338), a close diploid wild relative of potato, was also initially tested for recognition against inhibitors. CGN18338 displayed HR phenotype against EpiC2B (score = 3) and EpiC1 (score = 1), but not against their mutants. No HR phenotype was observed against Avr2 and Cip1 or their mutants in CGN18338 (**Figure 3.3(c)**). This demonstrated that purified wild-type inhibitor proteins, but not their respective mutants differentially induce HR in wild tomato and wild potato populations. Multiple concentrations from 1 µM to 5 µM of each inhibitor were tested on *Sp*LA2401 and *Sc*CGN188338 and based on HR phenotypes from 2 to 7 dpi, a concentration of 2 µM for Avr2 and Cip1 inhibitors and 4 µM for EpiC inhibitors was used for assessment of HR in our large pool of remaining 300 Solanaceae populations. A total of 1,58,760 infiltration injections were done in three screening rounds of in total1960 test and control plants.

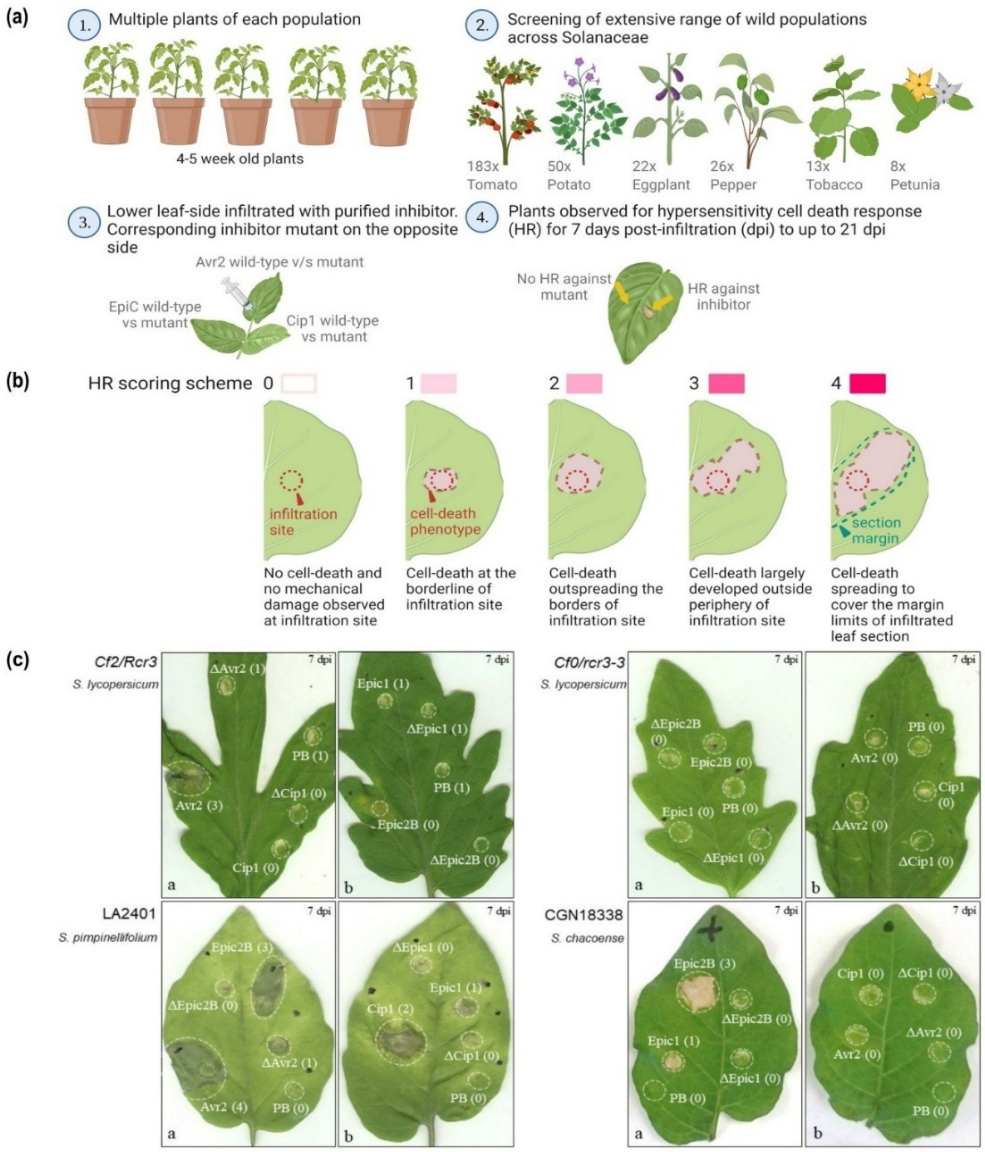


Figure 3.3 Screening of populations for response against four unrelated protein inhibitors.
(a) Illustration summarising hypersensitive response (HR) screening used to identify plants that can recognise Avr2 of *Cladosporium fulvum*, EpiC1 and EpiC2B of *Phytophthora infestans*, and Cip1 of *Pseudomonas syringae*. Eight plants from each tomato population and four plants from all other populations were tested. Number (x) of populations screened are mentioned with each crop; three independent syringae-infiltrations in different leaflets of leaves of same plant were done for each inhibitor. Mutant inhibitors were similarly infiltrated in the opposite leaf half. 2 µM of Avr2, Cip1 and their mutants was infiltrated whereas, 4 µM of EpiC1, EpiC2B and their mutants were used. HR was observed up to 7 dpi in tomato and potato. For other populations, HR was monitored up to 21 dpi. **(b)** Severity of HR symptoms used for numeric scoring (0 to 4) are shown. **(c)** Representative tomato (*S. pimpinellifolium* LA2401) and potato (*S. chacoense* CGN 18338) leaves show difference in inhibitor-induced HR (scores in bracket). Infiltration with 2 µM Tris-imidazole purification buffer (PB) was included as a negative control. Mutant inhibitor response was compared to PB, then HR against wild-type inhibitor was scored versus mutant. MM-*Cf-2/Rcr3* and MM-*Cf0/rcr3-3* tomato lines represented positive and negative control lines to show specific recognition of Avr2.

3.2.5 *Solanum pimpinellifolium* recognise Avr2 throughout distribution range with heterogeneity in HR in plants of same or different populations

Our first aim was to survey diverse *S. pimpinellifolium* populations for Avr2 recognition assessment in individuals of the same or different populations. This experiment analysed 896 plants, eight plants each from 112 *S. pimpinellifolium* populations across all regions. A total of 72,576 injections were done in three screening rounds of 112 populations. We infiltrated each inhibitor into three leaflets of each plant and combined the HR score of each plant for each inhibitor and its mutant in hierarchically clustered complex-map to establish response variations (**Figure 3.4**). These populations were first structured into four geographical regions: A (Ecuador: Carchi, El Oro, Galapagos Islands, Guayas, Loja, Los Rios and Manabi), B (North: Amazonas, Cajamarca, La Libertad, Lambayeque, Piura and Tumbes), C (Centre: Ancash and Lima), and D (South: Arequipa, Cusco and Ica), to represent variety of origin micro-habitats so that any variations in HR reveal local adaptations against inhibitors of multiple pathogens within same or different individual plants or populations. We observed that five of tested 17 total populations in region A responded to Avr2, where LA1263 and LA2933 had only one responsive plant each, LA0413 and LA1428 had three responsive plants each and LA2097 had five Avr2 responsive plants. However, not one population in this region displayed strong HR symptoms (score 3 or 4). Only three plants had moderate HR inductions of score 2 while ten plants showed HR score 1. The Avr2 mutant induced a weak HR only in one plant of LA0413 and not in any other population in region A (**Figure 3.4**).

As we move from region A to region B, Avr2 responsiveness is slightly increased, with 13 of 37 the tested populations showing Avr2-induced HR. Only LA1618 and LA2535 have one responsive plant while LA2181, LA2147, LA0114 and LA0400 contain two Avr2-responsive plants. In the remaining seven responsive populations, we observed three or more Avr2-

responsive plants out of eight tested plants each. While no population was found to be Avr2-responsive in all the eight plants, LA1589 had the most Avr2 response with six positive plants. Weak response (score 1) was also noted against Avr2 mutant in three plants, each from LA2186, LA1631 and LA0114. However, similar to region A, we observed that HR induction was mostly weak to moderate in region B, where 31 plants demonstrated HR score 1 and HR score 2 being noted in eight plants. Seven plants were identified to respond to Avr2 mutant, all with HR score 1 (**Figure 3.4**).

Moving onto region C, we noted a further increase in the number of Avr2 recognising populations, where 29 out of 39 tested populations responded. We identified LA1992 from Lima having Avr2 recognition ability in all eight of the tested plants, three showing HR score 2 and HR score 1 in remaining five. Furthermore, three populations, LA0375, LA1572 and LA0753 had seven responsive plants each. LA0375 responsive plants only displayed HR scores 4 (six plants) and 3 (one plant), whereas all responsive individuals in LA0753 showed HR with score 1. Five populations, LA1659, LA1342, LA1269, LA1602 and LA1280, had one Avr2 recognising plant each. Also, plants with an induced robust HR phenotype were frequently found in this region, where 24 plants responded with HR score 4 and 16 plants with HR score 3. Further 38 plants responded with HR score 2 and 30 plants were assessed showing HR score 1 (**Figure 3.4**).

In region D, our analysis showed that 14 out of 17 examined populations had HR triggered upon Avr2 infiltration. Although we recorded mostly weaker HR responses, where 29 plants had HR score 1 and eight responsive plants had HR score 2. Three plants in LA1679 (two with score 3 and one with score 4) and one plant (score 3) in LA1630 further indicate strong Avr2 recognition response (**Figure 3.4**). Our data demonstrate that Avr2 responsiveness in *S. pimpinellifolium* gradually increases in frequency along its Centres of origin from Ecuador (region A) to North Peru (region B), moving towards Centre Peru (region C) to highest responsiveness existing in the South Peru (region D). Avr2 responsive populations are

present throughout origin ranges, but concentrated in Ancash and Lima in the Centre and Ica in the South. Furthermore, the results uncover the diversity in HR phenotypes and natural variation in recognition of same inhibitor by individuals of the same population as well as between different populations of the same regions.

3.2.6 Inhibitor recognition in *S. pimpinellifolium*

Simultaneously to Avr2 response estimation in *S. pimpinellifolium* populations, we also evaluated if protease inhibitors from other pathogens (Shindo et al., 2016, Kaschani et al., 2010) can trigger HR. We infiltrated EpiC1, EpiC2B and Cip1 versus their mutants as described in **Figure 3.3**. In region A, no response against EpiCs or Cip1 was observed (**Figure 3.4**). In region B, we identified three of the 17 populations triggered HR against EpiC1, EpiC2B (LA2186, LA1589 and LA1578) and Cip1 (LA2186, LA1631 and LA0114). Only LA2186 can recognise all four unrelated inhibitors and trigger HR with variable strengths. 50% of the tested individuals of LA2186 recognise EpiC1, EpiC2B and Cip1, however, recognition is not always conferred by the same responsive individual. While all populations recognising EpiC1, EpiC2B and Cip1 also recognise Avr2, plants within a population may not confer recognition to both Avr2 and another inhibitor. Weaker HR (score 1) against mutants of EpiC1 and EpiC2B were also observed in two and three plants, respectively. No HR was observed in response to mutant Cip1 inhibitor. Further, only HR score 1 or 2 was visible against EpiCs and Cip1, only one but two different plants in LA2186 recognised EpiC2B and Cip1 with strong HR (score 3) (**Figure 3.4**).

In region C, 13 out of 39 populations had plants showing HR against Cip1 and three populations also showing HR with Cip1-induced HR (score 1). EpiC1 was recognised by 11 populations in region C while EpiC2B triggered HR in 12 populations (**Figure 3.4**). In region D, 11 of 13 tested populations responded to Avr2. Cip1 induced HR in five populations,

whereas four populations showed EpiC2B recognition and only two populations recognised EpiC1 (**Figure 3.4**).

Overall, out of 112 total tested *S. pimpinellifolium* populations consisting of a total of 896 test plants, 50 populations did not respond to any of the four inhibitors and their mutants. 61 populations had 201 plants responsive towards Avr2, but only 107 plants from 33 populations specifically recognised Avr2. We identified 62 plants from 22 populations showing HR against Cip1, where only 12 plants particularly recognised Cip1. 21 populations recognised EpiC2B whereas 17 populations recognised EpiC1 (**Figure 3.4**). While all the populations recognising EpiC2B and EpiC1 had plants responsive to Avr2, we identified individual recognition of EpiC2B and EpiC1 in 9 out of 70 plants responsive to EpiC2B and 2 out of 56 responsive plants against EpiC1. Mutant Avr2 triggered weak HR in 53 plants from 16 populations, however, only one plant specifically recognised mutant Avr2 without recognising wild type Avr2 or any other inhibitor. Four plants from four populations responded to mutant Cip1 and all these plants also recognised wild type Cip1. While 13 plants from eight populations and seven plants from five populations responded to mutant EpiC2B and mutant EpiC1, respectively, no plant showed HR in the absence of wild type EpiC2B and EpiC1 recognition. 17 plants, five plants from LA0753, two plants each from LA2186, LA0375, LA2401 and one plant each from LA1597, LA1520, LA1572, LA1614, LA2982 and LA1679 recognised all four inhibitors, but none of the mutants (**Figure 3.4**).



Figure 3.4 *Solanum pimpinellifolium* populations show variation in recognition of unrelated inhibitors and their mutants that target convergent apoplastic cysteine proteases with differential affinities.

Hierarchical clustering using a pre-defined Euclidean distance method and ComplexMap of all populations separated by geographical regions (A to D: Ecuador, North, Centre and South) allows visual representation of three or more variables in an experiment. Each row represents a population on y-axis (n = 112) and population's square represented on x-axis (P1 to P8; n = 896 plants) in each

row represent individual plants tested for a population. Eight plants per population were evaluated. Colour of squares indicate strength of HR phenotype (0 to 4). Average HR scores from three infiltrations in three rounds of screenings are shown. Tomato MM-*Cf-2/Rcr3* and MM-*Cf0/Rcr3* lines were assayed as reference. Populations on the left side of y-axis are clustered on basis of their overall similarity in response among populations within a geographic region represented on right side of y-axis. Plants are vertically clustered by response variations against an inhibitor and corresponding mutant within the same panel. Plants P1 to P8 on top are automatically clustered based on algorithm detection of responsive plants across populations in vertical panel. *R script and input scoring data are attached as supplementary S3.3.

Furthermore, we observed extensive variations in the strength of HR symptoms against each inhibitor by scoring HR on an ascending level of 0 to 4 (described in **Figure 3.3(b)**). Interestingly, 25 plants showed HR score 4 against Avr2 and only one plant against Cip1, while EpiC1 and EpiC2B did not trigger HR with score 4. HR score 3 was only scored in 21 plants against Avr2 and five plants against EpiC2B. HR score 2 was noted towards all inhibitor infiltrations, with 56 plants inducing it against Avr2, 34 plants against EpiC1, 33 plants against EpiC2B and 31 plants against Cip1. With 100 scored plants, HR score 1 was most frequently observed in response to Avr2, followed by 33 plants upon EpiC2B infiltration, 30 against Cip1 and 21 against EpiC1 (**Figure 3.4**). Further, we noted that the responsiveness to inhibitor mutants were significantly lower in comparison to their corresponding wild-type inhibitors. Avr2 mutant triggered the highest response with 53 plants displaying HR against it; 51 plants with HR score 1 and only two plants with score 2. 13 plants responded to EpiC2B mutant, where all the plants displayed HR score 1. Only seven plants recognised EpiC1 mutant and all displayed HR score 1. Cip1 mutant was the least recognised inhibitor, where only four plants conferred its recognition with HR score 1 (**Figure 3.4**). Comprehensively in *S. pimpinellifolium*, Avr2 is the most recognised inhibitor, followed by EpiC2B, Cip1 and EpiC1. Ascertained HR induction variations in populations of same species indicate the presence of genetic polymorphism underlying recognition of inhibitors from unrelated pathogens of tomato across geographies of origin.

3.2.7 Inhibitor recognition in wild tomato

Once HR phenotypes were well-established toward Avr2, Cip1, EpiC1 and EpiC2B in *S. pimpinellifolium*, we subsequently explored whether more distantly related and anciently evolved wild tomato species have the capability of recognising any or all of these inhibitors. We tested wild tomato species that were available at TGRC, spanning climate variations from most geographical origins structured in this study as: A (Colombia and Ecuador: Antioquia, Galapagos Islands, Loja, Pichincha and Zamora-Chinchipe), B (North: Amazonas, Cajamarca and La Libertad), C (Centre: Ancash, Ayacucho, Huanuco and Lima), D (South: Apurimac, Arequipa, Cusco, Ica, Moquegua and Tacna) and E (Chile: Antofagasta, Arica-Parinacota and Trapaca).

568 plants of 71 populations, representing 14 distantly related and four outgroup wild tomato species, were specifically infiltrated with Avr2, EpiC1, EpiC2B, Cip1 and their mutants. A total of 46,008 injections were done in three screening rounds of 71 populations. 64 infiltrated plants developed HR against Avr2 and responsive plants belong to 18 populations of nine species (**Figure 3.5**). We also observed response upon Avr2 mutant infiltrations in 20 plants of 11 populations of eight species. HR upon Cip1 infiltration was observed in 32 plants of nine populations of eight species, but mutant Cip1 did not induce HR in any plant. 23 plants from nine populations representing five species were responsive towards EpiC2B whereas 18 plants from six populations of five species recognised EpiC1. 48 populations from 17 species were non-responsive to any inhibitor treatment. Further, no population consisted all eight tested plants showing response against an inhibitor. Four plants from two populations of two species responded to EpiC2B mutant but no plant was observed to show response against EpiC1 mutant.

Of 11 populations in region A, three in-group populations had plants responsive against Avr2 and Cip1, but no responsiveness for EpiC1 or EpiC2B was noted. LA0532 and *S.*

cheesmaniae LA1043 had same plant recognising both Avr2 and Cip1, while *S. galapagense* LA0528 and *S. neorickii* LA2113, respectively responded to Avr2 and Cip1. In region A, only two populations (LA0532 and LA1043) showed HR symptoms against mutant Avr2. However, inhibitor mutants of Cip1, EpiC1 and EpiC2B did not trigger HR in region A (**Figure 3.5**).

Of eight populations in region B, *S. habrochaites* LA1353 and *S. arcanum* LA1346 responded to Avr2, where EpiC1, EpiC2B, mutants of Avr2 and EpiC2B were recognised additionally to Avr2 within same plant of LA1353. Only *S. arcanum* LA2157 showed Cip1-associated HR in region B while no response to mutant Cip1 was noted (**Figure 3.5**). In region C, six of 18 populations responded to Avr2 and five to mutant Avr2. Four populations recognised EpiC2B while EpiC1 and Cip1 were recognised by two populations each. *S. pennellii* LA1272 in region C is the only distant wild tomato species that conferred recognition of all four wild-type inhibitors, although EpiCs and Cip1 triggered HR in association with Avr2 in different plants (**Figure 3.5**).

Seven and two of 23 tested wild tomato populations in region D showed HR against Avr2 and its mutant, respectively. Four populations in region D responded to EpiC2B, where same plants of *S. pennellii* LA0716 and different plants of LA1932 were found to develop HR against EpiC2B as well as Avr2. In region D, EpiC1 and Cip1 induced HR in two populations each, with same plants of *S. corneliomulleri* LA1937 responding to Cip1, EpiC1 and EpiC2B. Further, *S. chmielewskii* LA2663 had same plants recognising Avr2 and Cip1 whereas, an individual of *S. chilense* LA1960 responded to EpiC1 and EpiC2B but conferred recognition of Avr2 in different individual plants (**Figure 3.5**).

In region E, we failed to observe any responsiveness towards Avr2, EpiCs or their mutants, but two individuals of an outgroup tomato species, *S. lycopersicoides* LA2730 recognised Cip1. 34 plants were responsive to Avr2, 23 plants particularly to Cip1, three plants

recognised only EpiC2B and only plant developed only EpiC1-associated HR. Any plant that exhibited responsiveness to a mutant inhibitor also recognised one or more inhibitors (**Figure 3.5**).

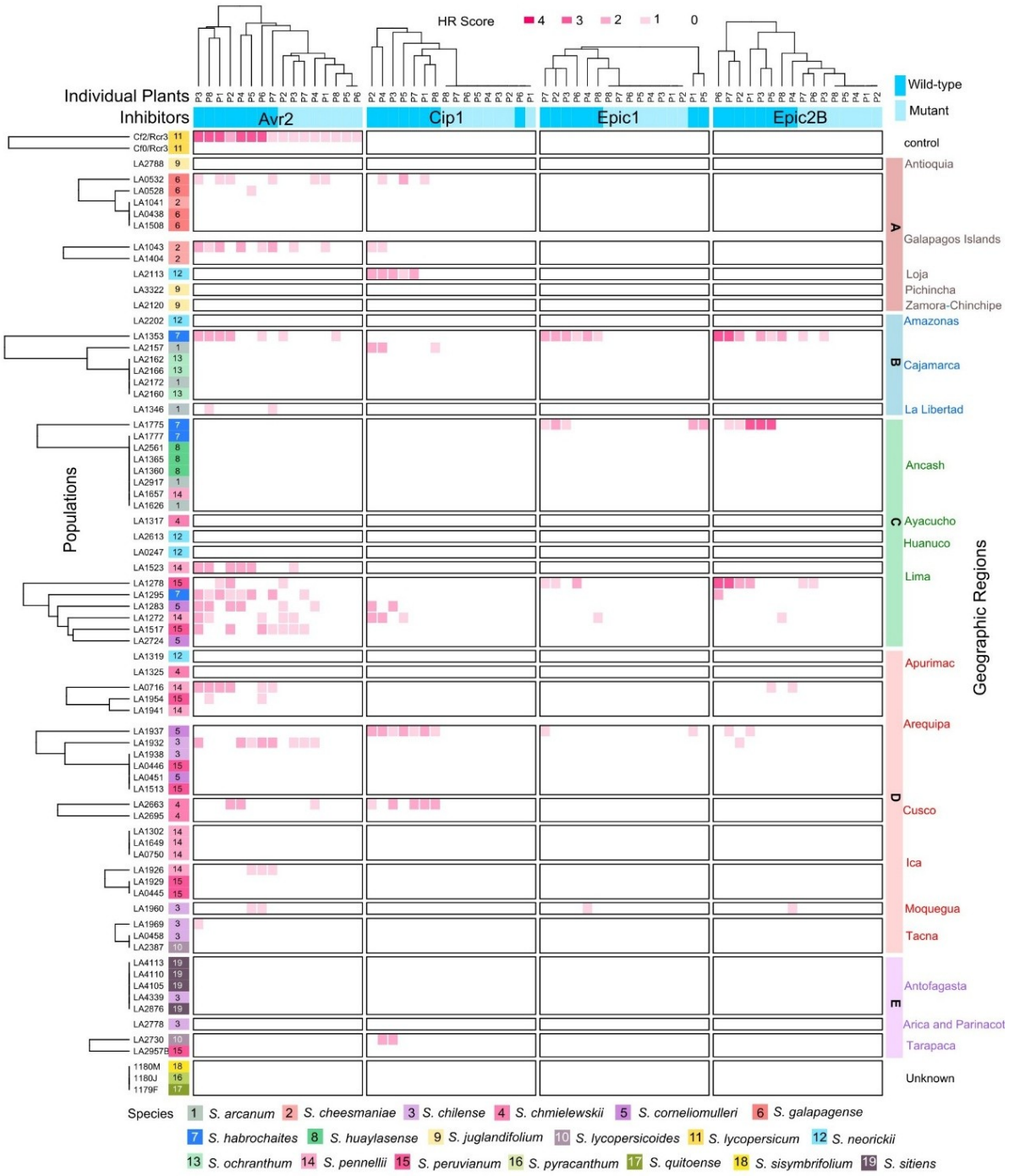


Figure 3.5 Wild tomato species show inter-specific and intra-specific differences in recognition against four inhibitors and their mutants tested in this study.

A ComplexMap and hierarchical clustering of wild tomato populations show variation in HR phenotype among species from a similar and distant geographical landscapes. Each row is a

population (n = 71 populations). Dendrogram on top cluster individuals of specific population on basis of response against an inhibitor and its mutant. Three leaves were infiltrated per plant (P1 to P8) and three independent HR screenings were conducted. Average response scores (0 to 4) are indicated as a square representing each plant score (n = 568 plants). MM-*Cf-2* and MM-*Cf0* were included as control lines. Grouping on left panel indicate closeness based on response to inhibitors. Right panel show geographical sectioning (A to E; Ecuador, North, Centre, South and Chile) of populations. *R script and input scoring data are attached as supplementary S3.4.

The relative severity of HR symptoms scored upon each inhibitor infiltration showed variations similar to those observed in *S. pimpinellifolium* in this study, except that robust HR score 4 was not observed in screening of remaining wild tomato relatives. Comparatively, stronger HR phenotypes (score 3) were only induced in six plants by EpiC2B whereas only HR score 1 and 2 were triggered by Avr2, Cip1 and EpiC1. Overall, the weakest HR score 1 was noted in 28 plants upon Avr2 infiltration, 11 plants upon Cip1 infiltrations and ten plants each upon EpiC1 and EpiC2B infiltrations. Further, HR score 1 was also observed in 20 plants against mutant Avr2 and all four plants responsive to mutant EpiC2B. 36 responsive plants were identified with score 2 against Avr2 while 21 plants were scored against Cip1. Eight and six plants respectively were observed with HR score 2 upon EpiC1 and EpiC2B infiltrations (**Figure 3.5**).

These results suggest that Avr2 recognition is conserved in distantly evolved wild tomato species, *S. cheesmaniae*, *S. galapagense*, *S. arcanum*, *S. chmielewskii*, *S. peruvianum*, *S. corneliomulleri*, *S. chilense* and *S. penellii*, but not in the most anciently evolved outgroup species, *S. ochranthum*, *S. sitiens*, *S. juglandifoliu*m and *S. lycopersicoides*. Moreover, through genus-wide HR screening, we identified that responsive and non-responsive plants recognising multiple unrelated inhibitors exist within same population as well as in same species. In addition to Avr2 and mutant Avr2 response concentration in Centre region C, responsive populations towards Cip1, EpiC1 and EpiC2B were also notable in this region. Populations from Chile (region E) exhibited HR response only against Cip1. Further, the differences in HR induction by multiple inhibitors indicate the existing diverseness in

perception of specific inhibitor within population of a species and among populations of different species.

3.2.8 Inhibitor recognition in wild potato populations

We further extended our inhibitor recognition profiling to wild potato and analysed 50 populations from three origin ranges we characterised as Region A: Mexico and Guatemala, Region B: Bolivia, Chile and Peru and Region C: Argentina and Paraguay. A total of 16,200 injections were done in three screening assays of 50 populations (**Figure 3.6**). All wild-type inhibitors and mutant EpiC2B were mostly recognised by a single plant from each of the three populations: *S. demissum* CGN17767 and CGN17815 from Mexico and *S. infundibuliforme* CGN17720 from Bolivia. Four plants per population were assessed and only *S. verrucosum* CGN17767 from Mexico and *S. chacoense* CGN24850 from Bolivia had all plants responding to Avr2 and EpiC2B, respectively (**Figure 3.6**). We did not detect the presence of any inhibitor-associated HR in multiple screening rounds in land variety. Two of eight populations from Guatemala, CGN22732 and CGN21363, both *S. bulbocastanum* responded to EpiC2B. Further, of seven populations from Peru, *S. orophilum* CGN23985 had response only against EpiC2B whereas *S. chacoense* CGN23044 responded to both EpiC1 and EpiC2B but not to their mutants. Similarly, the only representative population, *S. chacoense* CGN18338 from Paraguay recognised only wild-type EpiC1 and EpiC2B.

Interestingly, *S. venturii* CGN17755 from Argentina responded to Cip1 but not its mutant, inducing a weak HR in three of four tested plants. We did not identify any population that responded only to Avr2, however one plant from CGN17720 and two plants from *S. gourlayi* CGN24384 specifically identified Avr2 (**Figure 3.6**). Of 200 tested wild potato plants, we found 13 plants representing six populations were responsive to Avr2, eight plants from four populations to Cip1, 23 plants from 13 populations to EpiC1 and 47 plants depicting responsiveness of 23 populations to EpiC2B. Significantly lower recognition of mutant

inhibitors was also observed, where two plants, one each from CGN17815 and CGN24384 responded to mutant Avr2, two plants from CGN17720 to EpiC1 and 17 plants from 12 different populations to EpiC2B (**Figure 3.6**). There were also comparative variations in HR developed in response to different inhibitors. The highest HR score 4 was notable only against EpiC2B in six plants representing four populations from different regions. HR score 3 was prominent only against EpiC2B in 14 plants of 11 populations across regions and in two plants of CGN17720 upon EpiC1 infiltration. We noted HR score 2 against Avr2 in six plants, Cip1 and EpiC1 in five plants each, EpiC2B in ten plants and towards mutant EpiC2B in one plant. Overall, the weakest HR score 1 was induced by Avr2 in seven plants and in two plants by its mutant, by Cip1 in three plants, by EpiC1 in 16 plants versus in two plants by its mutant and by EpiC2B in 17 plants versus in 16 plants by its mutant (**Figure 3.6**).

The investigation of wild potato populations for response towards multiple inhibitors clearly show the occurrence of recognition across environmental conditions as well as the difference between common recognition of EpiCs in wild potato as compared to wild tomato. Although Avr2 and Cip1 failed to induce HR in distant wild potato, *S. bulbocastanum*, they are inconsistently recognised in South diploids and polyploid species of wild potato. A diverging inhibitor recognition pattern is present between native hosts, for Avr2 in wild tomato and EpiCs wild potato. Further, wild potato outgroup, *S. palustre*, originating from Chile and Argentina did not recognise any inhibitor, indicating the in-group restrictions of recognition specificities for Avr2, Cip1, EpiC1 and EpiC2B.

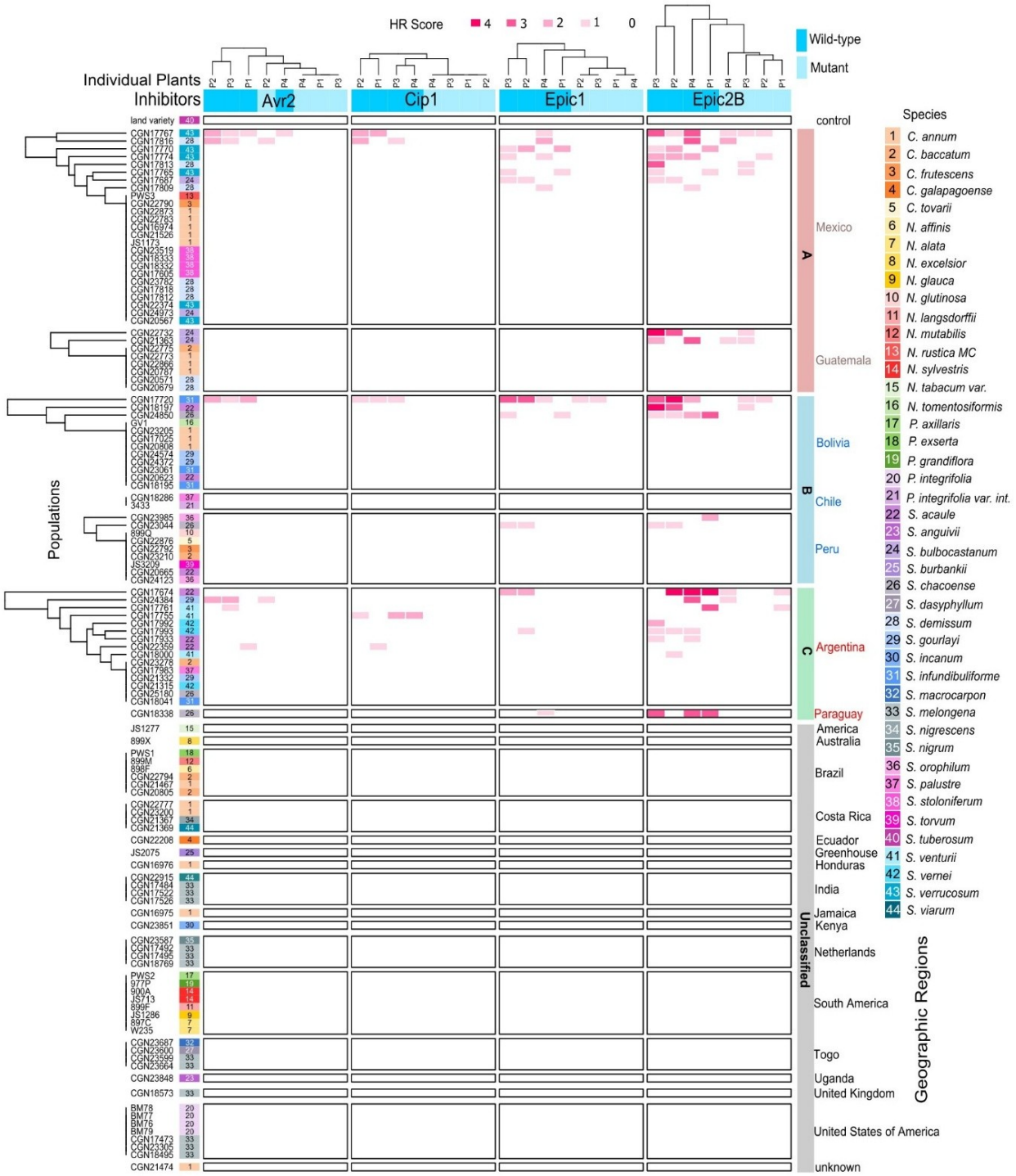


Figure 3.6 Inhibitor associated HR is induced in wild potato populations, but not in species beyond potato.

A cell-death response phenotype ComplexMap constructed using a Euclidean distance method showing variation in recognition of four different inhibitors. Populations as rows on left panel of y-axis are for potato species are clustered based on responsiveness within a region. Four plants (P1 to P4) from each population of potato (n = 50), eggplant (n = 22), pepper (n = 26), petunia (n = 8) and tobacco (n = 13) were treated with three infiltrations per plant per screening round. Average HR scores of each plant are indicated (0 to 4) as square in a row. Only potato populations were

responsive and clustering on x- and y-axis is similarly to analysis in figure 3.4. Other species were non-responsive, hence are region-wise unclassified. Land variety (*S. tuberosum*) was used as in-group control. MM-*Cf-2* and MM-*Cf0 t*omato lines in figures 3.4 and 3.5 represent overall HR assay controls in this study. *R script and input scoring data are attached as supplementary S3.5.

3.2.9 Inhibitor recognition in other solanaceous plants

To widen our search of populations responsive to unrelated inhibitors across Solanaceae family, we investigated plant species beyond tomato and potato (**Figure 3.6**). Of 88 plants representing 22 populations from ten cultivated and wild species of eggplant, we did not observe HR against any inhibitor treatment in three independent rounds of screening (**supplementary 3.1**). 104 plants from 26 populations of five cultivated and wild pepper populations also did not develop HR towards any inhibitor. Further, all 52 plants representative of 13 populations from 11 tobacco species, including most anciently evolved wild relative *N. tomentosiformis*, were non-responsive for all inhibitor infiltrations. We tested 36 plants from eight populations of four petunia species and did not detect HR phenotype against any inhibitor (**Figure 3.6**). A total of 22,356 injections were done in three HR assays for a total of 69 populations of other solanaceous plants. Our findings show that eggplant, pepper, tobacco and petunia species do not show visible HR opposite to any inhibitor infiltration, thereby suggesting that recognition specificities for Avr2, Cip1, EpiC1 and EpiC2B did not evolve beyond tomato and potato.

3.2.10 Recognition frequencies differ between geographic regions

Our HR analysis indicated that *S. pimpinellifolium*, wild tomato and wild potato from different regions harbour unique variations as local populations displayed visible differences in different inhibitor-associated HR (**Figures 3.4 3.5 and 3.6**). Therefore, to compare the recognition frequency, we estimated regional responses to each inhibitor. In *S. pimpinellifolium,* plants with highest responsiveness to all inhibitors were noticeable in the

Centre (region C) with a decreasing frequency order of 33.6% Avr2, 15.4% EpiC2B, 13.1% EpiC1, 11.8% Cip1, 2.9% mutant EpiC2B, 2.5% mutant Avr2, 1.6% mutant EpiC1 and 1% mutant Cip1 (**Figure 3.7**). The second highest responsiveness to all inhibitors, except mutant EpiCs, was observed in the South (region D) with specific recognition frequencies of 31.6% Avr2, 11.1% EpiC2B, 10.3% Cip1, 5.9% EpiC1, 4.4% mutant Avr2, 0.7% mutant Cip1 and 0.7% mutant EpiC2B. While percentage of total tested *S. pimpinellifolium* plants were the same in North (region B) and Centre, inhibitor recognition frequency was the third highest in North with frequencies 12.8% Avr2, 3.5% Cip1, 2.2% each of EpiC1, EpiC2B and mutant Avr2, with exceptions of mutant 1% EpiC2B and 0.6% mutant EpiC1. Avr2 and its mutant recognition frequency in *S. pimpinellifolium* were the least in Ecuador (region A), 9.5% and 0.7% respectively, with plants not responding to remaining inhibitors (**Figure 3.7**).

As was observed in *S. pimpinellifolium*, recognition frequency of Avr2 in other wild tomato species was highest in the Centre (16.7%), followed by South (11.4%), North (10.9%) and Ecuador (10.6%). Further, most response frequency to mutant Avr2 was found in Centre region. In contrast to *S. pimpinellifolium*, the maximum recognition frequency for EpiC1 (9.4%), EpiC2B (9.4%) and mutant EpiC2B (3.1%) in other wild tomato species were noted in North and not South. However, second highest recognition frequency for EpiC1 (6.2%), EpiC2B (7.6%) and mutant EpiC2B (1.4%) in other wild tomato species was observed in Centre (**Figure 3.7**). While no *S. pimpinellifolium* plant with response to Cip1 was found in region A, the highest Cip1 recognition frequency in other wild tomato species was determined in region A (9.6%), followed by regions D (6.5%), B (4.7%) and C (3.5%). Recognition frequencies of EpiC1 (1.6%), EpiC2B (2.7%) and Cip1 (6.5%) in South were significantly lower than in North and Centre for other wild tomato species (**Figure 3.7**).

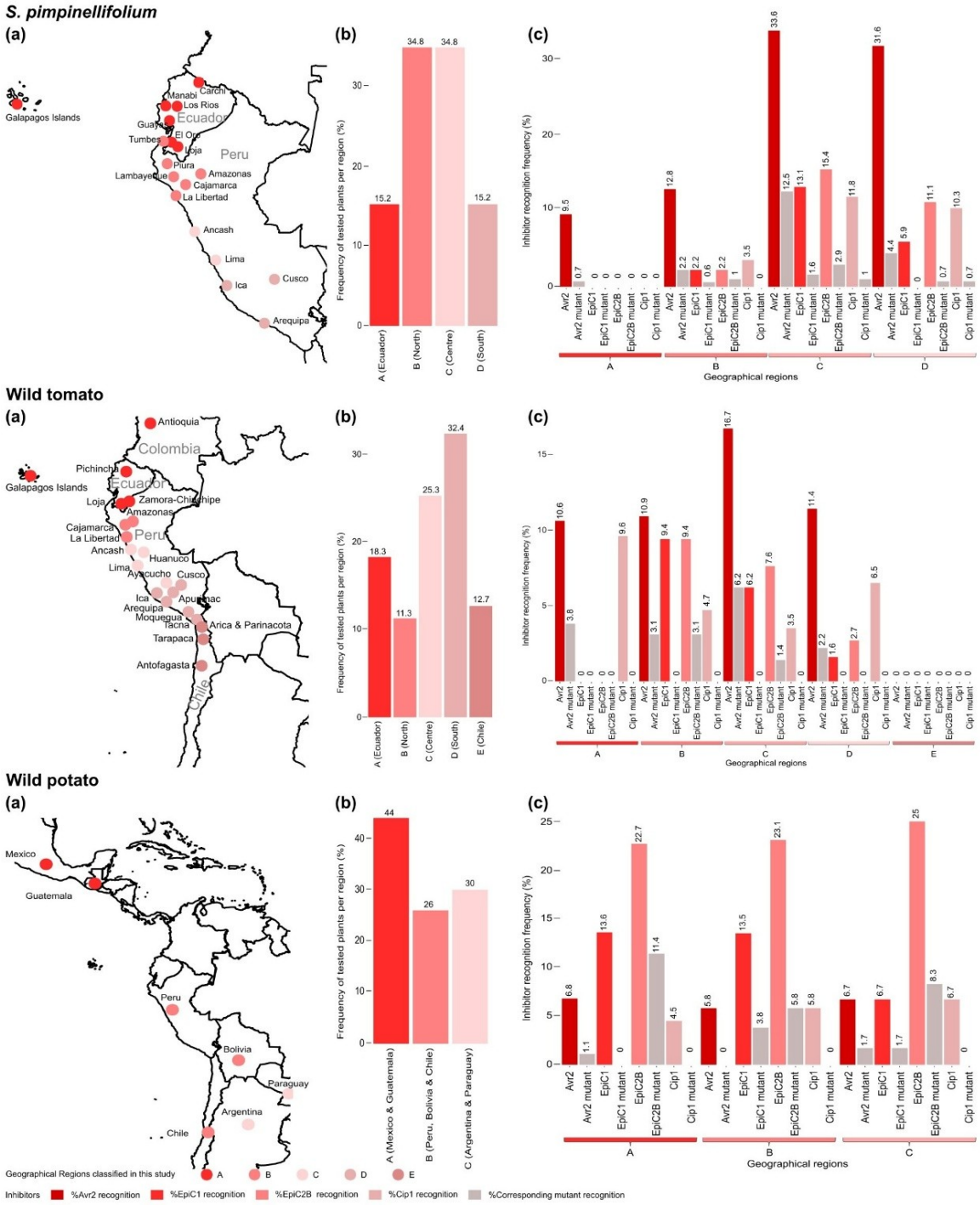


Figure 3.7 Estimated relative frequencies of inhibitor recognition reveal geographic disparity. Relative frequency distribution plots showing recognition of different inhibitors vs their mutants in different **(a)** geographical regions of population origin (Regions A to D for *S. pimpinellifolium*; A to E for wild tomato and A to C for wild potato, detailed in Materials & Methods chapter). **(b)** Frequency of tested plants for each region was estimated by dividing number of plants from all populations in a region by total plants tested for a group, for instance *S. pimpinellifolium*. **(c)** Relative recognition frequency (%) in a region (for example A) is expressed as number of plants responsive against a specific inhibitor (e.g. Avr2) divided by total number of plants in a given region. Average HR scores 0 to 4, from three independent assays were all included to calculate the frequencies.

Wild potato populations from region A, showed maximum response frequencies toward Avr2 (6.8%) and EpiC1 (13.6%), whereas highest response frequencies for Cip1 (6.7%) and EpiC2B (25%) were inferred in region C (**Figure 3.7**). Region B had the second most response frequency against Cip1 (5.8%), EpiC1 (13.5%) and EpiC2B (23.1%) while region C showed it for Avr2 (6.7%). Responsiveness to Avr2 and Cip1 is similar in regions B and C, however, significant difference is observed toward EpiC1 and EpiC2B in these regions. Mutant inhibitors also caused response with highest frequencies for EpiC2B (11.4%) in region A, for EpiC1 in region B (3.8%) and for Avr2 in region C (1.7%) (**Figure 3.7**). Inhibitor recognition regional frequencies are inconsistently and independently distributed in wild potato and wild tomato as compared to *S. pimpinellifolium*.

3.2.11 Inhibitor recognition varies by altitude

Altitude changes can profoundly impact the inhibitor recognition dynamics in locally adapted populations of same species, possibly due to environmental factors such as temperature and light (Yang et al., 2022). Therefore, we estimated cumulative recognition frequency by distinguishing tested populations across eight altitude ranges (in metres), 0 (sea level) to 500, 501 to 1000, 1001 to 1500, 1501 to 2000, 2001 to 2500, 2501 to 3000, 3001 to 3500 and 3501 to 4000. Most of *S. pimpinellifolium* (70.5%) and wild tomato (21.1%) plants were tested from sea level to 500 metres and maximum recognition frequency of Avr2 in *S. pimpinellifolium* (25.3%) and wild tomato (23.3%) was observed at this range (**Figure 3.8**). Further, altitude frequency of EpiC2B (8.1%), Cip1 (7.4%) in *S. pimpinellifolium* and most common recognition of mutants of Avr2 (7.4%), EpiC1 (0.95%) and Cip1 (0.5%) also occurred at sea level to 500 range. While 6% of tested wild potato plants belong to 0 to 500 metres category, only EpiC2B induced HR resulting in 41.7% of altitude recognition frequency.

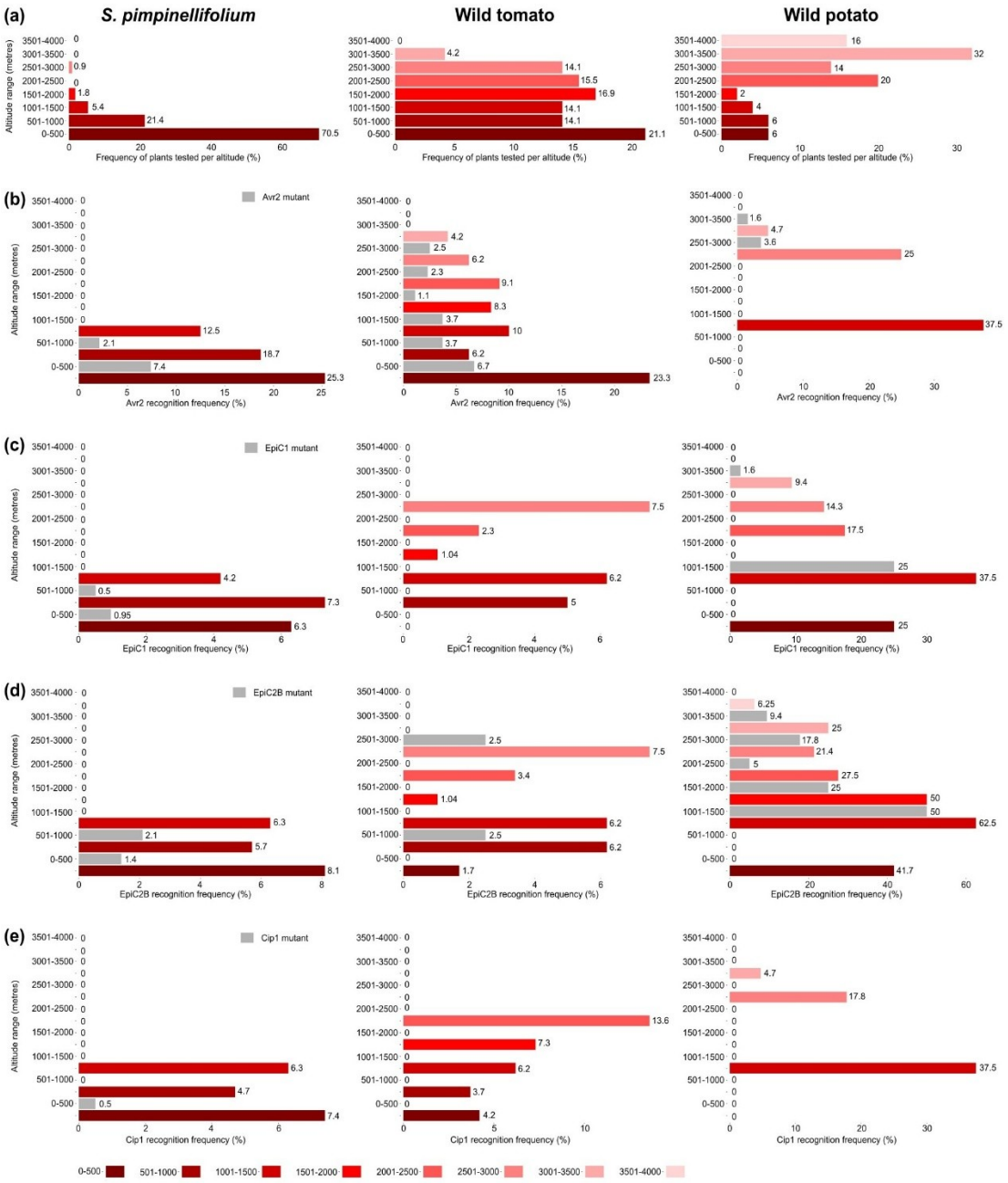


Figure 3.8. Altitude distribution of recognition frequencies against wild type and mutant inhibitors.

(a) Natural population distribution for *S. piminellifolium* in this study ranged from sea level (0) to 3000 metres, 0 to 3500 metres for wild tomato and 0 to 4000 metres for wild potato. Altitudes are distinctly classified into eight ranges 0 to 4000 metres. Percentage of tested plants in a range was estimated as number of plants for a particular group (*S. pimpinellifolium*, wild tomato or wild potato) in given range divided by the total number of tested plants of a group across all altitudes. **(b)** Relative altitude response frequency against Avr2 was calculated as number of plants responsive against Avr2 at a specific altitude range divided by total number of plants tested across a given altitude range of a group. Similarly, relative recognition frequency against EpiC1 **(c)**, EpiC2B **(d)** and Cip1 **(e)** were estimated. Average response HR scores (1 to 4) from three independent screenings were included. *R script and input data are attached as supplementary S3.6.

At 1001 to 1500 metres elevation, Avr2 response frequency was the highest in wild potato (37.5%), second highest in wild tomato (10%) and least in *S. pimpinellifolium* (12.5%). Highest response frequency of EpiC1 (37.5%), EpiC2B (62.5%) and Cip1 (37.5%) were also observed at 1001 to 1500 metres level (**Figure 3.8**). No inhibitor or their corresponding mutants were recognised beyond 1500 metres in *S. pimpinellifolium*, but we noted irregularly increased response frequencies for all wild-type inhibitors in wild tomato and potato.

Interestingly, plants from top altitude levels constituted maximum response frequency in wild tomato, with 7.5% each for EpiC1 and EpiC2B at 2501 to 3000 metres level and 13.6% at 2001 to 2500 metres level. Moreover, we observed responsiveness to all inhibitors and most mutants at altitudes extended up to 4000 metres in wild potato. At the highest altitude category of 3501 to 4000 metres, only EpiC2B recognition in wild potato with 6.25% frequency was estimated (**Figure 3.8**).

These results suggest that there was no directional altitude response frequency trend consistent for all inhibitors across *S. pimpinellifolium*, wild tomato and wild potato. However, an inconsistent pattern of decrease in Avr2 response frequency as we move from sea level to 500 metres upward to highest response range is common in each group. Further, throughout increasing altitude range, response frequency of EpiC1, EpiC2B and Cip1 is irregularly increasing and contrastingly decreasing in wild tomato and potato, respectively.

3.2.12 Distribution of responsive populations candidates for further studies

Finally, we identified competently responsive populations (HR score 3 and/or 4) as candidate wild germplasms for future studies by mapping these across geographical coordinates and altitude centres of collection to reflect distribution diversity range (**Figure 3.9**). Of 58 *S. pimpinellifolium* populations responsive to Avr2, 27 populations consisted

plants with robust HR, of 16 EpiC1 recognising *S. pimpinellifolium* populations, seven populations had strongly responsive plants and from 21 populations displaying EpiC2B and Cip1 associated HR phenotypes, 12 and 14 populations were effectively responsive. In region A, only Avr2 was perceived by LA0413 (80 mts, Ecuador) and by LA2097 (400 mts, Ecuador). In La Libertad of region B, LA1631 (50 mts) recognising Avr2 and Cip1, LA0121 (80 mts) and LA1578 (unknown elevation) recognising Avr2 and EpiC2B, respectively. In region B, LA2186 (550 mts, amazon tropical lowland) perceived all four inhibitors with similar HR strengths.

In Ancash of region C, LA0373 (60 mts) responded particularly to Avr2, LA0375 and LA2401 (both 100 mts) responded to all four inhibitors and LA1597 (200 mts) recognised Avr2 and Cip1. In Lima of region C, LA2982 (5 mts) responded to Avr2 and EpiC2B, LA2983 (5 mts) responded to Avr2 and Cip1, LA0753 (20 mts) and LA1520 (800 mts) recognised all four inhibitors. In Lima, LA1521 and LA2914A at 150 mts), LA1661 at 200 mts, LA0100 and LA0369 at 300 mts, LA1992 at 500 mts and LA1561, LA2934 and LA4138, collected at unknown elevations, responded only to Avr2. LA2983 (5 mts), LA1514 (800 mts) responded to both Avr2 and Cip1 in Lima, while LA2982 (5 mts) perceived Avr2 and EpiC2B. Three populations from Lima responded to three inhibitors each: LA1629 (sea level) and LA1572 (200 mts) were responsive to Avr2, Cip1 and EpiC2B, whereas, LA1614 (450 mts) recognised Avr2, EpiC1 and EpiC2B. In Ica of region D, LA1630 (sea level) responded to Avr2 and Cip1, whereas, LA1634 (700 mts) perceived only EpiC1, LA1637 (700 to 800 mts) recognised EpiC2B and LA1679 (unknown altitude) responded particularly to Avr2. From the coastal Arequipa desert in region D, we identified LA1335 (50 mts) responding to EpiC2B and LA1933 (140 mts) being responsive to Avr2 and Cip1.

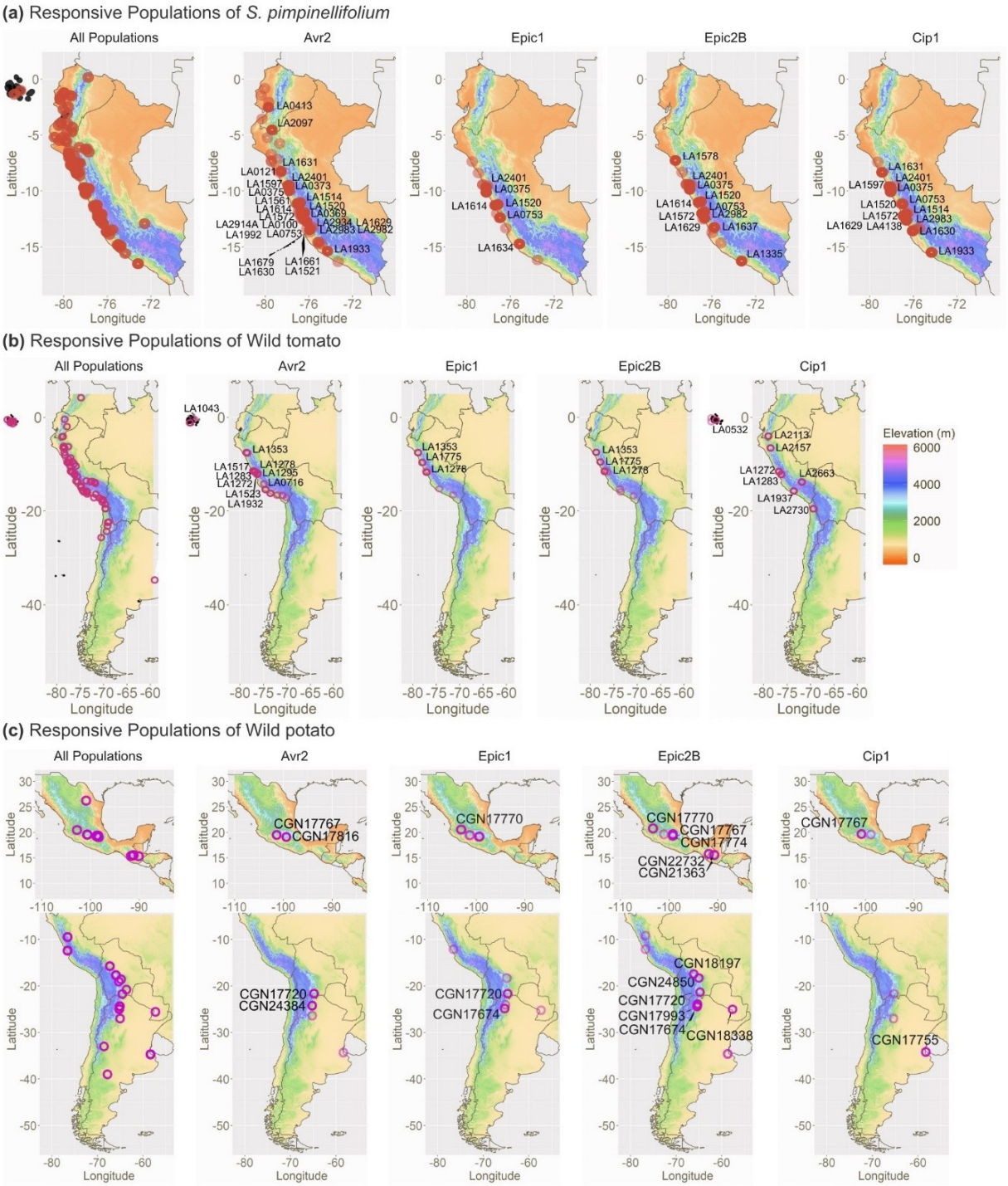


Figure 3.9. Distribution of responsive populations identified in *S. pimpinellifolium*, wild tomato and wild potato across latitude/longitude, altitude and geographical regions.

Maps combining latitude/longitude, altitude and geographical regions were generated using Raster terrain data in R (packages detailed in Chapter 2). The first panel in each row show distribution range of all populations assessed in this study. Second, third and fourth panels indicate populations responsive to Avr2, EpiC1, EpiC2B and Cip1, respectively. Strongly responsive populations are labelled and text highlighted. Weakly responsive populations in each group are shown in background with an increased opacity. Over-laying of raster map with population mapping was done using Inkscape. *R script and input data are attached as supplementary S3.7.

17 populations of eight other wild tomato relatives were determined to have plants responsive toward Avr2, but only ten populations of six species showed strong HR. Six and eight populations from five wild tomato species had plants responding respectively to EpiC1 and EpiC2B, however three populations from two species could uniquely exhibit severe HR. Further, of nine populations representative of eight wild tomato species had responsiveness to Cip1, but eight populations sampling seven populations had well-developed HR phenotypes. In region A, the closest wild tomato in-group species, *S. cheesmaniae* LA1043 (60 mts, Galapagos Islands) recognised Avr2, while two populations, one from an in-group *S. galapagense*, LA0532 (5 mts, Galapagos Islands) and another from farther evolved *S. neorickii*, LA2113 (1300 mts) conferred recognition to Cip1.

In Cajamarca in region B, *S. arcanum* 2157 (1600 mts) responded to Cip1, but *S. habrochaites* LA1353 (2650 mts) responded to Avr2, EpiC1 and Epic2B. Populations from Lima in region C, *S. peruvianum* LA1517 (236 mts), *S. pennellii* LA1523 (400 mts) and *S. habrochaites* LA1295 (2100 mts), all recognised only Avr2. However, *S. pennellii* LA1272 (1000 mts) and *S. corneliomulleri* LA1283 (2000 mts) responded to both Avr2 and Cip1. *S. habrochaites* LA1775 (1200 mts, Ancash) in region C recognised both EpiC1 and EpiC2B. Only *S. peruvianum* LA1278 (800 mts, Lima) recognised at least three inhibitors, Avr2, EpiC1 and EpiC2B. In region D, *S. pennellii* LA0716 (50 mts, Arequipa) and *S. chilense* LA1932 (1100 mts, Arequipa) responded specifically to Avr2 while *S. corneliomulleri* LA1937 (2500 metres, Cusco) and *S. chmielewskii* LA2663 (2500 mts, Cusco), specifically responded to Cip1. Among the analysed outgroup wild tomato species, only *S. lycopersicoides* LA2730 (1700 mts), with HR-induced upon Avr2 infiltration was responsive in Chile region E.

We detected HR against Avr2 in wild potato plants from six populations, one each from six different species, but intense recognition occurred in four populations from four species each. 13 populations from six wild potato species recognising EpiC1, three species

consisting of responsive plants in one population each. While EpiC2B was perceived in wild potato plants of ten species consisting of 23 populations, plants from 11 populations constituting six species strongly responded to EpiC2B. Cip1 responsiveness was discovered in five populations, each from five different wild potato species, but only two species with one population each had plants with well-defined HR. In region A, diploid wild potato *S. verrucossum* populations from Mexico, CGN17767 (2950 mts) showed response to three inhibitors (Avr2, EpiC2B and Cip1), CGN17770 (3250 mts) responded to two inhibitors (EpiC1 and EpiC2B) and CGN17774 (2300 mts) recognised only EpiC2B. A polyploid population, *S. demissum* CGN17816 (3000 mts) perceived only Avr2. Further, diploid *S. bulbocastanum* populations from Guatemala in region A, CGN22732 (1900 mts) and CGN21363 (1430 mts) specifically responded to EpiC2B.

Diploid populations from Bolivia in region B, *S. infundibuliforme* CGN17720 (1420 mts) recognised three inhibitors (Avr2, EpiC1 and EpiC2B), whereas, *S. chacoense* CGN24850 (2400 mts) and *S. acaule* CGN18197 (3300 mts) showed specific recognition toward EpiC2B. In populations from Argentina in region C, variation was observed at same elevation of 3200 mts, where polyploidy *S. acaule* CGN17674 recognised EpiC1 and EpiC2B, however, diploids *S. venturii* CGN17755 and *S. vernei* CGN17993 individually recognised Cip1 and EpiC2B. In region C, Avr2 was only recognised by *S. gourlayi* CGN24384 (3100 mts, Argentina). The only tested population from Paraguay in region C, diploid *S. chacoense* CGN18338 (200 mts) responded only to EpiC2B. These candidate populations/species serve as valuable repositories to study plant-pathogen interactions in Solanaceae.

3.3 Discussion

This chapter provides a valuable comprehensive investigation of wide-ranging natural populations across Solanaceae, for responses to four distinct protease inhibitors from three unrelated pathogens, Avr2 of *C. fulvum*, EpiC1 and EpiC2B of *P. infestans* and Cip1 of *P. syringae*. We constructed and expressed the mutants of these inhibitors in *E. coli*. SDS-PAGE and Competitive-ABPP analysis showed that purified mutant inhibitors are stable proteins that do not inhibit Rcr3, whereas their wild-type counterparts caused Rcr3 inhibition with variable strengths. However, there was little difference in the sensitivity of EpiC1 and its mutant to Rcr3. This observation may be explained by appropriate modifications to optimally known inhibitor concentration range and inhibitor exposure duration requirements of EpiC1 proteins.

3.3.1 Avr2 is the most recognised inhibitor in wild tomato and EpiC2B in wild potato

We found that Avr2-induced HR is present in tomato and potato but not in other tested Solanaceae species. *S. pimpinellifolium* plants confer the highest Avr2 recognition frequency in regions C (Centre, 33.6%) and D (South, 31.6%), followed by remaining wild tomato group in regions C (Centre, 16.7%) and D (South, 11.4%). Response frequency to Avr2 in wild potato plants was nearly similar across regions A (North, 6.8%), B (Centre, 5.8%) and C (South, 6.7%). Previous assessment of several *S. pimpinellifolium* populations, for response against Avr9, a *C. fulvum* inhibitor recognised directly in tomato plants carrying *Cf-9* gene, showed that Avr9 responsive plants were distributed across origin range of *S. pimpinellifolium*, where recognition frequency in South was nearly three times more than in North (van der Hoorn et al., 2001). Our finding that Avr2 recognition in *S. pimpinellifolium*

occurs throughout distribution range reflect similarity to frequent Avr9 recognition (van der Hoorn et al., 2001).

However, Avr2 recognition pattern in plants from distant wild tomato species show that response frequency is comparable in North (10.6%) and South (11.4%). This difference might be due to several species being assessed with a small size of representative population from each. Since different wild tomato species inhabit varied microclimatic geographies across South America, their inhibitor recognition patterns even in small population pools could be indicative of pathogen pressures in local regions. Screening of *S. chilense* populations against *C. fulvum* Avr9 and Avr4 previously showed that recognition is not as consistent in North and Centre regions as was shown in *S. pimpinellifolium* by Krujit et al., 2005, whereas Avr9 recognition seems to completely disappear in species from the South (Kahlon et al., 2020). Previously, study of tomato species for Pto-mediated indirect recognition of AvrPto and AvrPtoB, sequence divergent effectors from *Pseudomonas syringae* revealed recognition occurs in *S. pimpinellifolium* and in distantly related wild tomato species. It was noticed that AvrPto and AvrPtoB are differentially recognised and also that responsive populations of *S. chmielewskii* were observed to specifically recognise AvrPtoB, but not AvrPto in their origin ranges across South region (Kraus et al., 2016).

An interesting observation was that Avr2 is weakly and homogeneously recognised across independently evolved Centres of wild potato origin by a diploid *S. verrucosum* and a polyploid *S. demissum* population in North (Mexico), by a diploid *S. infundibuliforme* in Centre (Bolivia) and by a polyploid *S. acaule* and two populations of unknown ploidy levels (*S. gourlayi* and *S. venturii*) in the South (Argentina). High relative humidity and warm temperatures promote *C. fulvum* infections in tomato, and Avr2 responsive wild potato come from tropical wet climate of Mexico, humid subtropical climate of Bolivia and humid/arid ranges of Argentina. The precise mechanism of *C. fulvum* interaction with potato host likely

possess allelic variations from tomato, yet the recognition of Avr2 in non-host potato indicate overlapping interplay of multiple signalling components across the genus. A published study of screening wild potato genotypes for response against Avr2 of *P. infestans*, which is unrelated to Avr2 of *C. fulvum* used in this study, showed that *R* genes conferring recognition are present at different genetic loci and resistance specificities evolved independently in two Centres of potato diversity (Aguilera-Galvez et al., 2018). Therefore, a possible scenario could be that Avr2 recognition capabilities evolved independently in tomato and potato as the origin Centres of their responsive populations do not coincide.

Additionally, our finding reports the occurrence of recognition of EpiC1, EpiC2B and Cip1. These inhibitors share no coinciding recognition patterns with each other or with Avr2 in *S. pimpinellifolium*, other wild tomato and wild potato genotypes. *S. pimpinellifolium* has been the source of introgression of *Cf-2/Rcr3* system of Avr2 perception in cultivated tomato (Dixon et al., 1996 and Kruger et al., 2002), hence the high frequency of Avr2 recognition over EpiC2B, EpiC1 and Cip1 in *S. pimpinellifolium* suggest a natural selective advantage. Being the main host of *P. infestans*, wild potato displayed significant recognition of EpiC2B as compared to Avr2 and Cip1, which is consistent with the native host-pathogen co-evolution dynamics. We further noticed that EpiC2B is more frequently recognised than EpiC1. *P. infestans* cause disease at low temperatures with damp weather, but the elevated air temperatures impacted by global warming may explain geographic variations in temperature preferences of pathogen, increasing the potential to infect broad spectrum of hosts. However, we did not observe any HR symptoms with EpiCs, Avr2 or Cip1 in multiple screenings in eggplant, pepper, tobacco and petunia populations.

3.3.2 Recognition intensity variations within and cross-species

We observed that an array of HR phenotypes ascending on a score scale 0 to 4, are triggered by same inhibitor or by different inhibitors, within the same population and among

different species. Moreover, recognition intensity against particular inhibitor is not commonly shared among populations from same geographical region or altitude range. Previously, sequencing data from 314 *S. acaule* population analysis suggested that populations collected from same regions or different plants of a population can have different genetic variations while populations that originated at geographically distant locations can have redundant genotypes (van Treuren et al., 2004).

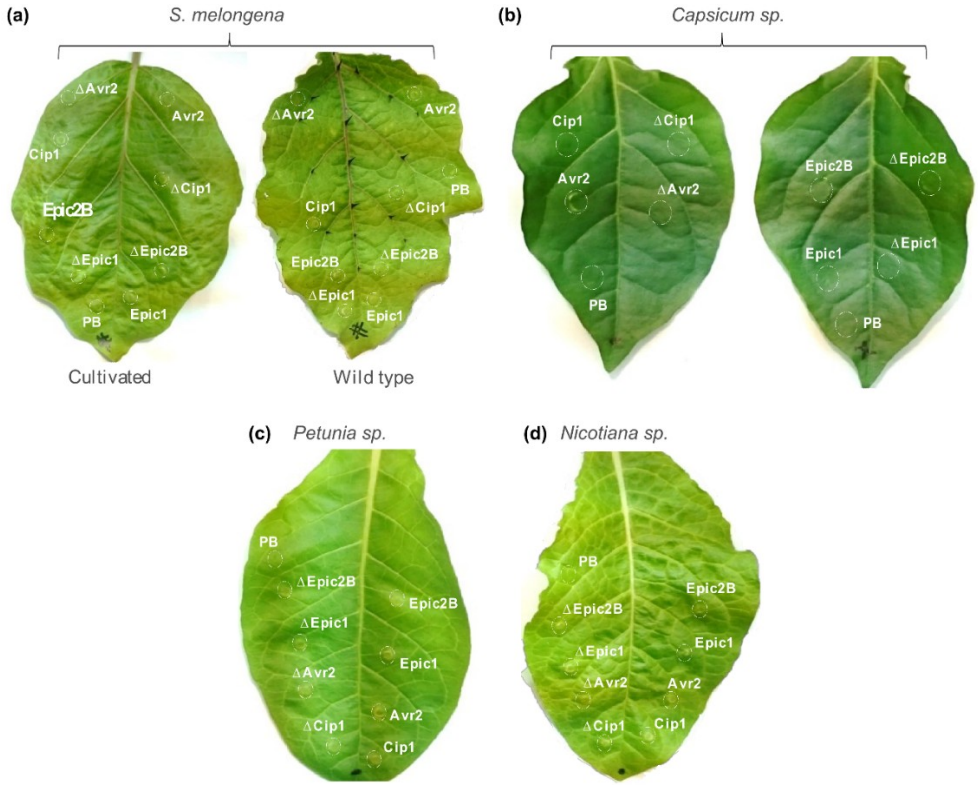
The absence of inhibitor recognition correlation with each other and versatility in HR-mediated recognition intensities against same inhibitor among different populations indicate the existence of allelic variations of underlying genetic components conferring extracellular inhibitor recognition. In a heterogeneous environment, infections of multiple pathogens at same time are not uncommon in natural populations of plants. Under different environmental conditions, alternative host species or genotypes of the same species may be available. This could maintain or promote the polymorphism at specific resistance gene locus and presence of broad-spectrum conferring genes. Hence, micro-environment driven balancing selection may be more prevalent across native geographic ranges of tomato or potato species.

3.3.3 Recognition of inhibitors in different species does not follow a gradient along altitude

We found that there are variations in recognition of same inhibitor in different species and of different inhibitors in same species across environmental geographic and altitude ranges. For instance, the highest Avr2, EpiC2B and Cip1 recognition within *S. pimpinellifolium* occurs at 0-500 mts, whereas in other wild tomato, Avr2 is mostly recognised at 0-500 mts, but recognition frequency of EpiC2B and Cip1 occurs highly at 2501-3000 mts and 2001-2500 mts, respectively. In contrast to *S. pimpinellifolium* and wild tomato, the highest

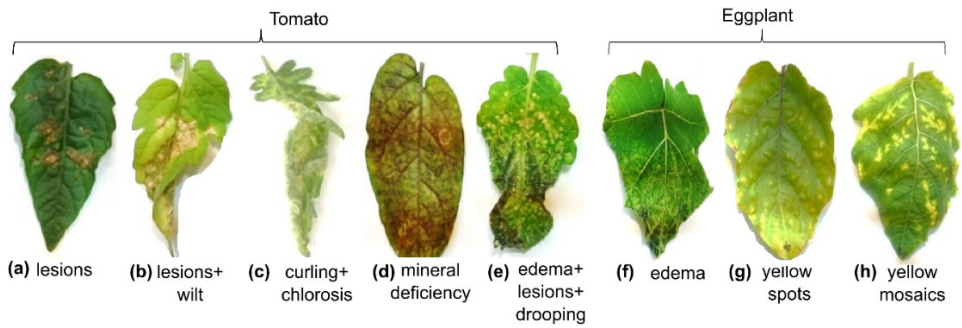
recognition frequency in wild potato for EpiC2B was noted at 1001-1500 mts. Similarly, highest recognition frequency of EpiC1 varied across altitudes, where it was observed at 501-1000 mts in *S. pimpinellifolium*, at 2501-3000 mts in wild tomato and at 1001-1500 mts in wild potato.

Several studies have explored the effect of altitudinal climatic variations on evolution of pathogens or their effectors, such as *P. infestans* effector Pi02860 (Yang et al., 2022), which suppress cell death triggered by *INF1* in wild potato (Yang et al., 2016b, Wang et al., 2021a). Previous studies on *P. infestans* effectors, Avr3a (Yang et al., 2018), Avr1 (Shen et al., 2021) and Avr2 (Yang et al., 2020) in pathogen populations collected from sites with temperature variations revealed that air temperatures locally influence evolution of effectors. How plant populations genetically vary and adapt across altitudes has been a research interest for long. However, while candidate genes are identified, molecular mechanisms that link natural response variations in different populations/species in correlation to altitude has not been significantly explored and established (Montesinos-Navarro et al., 2011, Zaborowska et al., 2021, Holdsworth et al., 2025). While we showed natural variation in recognition of Avr2, EpiC1, EpiC2B and Cip1 in wild tomato and potato across different geographic origins and altitudes, it remains to be understood whether these recognition variations biologically correspond to multiple disease resistance against fungal pathogen *C. fulvum*, oomycete pathogen *P. infestans* and bacterial pathogen *P. syringae*. Therefore, it would be useful to estimate geographic frequency and nucleotide variations in genes of interest that likely underlie recognition of distinct inhibitors evaluated in this chapter.



Supplementary 3.1 No HR response phenotypes observed against inhibitor infiltrations in eggplant (both cultivated and wild populations shown), pepper, petunia and tobacco populations.

HR assays were performed as schematically shown in Figure 3.3. Representative test leaves were observed for up to 21 dpi when the photographs were taken.



Supplementary 3.2 Different symptoms observed in a few tomato and eggplant populations.

Some unexpected symptoms were observed in tomato and eggplant populations. Plants in visibly good condition were still tested from these populations. However, all these populations were non-responsive to all wild-type and mutant inhibitors. Most of these symptoms were possibly greenhouse environment-induced, such as, (d) mineral deficiency as is seen during initiation of purple leaf disorder, (e) drooping and chlorotic spots along with water retention or edema, (f) edema only and (g) chlorotic spots.

Chapter 4

Genotyping tomato *Cf-2* family and apoplastic proteases show variability associated with inhibitor recognition

Shivani Malik[1], Jiorgos Kourelis[1,2] and Renier A.L. van der Hoorn[1*]

[1]Plant Chemetics Laboratory, Department of Plant Sciences, University of Oxford, South Parks Road, OX1 3RB Oxford, UK. [2]Current address: Department of Life Sciences, Imperial College, SW7 2AZ, London, UK. *Correspondence: renier.vanderhoorn@biology.ox.ac.uk

Author Contributions:

Research design: SM and RvdH; Seed collection procurement: SM; Experimental investigations: SM; *Cf-2/Hcr2* primer design: JK; Data analysis, Figures, and writing: SM with critical inputs from RvdH; Funding acquisition: RvdH.

Acknowledgement:

We thank Tomato Genetics Resource Centre (TGRC), Davis and Centre for Genetic Resources (CGN), Netherlands, for seed donations; Ursula Pyzio and Timothy Wroe for greenhouse assistance; Sarah Rodgers and Caroline O' Brien for technical support; SM was supported by Oxford-Indira Gandhi Scholarship.

4.1 Introduction

Genetic diversity in both plants and their pathogens is promoted through a back and forth dynamics, where pathogen adaptations lead to evolution of new infection strategies while plants develop counter-adaptation resistance responses. Presumably, where effectors are evolving to suppress or evade recognition in specific plant population or species, the host plant may also have developed distinct receptor repertoires that can have redundancy or different sensitivities to effectors. Identifying this natural genetic polymorphism in resistance genes, such as receptor-like proteins (RLPs) and their co-receptors is thus essential for developing effective broad spectrum resistance against multiple pathogens.

Cladosporium fulvum resistance genes *Cf-2 (*Dixon et al., 1996) and *Cf-9* (Parniske et al., 1997) are part of multigene families *Hcr2* (*Homologs of C. fulvum resistance gene 2*) and *Hcr9* (*Homologs of C. fulvum resistance gene Cf-9*), respectively. Both *Cf-2* and *Cf-9* are cell surface RLPs encoding leucine-rich repeat domains and were originally sourced into near-isogenic lines of cultivated tomato, *S. lycopersicum* from its closest wild relative species, *S. piminellifolium*. Genes at the *Hcr9* locus are well characterised in comparison to *Hcr2* and a contrasting difference in the members of both is that *Hcr2* family members significantly differ in their number or combinations of LRR domains that range from 25 to 38 (Dixon et al., 1998). LRR binding motifs are highly specialized and whereas the Hcr9s have a more fixed number of LRRs, their variations play major role in determining inhibitor recognition specificities (Seear and Dixon., 2003).

Pathogen pressure studies on fungal pathogen *C. fulvum* and wild tomato species interactions are limited, however *C. fulvum* disease assays were shown to induce different levels of resistance in wild tomato species, *S. pimpinellifolium*, *S. peruvianum*, *S. habrochaites* (Kerr et al., 1971) and *S. chilense* (Kahlon et al., 2020). Since the discovery

of first *Cf* locus (Langford., 1937), there are over 20 *Cf* genes conferring specific resistance to different races of *C. fulvum* that have been transferred into cultivated tomato till date (Kanwar et al., 1980, Dickinson et al., 1993, Joosten et al., 1999, Zhao et al., 2016 and Liu et al., 2019). *Cf* gene homologs are located at a single locus or multiple loci, for instance, a large number of *Hcr9s* have been identified at multiple loci on Chromosome 1 (Parniske et al., 1999) and their differential Avr9 recognition capacity has been evaluated for a few members, including *9DC* (van der Hoorn et al., 2001) and *Cf-9B* (Panter et al., 2002). Genes conferring recognition of *C. fulvum* derived Ecp5 inhibitor are also reportedly present at multiple loci under convergent evolution in different wild tomato populations (Lakovidis et al., 2020). Further, a survey study of *Cf-2* evolution in *S. pimpinellifolium* revealed that heterogeneous evolutionary processes are exerted on *Cf-2* gene family, consisting at least 26 *homologs* additionally to initially identified *Hcr2-2A* (Caicedo and Schaal, 2004). *Cf-like* receptor gene clusters have been identified outside Solanaceae (Vlnatzer et al., 2001) and while *Cf-9* and *Cf-4* are known to be conserved in wild tomato species (Krujit et al., 2005 and Kahlon et al., 2020), *Cf-2* still remains to be characterised outside *S. pimpinellifolium*.

Cf-2 and *Cf-9* distinctly resist leaf mould pathogen *C. fulvum* through perception of Avr2 (Luderer et al., 2002) and Avr9 (Joosten et al., 1994), respectively. Recognition of Avr2 by Cf-2, on the other hand occurs indirectly, where Avr2 physically binds to Rcr3, a papain-like cysteine protease (Krüger et al., 2002). Interaction of Avr2 with Rcr3 are sensed by Cf-2, leading to the induction of a localised cell-death response to restrict infection. Vap1, a potato cyst nematode (*Globodera rostochiensis*) derived inhibitor is also reported to get recognised by Cf-2 in a similar manner as Avr2 (Lozano-Torres at al., 2012). While various *Rcr3* homologs within the genus *Solanum* are capable of inducing Cf-2- dependent recognition of Avr2, *Rcr3* homologs beyond *Solanum*, despite being inhibited by Avr2 do not trigger Cf-2-mediated HR (Kourelis et al., 2020). Cysteine-rich Avr2 (Rooney et al., 2005, van Esse et al., 2008, Shabab et al., 2008), cystatin-like EpiC1 and EpiC2B of oomycete pathogen *Phytophthora infestans* (Tian et al., 2007, Song et al., 2009) and chagasin-like Cip1 of

bacterial pathogen *Pseudomonas syringae* (Shindo et al., 2016), are known secreted inhibitors of convergent cysteine protease targets, Rcr3, Pip1 and C14 in the apoplast of tomato. However, unlike Avr2 and Vap1, EpiC1, EpiC2B and Cip1 do not induce Cf-2-mediated hypersensitive response (HR). The functional consequences of independently evolving natural variations in *Rcr3*, *Pip1* and *C14* has been investigated in previous studies in wild tomato and wild potato species, where high frequency of intraspecific and interspecific natural variation has been detected at nucleotide and amino acid levels (Shabab et al. 2008, Kaschani et al., 2010, Hörger et al., 2012, Kourelis et al., 2020). Further, differences in strength of response against Avr2, EpiC1, EpiC2B and Cip1 due to underlying amino acid polymorphisms was also observed in *in-vitro* and *in-planta* assays (Hörger et al., 2011).

The Guard hypothesis (reviewed by van der Hoorn et al., 2002) suggest that Rcr3 being the virulence substrate 'guardee' of pathogen-derived Avr2 is 'guarded' by Cf-2 receptor. It is thus proposed that coevolution of guard, Cf-2 and its guardee, Rcr3 (Hörger et al., 2012) is a significant factor that potentially results in novel indirect recognition specificities. Targeting of common extracellular host cysteine proteases by protease inhibitors from different microbial kingdoms show that guarding the 'guardee' targets is beneficial in the expansion of a variety of pathogens that might get recognised by guard receptors. Since natural host species co-evolve with their pathogens through imposed selection pressures in the host system, it is thus important to study the existing evolutionary dynamics of the guard/guardee. In Chapter 3, we determined the recognition pattern of Avr2, EpiC1, EpiC2B and Cip1 in natural populations of Solanaceae. In this chapter, our aim was to genotype variation in number of *Cf-2* homologs and sequence allelic variants of *Rcr3* that potentially correlate with differential recognition of Avr2. We hypothesised that all Avr2 recognising plants have *Cf-2* and there are likely other *Hcr2s* capable of recognising Avr2.

There are a few LRR-RLP immune receptors in tomato outside *Cf* gene superfamily, particularly *Ve1*, which is known to confer recognition of Ave1 from race 1 of fungal pathogen *Verticillium dahlia* (Kawchuk et al., 2001, Frandin et al., 2009 and Wang et al., 2010). Interestingly, *Ve1* is capable of differentially recognising Ave1 homologs from other fungal pathogens, *Colletotrichum higginsianum*, *Fusarium oxysporium* f. sp. *lycopersici* and *Cercospora beticola* as well from bacterial pathogen *Xanthomonas axonopodis* pv. *citri* (de Jong et al., 2012). Further, recognition of Ave1 by *Ve1* homologs from potato *S. tubersoum* (Simko et al., 2004), eggplant *S. torvum* and tobacco *N. glutinosa* has been shown (Song et al., 2017). Homologs of *Ve1* are also known to exist outside Solanaceae family (Tang et al., 2016, Chen et al., 2016). We further hypothesised that HR in response to EpiCs and Cip1 is either conferred by a natural variant of *Hcr2* family that can strongly recognise their interaction with a natural variant of *Rcr3* or natural populations harbour a *Pip/C14* variant capable of interacting with an *Hcr2/Cf-like* LRR-RLP to confer recognition of unrelated inhibitors. We therefore investigated the correlation of *Hcr2s* in relation to responsiveness to EpiC1, EpiC2B and Cip1 using PCR-based genotyping approach.

We also used DNA sequencing on a set of randomly chosen individuals to identify whether existing natural variations in *Rcr3, Pip1* or *C14* correlate with specific recognition of different inhibitors. Combining Likelihood-based and Bayesian counting statistical methods available publicly at Datamonkey 2.0 (www.datamonkey.org) (Weaver et al., 2018), we inferred evolutionary selection pressure across species-specific variant branches/clades and found that Rcr3 is under diversifying selection in *S. pimpinellifolium* and wild tomato, whereas Pip1 is under diversifying selection in wild tomato outside *S. pimpinellifolium*. In contrast to previous finding that C14 is under positive selection in wild potato, we found that C14 is under diversifying selection in *S. pimpinellifolium* only. To identify any signatures of positive selection that are often missed in clade/branch-wide analysis, we used approaches to pinpoint individual sites in a coding sequence alignment that are overall targets of diversifying selection in *Rcr3*, *Pip1* and *C14*.

4.2 Results

4.2.1 Genotyping highly homologous *Cf-2* gene family, *Cf-9* and *9DC* in control plant line

We employed a genomic PCR based approach for using newly designed primers SM_Cf-2/Cf5_F and SM_Cf-2/Cf5_R, to amplify *Cf-2* and *Hcr2s* known so far to exist in *S. pimpinellifolium* (Caicedo et al, 2004). An illustration (**Figure 4.1(a) and (b)**) shows the position of the PCR primers on the coding sequences of genes at the *Cf-2* locus in *S. pimpinellifolium* (*Cf-2.1*, *Cf-2.2* and *Hcr2-2A*) and *S. lycopersicum* (*Hcr2-0A* and *Hcr2-0B*). Initially we performed PCR on positive and negative control lines, MM-*Cf-2* and MM-*Cf0*, respectively. PCR products were separated on 1.5% agarose gel and we obtained the expected resultants *Cf-2* (2893 bp) and *Hcr2-2A* (1961 bp) in MM-*Cf-2* and *Hcr2-0B* (2389 bp) and *Hcr2-0A* (2035 bp) in MM-*Cf0* (**Figure 4.1(c)**). However, unexpectedly we also obtained two *Hcr-like* products of ~2100 bp and ~1500 bp in both MM-*Cf-2* and MM-*Cf0* lines and the identity of PCR products was further confirmed by sanger sequencing (primer listed in Table 2.6).

Two member genes of *Hcr9* family recognising Avr9, *Cf-9* and *9DC* have previously been studied for occurrence frequency and polymorphism in *S. pimpinellifolium* (van der Hoorn et al., 2001) and a few other wild tomato species (Krujit et al., 2005 and Kahlon et al., 2020). Therefore, additionally to *Cf-2* gene family, we were also interested in identifying segregation of *Cf-9* and *9DC* in our responsive and non-responsive populations. We performed PCR on same genomic DNA samples as for *Hcr2s* using specific primer pairs CS5 and CS1 to detect *Cf-9* and CS5 and DS1 to detect *9DC* (van der Hoorn et al., 2001).

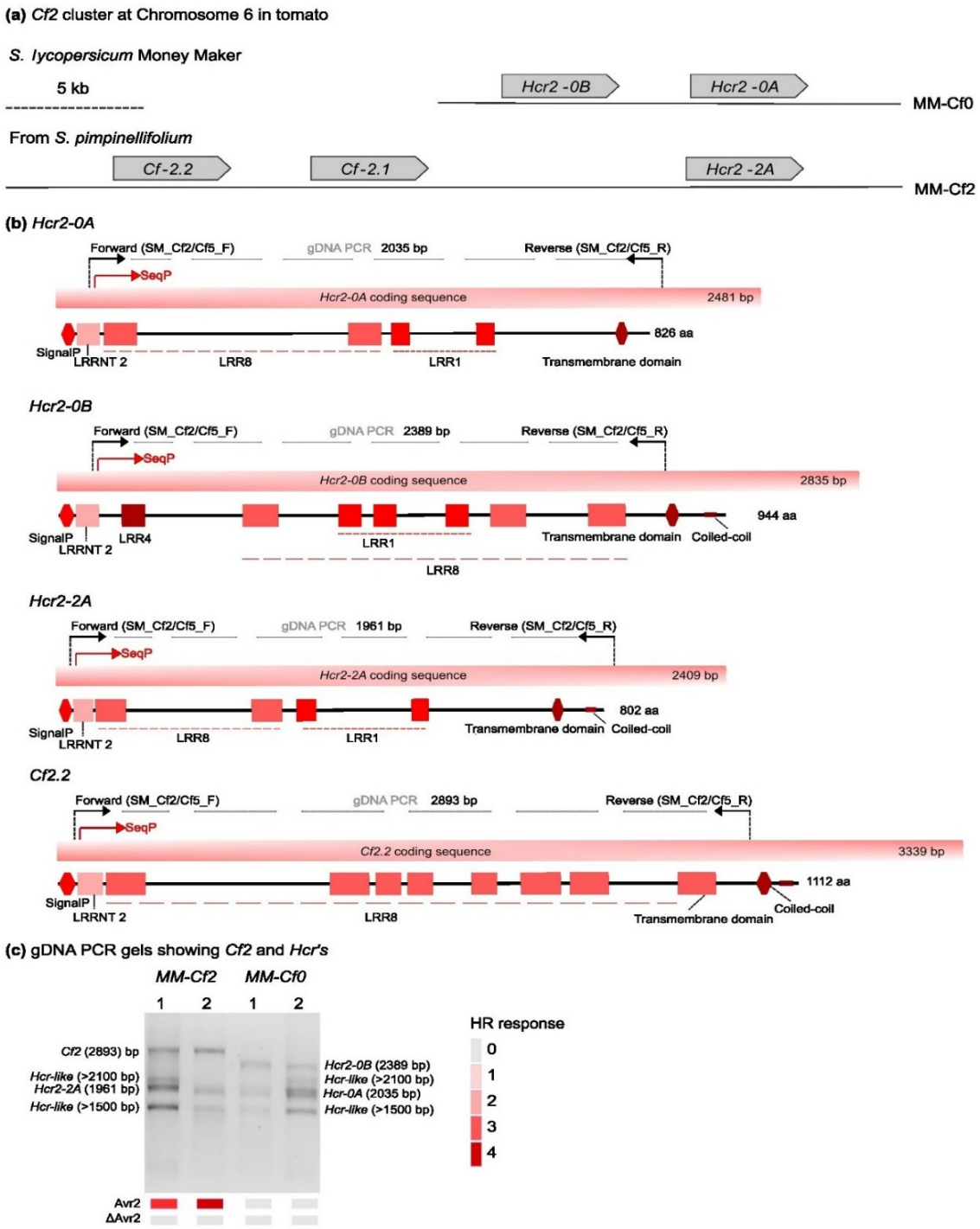


Figure 4.1 Schematic illustration showing intron-less *Cf-2* gene cluster on chromosome 6.
(a) Allelic regions of *Cf-2* gene cluster in near isogenic line Money Maker (MM)-*Cf0* and MM-*Cf-2* are detailed. Bar length is 5 Kb and grey boxes represent Open Reading Frames (ORFs) with directional representation indicating direction of transcription. **(b)** Coding sequence and protein domain architecture of Cf-2.2 and *Homologs of Cf-2* (*Hcr2*'s): *Hcr2-0A*, *Hcr2-0B* and *Hcr2-2A*, were expected products in gDNA PCR on control lines MM-*Cf-2* and MM-*Cf0.* Annealing sites of PCR and sequencing primers are described (primer details in Table 2.6). Protein products with predicted domain architectures are also shown. **(c)** gDNA PCR products from control lines MM-*Cf-2* and MM-*Cf0* were separated on 1.5% agarose gel.

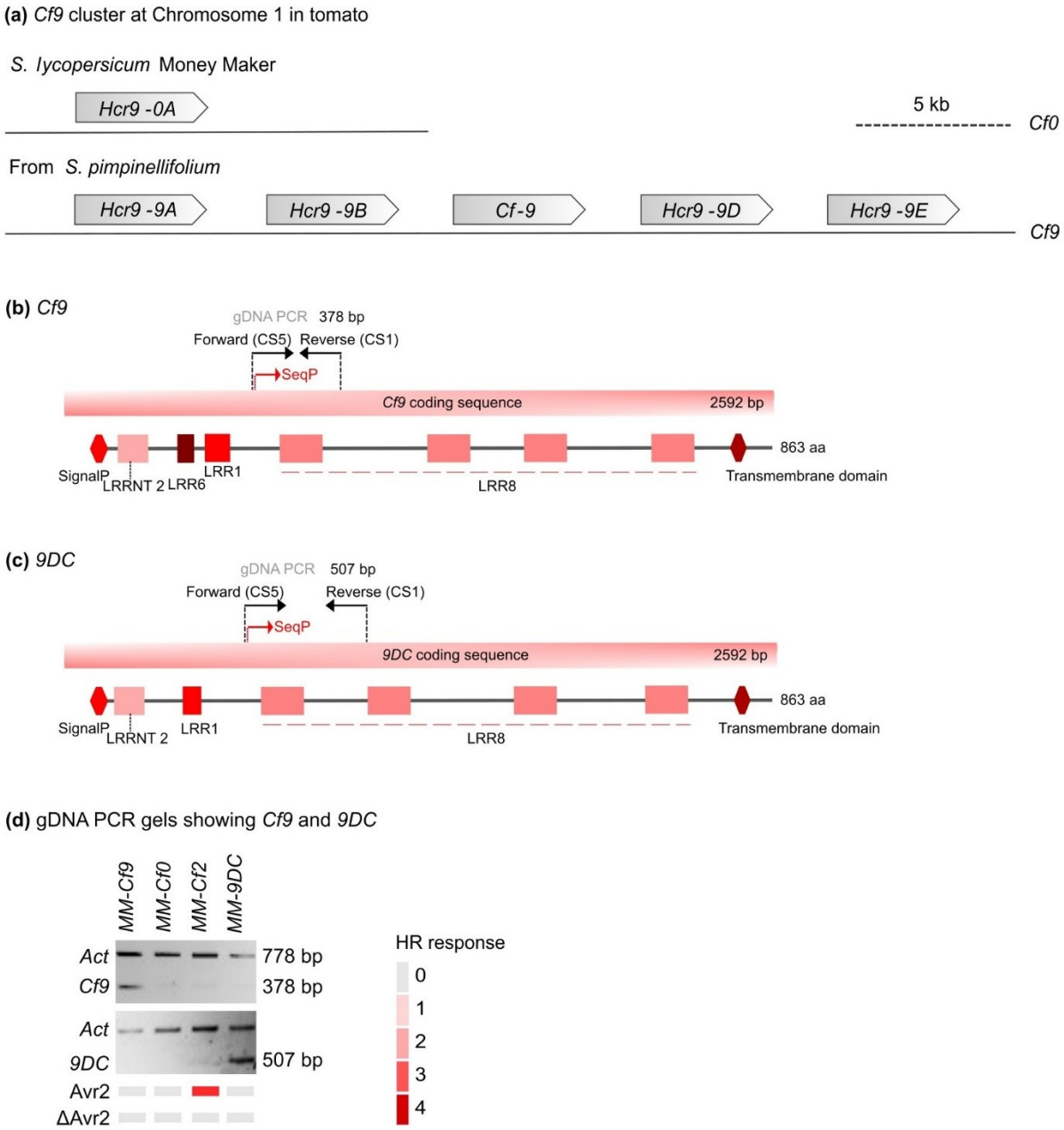


Figure 4.2 Allelic regions and PCR of *Cf-9* gene cluster on chromosome 1.

(a) ORFs of *Cf-9* and four *Homologs of Cf-9* (*Hcr9*'s) are shown as grey boxes sourced from *S. pimpinellifolium* and accordingly in *S. lycopersicum* Money Maker near isogenic MM-*Cf0*. Directional schematic show transcription direction. **(b)** *Cf-9* coding sequence detailing translated protein domains and alignment with *Hcr9,* **(c)** *9DC* show PCR primer binding sites. **(d)** gDNA PCR products from control lines were separated on 1.5% agarose gel. *Act* gene was used as reference. *primers and control lines are detailed in Tables 2.6 and 2.3, respectively.

A schematic representation of the *Cf-9* cluster in *S. lycopersicum* and *S. pimpinellifolium* and annealing of PCR primers on *Cf-9* and *9DC* are shown in **Figure 4.2(a) and (b)**. We tested these primers in positive control lines MM-*Cf-9* and MM-*9DC* to obtain expected products *Cf-9* (378 bp) and *9DC* (507 bp), respectively. *Act* (700 bp) (van der Hoorn et al., 2001) was amplified as control. As expected, we did not obtain *Cf-9/9DC* from in MM-*Cf-2* and MM-*Cf0* (**Figure 4.2(c)**). The optimised PCR conditions on control lines were further used for genotyping our test population pool of *S. pimpinellifolium*, distant wild tomato species and wild potato species in this study. We sequenced *Cf-2/Hcr2s*, *Cf-9* and *9DC* from control lines using primers listed in **Table 2.6** to confirm *Cf-2/Hcr2* identity and therefore based on PCR product lengths expected for *Cf-2/Hcr2*, *Cf-9* and *9DC*, we counted genotyped wild populations as positive for the respective genes.

4.2.2 *Cf-2/Hcr2s*, *Cf-9* and *9DC* show variation among individuals of same population and their presence does not specifically correlate with inhibitor recognition

We genotyped a randomly selected set of responsive and non-responsive *S. pimpinellifolium* populations based on our HR screening against four unrelated inhibitors, Avr2, EpiC1, EpiC2B and Cip1, in chapter 3. We had grouped populations based on their geographical origins in four regions A to D in chapter 3, and all regions are represented in this genotyping. To detect the presence of *Cf-2* and number of other *Hcr2s*, genomic DNA from four of eight HR assessed plants of each *S. pimpinellifolium* population was isolated. We chose five of 17 populations screened for HR from Ecuador (region A), 14 of 39 populations from North Peru (region B), 13 of 39 populations from Central Peru (region C) and eight of 17 populations from South Peru (region D). PCR analysis was also performed to detect *Cf-9* and *9DC* in three of five populations for *Cf-2/Hcr2s* from Ecuador, seven of

14 genotyped populations from North Peru, all 13 *Cf-2/Hcr2* genotyped populations from Central Peru and five of eight genotyped populations from South Peru.

Surprisingly, in some cases, a weak PCR amplification signal was detected at ~2893 bp, hence we distinguished clearly visible *Cf-2* signal (asterisk) from a weak signal (denoted as 0) (**Figures 4.3 and 4.4**). We found that 11 of 12 plants with a robust HR (score 3 or 4) against Avr2 carry a clear signal for *Cf-2*, irrespective of their geographic origin. Remarkably, plants lacking *Cf-2*, but having *Hcr2-2A* or other *Hcr2-like* genes possess the capability to confer weaker Avr2 recognition. For example, LA0400 (P1) and LA0400 (P3), both weakly recognise Avr2, but we detected a predicted full-length *Hcr2* amplicon in LA0400 (P3), wherease a predicted *Cf-2* amplicon in LA0400 (P1) (**Figure 4.3(b)**).

We further noticed variation in the presence of *Cf-2*, number and types of *Hcr2s* among plants of the same population. An unexpected observation was that all four genotyped plants of LA2186 from region B (**Figure 4.3(b)**), recognising all four inhibitors in same or different plant contained only an amplification product *Cf-2* without hardly any other *Hcr2* association. Interestingly, two plants of LA2186 recognising all inhibitors had both *Cf-2* and *9DC* amplification products in contrast to remaining two plants recognising only Avr2 and Cip1 in the presence of *Cf-2* and *Cf-9* amplification. Further, we noted that despite a similar *Cf* genetic profile of plants from same population or from same geographical region, recognition can be visibly differentially conferred to similar or different inhibitors, for example in plants of LA0375 (P3, P4, P5 and P7) and LA2401 (P2 and P6) from the Centre region C. On the other hand, in individuals from populations like LA0753, P3 and P4, having similar genetic backgrounds of *Cf-2*, number and types of *Hcr2s* and *Cf-9*, inhibitor recognition is consistent.

It was also discovered that Avr2 recognition does not occur in all plants from which a *Cf-2*-size fragment was amplified (**Figures 4.3 and 4.4**). Segregation of *Cf-2*, *Cf-9* and *9DC* appears independent in the tested plants and does not show a relationship with HR-associated recognition of EpiC1, EpiC2B and Cip1. Populations with *Cf-2*, *Cf-9* and *9DC* are present throughout regions A to D of *S. pimpinellifolium* distribution. *Cf-2* gene family reportedly contain nearly nine homolog classes with 26 variants (Caicedo et al., 2004), however, in our PCR analysis only a few were amplified (**Figures 4.3 and 4.4**). A more degenerate mix of *Cf-2/Hcr2* primers could amplify other existing *Hcr2s* in *S. pimpinellifolium* populations (Caicedo and Schaal, 2004). There may also be single nucleotide polymorphism (SNP) variations in *Cf-2* genes. Sanger sequencing of the PCR products identified several mixed signals indicating that more than one *Hcr2* was amplified at a similar size. Our results indicate that Avr2 recognition in addition to *Cf-2*, is also conferred by another *Hcr2.* The recognition of Cip1 may or not occur in the presence of *Cf-2* and an *Hcr2* family member. Recognition of EpiC1 and EpiC2B can occur in the absence of *Cf-2* or a range of *Hcr2s* and most responsive plants have either *Cf-9* or *9DC*, indicating that EpiC1 and EpiC2B recognition possibly involves a different gene than *Cf-2*. Taken together, the underlying molecular basis of inhibitor recognition is more complex than anticipated.

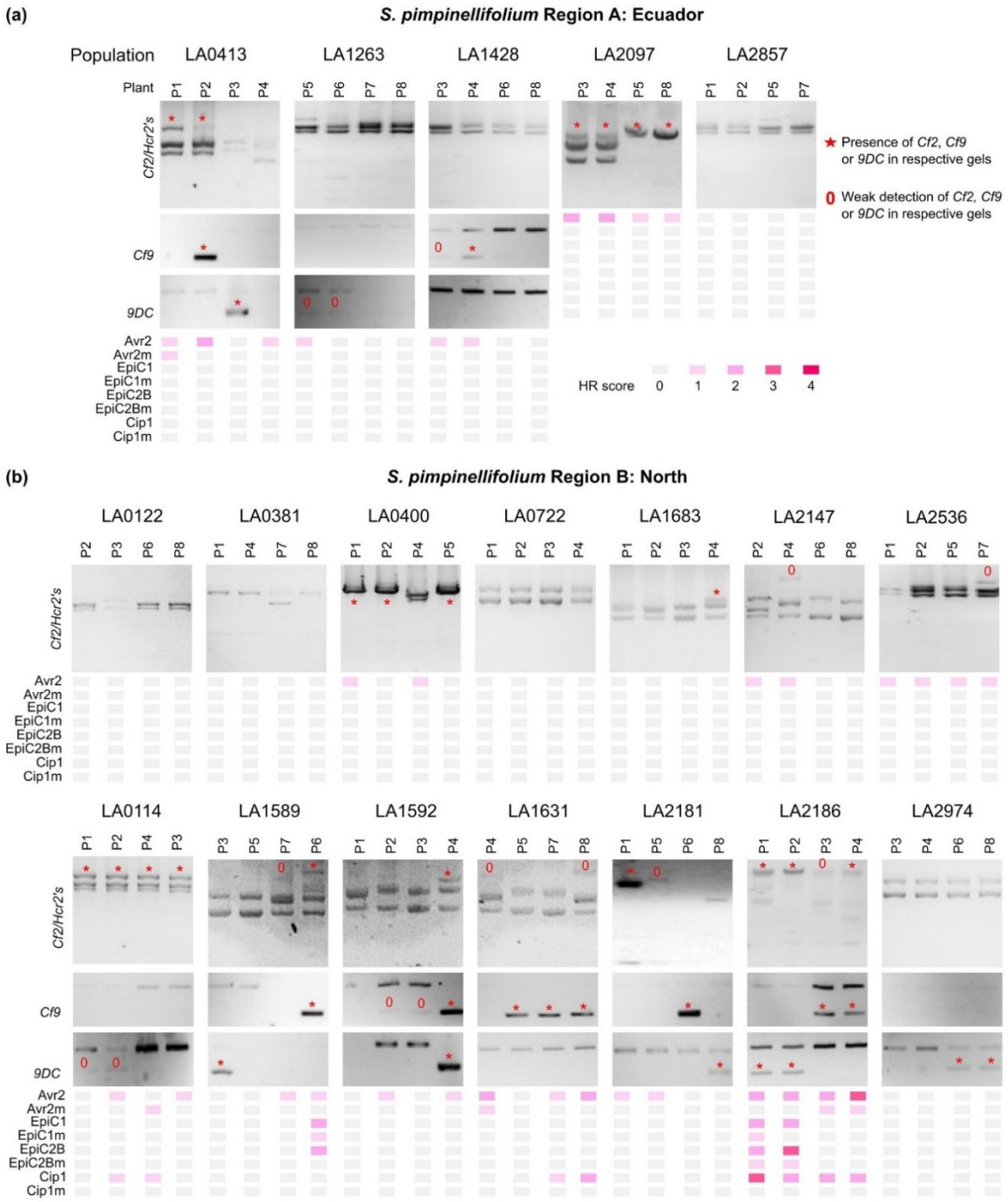


Figure 4.3 Occurrence of *Cf-2*, *Hcr2's*, *Cf-9* and *9DC* in relation to responsiveness towards each inhibitor in *S. pimpinellifolium* populations from Region A (Ecuador) and Region B (North).

A set of populations from **(a)** Ecuador and **(b)** North were selected to detect specific *Cf/Hcr* genes in responsive and non-responsive genotypes. DNA samples of four out of eight tested individuals in HR screening were randomly chosen. PCR amplification of *Cf-2* and *Hcr2* fragments are shown in the first panel of each population. *Cf-9* and *9DC* fragments were not tested in all populations and where tested, are shown in the second and third panel, respectively. Y-axis represent tested Cf-genes, whereas associated intensities of HR phenotype towards each inhibitor and its mutant are indicated on x-axis. Control gels are shown in figures 4.1 and 4.2.

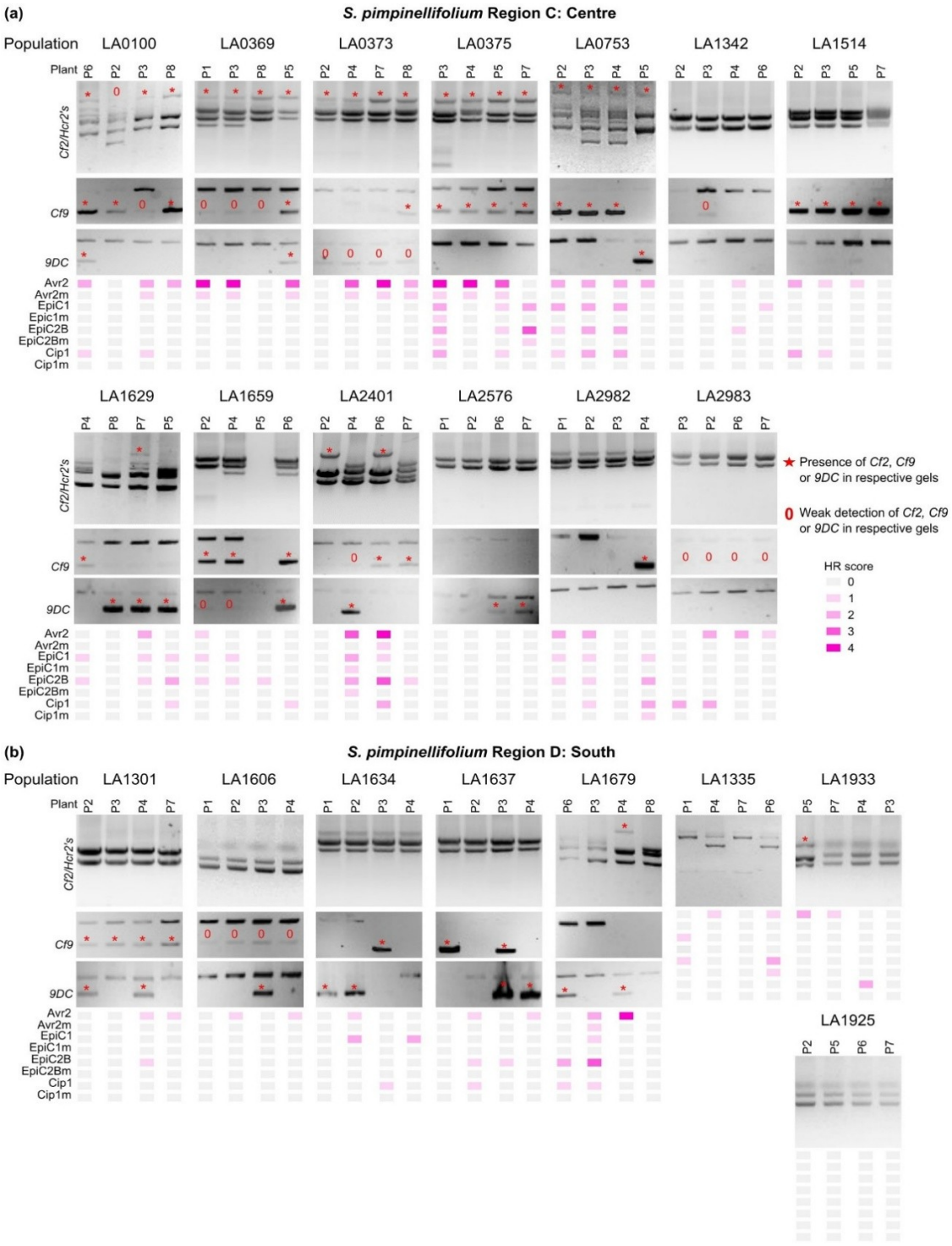


Figure 4.4 Association of *Cf-2*, *Hcr2*'s, *Cf-9* and *9DC* to inhibitor recognitions in *S. pimpinellifolium* populations from Region C (Centre) and Region D (South).

A few populations from **(a)** Centre and **(b)** South regions were selected to amplify specific *Cf/Hcr* genes in responsive and non-responsive individuals. DNA samples of four out of eight tested plants per population in HR screening were randomly used. PCR products for detected *Cf-2* and *Hcr2*'s, are shown in the first panel. *Cf-9* and *9DC* fragments, where tested, are shown in second and third panels. HR phenotype intensity against each inhibitor vs mutant is indicated in genotyped individual plants. Control gels are shown in figures 4.1 and 4.2.

4.2.3 Variation in *Cf* gene frequencies and their relatedness to inhibitor recognition across natural distribution ranges of *S. pimpinellifolium*

To assess the overall region-wise frequency of *Cf* genotypes, their co-occurrence and correlation with inhibitor recognitions, we summarised genotyping data using bar plots (**Figure 4.5**). We found that highest frequency of the *Cf-2*-size signal exists in populations from Centre region C, where 44.2% of genotyped plants had a *Cf-2*-like signal (**Figure 4.5(b)**). Further, *Cf-9* (63.5%) and *9DC* (45%) gene frequencies were the highest in regions C and D (South Peru), respectively. A significant difference in *Cf-2* gene frequencies between regions A (35%) and D (6.25%) is a striking result in correlation to nearly three-fold higher Avr2 recognition in region D (31.6%) in comparison to region A (9.5%). Considering that both Ecuador (Region A) and South Peru (Region D) are within the natural occurrence range of *C. fulvum* and no evidence suggests difference in *C. fulvum* prevelance in both regions, it is possible that unique *Cf-2/Hcr2* variants with different sensitivity to recognise Avr2 are present in each region. Overall, across all regions, the *Cf-9* gene is the most frequent, followed by *Cf-2* and *9DC.* Our finding is in contradiction with a published survey study of *Cf-9* and *9DC* occurrence in *S. pimpinellifolium*, where *Cf-9* containing plants were only reported in North and Central Peru and *9DC* was more frequently present than *Cf-9* (van der Hoorn et al., 2001). However, evaluation of *Cf-9* and *9DC* in *S. chilense* showed that *Cf-9* is present in populations from South Peru whereas no *9DC* fragment was detected in any tested plant (Kahlon et al., 2020). Evaluation in Avr9-responsive plants showed that either *Cf-9* or *9DC* is present but not both (van der Hoorn et al., 2001).

We estimated the frequency of co-occurrence of *Cf* genes in *S. pimpinellifolium* in various combinations, *Cf-2/Cf-9*, *Cf-2/9DC*, *Cf-9/9DC* and *Cf-2/Cf-9/9DC* (**Figure 4.5(c); Supplementary file S4.6**). All four combinations were detected in plants from North and Central Peru and a prominent finding was the presence of *Cf-2* with *Cf-9* or *9DC* in the same

plant in 3.6% and 5.8% of the total tested plants, respectively. We noticed that both *Cf-9* and *9DC* are present in 20% of the tested plants in South Peru, however, this combination was not found in plants from Ecuador. We further found that 3.6% plants in North and 13.5% plants in Central Peru contain both *Cf-9* and *9DC*. *Cf-2/Cf-9* genotype was prevailing in Central Peru (32.7%), while *Cf-2/Cf-9* and *Cf-2/9DC* were equally common in North Peru (17.8% each). An interesting finding is that the *Cf-9* gene frequency was the highest in plants recognising Avr2 (60%), EpiC1 (56.5%), EpiC2B (59.2%) and Cip1 (67.8%) (**Figure 4.5(d)**). The second highest gene frequency was estimated to be for *Cf-2* in plants individually conferring recognition of all four inhibitors.

While *Cf-9* and *9DC* sequences in *S. pimpinellifolium* have been reported (van der Hoorn et al., 2001), this is the first report of *Cf-2/Hcr2* prevalence in *S. pimpinellifolium* in association with Avr2 recognition and holds a potential to further investigate role of their allelic variations in recognition of Avr2 as well as other inhibitors, EpiC1, EpiC2B and Cip1. Our results suggest that a variable *Cf* genetic architecture underlying variation in recognition cell-death phenotypes within different micro-habitats are a common occurrence and may appear significantly clearer on a larger scale of population/species genotyping. Further, local environmental selection rather than genetic selections on a *Cf* gene, differential expressions of *Cf/Hcr* genes and variation in other immunity signalling components could possibly explain regional patterns of inhibitor recognition variations.

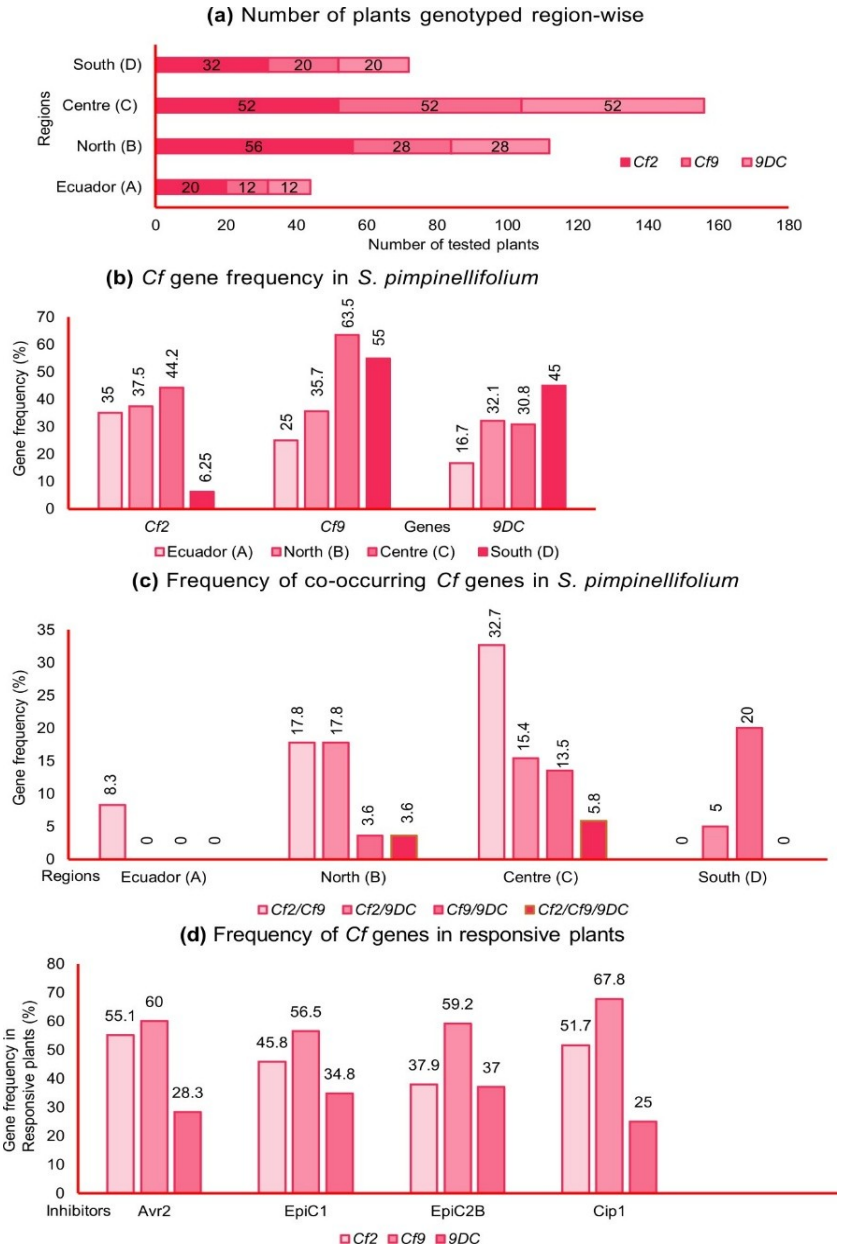


Figure 4.5 Variation in *Cf* gene frequencies across *S. pimpinellifolium* natural geographical distribution ranges.

Bar plot showing **(a)** number of plants genotyped for *Cf-2*, *Cf-9* and *9DC* from geographical ranges (A to D). **(b)** Region-wise frequency of *Cf-2*, *Cf-9* and *9DC* genes was estimated as number of plants with specific *Cf* gene in a given region divided by total number of plants genotypes in that given region. **(c)** Categories of co-occurring *Cf* genes were calculated as percentage by dividing number of plants having specific *Cf* genotype category to total number of plants genotyped in a region. **(d)** Estimated frequency of specific *Cf* gene in responsive plants against each inhibitor treatment is shown as number of responsive plants to a specific inhibitor having a particular *Cf* gene divided by total number genotyped plants responsive to that inhibitor. All individuals from PCR's in Figures 4.3 and 4.4 were included. *Raw frequency data file is attached as Supplementary S4.6.

4.2.4 *Hcr2* family is conserved in wild tomato and show intra-population and inter-specific variations

We next evaluated whether *Cf-2* and *Hcr2s* are detected in wild tomato species beyond *S. pimpinellifolium* and is there a correlation with responses to one or multiple inhibitors. We performed PCR on genomic DNA samples from four of eight plants that were phenotypically assessed for HR against inhibitors, representing a single population of two different species, each from geographically distinct North, Centre and South (**Figure 4.6**). Through an *in-silico* search in *S. pennellii* LA0716 genome (Bolger et al., 2014), we found an annotated *Cf-2* gene and a few *Hcr2s* at Chromosome 6, so we selected populations recognising more than one inhibitor, LA0716 from South and LA1272 from Centre. We detected Avr2 recognition in the presence of *Cf-2* amplification products in two plants and EpiC2B recognition in the absence of a *Cf-2* amplification but presence of *Cf-9* or *9DC* in two other plants of LA0716. In *S. corneliomulleri* population LA1937 in South, we found the presence of *Cf-9* and *9DC* in plants responsive to EpiCs and Cip1. However, the absence of *Cf-2* in LA1937 and no Avr2 recognition can indicate the lower frequency of *Cf-2* in wild tomato species from South as was found in *S. pimpinellifolium* populations where low *Cf-2* frequency implied the existence of allelic *Hcr2* variations conferring a high degree of Avr2 response in South.

S. habrochaites populations responded differently to inhibitors, where LA1775 in Centre region specifically responded to EpiCs while LA1353 in North additionally recognised Avr2 in the presence of *Cf-2*. Interestingly, we detected *Hcr2s* but not *Cf-2* in outgroup wild tomato species, *S. ochranthum* population LA2166 in North (**Figure 4.6**). These findings do not clearly establish a *Cf* genotypic relation with inhibitor recognition associated HR phenotypes. However, our results indicate that a number of *Hcr2s* and *Cf-9* genes are present in responsive and non-responsive populations of all tested wild tomato species from

different geographical regions, hinting towards their higher prevalence and primordial origin over *Cf-2* and *9DC*.

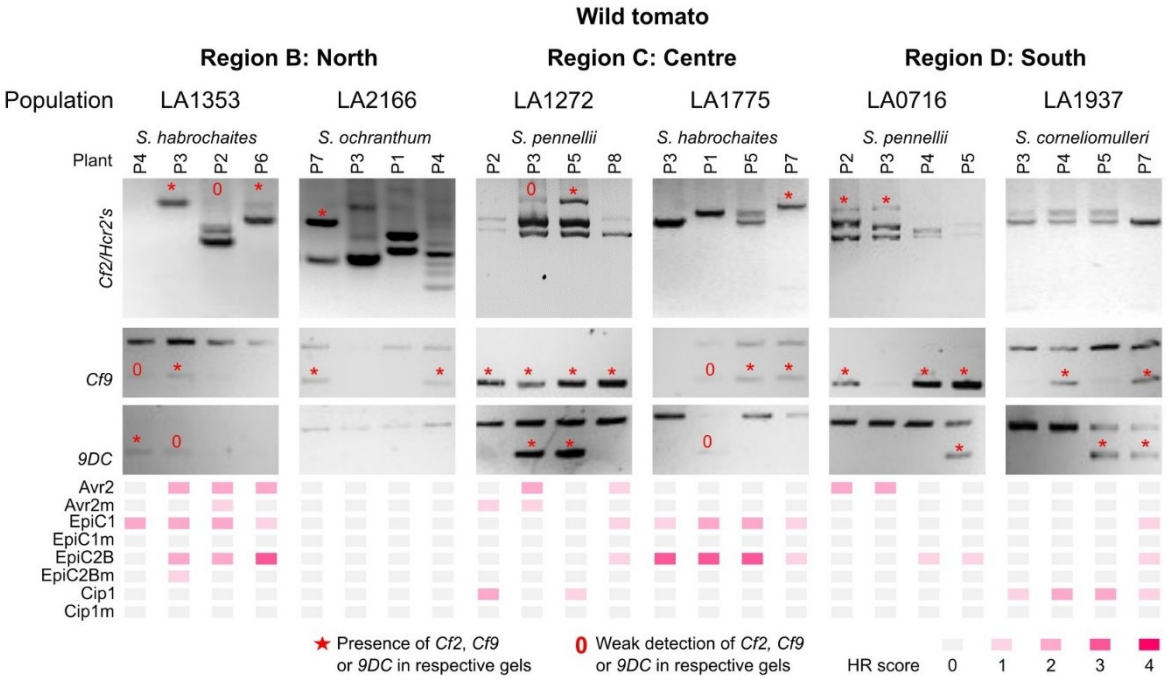


Figure 4.6 *Cf-2* amplification in *S. habrochaites* and *S. pennellii* correlate with strong HR phenotype against Avr2. EpiC1, EpiC2B and Cip1 recognitions do not fully associate with presence of *Cf-2*, *Cf-9* or *9DC* in *S. habrochaites*, *S. pennellii* and *S. corneliomuelleri*.
DNA gels showing amplification of *Cf-2/Hcr2*'s (first panel), *Cf-9* (second panel) and *9DC* (third panel) using genomic DNA of four individuals (P1 to P4) each from the two populations genotyped from three different regions of wild tomato distribution. Corresponding HR scores are detailed for each plant. *Act* gene was used as control; PCR of control lines are shown in figures 4.1 and 4.2.

4.2.5 *Cf-2-like* genes are found throughout diploid wild potato species from different origin centres

Four plants per wild potato population were screened for HR against all four inhibitors (chapter 3) and we analysed all four plants that were screened for HR from six different populations, representing two different species each from regions A, B and C. To observe a less complex genotype to phenotype relation, we assessed only diploid populations in our PCR-based approach for identification of *Cf-2/Hcr2-like*, *Cf-9* and *9DC* genes. *Cf-2*-size

gene fragments were amplified in eight of 24 genotyped plants including six of eight plants responsive to Avr2 (**Figure 4.7**). Three of five Cip1 responsive plants had *Cf-2* amplification product, whereas, two of five EpiC1 responsive plants and five of 12 EpiC2B responsive reportedly carried amplified *Cf-2*. Further, the number of amplified *Hcr* genes were less as compared to profiling in wild tomato species. Avr2 triggered HR occurred only in the presence of *Cf-2-like* fragment in *S. verrucosum* CGN17767 from region A and *S. venturii* CGN17761 from region C, both species are related phylogenetically close to cultivated potato *S. tuberosum*. In *S. infundibuliforme* CGN17720 from region B, we discovered two plants with response to all four inhibitors, however their genotypes showed the presence of one *Hcr2-like* gene in one individual while the other carried only *Cf-2*. Strikingly, Avr2 recognition was weaker in plants carrying *Cf-2* while slightly more intense Avr2-triggered HR was observed in another plant carrying an *Hcr2* only.

All plants of *S. bulbocastanum* CGN22732, a more distantly evolved wild potato species in the North Region A clearly lacked *Cf-2* where very strong EpiC2B recognition was identified. One of four plants from *S. palustre* CGN18286, an outgroup wild potato species contained *Cf-2-like* gene and a few *Hcr2s* in separate plants (**Figure 4.7**). This is a surprising finding in contrast to wild tomato outgroup species, *S. ochranthum*, where we did not detect *Cf-2*. Therefore, *Cf-2* presence as detected based on amplified PCR product size is not restricted to tomato only and extend at least up to potato. We did not test for presence of *Cf-9* and *9DC* genes in our wild potato genotyping (or beyond to eggplant, pepper, tobacco and petunia) as we failed to amplify their canonical regions in a DNA sample from control potato line *S. tuberosum* and because we did not identify any pattern of *Cf-9/9DC* in relation to responsiveness to different inhibitors. Hence, it remains to be investigated whether *Cf-9* and *9DC* exist in potato and if they show any segregation pattern concurrent to inhibitor responses. There may, however, be single nucleotide polymorphism variations between tomato and potato *Cf-2/Hcr2* genes that we could not resolve fully in our DNA PCR product sequencing experiment. Furthermore, it could be that wild tomato and potato independently

evolved the ability to recognise Avr2 and other inhibitors, where different *Hcr2s* or related receptors confer recognition of the same inhibitor.

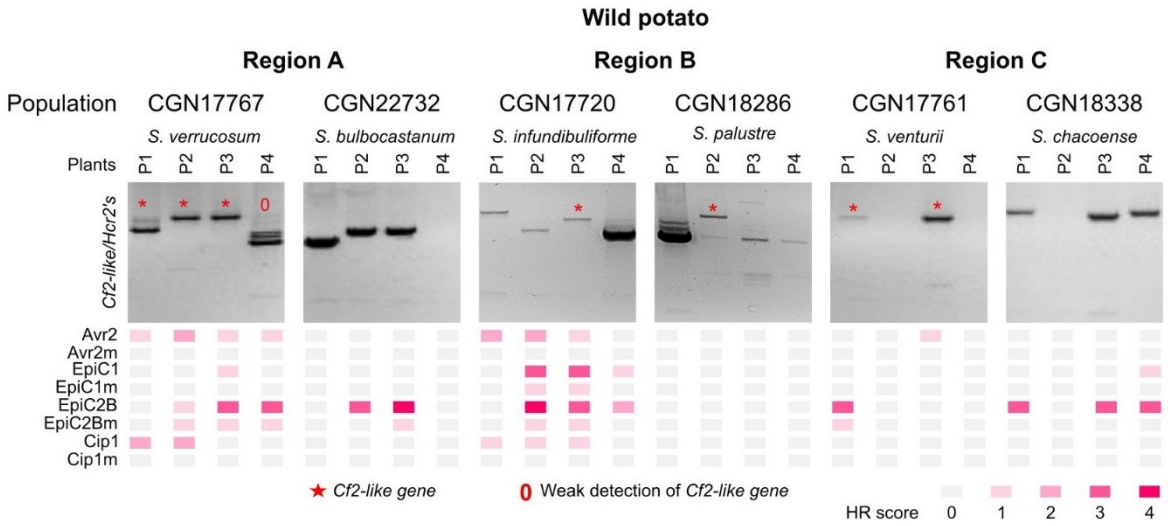


Figure 4.7 *Cf-2-like* genes are present in genotyped wild potato populations.
Genomic DNA PCR amplification of *Cf-2-like* fragments obtained using *Cf-2/Hcr2* primer in plants from selected two populations per region are shown. *Cf-2* controls are shown in figure 4.1. *Fragments are not sequenced and classified based on estimated product length.

4.2.6 Sequencing apoplastic cysteine proteases for relatedness with HR-associated recognition of unrelated inhibitors

Since the differences in recognition of distinct inhibitors Avr2, EpiC1, EpiC2B and Cip1 could not evidently be explained by the presence of *Cf-2, Cf-9* or *9DC* signals, we next aimed to investigate natural variations in relevant apoplastic cysteine proteases *Rcr3*, *Pip1* and *C14*, which are reportedly subject to contrasting selection pressures within and between tomato and potato (Hörger et al., 2012, Kaschani et al., 2010, Ilyas et al., 2015 and Kourelis et al., 2020). Therefore, we used PCR on genomic DNAs to isolate *Rcr3* fragments using previously published r072 forward/r073 reverse primers (Hörger et al., 2012). Similarly, we amplified *Pip1* fragments using SM_PIP1_1 forward/SM_PIP1_2 reverse primers and *C14* fragments using forward SM_C14_1/reverse SM_C14_2 primer set (**Table 2.6**). The *Act* gene (van der Hoorn et al., 2001) was amplified as PCR control in

all reactions (**Table 2.6**). After PCR, the products were purified and sequenced using specific primers in a sanger sequencing assay. The coding sequences of the cysteine proteases with the positions of PCR and sequencing primers are shown in **Figure 4.8(a)**.

We first tested the primers on a control plant line *S. lycopersicum Cf-2/Rcr3* and a representative population of *S. pimpinellifolium* (LA0753), distant wild tomato *S. pennellii* (LA0716) and a diploid wild potato *S. chacoense* (CGN18338). We obtained the expected *Rcr3* product of 1109 bp in all samples and a smaller fragment of 778 bp for the *Act* fragment (**Figure 4.8(b)**). Likewise, expected products for *Pip1* (1232 bp) and *Act* gene (778 bp) were amplified in all samples. For *C14* PCR, we obtained a single predicted product of 1298 bp with our designed primer set in control plant line *Cf-2/Rcr3* and *S. pimpinellifolium* LA0753. However, PCR reactions in *S. pennellii* LA0716 and *S. chacoense* CGN18338 delivered two products, one of expected size 1298 bp and another protease gene of ~923 bp were obtained in addition to *Act* control fragment of 778 bp. We next eluted the products of each cysteine protease and sequenced them using specific sequencing primers (Table 2.6). Similarly, samples from different *S. pimpinellifolium*, wild tomato and wild potato populations were used to PCR, purify and sequence *Rcr3*, *Pip1* and *C14*.

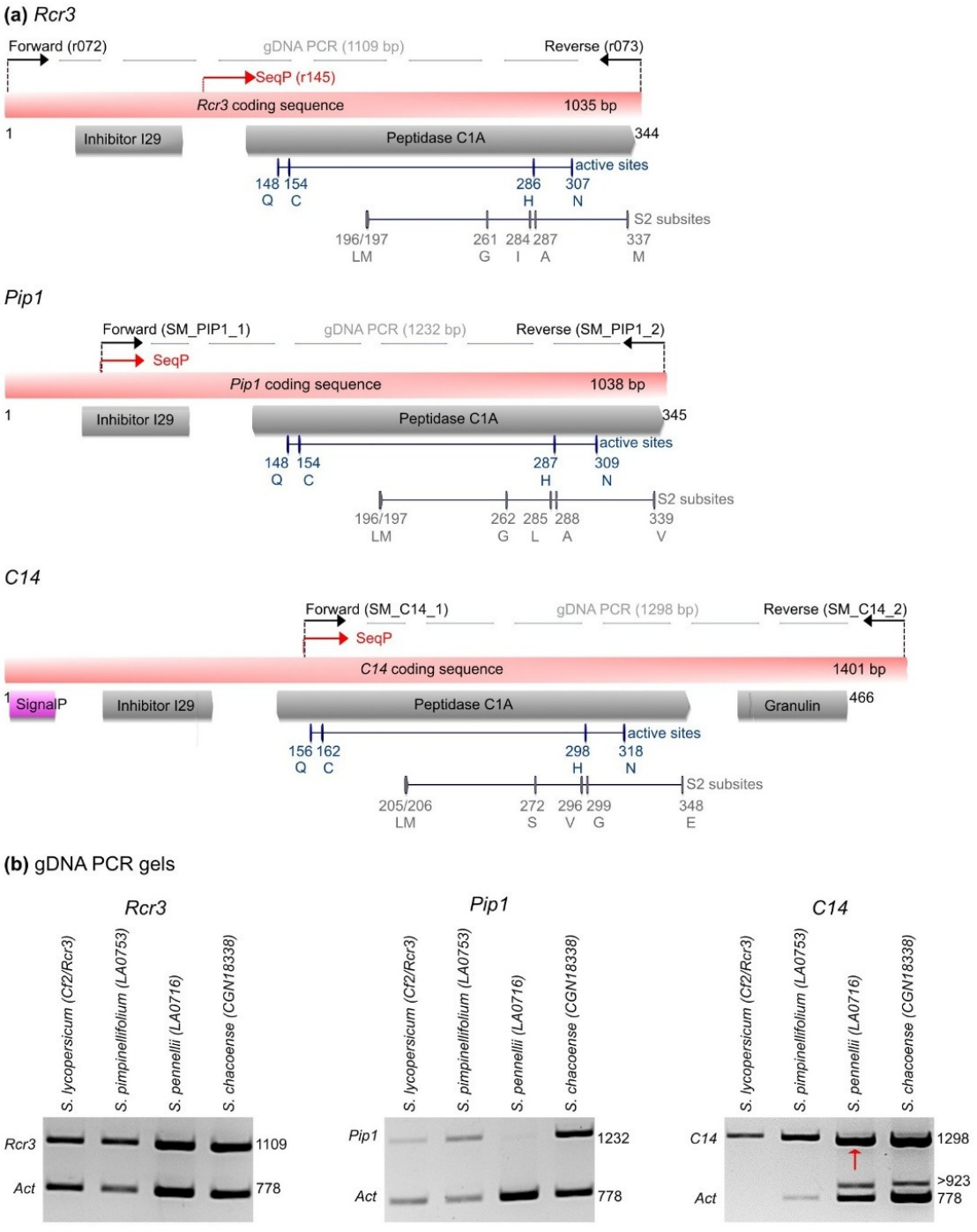


Figure 4.8 Detection and sequencing scheme of *Rcr3*, *Pip1* and *C14*.

The coding sequences of apoplastic cysteine proteases **(a)** *Rcr3*, *Pip1* and *C14*, and structural features of their products are shown. Positions of specific primer sets used for PCR and sequencing are highlighted. **(b)** DNA gels showing PCR products of *Rcr3*, *Pip1* and *C14* in representative *S. pimpinellifolium*, wild tomato and wild potato. *Act* gene was used as control. Red arrow in C14 gel indicate the product sequenced.

4.2.7 Effect of natural variation in *Rcr3* on recognition of inhibitors and evidence of positive selection revealing species-wide and Solanaceae-wide hotspots in *Rcr3*

To analyse sequence variation and evolutionary forces acting on *Rcr3*, we sequenced the region encoding the mature Rcr3 protease (without pro domain) from 86 individual plants from several populations representing multiple distantly related wild tomato and wild potato species from different geographical regions and displaying variations in HR phenotype against four inhibitors. High degree of *Rcr3* polymorphism has already been described, so we included 54 previously published tomato *Rcr3* alleles (Shabab et al., 2008, Hörger et al., 2012) and found an additional 32 *Rcr3*, across Solanaceae using BLAST (NCBI Gene/RefSeq database). A MUSCLE nucleotide alignment of 172 sequences were assembled in a multiple sequence alignment to construct a maximum-likelihood tree (**supplementary file 4.7**) (**Figure 4.9**). *Rcr3* alleles of *S. pimpinellifolium*, homologs from different wild tomato and wild potato taxa noticeably cluster into specific branches following phylogenetic orders of species evolution.

We noticed different *Rcr3* alleles existing in different plants from same population, therefore heterozygosity in *Rcr3* indicates genetic diversity that may improve host's capability to recognise Avr2 strongly or other inhibitors, EpiCs and Cip1. Further, three pruned trees were extracted specially for *S. pimpinellifolium* (**Figure 4.10**), other wild tomato (**Figure 4.11**) and wild potato (**Figure 4.12**) groups for detailed analysis of shared and unique allelic/selection pressure variations at *Rcr3*. Although eight individuals of each population were screened for HR against inhibitors in Chapter 3, not all individuals or populations were sequenced for cysteine protease variation analysis. Of 38 *S. pimpinellifolium Rcr3* alleles generated in this study, three were from Ecuador (region A), eight from North (region B), 17 from Lima province and seven from Ancash province in the Centre (region C) and three

were from Ica province in the South (region D) (**supplementary 4.8**). We focussed our analysis on 33 amino acid positions in *Rcr3* that showed a site substitution frequency spectrum of over 10%.

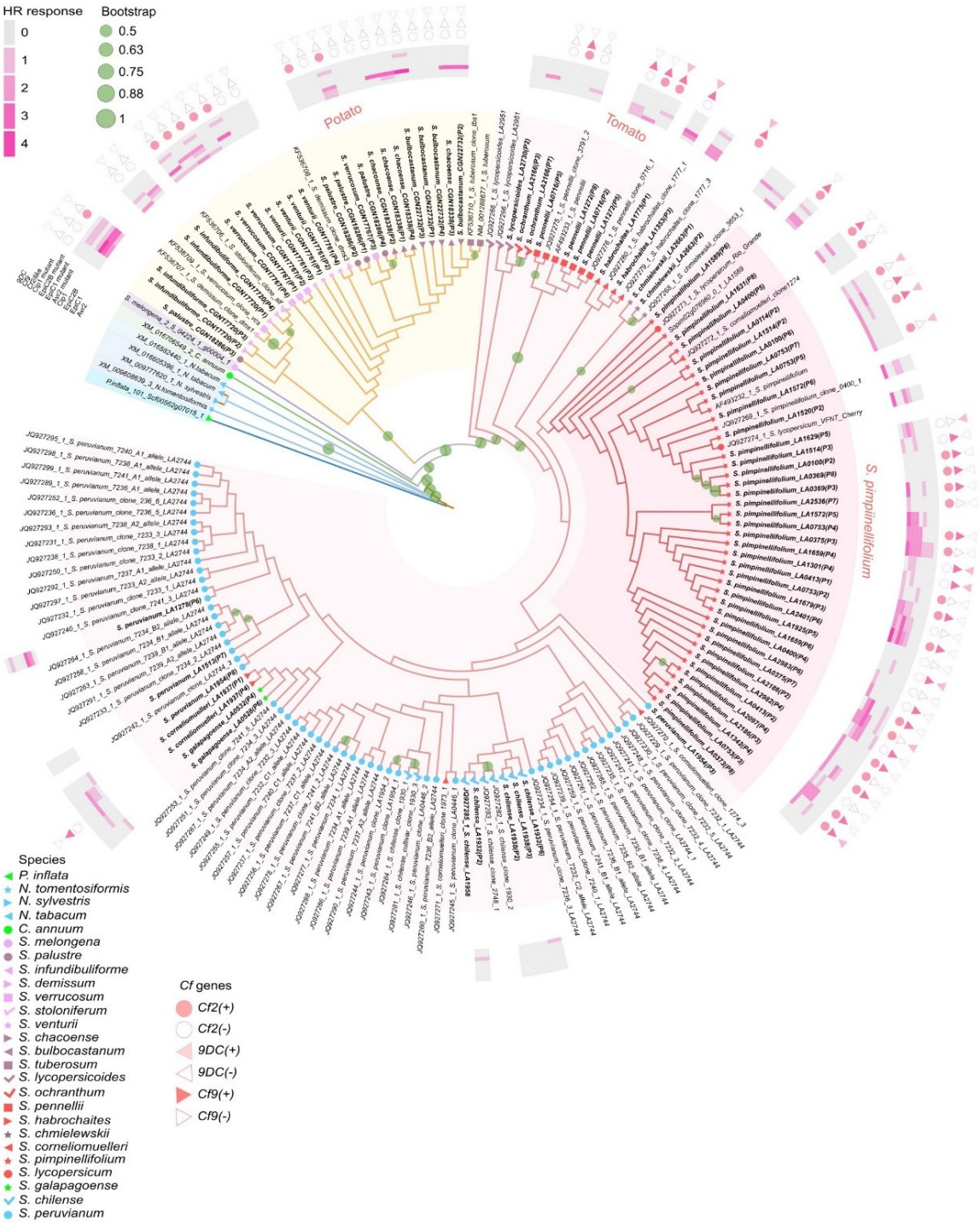


Figure 4.9 Phylogenetic tree of *Rcr3* gene family in Solanaceae.

Maximum-likelihood phylogenetic tree of 172 *Rcr3* genes, including 86 newly sequenced *Rcr3* in this study was constructed using a MUSCLE nucleotide alignment of 241 codons in MEGA12. The tree

is rooted at the most anciently evolved species, *Petunia inflata* as outgroup. Source species of *Rcr3* genes are depicted as symbols on branch tips. Green dot on a branch represent bootstrap value over 50% as derived from 500 replications. *Rcr3* generated from DNA sequencing in this study are distinguished in bold and HR scores from their source species tested against inhibitors are shown. Further, presence or absence of *Cf* genes genotyped in this study, are shown with certain new *Rcr3* sequences. *S. pimpinellifolium*, other wild tomato species and wild potato clades are depicted by three coloured branches and domains. These three clades are analysed in detail in figures 4.10, 4.11 and 4.12. *Phylogenetic tree in newick format and iTOL annotations are attached as supplementary S4.7.

Of 24 *Rcr3* alleles obtained for wild tomato species beyond *S. pimpinellifolium*, two variants of *S. galapagoense* populations in Ecuador, three variants representing *S. ochranthum* and *S. habrochaites* in North, four variants constituting *S. pennellii*, *S. peruvianum* and *S. habrochaites* in the Centre, 12 variants from *S. chilense*, *S. pennellii*, *S. corneliomuelleri*, *S. chmielewskii* and *S. peruvianum* in South and two variants of outgroup tomato species *S. lycopersicoides* from Tarapaca in Chile were included (**Figure 4.11**). Four plants from each wild potato population were tested in HR assay in Chapter 3 and for identifying natural variation in cysteine proteases, we sequenced *Rcr3* in all four plants of two wild potato species from each of the three geographic regions. *Rcr3* natural variants sequenced from 24 individuals of wild potato species (**Figure 4.12**) consisted of all four individuals of *S. verrucossum* (CGN17767) from Mexico and of *S. bulbocastanum* (CGN22732) from Guatemala in region A, of outgroup wild potato species *S. palustre* (CGN18286) from Chile and *S. infundibuliforme* (CGN17720) from Bolivia in region B and all individuals of *S. chacoense* (CGN18338) from Paraguay and *S. venturii* (CGN17761) from Argentina in region C.

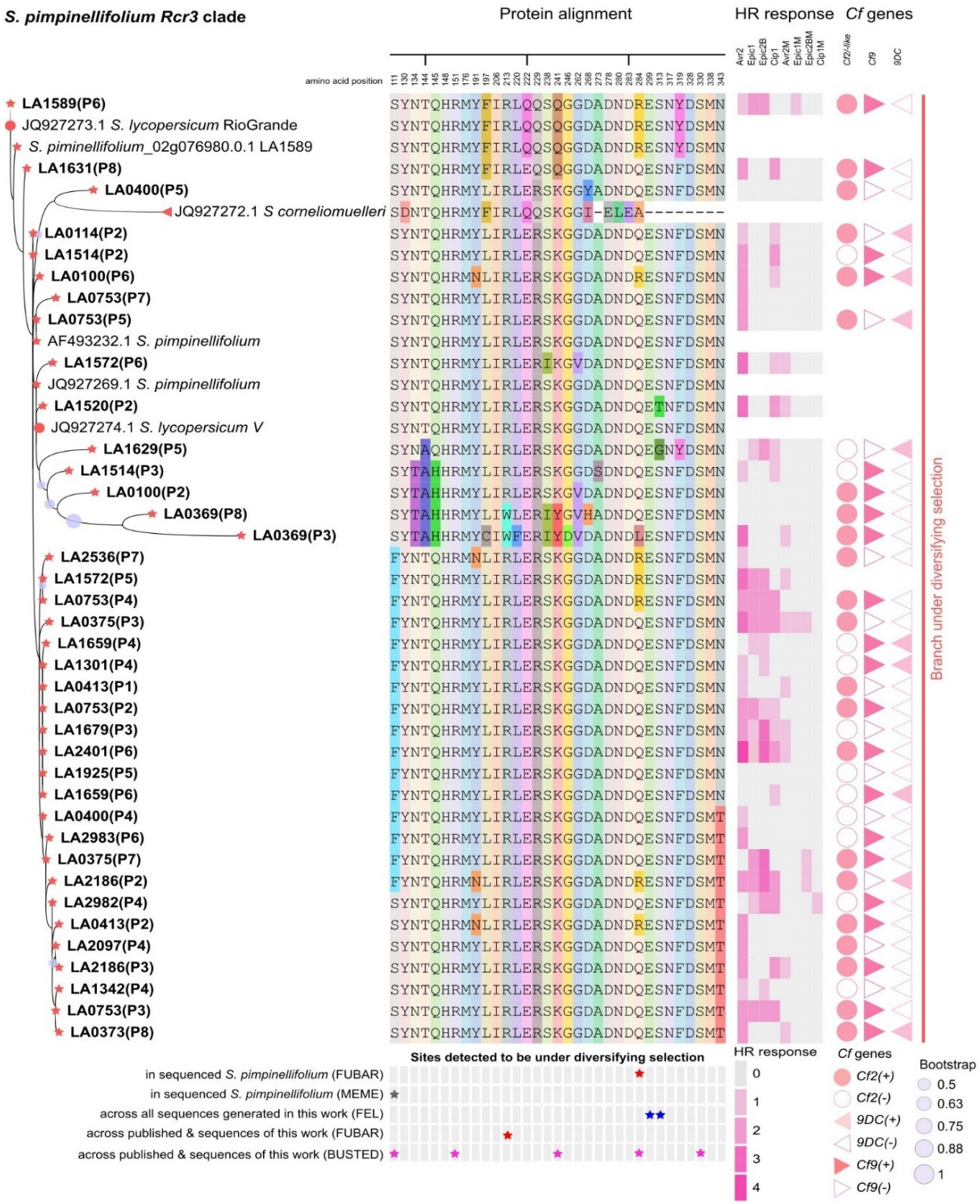


Figure 4.10 *Rcr3* is under diversifying selection in *S. pimpinellifolium*.

This tree shows detailed section of *S. pimpinellifolium* clade from *Rcr3* gene tree in figure 4.9. Bootstrap score of over 50% is shown as grey circles at branch midpoints. 38 *Rcr3* sequences newly generated in this study are shown in bold. MUSCLE alignment of 33 amino acid positions having site frequency spectrum of over 10% in overall Solanaceae-wide analysis are shown. HR scored in response to inhibitors tested in this study are indicated. Symbols on branch tips indicate species origin (figure 4.9). *Cf* genes from genotyping of selected individuals are also shown. A BUSTED

method with only non-synonymous substitutions was used to detect gene-wide selection pressure on *S. pimpinelifolium Rcr3* clade. Next, a Bayesian counting approach using FUBAR was used to pinpoint sites that are under positive selection. A maximum-likelihood test based on mixed-evolutionary model. MEME, was further used to correlate FUBAR results or identify missed sites under episodic positive selection. Sites that are broadly under diversifying selection in *Rcr3* are also detailed and were identified using FEL, FUBAR and BUSTED. *Nucleotide sequences generated in this study and alignment sites displayed in iTOL annotation are attached as supplementary S4.8.

Most amino acid variation in Rcr3 in *S. pimpinellifolium* were detected in the Centre region C, where high frequency of response and variations in HR against multiple inhibitors were also observed (Chapter 3). Structural predictions on Rcr3 protease domain previously showed that highly variable residues are located around the substrate-binding groove and are exposed to the surface, whereas residues constituting the substrate binding groove and catalytic site are well conserved (Kourelis et al., 2020). While we observed no changes in three active site residues C155, H287 and N308, we found substitutions at component sites of the substrate binding groove. F197 was conserved only in Avr2 and Cip1 recognising LA1631(P8) in North whereas leucine (F197L) was found in all other *S. pimpinellifolium* populations and cysteine (F197C) in plant 3 of LA0369 that specifically recognise Avr2. Further, highly conserved glycine at 262 showed substitutions to valine (G262V) in LA0100(P2), LA1572(P6), LA0369(P8) and LA0369(P3) in Lima region. LA0369(P8) does not recognise any inhibitor, however, LA0100(P2) and LA1572(P6) weakly perceived Cip1 in consolidation with other different substitutions. Methionine to valine substitutions at conserved site M338V were detected in four individuals of *S. pennellii*, LA1272(P5) and LA1272(P8) in Lima of Centre region and LA0716(P2) and LA0716(P5) in Arequipa of South region. Despite no other Rcr3 sequence variations in these four plants, all four plants displayed variation in inhibitor recognition in different *Hcr2* genetic backgrounds (**Figure 4.10**).

Previous studies identified amino acid polymorphisms in Rcr3 that are functionally capable of influencing strength of HR against Avr2, but not HR with EpiC1, EpiC2B and Cip1 via

Rcr3/Cf-2 (Hörger et al., 2012, Shindo et al., 2016, Kourelis et al., 2020, Kourelis et al., 2024). Substitutions into aspartic acid (D) and glycine (G) at site 194 otherwise carrying a conserved asparagine (N) were shown to cause reduced sensitivity to Avr2 inhibition (Shabab et al., 2008, Kourelis et al., 2020). Plant P3 of LA0369 recognises Avr2 while P8 does not, even though it is *Cf-2* positive, both carry a cysteine substitution N194C. However, Plant 3 of LA0369 contains four additional substitutions (F197C, L220F, G246D and R284L) that are absent in Plant 8 and potentially either compensate for N194 or collectively increase recognition of Avr2 (**Figure 4.10**). Lysine at 194 (K194) were found in Avr2 insensitive plants P3 and P7 of *S. ochranthum* LA2166. Avr2 insensitive natural Rcr3 variants of *Nicotiana* also have K194 and their replacement with N enhances the variant's sensitivity to Avr2 inhibition (Kourelis et al., 2020). K194 in Rcr3 could possibly explain why Avr2 is not recognised in the presence of *Cf-2* in LA2166(P7). Moreover, R151Q associates with elevated Rcr3 inhibition by Avr2 (Hörger 2011) and Q151 was found in LA2166 in combination with K194, yet no response against Avr2 was observed in the presence or absence of *Cf-2* in P7 and P3 of LA2166 (**Figure 4.11**).

Rcr3 variants carrying substitutions H148N and R151Q are increasingly inhibited by EpiC1 whereas H148N and D283N cause enhanced inhibition by EpiC2B (Hörger 2011, Ilyas, 2014). H148D is also crucial for Rcr3 inhibition by EpiC1 of *Phytophthora mirabilis* (Dong et al., 2014) and its additive effect on increased Avr2 inhibition of Rcr3 has been revealed in combination with R151V/N194D or N194D/Q284R (Kourelis et al., 2020). We found no variations at H148 in our tested *S. pimpinellifolium* samples, however H148N substitutions were detected in wild tomato and potato populations and H148Y in wild potato populations in regions B and C (**Figure 4.11 and 4.12**). We identified *Cf-2*-carrying *S. habrochaites* LA1353(P3) in North region recognised Avr2, EpiC1 and EpiC2B, but not Cip1 with equal HR strength and had genetic variations H148N and D283N in combination with R151, K241 and R284. Further, *S. galapagoense* LA0532 from Ecuador weakly recognised only Cip1

and mutant Avr2 in the presence of D283E and F319S substitutions as well as H148, R151, K241 and R284 (**Figure 4.11**).

We also noted novel variations S313T in combination with R284Q in LA1520(P2) from Lima that conferred strong HR against Avr2, moderate HR upon Cip1 treatment. Similarly, S313G differing from LA1520 in combination with T144A, R284Q and F319Y in *Cf-2*-lacking LA1629 potentially relates to inhibitor recognition difference as LA1629 did not recognise Avr2, but EpiC1 (HR score 1), EpiC2B (HR score 2) and Cip1 (HR score 1) (**Figure 4.11**). Surprisingly, we did not find Rcr3 substitutions uniquely present in plants/populations that were responsive to all four inhibitors. However, we did find a few variations specifically in *S. pimpinellifolium*, wild tomato and wild potato groups that likely impact the strength of HR-associated inhibitor recognition, in combination with substitutions occurring at other sites in Rcr3 as well as in presence of absence of corresponding receptor. Most Rcr3 substitutions detected in our samples did not explicitly associate with differential recognition of distinct inhibitors in *Cf-2*-carrying genetic backgrounds across geographical regions.

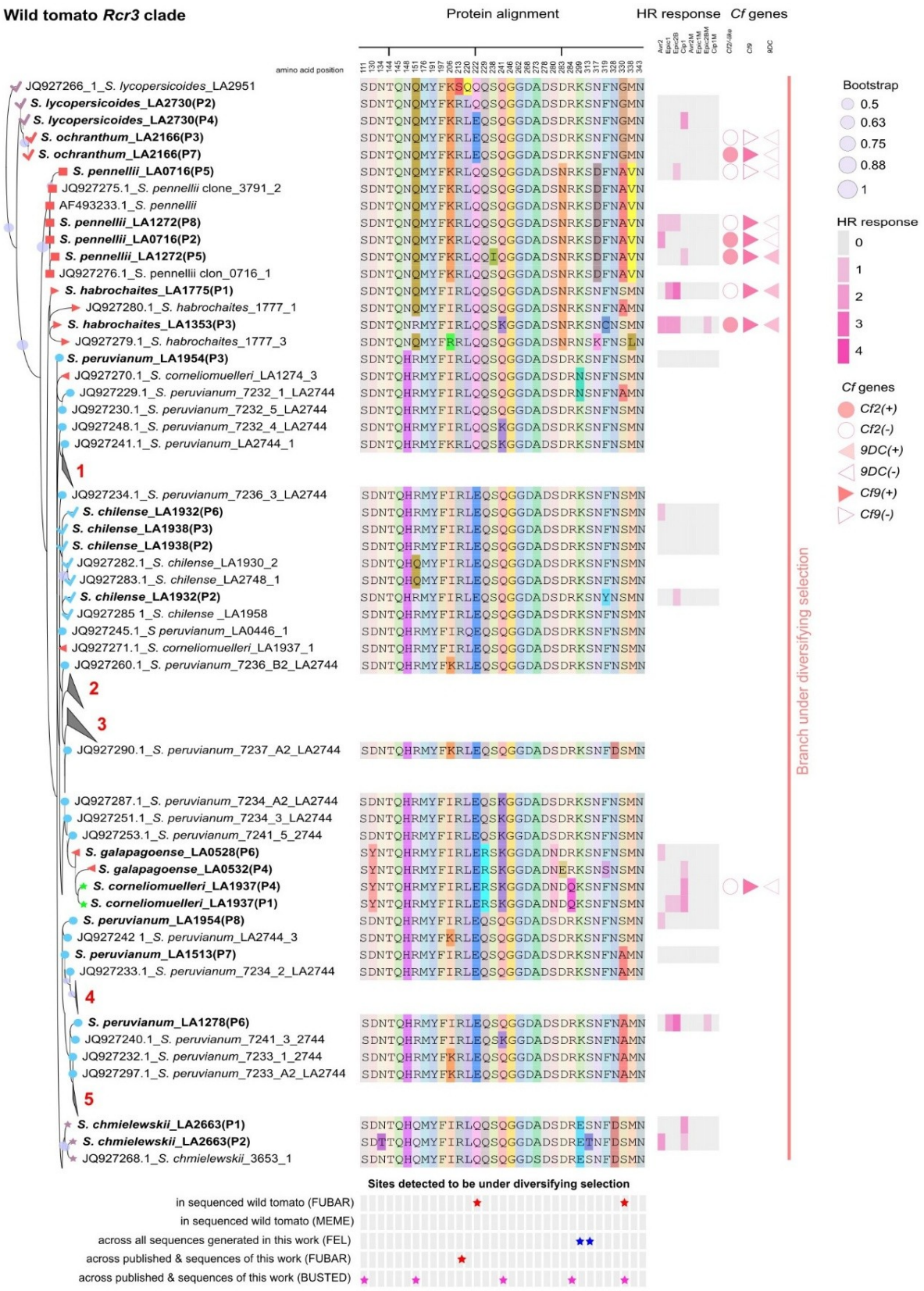


Figure 4.11 *Rcr3* is under diversifying selection in wild tomato.

Section of wild tomato clade from *Rcr3* gene family tree in figure 4.9 is shown. *Rcr3* sequences obtained in this study are indicated in bold. Grey circles represent over 50% bootstrap values and symbols on branch tips represent *Rcr3* source species (detailed in figure 4.9). HR scores and *Cf*

genes are detailed where analysed in *Rcr3* source population/plant. Approaches to identify selection pressure on *Rcr3* in wild tomato and allelic sites under selection are detailed in figure 4.10. Collapsed clades indicate previously published sequences with shared similarities at highlighted amino acid positions (**1**: *S. peruvianum* clones JQ927247/35/65/62/61/59/39/54 having shared homology to JQ927248; **2**: JQ927246 identical to JQ927260 and JQ927243/44 having substitutions represented in expanded *S. peruvianum* clades; **3**: *S. chilense* JQ927281/84 do not have any substitutions unique from described sequences; **4**: *S. peruvianum* JQ927291/63/58/64 identical to JQ927233, except for position 208 (K); **5**: *S. peruvianum* JQ927292/50/38/31/93/36/52/89/99/98/95/96 all are identical to JQ927232. *Data attached as supplementary S4.8.

To detect the evolutionary selection pressure acting on *Rcr3*, we first performed BUSTED (Branch-site Unrestricted Statistical Test for Episodic Diversification) (Murrell et al., 2015), a likelihood ratio based test for aggregated evidence of gene-wide episodic diversifying selection by analysing 145 of 172 unique variants, testing 241 *in-frame* codon sites in global nucleotide MUSCLE alignment (**supplementary files 4.8**). The BUSTED hypothesis states that at least one branch of the *Rcr3* gene tree has positive selection evidence on at least one site (Figure 4.9). BUSTED also does a quick evidence-ratio based analysis to look for specific sites that might have been the target of positive selection after a gene-wide signal of positive selection has been established. This analysis only included site to site non-synonymous rate variation resulting in the identification of ten codons in *Rcr3* with Evidence ratio (ER) ≥ 10 indicating positive selection across Solanaceae. Five of the ten codons under diversifying selection are 111, 151, 241, 284 and 330 and are highlighted in the displayed alignment of 33 amino acids in **Figures 4.10, 4.11 and 4.12** (detailed BUSTED analysis is shown in **supplementary 4.3**). While BUSTED found evidences of diversifying selection occurring at *S. pimpinellifolium* and wild tomato, it did not detect gene-wide evidence of positive selection within wild potato. BUSTED offered an advantage in our case where we had limited representatives from specific taxa, but since there were no clade-wide signatures of diversifying selection outside wild tomato, we next aimed at identifying individual sites in *Rcr3* under positive selection across Solanaceae.

Assuming that selection pressure at each site remains constant throughout phylogeny, we used FUBAR (Fast, Unconstrained Bayesian Approximation) (Murrell et al., 2013) to determine dN/dS substitution rates (represented through posterior probability; dN > dS) at individual sites in global nucleotide alignment. This approach identified only codon site 213 to have posterior probability of >0.9 indicating it is under positive selection across Solanaceae. We were further interested in identifying whether any site in 86 *Rcr3* sequences newly generated in this study have experienced positive selection that may have been missed in an overall Solanaceae-wide analysis, we therefore used FEL (Fixed-Effects Likelihood) (Kosakovsky-Pond et al., 2005), a pervasive maximum likelihood selection test suitable for small to medium datasets and individually tests whether dN=dS≠1 or not at each site in a given alignment.

Using a contrast FEL test, we attempted to determine contrast in selection pressure at same sites between three clades (*S. pimpinellifolium*, wild tomato and wild potato), but did not obtain any site with variable selection pressure across our tree. The significance of random effects was evaluated using Likelihood Ratio Test (LRT) for fixed effects, which used a parametric bootstrap resampling of 500 replicates to derive site by site null LRT distributions with a *p*-value threshold of $p \leq 0.05$ and dN/dS ratio ≥ 1. Using FEL, we identified amino acid sites 299, 313 and 341 to be under positive selection in *S. pimpinellifolium*, other wild tomato species and wild potato species. Overall distribution of each selection type site ratios of asymptotic and bootstrap *p*-value are shown as **supplementary 4.2 (a)**. However, FUBAR has a speed advantage as well as superior statistical estimates over FEL approach.

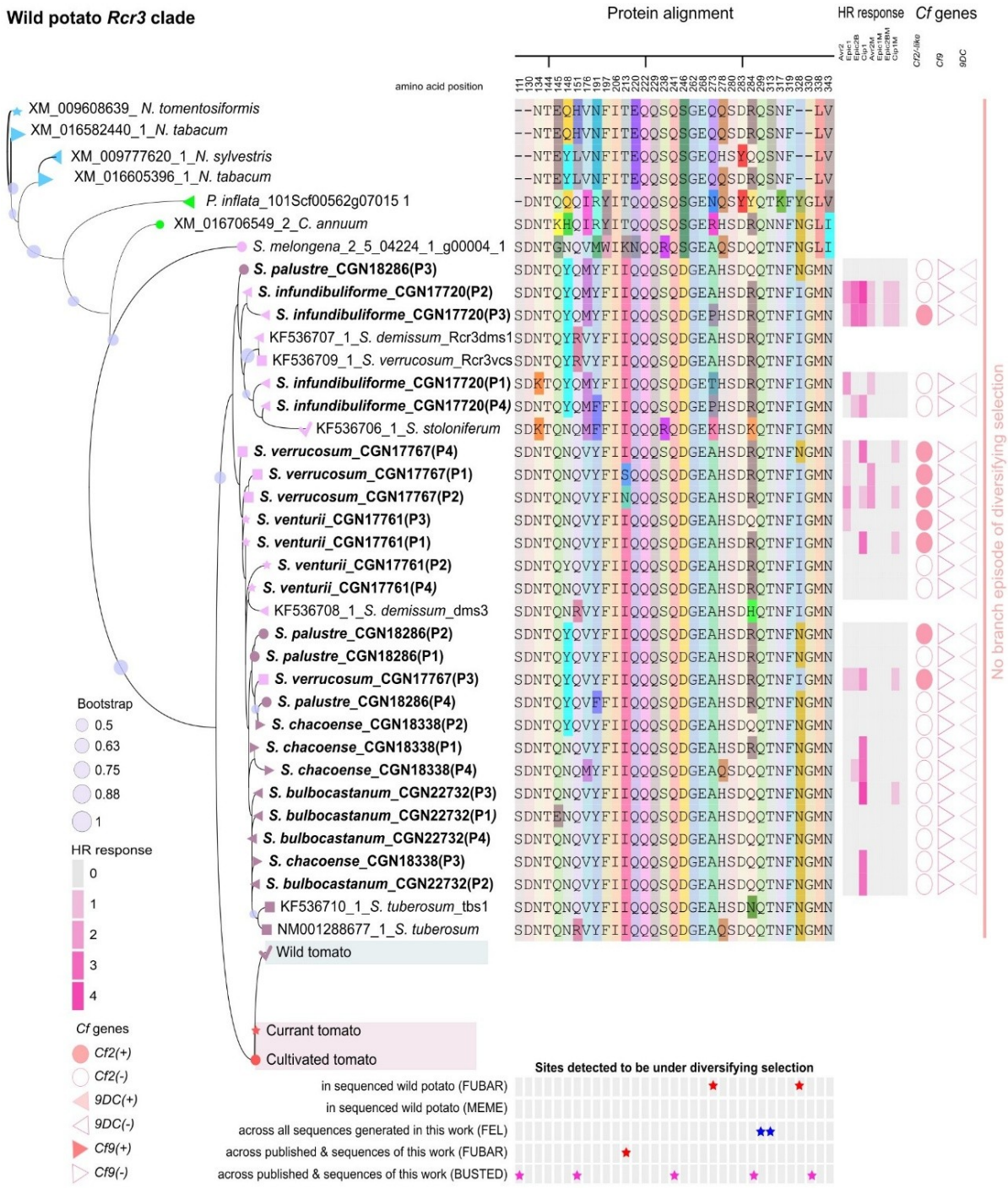


Figure 4.12 Clade-wide signature of diversifying selection not detected on *Rcr3* in wild potato. Pruned tree of wild potato clade sectioned from *Rcr3* phylogenetic analysis performed in figure 4.9 is shown. *Rcr3* sequences generated in this study are highlighted in bold, with grey circles on branches implying >50% bootstrap scores. Symbols at branch tips indicate *Rcr3* source species and are listed in figure 4.9. HR assay scores against inhibitors and *Cf* genotyping evaluated for *Rcr3* source populations/plants in this work are described. Selection pressures on *Rcr3* and individual allelic sites in wild potato were estimated as detailed in figure 4.10. *Data attached as supplementary S4.8.

Narrowing down to identify sites under positive selection in each group, we used MEME (Mixed Effects Model of Evolution) (Murrell et al., 2012) on group-specific nucleotide alignments of *Rcr3*. MEME is capable of revealing sites in branches even when there is selection difference among various branches in a tree by estimating site-wise synonymous (alpha) and categorical mixture of non-synonymous (beta) rates likelihood ratios that determine if beta > alpha at a site. The results aggregate information estimated at each site over branches in each group. Hence, the selection signal is derived from site-level episodic diversification, which estimated a combination of strength of evolution [effect size] and the fraction of the tree affected by an episode. At *p*-value threshold of 0.05 in MEME, five sites (111, 293, 294, 343 and 344) were detected to be under positive selection in *S. pimpinellifolium*. Group-specific nucleotide instead of global alignment revealed different selection pressures acting on same sites in different groups.

MEME identified that *Rcr3* amino acid 174 is under diversifying selection in wild tomato whereas no site in *Rcr3* was detected to be under diversifying selection in wild potato. We also used FUBAR as an alternative approach to identify amino acid positions under diversifying selection. Sites 213, 186, 196 and 284 in specifically in *S. pimpinellifolium*, sites 222 and 330 in wild tomato species group and sites 161, 273 and 328 in wild potato species group (**supplementary 4.1(a)**). Balancing selection at tomato *Rcr3* locus has been reported as a key driver in maintaining variation in response strength to Avr2 (Hörger et al., 2012). In consistence with previous finding (Shabab et al., 2008), we found that *Rcr3* is under positive selection in *S. pimpinellifolium* and across wild tomato species. We further identified the sites that are targets of positive selection specifically in *S. pimpinellifolium*, wild tomato, wild potato and overall across Solanaceae.

4.2.8 Natural diversity in *Pip1* gene and their consequences in relation to observed variations in inhibitor recognition and evolutionary selection pressure

Pip1 and *Rcr3* are independently evolved paralogs from the same genomic locus (Ilyas et al., 2015, Kourelis et al., 2020) and Pip1 is also inhibited by Avr2 (Tian et al., 2007). While there is no direct evidence that cysteine proteases play a role in the recognitions of EpiC1, EpiC2B and Cip1, these inhibitors do inhibit cysteine proteases with varying sensitivity in tomato (Shabab *et al*., 2008, Kaschani *et al*., 2010, Shindo *et al*., 2015). Therefore, we looked for a correlation between *Pip1* variation and HR induced by Avr2, EpiCs and Cip1 (**Figure 4.13**). Amino acid residues constituting the substrate binding groove are conserved in Rcr3 and Pip1, but variations between these proteins exist primarily in amino acids around substrate binding groove or over solvent-exposed surface (Shabab et al., 2008, Ilyas et al., 2015, Kourelis et al., 2020). Hence, we sequenced regions encoding the mature Pip1 protease domain from 24 different individuals of *S. pimpinellifolium* consisting one population from Ecuador (LA0413), four populations from North and Centre each and three populations from South. Further, Pip1 alleles were derived from wild tomato species including *S. ochranthum* LA2166(P7) and *S. habrochaites* LA1353(P3)/(P4) from North, *S. pennellii* LA1272(P5)/(P8) and *S. habrochaites* LA1775(P1) from Centre and *S. pennellii* LA0716(P2)/(P5) and *S. corneliomulleri* LA1937(P4)/(P7) from South (**Figure 4.13**).

Pip1 alleles were also sequenced from six different wild potato species representing *S. verrucosum* CGN17767(P1)/(P2) and *S. bulbocastanum* CGN22732(P3) from region A, *S. infundibuliforme* CGN17720(P1)/(P3)/(P4) and *S. palustre* CGN18286(P1)/(P2) from region B and *S. chacoense* CGN18338(P4) and *S. venturii* CGN17761(P1) from region C. In addition to 34 newly sequenced *Pip1* alleles, 13 *Pip1* genes were extracted from NCBI RefSeq database as reference, we built a global nucleotide MUSCLE alignment of 295

codons (283 without gaps) of full-length 345 codons (Reference: Solyc02g077040.2.1 or NP_001233949). In a 500 bootstrap replication maximum-likelihood tree, group specific *Pip1* alleles visibly align within *S. pimpinellifolium*, other wild tomato taxa and further wild potato taxa in a phylogenetic genus order (**Figure 4.13**).

Only 31 amino acid sites in Pip1 that showed a frequency spectrum variation of more than 10% were examined in detail. Our findings did not identify remarkable substitutions that were unique to a species group or geographical area and that did not appear to be correlated with differences in inhibitor recognition variations. We did not detect any variation in active site residues C154, H287 and N309, but out of six highly conserved S2 sub-site residues, we detected variation V339I in wild tomato *S. pennellii* LA1272(P8) that weakly recognised Avr2, EpiC1 and EpiC2B and in wild potato *S. verrucossum* CGN17767(P2) that responded moderately to Avr2/Cip1 and weakly to EpiC2B and its mutant. Pip1 variations D147R and V150E reportedly are insensitive to EpiC2B (Schuster et al., 2024), but we did not find either in our tested natural populations (**Figure 4.13**). Interestingly we noticed that CGN17767(P2) carry V150G in combination with other substitutions that differ from LA1272(P8) and this may underlie the slight differences in their inhibitor recognition profiles. Previously displayed natural variations from different wild tomato species occurring at nine selected sites in Pip1 displayed minor differences in Avr2 or EpiC2B inhibitions (Hörger 2011, Ilyas, 2014).

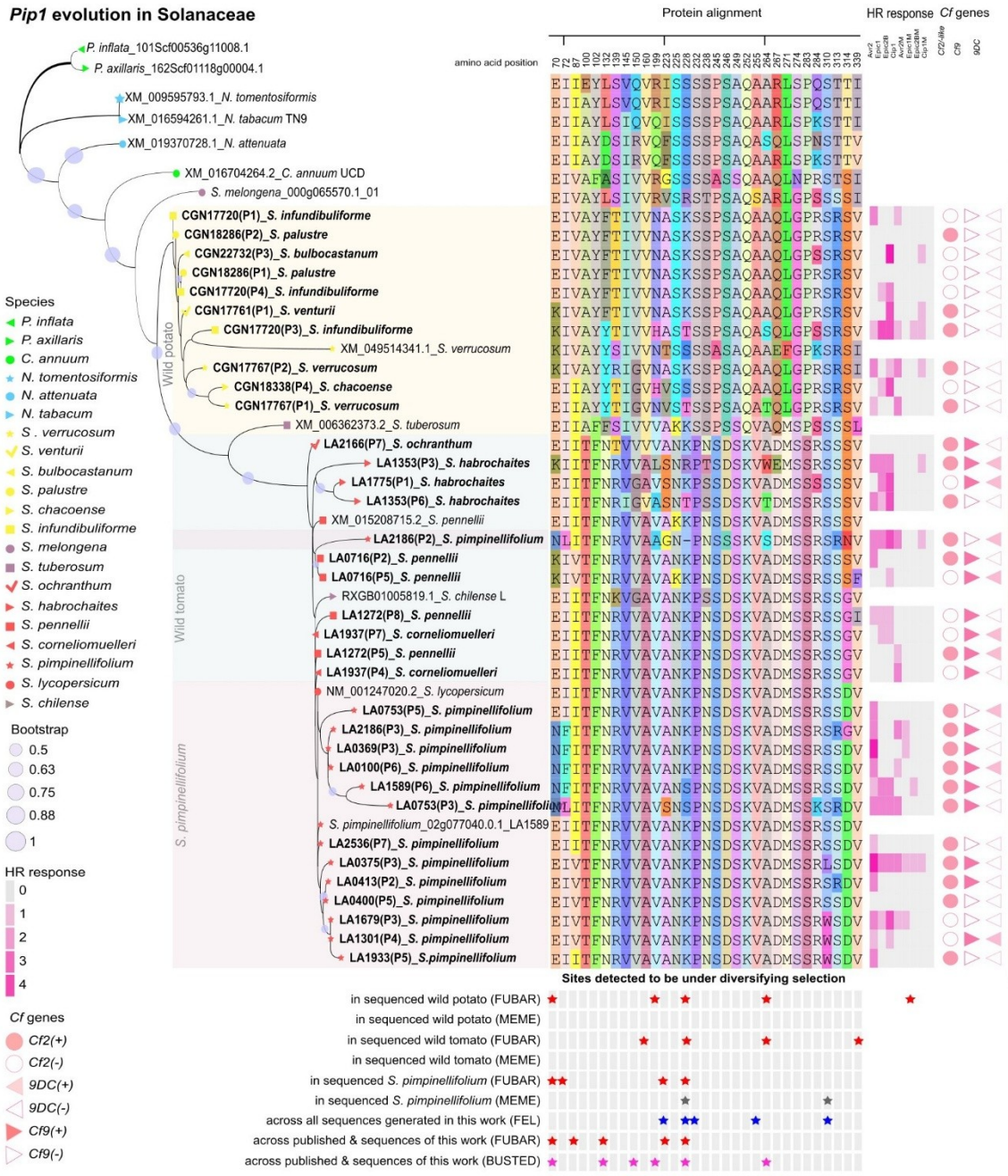


Figure 4.13 Evolutionary analysis in Solanaceae suggests *Pip1* is under diversifying selection in wild tomato, but not in *S. pimpinellifolium* and wild potato.

A maximum-likelihood phylogenetic DNA tree with 500 bootstrap replication method was constructed using MEGA12. Bootstrap score of over 50% are shown as grey circles on branch lengths. 34 newly sequenced *Pip1* alleles obtained in this study are shown in bold, with 14 from *S. pimpinellifolium*, ten from wild tomato and ten from wild potato populations/plants. A MUSCLE alignment of 295 *Pip1* codons was generated and 31 highlighted amino acid positions correspond sites with frequency spectrum of over 10% among sequenced in this work. Symbols at branch tips are species listed on left. Associated HR scores against all four inhibitor treatments and their mutants indicate potential variability in *Pip1* allelic strength towards recognition. Further, *Cf* genes in correlation to allelic sites and HR phenotypes are shown. The tree is rooted at *Petunia inflata Pip1* as outgroup for entire

family, Natural selection was detected for Solanaceae and independently within *S. pimpinellifolium*, wild tomato and wild potato using methods described in figure 4.10. *DNA sequences generated in this study, phylogenetic tree in newick format and iTOL annotations are attached as supplementary S4.9.

S. chilense Pip1 carrying R139K, N238S and D314S and *S. habrochaites* carrying A223S in combination with D267H, S283Y and D314S are inhibited by Avr2 and EpiC2B with nearly identical strengths (Ilyas, 2014). In our tested *S. habrochaites*, we identified N238T/D314S in LA1353(P3) and N238S/D314S in LA1353(P6), both individuals carry *Cf-2* and respond to Avr2, EpiC1 and EpiC2B (**Figure 4.13**). However, LA1353(P6) confer marginally stronger recognition of EpiC2B and we noticed that it also has V150G along with a few other site variations as compared to LA1353(P3). We also detected substitution combinations of R139T, N238S and D314S in non-responsive outgroup wild tomato species *S. ochranthum* 2166(P7) and in different wild potato species, including non-responsive outgroup *S. palustre* CGN18286. Strikingly, we detected R284K in *S. pimpinellifolium* LA0753(P3) that well recognised all four inhibitors Avr2, EpiC1, EpiC2B and Cip1 in the presence of *Cf-2*. Further, R284S was detected in *S. habrochaites* LA1775(P1), *S. bulbocastanum* CGN22732(P3) and *S. infundibuliforme* CGN17720(P3) that either strongly responded to EpiC2B or additionally to other inhibitors in the presence of absence of *Cf-2* (**Figure 4.13**). Of course, there were other substitutions present in these responsive versus non-responsive plants. Our findings of limited unique *Pip1* variation correlation with differential recognition of distinct inhibitors indicate various other components essentially and additively may play a part in conferring recognition specificities with variable strengths.

After identifying natural variation in *Pip1*, we next performed several statistical tests to analyse evolutionary signatures of positive selection on Pip1 across Solanaceae. Firstly, we used BUSTED (Murrell et al., 2015) and identified gene-wide episodes of diversification on wild tomato clade, but not specifically on *S. pimpinellifolium* and wild potato clades (**Figure 4.13**). Further, BUSTED revealed that amino acid sites 70, 77, 132, 150, 186, 196

199, 228 and 264 in *Pip1* gene are under positive selection overall in Solanaceae (**supplementary 4.4**). Secondly, FUBAR (Murrell et al., 2013) analysis identified amino acid sites 70, 77, 87, 132, 186, 223, 228 and 285 of *Pip1* are under positive selection across Solanaceae. Thirdly, FEL (Kosakovsky-Pond et al., 2005) test on 34 newly sequenced Pip1 alleles determined amino acid sites 223, 228, 232, 255, 268, 272, 273, 277, 280, 294 and 310 to be positively selected (**supplementary 4.2(b)**).

Because gene-wide evidences of selection were not obtained in *S. pimpinellifolium* and wild potato clades, we ensured that any signatures of positive selection on individual sites are not missed. Hence, we used two different statistical approaches, FUBAR and MEME on group-specific *Pip1* nucleotide alignments. FUBAR analysis identified that amino acid sites 70, 72, 223 and 228 in *S. pimpinellifolium*, 160, 228, 264, 285, 294, 324 and 339 in wild tomato and 70, 77, 142, 186, 199, 228 and 264 in wild potato are under positive selection (**supplementary 4.1(b)**). A MEME (Murrell et al., 2012) analysis resulted in different site selections where 228 and 310 are revealed to be under positive selection in *S. pimpinellifolium*, but no sites were detected to be positively selected in wild tomato and wild potato. Our results are consistent with previous reports suggesting *Pip1* is under diversifying selection in wild tomato (Shabab et al., 2008). Although *Pip1* displays higher amino acid variation in comparison to many cysteine proteases, it exhibits lesser diversity when compared to its paralog *Rcr3* in wild tomato (Shabab et al., 2008, Ilyas et al., 2015). Our finding of diversifying selection in *Rcr3* but not in *Pip1* within *S. pimpinellifolium* is complementary to this view.

4.2.9 Natural variation and sites under positive selection identified in *C14*

C14 is another host protease targeted by EpiCs (Tian et al., 2007, Song et al., 2009) and a direct interaction between EpiC2B and C14 was previously demonstrated (Kaschani et al., 2010). Moreover, tomato C14 has been shown to contribute to resistance against *P.*

infestans infection (Kaschani et al., 2010). *Arabidopsis RD21* is a *C14* ortholog known to play different roles in resistance against different pathogens. RD21 contributes to resistance upon infection by fungal pathogen *Botrytis cinerea*, but not against oomycete *Hyaloperonospora arabidopsidis* and bacterial pathogen *Pseudomonas syringae* (Shindo et al., 2012). We hypothesised that significantly stronger and frequent recognition of EpiCs could be due to underlying high variation in *C14* in natural *P. infestans* host wild potato in comparison to wild tomato. Therefore, individuals/populations that were source of allelic variations in *Pip1* in this study were also studied for *C14* variation (**Figure 4.14**). We thus aimed to seek correlation between natural variation in *C14* and HR-triggered by inhibitors, particularly EpiCs in this study.

A MUSCLE alignment was created using 19 already published *C14* references (Kaschani et al., 2010, NCBI Genes database) and 34 *C14* sequences generated in this study by DNA sequencing of 272 codons of original full-length 466 amino acids long C14 (NCBI Reference: *S. lycopersicum* CYP1 CAA05894 and *S. tuberosum* AJ245924). In a maximum-likelihood tree, we noted that although *C14* from *S. pimpinellifolium*, other wild tomato and wild potato taxa cluster into their specific groups, two allelic subsets were formed within wild potato (**Figure 4.14**). Ten wild potato *C14* alleles that are newly sequenced in this study cluster separately from previously described *C14* alleles (Kaschani et al., 2010). A possible reason could be that both subsets contain representatives from different wild potato species/populations, where our sequenced subset 2 specifically consists alleles from diploid relatives. The tree displays alignment of sites that had over 10% site variation frequency overall, therefore only 13 amino acid positions, 195, 221, 277, 284, 291, 302, 326, 327 and 336 of C14 protease domain and 383, 393, 396 and 425 of granulin domain are shown (corresponding sites in 292 alignment attached in **supplementary 4.10** are 1, 27, 83, 90, 97, 108, 132, 133, 142, 189, 199, 202 and 231).

The amino acid triad that make up active site/catalytic region were found to be conserved in our study. We discovered that amino acid site 277 and 326 were especially variable in *S. pimpinellifolium*, whereas sites 393 and 396 displayed variations restricted only to the wild potato clade. The R195K substitution that has previously been reported in wild tomato is also present in our tested individuals from more distant species from *S. pimpinellifolium*, *S. pennellii*, *S. habrochaites* and *S. ochranthum* but not in closer *S. corneliomulleri*. Since amino acid positions 148, 151, 194 and 284 surround the substrate binding groove in papain-like cysteine proteases, any variations detected in these can impact the alterations in inhibitor binding (Kourelis et al., 2020). However, our results indicate variations only at 284 among these crucial sites. Plant 6 of LA1589 has substitution K284N, which showed enhanced recognition of EpiC1 and EpiC2B in comparison to Avr2. Similarly, *S. chacoense* CGN18338(P4) also has K284N, where recognition of EpiC2B is better than EpiC1 (**Figure 4.14**).

Further K284I variation was detected in LA1301(P4) that weakly recognises both Avr2 and EpiC2B. We uncovered variations occurring at sites 221, 302 and 336 that have also been identified earlier (Kaschani et al., 2010). Substitution T221S formerly detected only in wild potato was also identified in wild tomato *S. pennellii* LA1272(P5) together with wild potato *S. verrucosum* CGN17767(P2) and *S. venturii* CGN17761(P1) and all displayed variable inhibitor recognitions. *S. palustre* CGN18286(P1) has T221G, but the plant did not recognise any inhibitor (**Figure 4.14**). Variation A302V known to exist in wild potato (Kaschani et al. 2010) was also found in *S. chacoense* and *S. palustre* in this study.



Figure 4.14 *C14* is under diversifying selection in *S. pimpinellifolium* while no other branch-specific episodes of positive selection were identified in this study.

Maximum-likelihood phylogenetic tree based on 53 *C14* gene sequences generated using MUSCLE alignment of 272 codons in MEGA12. 34 *C14* sequences generated in this study are shown in bold and their source population/plant with species indicated on branch tips are listed on the right. Bootstrap values over 50%, derived from 500 replicates are shown as grey circles on branch. The tree is rooted at *Petunia inflata*, representing family outgroup. *S. pimpinellifolium* LA1589 *C14* was used as tomato reference. Amino acid alignment on the right display 13 sites that had over 10% site frequency across *C14* genes sequenced in this study. Positions correspond to sites in a Solanaceae-

wide alignment. HR scores toward inhibitors and *Cf* genotyping from this work, for source plants of new *C14* alleles are also shown. Statistical tests to estimate clades and allelic sites under diversifying selection were performed as detailed in figures 4.10. *DNA sequences generated in this study, phylogenetic tree in newick format and iTOL annotations are attached as supplementary S4.10.

Surprisingly we noticed this amino acid site is highly variable showing alterations A302L/N/I/T in *S. pimpinellifolium* and also extending as A302P in *S. habrochaites* LA1353(P6). It should be highlighted that while *S. chacoense* recognised EpiCs and *S. habrochaites* responded to Avr2 and EpiCs, and *S. palustre* did not respond to any inhibitor despite the presence of shared substitutions. Therefore, amino acid substitutions singularly, including at 221 and 302 unlikely have major influence on inhibitor recognition, but when in combination with other substitutions they may add to the overall interaction affinity of the inhibitor. For instance, we identified that *S. pimpinellifolium* LA0375(P3) from the centre region with high diversity, confer moderate to strong HR against all four inhibitors and has C14 substitution A302T in addition to G277S and V336D (**Figure 4.14**). V336I substitutions are already known to exist in wild potato (Kaschani et al., 2010), but since we found them our *S. palustre* samples as well indicated the importance of multiple site variations exerting an aggregative influence instead as compared to single site variations. Comparatively lesser variations in *C14* alleles were identified in wild tomato than wild potato (Kaschani et al., 2010), however, our results indicate increased variation levels in *C14* from tomato. This led us to investigate whether the diversifying selection on *C14* extends outside wild potato and also occurs in natural populations of *S. pimpinellifolium* and wild tomato.

We next used statistical approaches as were used for *Rcr3* and *Pip1* to detect gene-wide and site-specific diversification in *C14*. The global *in-frame* codon alignment of all *C14* sequences in tree (**Figure 4.14**) was used as an input in BUSTED (Murrell et al., 2015) to analyse gene-wide selection signatures across *C14* variants. BUSTED revealed that only *S. pimpinellifolium* branch is under diversifying selection and not wild tomato and wild potato clade. BUSTED further identified amino acid sites 245, 291 and 302 overall to be under

positive selection (**supplementary 4.5**). We next investigated Solanaceae-wide diversifying sites by using FUBAR (Murrell et al., 2013) and uncovered sites 221, 291, 302, 336, 375, 380 and 396 (**supplementary 4.1(c)**). To assess whether the sequences that we generated have specific sites experiencing variable selection pressures, we performed FEL (Kosakovsky-Pond et al., 2005) on a MUSCLE nucleotide alignment of 34 new *C14* alleles. FEL determined that sites 277, 281, 291, 302, 317, 323, 326, 329, 331, 342, 344, 345, 350, 355, 371, 393, 397, 430, 441 and 452 are under positive selection across the three groups of species, *S. pimpinellifolium*, wild tomato and wild potato in our study. Since there exist variations in selection pressure at same site in different groups, a group-specific MUSCLE nucleotide alignment was then used to analyse difference in site selection.

Using FUBAR, we identified that sites 277, 291, 302 and 303 in *S. pimpinellifolium*, 302 and 336 in wild tomato and 221 and 336 in wild potato are under diversifying selection (**Figure 4.14**). Contrarily, MEME (Murrell et al., 2012) only estimated site 291 is under positive selection in *S. pimpinellifolium*, whereas it failed to estimate any diversifying selection occurring at any site in wild tomato and wild potato specifically. Our *C14* evolutionary analysis indicating diversifying selection occurs particularly in *S. pimpinellifolium* tomato but not in wild potato is in contradiction to previous finding that *C14* is under diversifying selection in wild potato and experienced conservative evolution in wild tomato (Kaschani et al., 2010).

4.3 Discussion

Pathogen pressure variations in differing geographical environments can locally drive an evolutionary arms race in the constant interactions between plant hosts and pathogens. This can sometime lead to distinct genotypes having variations in alleles of a resistance gene within a same population. *Hcr2* family is an actively evolving resistance gene family in

S. pimpinellifolium, where heterogeneous modes of selection have generated a large number of potentially functional *homologs* maintained through intragenic recombination and balancing selection within populations of *S. pimpinellifolium* and among different wild tomato species (Caicedo and Schaal, 2004).

Cf-2 is presumably one of the most recently evolved members of *Hcr2* gene family (Kourelis et al., 2020) and so far was identified only in *S. pimpinellifolium*. Our PCR amplification of *Cf-2* suggest that *Cf-2* is likely conserved across wild tomato and wild potato species. We further estimated a pattern of geographical distribution of *Cf-2* within native species, *S. pimpinellifolium*, and inferred that *Cf-2* is most frequent in the Centre region C, the region that showed high recognition against inhibitors as well. It was interesting to find that *Cf-9* is the most frequently occurring gene when compared to its homolog *9DC* and *Cf-2* and their segregation appears independent of each other. Despite an approximately three times more frequent Avr2 recognition in region D when compared to region A, the frequency of *Cf-2* gene in region A is roughly five times greater. We detected Avr2 recognition in plants lacking *Cf-2*, for example Plant 4 and Plant 6 of *S. pimpinellifolium* LA2401 in Central Peru HR-triggered by Avr2 was noted, however *Cf-2* was detected in Plant 6 but not in Plant 4, which carry *9DC* (**Figure 4.4**). These results suggest that either the existence of specific allelic variations in *Cf-2* in different geographical regions or a presence of another *Hcr2* or related gene that may be conferring a response towards Avr2. We observed intra-specific and inter-specific variations in number and combinations of *Cf-2/Hcr2s*, however, a clear pattern of correlation with recognition of pathogen inhibitors EpiC1, EpiC2B and Cip1 could not be established.

Cf-5 is homologous to *Cf-2* and confers recognition of *C. fulvum* secreted Avr5 (Dixon et al., 1998). When *Cf5* was co-expressed with *Rcr3* and *Avr5,* no HR was triggered, implying that Rcr3 is not a required component in recognition specificity of Cf-5 (Dixon et al., 2005). Further, previous studies identified that co-expression of *Cf-5* and *Avr2* in the presence of

Rcr3 does not induce HR, showing that Avr2 induced HR is specifically dependent on Cf-2/Rcr3 interaction (Dixon et al., 2000 and Kourelis et al., 2020). It is possible that different *Hcr2s* confer specific recognitions of distinct inhibitors and the recognition functions are not substituted by allelic variations in *Hcr2s*. Polymorphism in resistance genes often occur due to recombination and are maintained by balancing selection, causing allelic variations in a resistance gene conferring resistance against specific pathogen variants/strains. Therefore, balancing selection promotes the maintenance of multiple alleles of a gene, enhancing plant adaptation to a range of pathogen pressures and consequently leading to different population genotypes. Moreover, variation in genotypes of populations across different geographic origin ranges develop through a complex interplay between environmental conditions, selective pathogen pressures and host genetic factors. The additive effects of these factors lead to genetic profile differences in a gene within same or among populations in a particular region.

Ve1 in tomato, conferring resistance against *V. dahlia*, is an example of an LRR domain-rich receptor that has the capacity to detect a similar avirulence protein, *Ave1* from multiple pathogens, including *F. oxysporum* f. sp. *lycopersici* and *C. higginsianum* (de Jonge et al., 2012). Further, homologs of *Ve1* exist in various species outside Solanaceae and functionally active transferability of *Ve1* across plant families has been shown (Thomma et al., 2011). As EpiCs are expressed in the apoplast during early stages on *P. infestans* entry (Tian et al., 2007), similar to Ve1, extracellular receptor involved in EpiCs or Cip1 recognition likely functions as PRR in MAMP-triggered immunity against EpiCs and Cip1, where it associates with co-receptor RLKs, SERK/BAK1/SOBIR1 to confer a relatively weaker recognition function in comparison to Avr2. Further, *Hcr2* family members are subdivided into several full-length and truncated classes based on their sizes that resulted from variations in number of LRR domains (Caicedo and Schaal, 2004). It remains to be investigated whether *Hcr2* family overall or a specific class is under positive selection and

how SNP variations in LRR domains among plants from different populations/species impact the interaction with co-receptor and ultimately recognition of different inhibitors.

Not all *Cf-2* containing plants were responsive to inhibitor treatment and since we did not decipher a specific correlation between *Cf-2/Hcr2* or *Cf-9/9DC* genetic architectures, we then detected natural variation in *Rcr3*, *Pip1* and *C14* in wild tomato and wild potato clades. However, whether the observed amino acid variations translate into active protein state and functional diversity in recognition of pathogen inhibitors from three microbial kingdoms (fungi, bacteria and oomycete) remains to be explored in further studies. A correlation analysis of 54 alleles in the past revealed sensitivity variations of *Rcr3* towards Avr2 (Hörger et al., 2012), EpiCs and Cip1 (Hörger 2011, Cip1 referred in publication as Rip1). For instance, Rcr3 substitution of histidine by asparagine, H148N is at close interaction proximity of conserved QxVxG motif of EpiCs and has been shown as crucial for EpiC recognition (Hörger, 2011, Ilyas, 2014). However, the extent of *P. infestans* co-evolution with wild tomato species have not been documented extensively so far.

Rcr3 and *Pip1* have evolved independently and while their surface binding grooves are conserved, they display differences in amino acids mainly in solvent-exposed surface residues of the proteins. Therefore, both Rcr3 and Pip1 potentially recognise same inhibitors interacting with substrate binding groove region, but may have substrate binding preferences when surface residues are the targets of inhibitors from different pathogens (Ilyas et al., 2014). Presence of *S. lycopersicum Pip1* in *MM-Cf-2/rcr3-3* or when transiently expressed with *Cf-2* in *N. tabacum* cv. Petite Havana SR1 does not trigger Cf-2 dependent HR upon Avr2 infiltration (Kourelis et al., 2020). Pip1 is comparatively an abundant protease in the apoplast during pathogen infection, however *Pip1* natural variation did not show significantly altered response against Avr2 and EpiCs (Ilyas, 2014). Natural genotypic variations in *Pip1* and *C14* have also previously been revealed (Shabab et al., 2008, Kaschani et al., 2010, Hörger 2011, Ilyas, 2014 and Kourelis et al., 2020). The functional

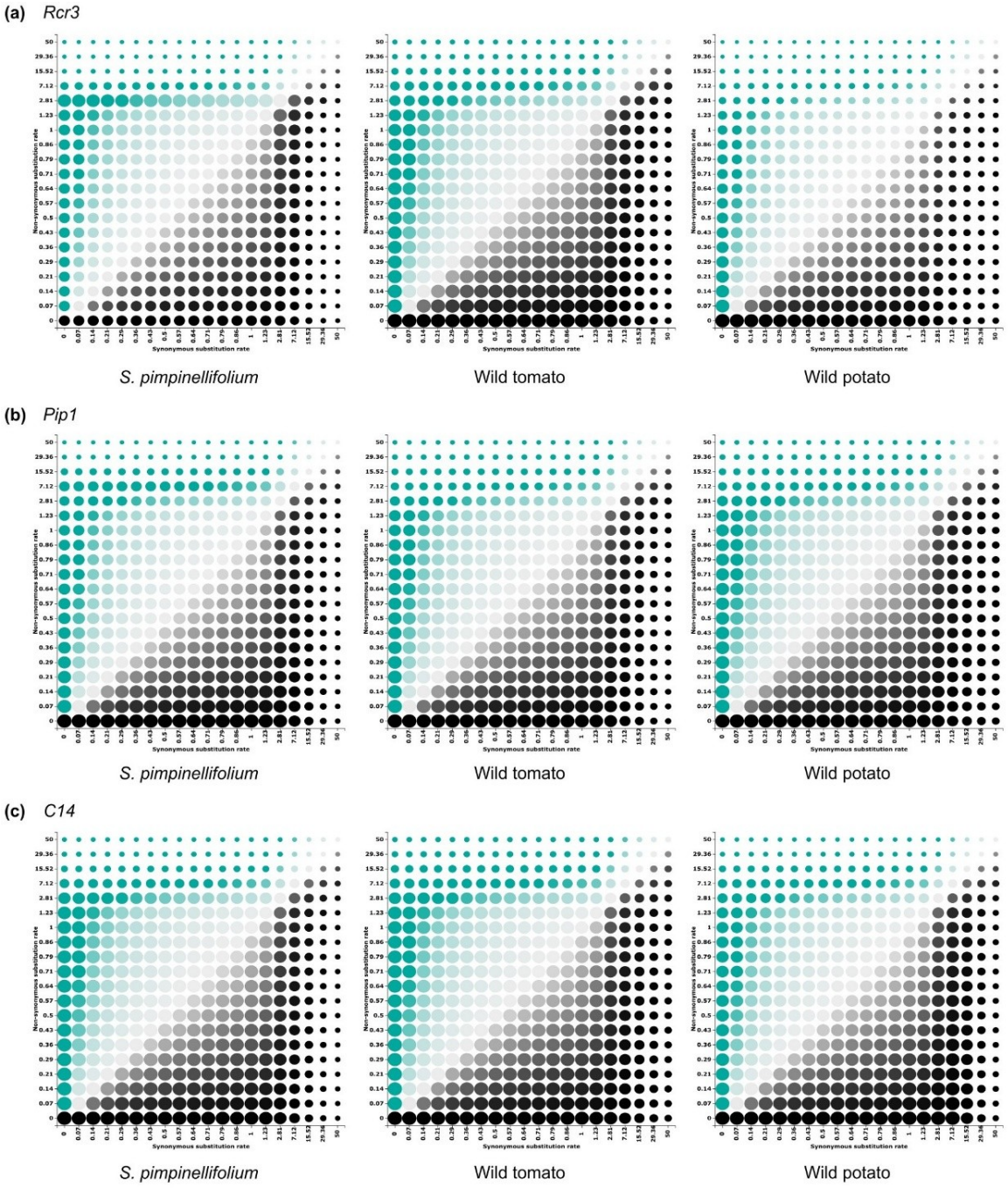
conservation and importance of Pip1 in basal defence (Caldwell and Michelmore, 2009, Ilyas et al., 2015) may point towards low levels of polymorphism in *Pip1* translating into functional variations against different inhibitors.

C14 has not been studied in natural *S. pimpinellifolium* populations, but a few variations have been published in other wild tomato species and in wild potato species (Kaschani et al., 2010). In this study, we did not observe any variants of *Rcr3*, *Pip1* and *C14* that are specifically present in plants/populations recognising all four inhibitors, Avr2, EpiC1, EpiC2B and Cip1. Amino acid variations in apoplastic cysteine proteases add to their functional diversification favouring substrate specificities and distinct affinities that improve host fitness in changing environmental conditions. The diversifying selection on cysteine proteases may facilitate fine tuning of positive selection on *Cf-2/Hcr2* gene. Therefore, figuring out a compatible interaction between an allele of *Rcr3*, *Pip1* or *C14* in association with variations in *Cf-2/Hcr2* in native host would be a fascinating future direction to explore.

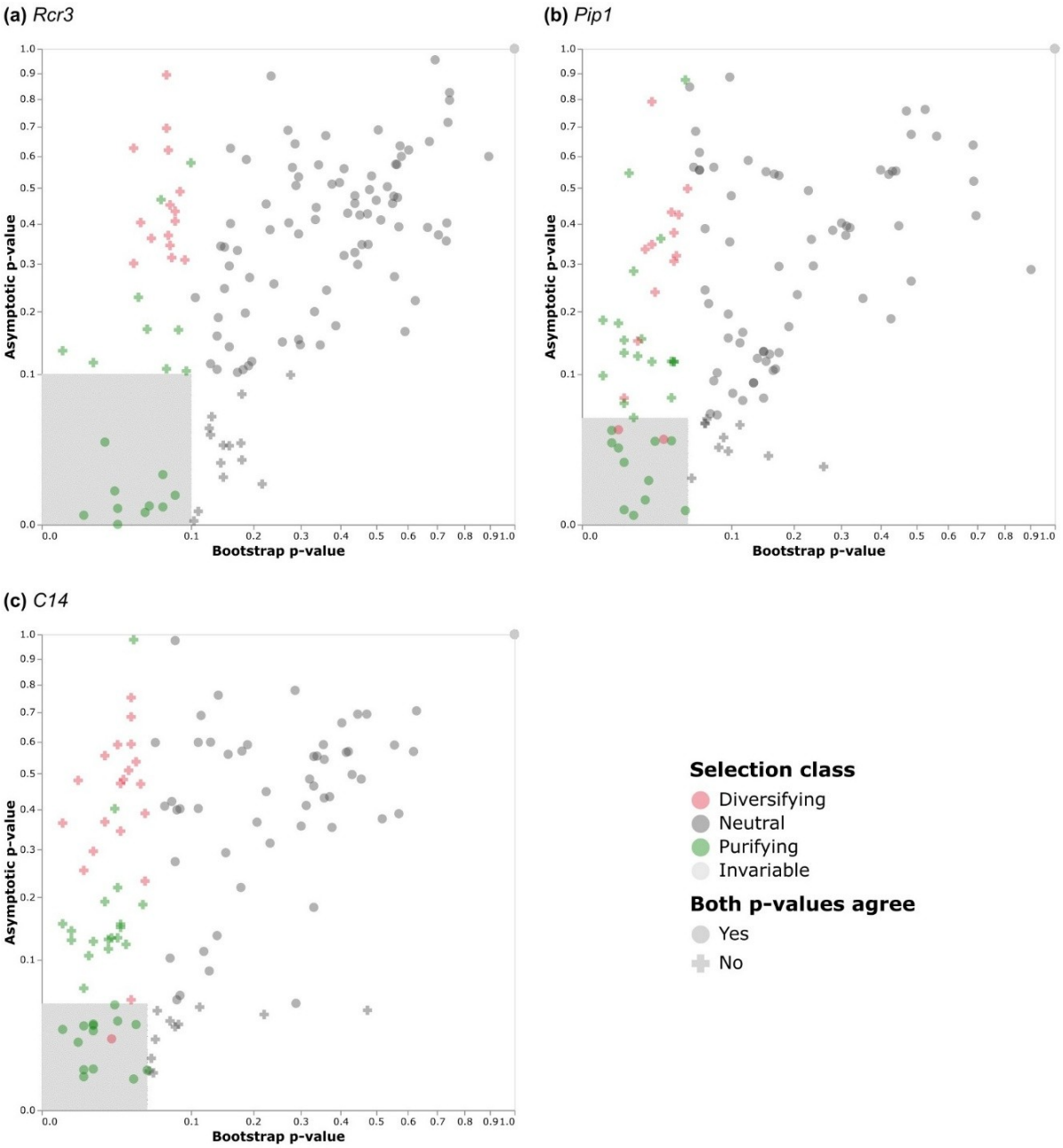
We identified different selection forces acting on *Rcr3*, *Pip1* and *C14* in similar and different species groups. Using likelihood ratio (Murrell et al., 2015) and Bayesian counting (Murrell et al., 2013) based evolutionary tests, we identified that *Rcr3* and *C14* are under diversifying selection in *S. piminellifolium*, whereas diversifying selection is acting on *Pip* additionally to *Rcr3* in wild tomato group consisting of species beyond *S. pimpinellifolium*. *Rcr3* and *Pip1* have previously been shown to have experienced positive selection in wild tomato (Shabab et al., 2008, Hörger et al., 2012). Surprisingly, we did not detect any gene-wide positive selection on *Rcr3*, *Pip1* or *C14* in wild potato. *C14* has previously been reported to be under diversifying selection in wild potato but conserved in wild tomato (Kaschani et al., 2010). Since EpiCs are known to strongly interact with C14 in comparison to Rcr3 and Pip1, less C14 diversification in the native host of *P. infestans* would imply a conserved role of C14 in extracellular defence in wild potato.

In conclusion, different wild relatives of a Solanaceaous crop species may possess exclusive genetic backgrounds, having unique set of alleles of *Hcr2* members and corresponding cysteine protease co-receptors that result in broad capacity of different host responding to same or different pathogen-derived inhibitors with different specificities. Our preliminary results indicate that functional diversity of *Hcr2* gene family is larger and more complex than originally hypothesised. The available redundancy may compensate for the absence of primary receptor or co-receptor in the presence of a homolog variant with same or overlapping specificities, ensuring the plant has a sustainably enhanced capacity to withstand multiple unrelated pathogens.

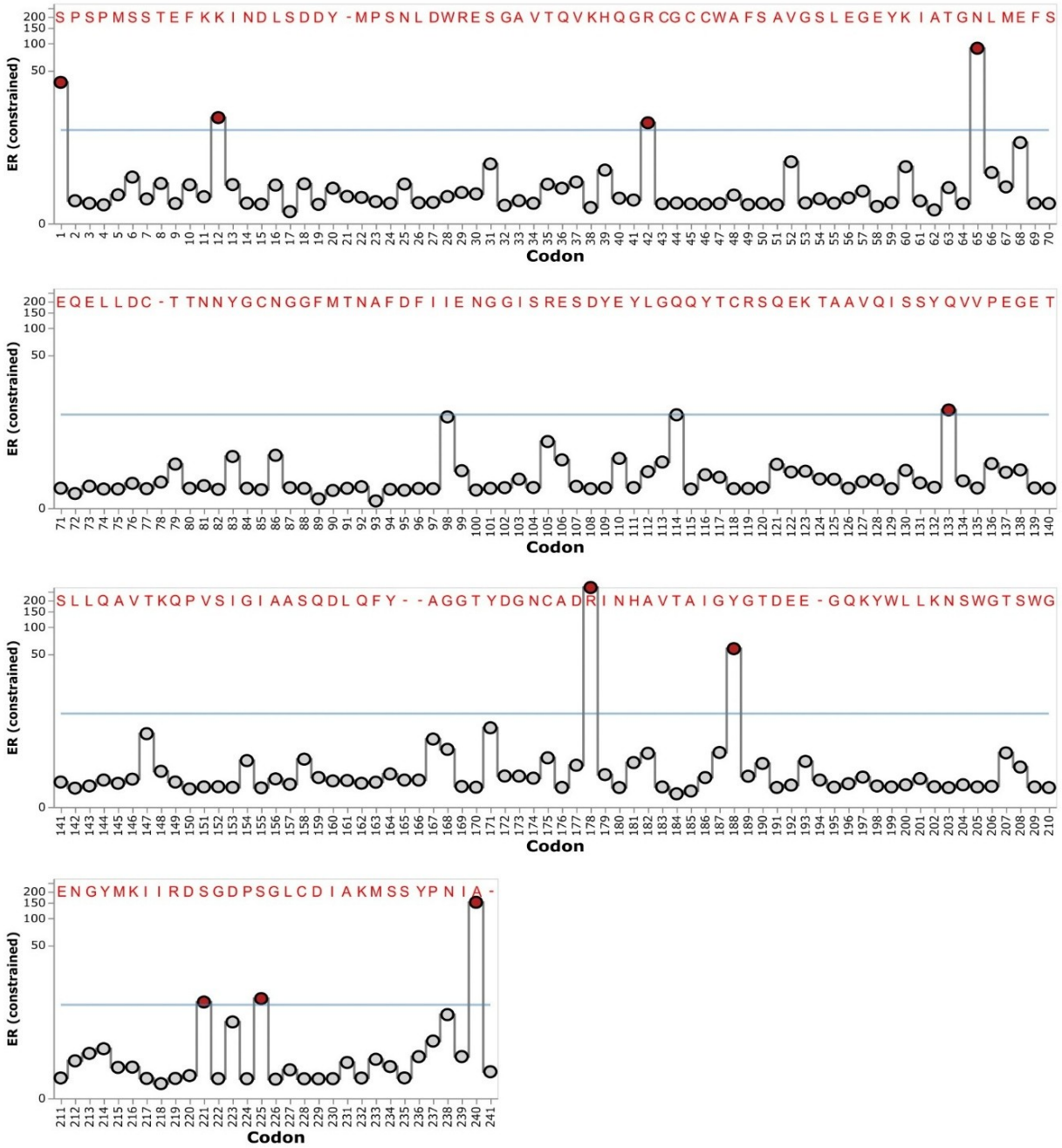
Many anciently specialised pathogens now have expansive host ranges with their rapidly evolving capacity to overcome host defence mechanisms. This expansion in host range pose a challenge when multiple pathogens with similar perception infect a host together. The presence of a particular pathogen potentially impacts the trajectories of virulence and transmission of another pathogen within the same host. Such complicated interactions may involve trade-offs among different pathogens as well as with host resource allocations in resistance responses. Understanding the genetic variations in cell-surface receptor *Hcr2s* and associated signalling components is thus important in developing durable crops varieties with broad spectrum resistance to pathogens.



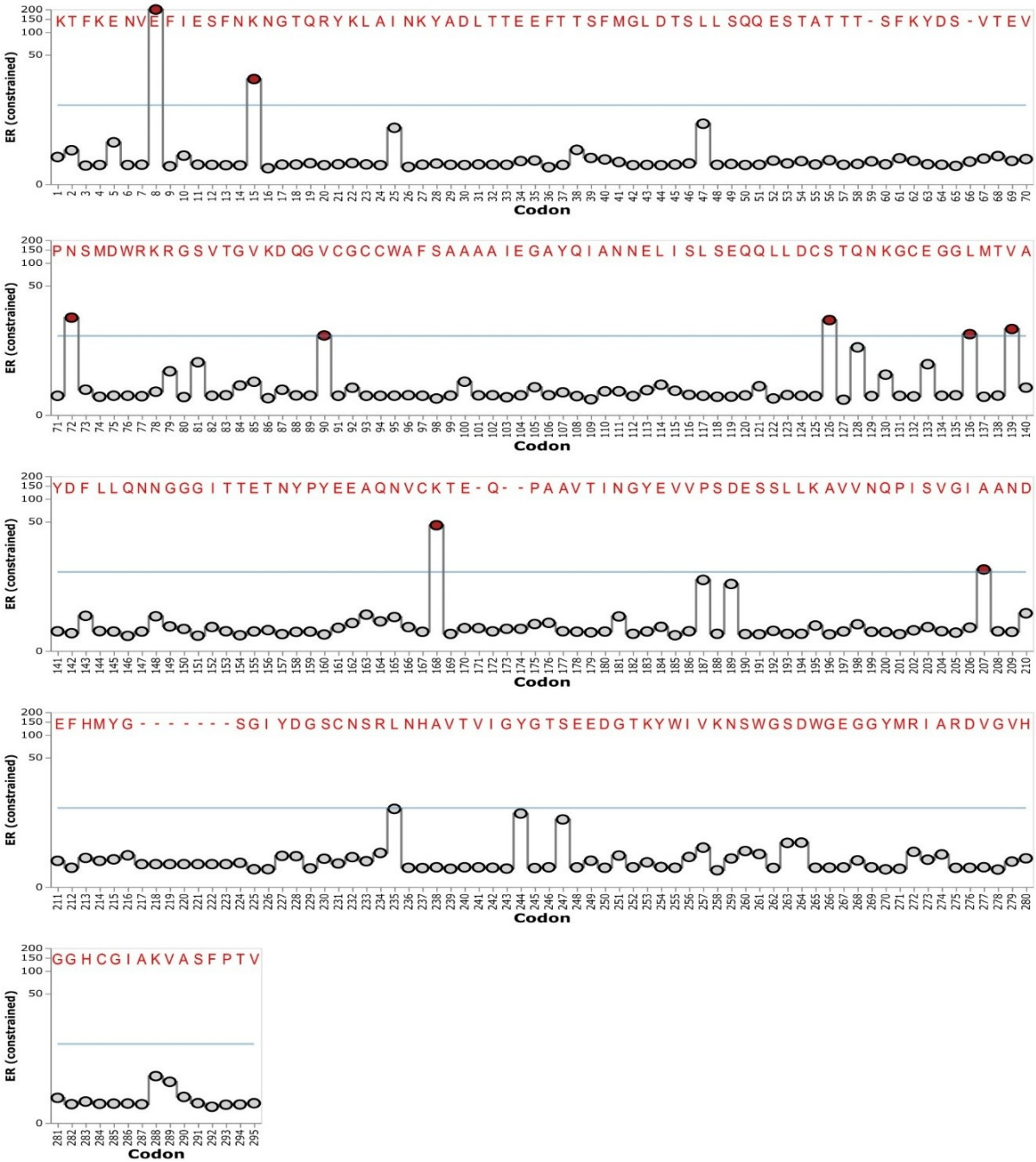
Supplementary 4.1 In order to identify site-selection in **(a)** *Rcr3* in *S. pimpinellifolium* (figure 4.10), wild tomato (figure 4.11), and wild potato (figure 4.12), graphs displaying the posterior distribution through discretized rate grid were created using the Fast Unconstrained Bayesian Approximation (FUBAR) test. Similarly, in Solanaceae-wide alignments, FUBAR analysis was used to **(b)** *Pip1* (figure 4.13) and **(c)** *C14* (figure 4.14). The posterior weight assigned to a particular grid point determines the dot size. Positive and negative selection strengths are shown by the black and green color variations, respectively. Individual site-specific distributions of synonymous vs. non-synonymous rates are not displayed because this is an alignment wide distribution. Positive selection was applied to sites having a posterior probability greater than 0.9.



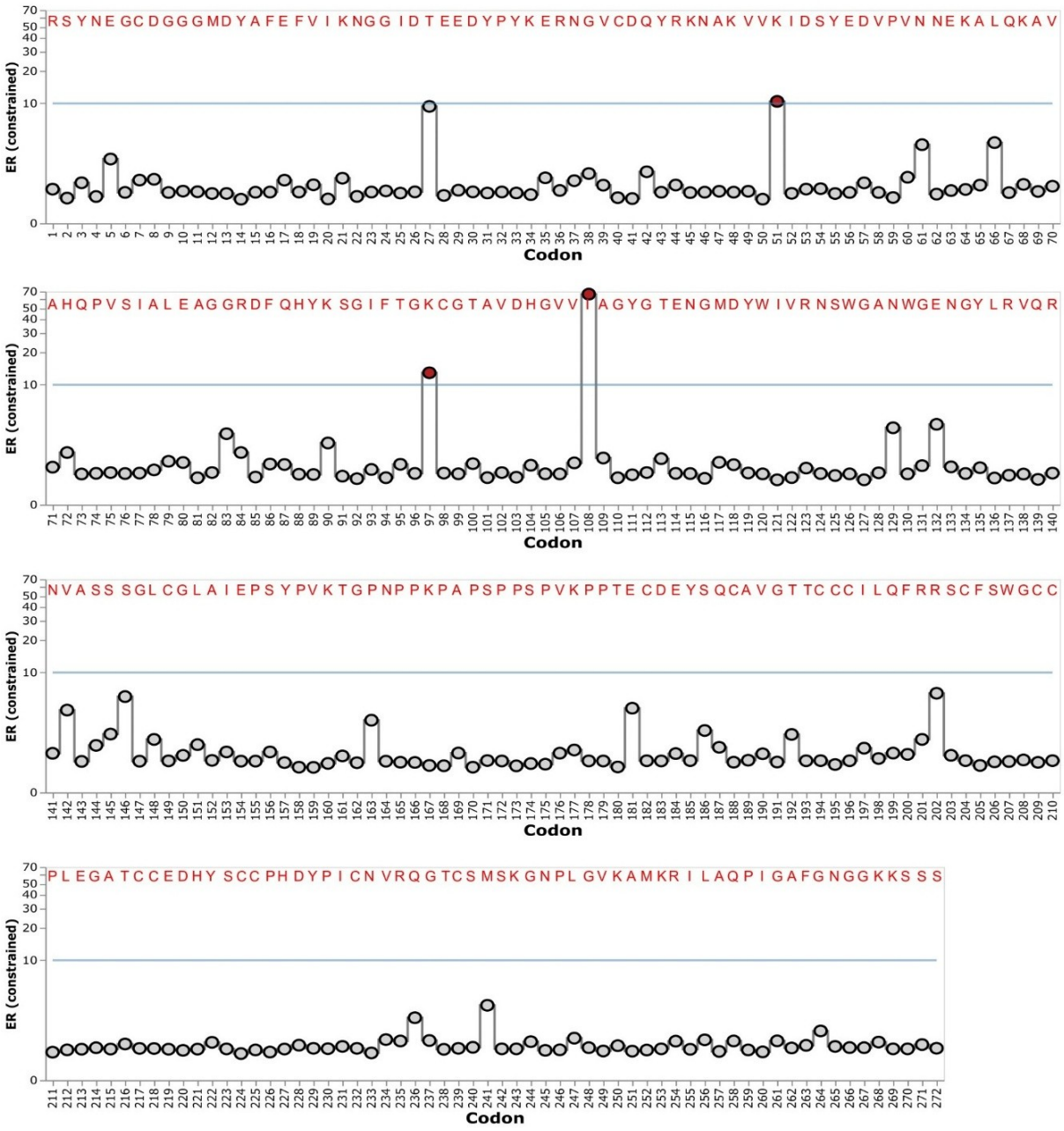
Supplementary 4.2 Fixed-effects likelihood test for statistical significance was estimated on the basis of 500 site-level parametric bootstrap replicates for combined selection signatures on sequences generated in this study for **(a)** *Rcr3* (figures 4.9, 4.10 and 4.11), **(b)** *Pip1* (figure 4.13) and **(c)** *C14* (figure 4.14). The analysis included site to site synonymous and non-synonymous rate variations. Graphs are shown comparing site-level *p*-values for non-neutrality using parametric bootstrap and asymptotic approximation. Grey rectangle indicate test rejection region ($p \leq 0.05$). Sites under diversifying selection are highlighted in pink.



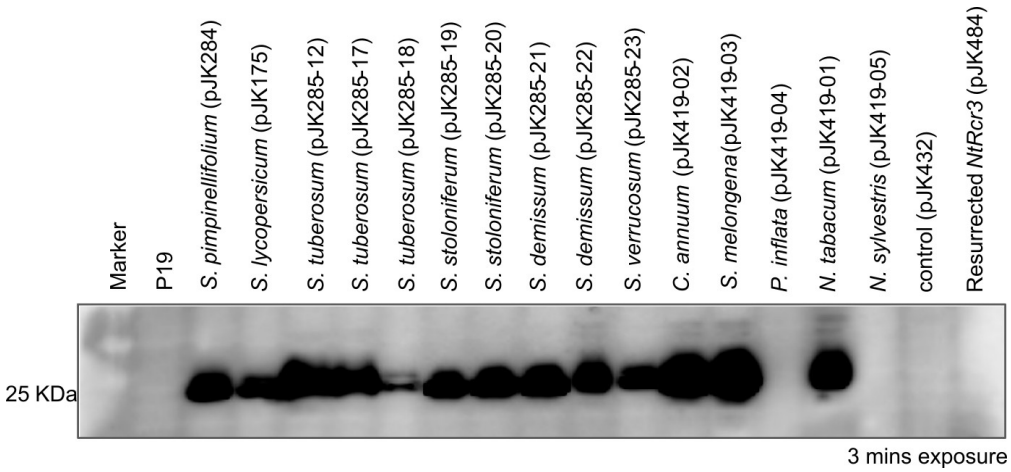
Supplementary 4.3 Branch-site Unrestricted Statistical Test for Episodic Diversification (BUSTED) to detect episodes of positive selection in *Rcr3* gene family (figures 4.10, 4.11 and 4.12) in Solanaceae. Evidence ratio/site level likelihood ratio plot (ω>1) for 241 sites, including 234 in-frame codon in a MUSCLE alignment of all *Rcr3* sequences in tree suggest sites that are under positive selection. Representative 241 amino acid positions tested in a Solanaceae-wide alignment are shown from *S. pimpinellifolium* (*Sopim02g076980_1*; LA1589). Solid line marks significance threshold (ER≥ 10; test *p*-value ≤0.05).



Supplementary 4.4 Branch-site Unrestricted Statistical Test for Episodic Diversification (BUSTED) to detect episodes of positive selection in *Pip1* gene family (figure 4.13) in Solanaceae. Evidence ratio/site level likelihood ratio plot (ω>1) for 295 sites, including 283 in-frame codon in a MUSCLE alignment of all *Pip1* sequences in tree indicate sites that are under diversifying selection. Reference 295 amino acid positions tested in a Solanaceae-wide alignment are shown from *S. pimpinellifolium* (*Sopim02g077040_1*; LA1589). Solid line marks significance threshold (ER≥ 10; test *p*-value ≤0.05).



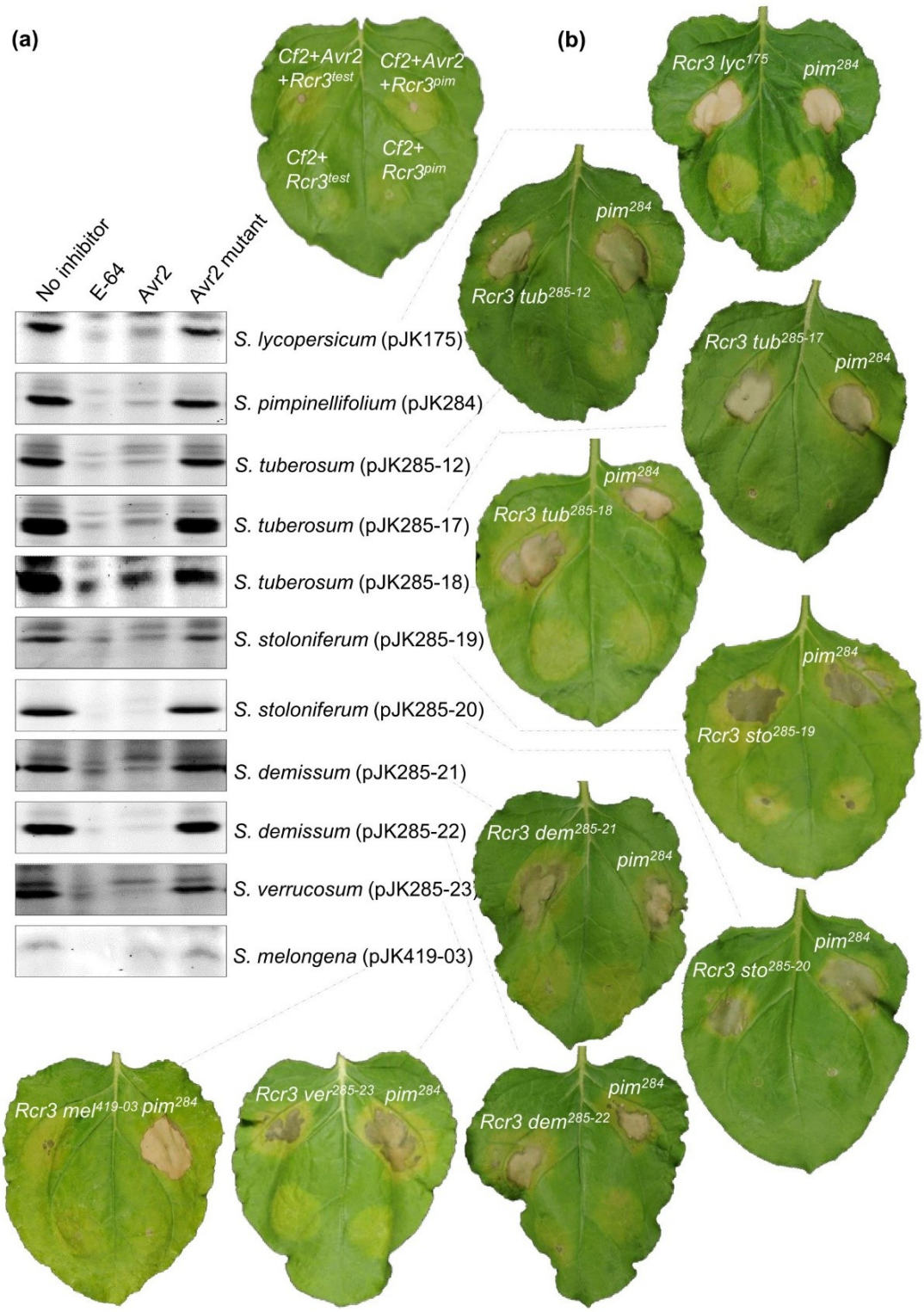
Supplementary 4.5 Branch-site Unrestricted Statistical Test for Episodic Diversification (BUSTED) to detect episodes of positive selection in *C14* gene family (figure 4.14) in Solanaceae. Evidence ratio/site level likelihood ratio plot (ω>1) for 272 in-frame codons in a MUSCLE alignment of all *C14* sequences in a tree show sites under positive selection. Reference 272 amino acid positions tested in a Solanaceae-wide alignment are shown from *S. pimpinellifolium* (*Sopim12g088670_1*; LA1589). Solid line marks significance threshold (ER≥ 10; test *p*-value ≤0.05).

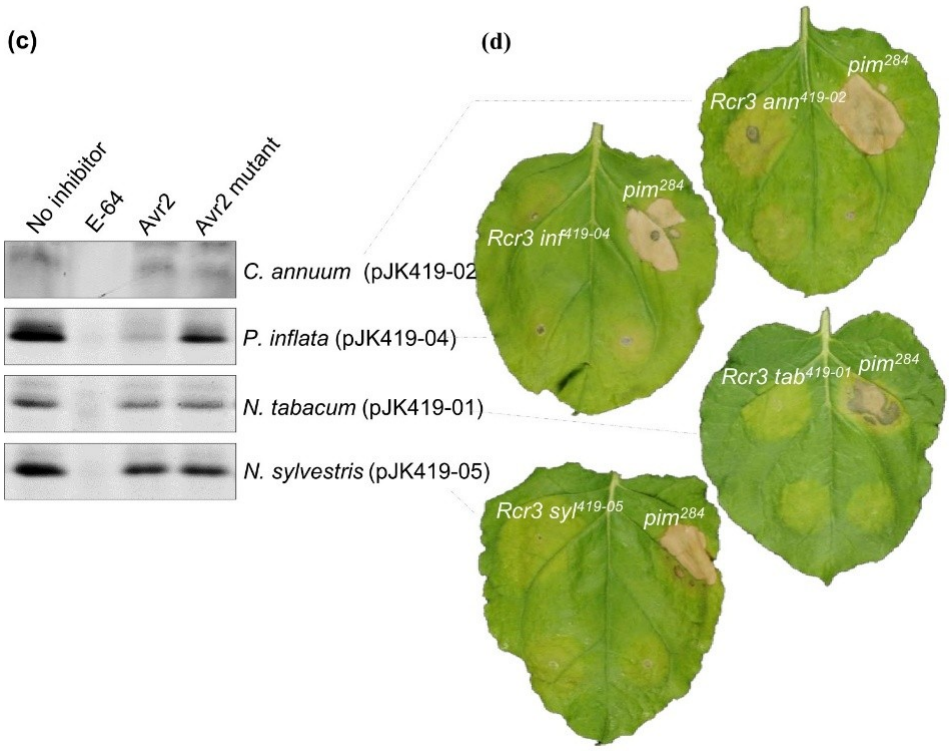


Appendix 4.1 αRcr3 western blots showing natural Rcr3 variants tested.

Rcr3 constructs were independently over-expressed in N. benthamiana and apoplastic fluid (AF) was isolated 4 dpi and used to detect Rcr3 using a primary αRcr3 (1:5,000) and a secondary HRP-conjugated anti-rabbit (1:10,000) antibody. S. lycopersicum (pJK175) and a truncated Rcr3 (pJK432) were used as positive and negative controls respectively. Of the total 15 variants, PiRcr3 and NsylRcr3 alleles repeatedly could not be detected on protein blots.

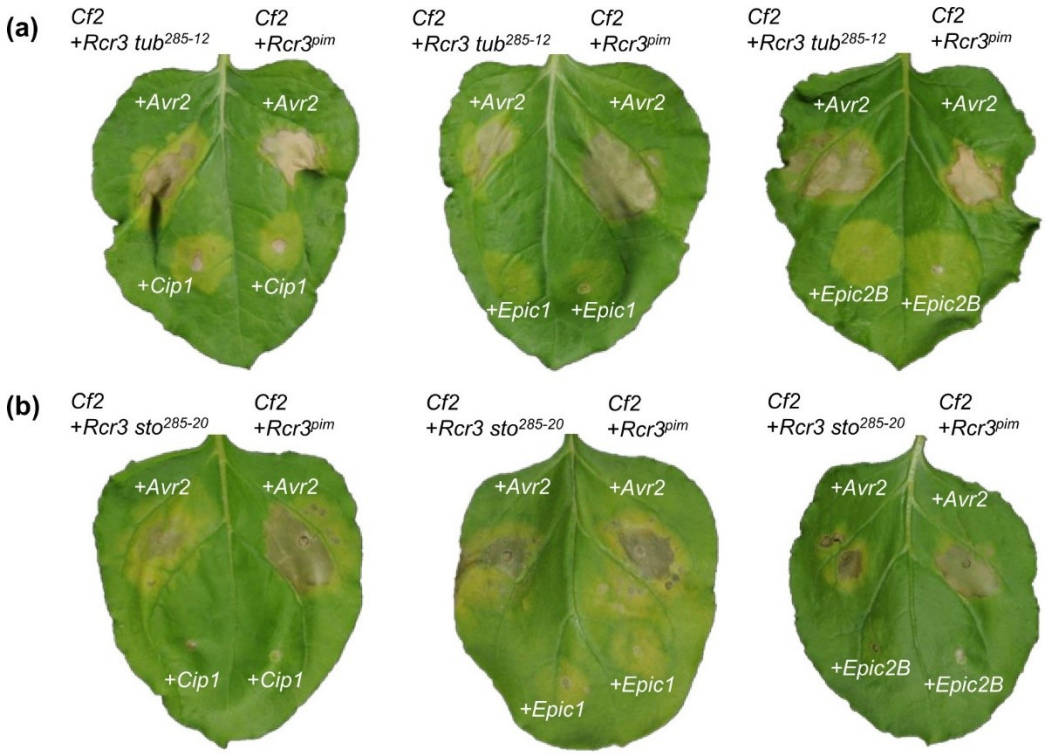
*Appendix Figures 4.1, 4.2 and 4.3 are data supporting Kourelis et al., 2020 publication; author contribution is clearly stated in the published article and these are not part of main results presented in this thesis.


(a)
Cf2+Avr2 +Rcr3test
Cf2+Avr2 +Rcr3pim
Cf2+ Rcr3test
Cf2+ Rcr3pim
No inhibitor
E-64
Avr2
Avr2 mutant
S. lycopersicum (pJK175)
S. pimpinellifolium (pJK284)
S. tuberosum (pJK285-12)
S. tuberosum (pJK285-17)
S. tuberosum (pJK285-18)
S. stoloniferum (pJK285-19)
S. stoloniferum (pJK285-20)
S. demissum (pJK285-21)
S. demissum (pJK285-22)
S. verrucosum (pJK285-23)
S. melongena (pJK419-03)
(b)
Rcr3 lyc175 pim284
pim284 Rcr3 tub285-12
Rcr3 tub285-17 pim284
pim284 Rcr3 tub285-18
pim284 Rcr3 sto285-19
Rcr3 dem285-21 pim284
pim284 Rcr3 sto285-20
pim284 Rcr3 dem285-22
Rcr3 mel419-03 pim284
Rcr3 ver285-23 pim284



Appendix 4.2 Active *Rcr3* variants exist in other Solanaceae species and some of them have the ability to trigger HR in the presence of transiently co-expressed *Avr2* and *Cf-2* in *N. benthamiana*.

Rcr3 were cloned in a *P19* background and agroinfiltrated in *N. benthamiana*. Apoplastic fluids (AFs) from *Solanum* species were extracted at 4 dpi and **(a)** a competitive-activity based protein profiling assay (C-ABPP) was performed by pre-incubating AFs with 3 µM affinity-purified Avr2 or its mutant in a 50 mM sodium acetate labelling buffer (pH 5.5) and 3 nM DTT. The reaction was further labelled using 0.9 µM fluorescent MV201 for 3.5 hours. The samples were precipitated using 5 volumes of ice-cold 100% acetone, centrifuged for 15 minutes at 4°C, maximum speed. Pellets were air dried and dissolved in 2X gel-loading buffer and samples were heated at 95°C to separate proteins on 15% SDS-PAGE gels. A negative control without inhibitor and a positive control with 100 mM E-64 were used. **(b)** Representative leaves show transient analysis of *Rcr3* variants, where *A. tumefaciens* GV3101 overnight grown cultures of $Rcr3^{test}$, *Cf-2* and *Avr2* were mixed in 1:1:1 ratio to OD_{600} = 0.5. The samples were suspended in 10 mM MES/10 nM $MgCl_2$ infiltration buffer (pH 5.7) and incubated for 2 hrs at 28°C. Scheme of infiltration is shown in the first leaf and 5-week old *N. benthamiana* plants were used for infiltration. HR was observed from 1 to 7 dpi and leaves were photographed at 8 dpi. Similarly, **(c)** and **(d)** show *Rcr3* variants C-ABPP and transient analysis, respectively, from Solanaceae species that are distant relatives of tomato.



Appendix 4.3 Cip1 and EpiCs do not trigger HR when transiently co-expressed with *Cf-2* and tomato or potato *Rcr3*.

5-week old *N. benthamiana* leaves were infiltrated with 1:1:1 *Agrobacterium* cultures of *Rcr3*^{test}, *Cf-2* and *Cip1*, *EpiC1* or *EpiC2B*. HR was observed 1 to 7 dpi and photographs were taken at 8 dpi. *Cf-2+Avr2+Rcr3*^{pim} was used as a positive control combination while *Cf-2+Avr2+Rcr3*t^{est} was used as reference control. Two potato *Rcr3* variants were tested, *Rcr3 tub*$^{285-12}$ and *Rcr3 sto*$^{285-20}$ that were found to trigger HR upon *Avr2* infiltration in the presence of *Cf-2*.

*Appendix Figures 4.1, 4.2 and 4.3 are data supporting Kourelis et al., 2020 publication; author contribution is clearly stated in the published article and these are not part of main results presented in this thesis.

Chapter 5

Functional characterisation of *Cf-2*-homologs and likely co-receptors using virus-induced gene silencing and phylogenetic analysis of Cf-like RLPs

Shivani Malik[1], Jiorgos Kourelis[1,2], Matthieu H.A.J. Joosten[4] and Renier A.L. van der Hoorn[1*]

[1]Plant Chemetics Laboratory, Department of Plant Sciences, University of Oxford, South Parks Road, OX1 3RB Oxford, UK. [2]Current address: Department of Life Sciences, Imperial College, SW7 2AZ, London, UK. [3]Laboratory of Phytopathology, Wageningen University, Drevendaalsesteeg 1, 6708 PB, Wageningen, the Netherlands. *Correspondence: renier.vanderhoorn@biology.ox.ac.uk

Author Contributions:

Research design: SM and RvdH; Seed collection procurement: SM; Silencing vector and experimental design: SM, JK and RvdH; *Cf-2.2* parent plasmid and *SOBIR1* silencing construct: MJ; Experimental and *in-silico* evolutionary investigations: SM; Data analysis, figures and writing: SM with critical inputs from RvdH; Funding acquisition: RvdH.

Acknowledgement:

We thank Tomato Genetics Resource Centre (TGRC), Davis and Centre for Genetic Resources (CGN), Netherlands, for seed donations; Ursula Pyzio and Timothy Wroe for greenhouse assistance; Sarah Rodgers and Caroline O' Brien for technical support; SM was supported by Oxford-Indira Gandhi Scholarship. SM would also like to acknowledge the assistance of Dr Zhe Ji at the Department of Biology, Oxford, for qPCR data analysis.

5.1 Introduction

A multi-layered plant immune system consists of resistance genes (*R*-genes) that encode a diverse repertoire of cell-surface and intracellular receptors and enable plants to mount defence response, specifically and broadly against corresponding avirulence genes (*Avr*) of pathogens encoding secreted inhibitors or effectors. The ever-evolving co-evolutionary interactions between pathogens of various microbial kingdoms and plants drive the expansion of host cell surface receptors that trigger extracellularly-triggered immunity (ExTI) through effective recognition of secreted proteins of a pathogen in the apoplast or structural features called pathogen-associated molecular patterns (PAMPs) or extracellular immunogenic patterns (ExIPs) (Flor, 1946, Couto and Zipfel, 2016, van der Burgh and Joosten, 2019).

Two largest and most extensively studied families of cell surface localised receptors are categorised as Receptor-like proteins (RLPs) and Receptor-like kinases (RLKs) (Monaghan and Zipfel., 2012, Couto and Zipfel, 2016). RLPs are often characterised by extracellular leucine-rich repeat (LRR) domains that are involved in direct or indirect ligand binding of pathogen-secreted proteins (Boutrot and Zipfel 2017, Kourelis and van der Hoorn, 2018). This further leads to activation of downstream signalling through association with RLKs carrying a cytoplasmic kinase domain that is lacking in RLPs (Wang et al., 2010, Liebrand et al., 2013, Fischer et al., 2016, Aranka et al., 2019). The downstream signalling cascade activated by receptor/co-receptor(s) and other signalling components ultimately generates defence responses, including the release of reactive oxygen species (ROS), activation of the mitogen-activated protein kinase (MAPK) cascade, transcriptional reprogramming inducing the production of antimicrobial peptides and in some cases, the hypersensitive response (HR), a type of programmed cell-death (Schwessinger et al., 2011, Paulus et al., 2020, Lu and Tsuda, 2021).

In tomato, nearly twenty-four functional RLPs, located on twelve chromosomes, have been characterised as members of *Cladosporium fulvum (Cf)* resistance gene family (Pei et al., 2024) known to mediate resistance against different strains of *C. fulvum* (currently *Fulvia fulva*), the fungal pathogen causing common leaf mould disease in tomato (Thomma et al., 2005). For example, *Cf-9* originally identified on chromosome 1 in the closest species to cultivated tomato, *Solanum pimpinellifolium*, mediates resistance against *C. fulvum* strain expressing Avr9 (Jones et al., 1994). *Cf-2* is also introgressed from *S. pimpinellifolium*, but is located on chromosome 6 and mediates recognition of Avr2, a cysteine-rich protein secreted into the host apoplast by *C. fulvum* (Dixon et al., 1995). Two functional and almost identical alleles, *Cf-2.1* and *Cf-2.2* were identified at the *Cf-2* locus. Their translated RLPs of 1112 amino acid residues differ only in three residues. *Cf-2* is a member of the *Hcr2* family (*Homologs of C. fulvum resistance gene 2*) and *Cf-9* belongs to *Hcr9* family. Although representative examples, *Cf-9* and *Cf-2* are unlinked, they share greatest homology that is to an extent conserved among other *Cf* genes and their homologs. Both Cf-2 and Cf-9 have a putative signal peptide, N-terminal extracellular stretch of LRRs and a membrane anchor domain at the C-terminus. Thirty-eight LRR motifs are present in Cf-2-RLP, where twenty extremely conserved motifs consist of alternating repeats and sites for potential *N*-linked glycosylation. The conserved regions of Cf-RLPs are postulated to interact with cognate partner proteins and co-receptors to activate resistance response (Dixon et al., 1996).

Hcr9's in gene clusters were discovered to contribute to sequence exchange among members leading to novel recognition specificities and Hcr9s contain mostly identical number of LRR motifs. Contrarily, the Hcr2s have variation in the number of LRRs. Variation in solvent-exposed nucleotides of LRR structural motifs is important in the generation of novel pathogen/inhibitor recognition specificities (Song et al., 1995, Dixon et al., 1998, van der Hoorn et al., 2001, Caicedo and Schaal, 2004). Around twenty-six members of Hcr2s, distinguished into 9 categories based on protein size and architecture have been detected in *S. pimpinellifolium* populations, mostly differing by indels and single base pair

substitutions in LRR encoding regions. Further, intraspecific differences in number of Cf-2 homologs present in a survey of *S. pimpinellifolium* populations revealed that natural selection acts heterogeneously and is complex on the *Hcr2* family (Caicedo and Schaal, 2004). *Cf-2* is reportedly restricted within tomato and is thus presumably a lately evolved functional gene among *Hcr2* and *Hcr9* families (Kourelis et al., 2020). Since LRR regions in *R* genes are predicted to be mostly under diversifying selection, it is likely that *Cf-2* and other *Hcr2s* in tomato are actively expanding through accumulation of mutations that can be a source of variants capable of conferring specific or broad recognitions towards unrelated pathogens.

Cf-5 is a member of *Hcr2* family that is allelic to *Cf-2* with over 90% similarity in RLP sequence (Dixon et al., 1996). However, both were indicated to confer recognition of specific proteins (Dixon et al., 2000). Rcr3, a papain-like cysteine protease (PLCP) presumably evolved before Cf-2 (Ilyas et al., 2015) is required as a co-receptor to mediate perception of Avr2 (Kruger et al., 2002). In addition to recognising Avr2, Cf-2 is reported to also recognise Venom-allergen-like protein 1 (VAP1), produced by nematode *Globodera rostochiensis* (Torres et al., 2012). In addition to Rcr3, *Phytophthora*-inhibited protease 1 (Pip1), a paralog PLCP encoded at the same locus as Rcr3 (Tian et al., 2005; Tian et al., 2007, Ilyas et al., 2015) and a different PLCP, C14 (Kaschani et al., 2010, Shindo et al., 2016), are targeted by distinct inhibitors of pathogenic bacteria, fungi and oomycete.

Fungal Avr2 targets both Rcr3 and Pip1 (Rooney et al., 2005, Shabab et al., 2008). Oomycete cystatin-like EpiC2B and bacterial chagasin-like Cip1, both have a greater affinity for C14 than Rcr3, which may be the reason tomato plants carrying $Cf\text{-}2^{pim}$ and $Rcr3^{pim}$ did not recognise EpiC2B or Cip1. Interestingly, EpiC1 is another cystatin-like inhibitor of *P. infestans* that inhibits Rcr3, but not Pip1 and also evades recognition by Cf-2 (Tian et al., 2007, Song et al., 2009, Kaschani et al., 2010, Shindo et al., 2016). Sequence exchange studies between Rcr3 and Pip1 revealed the residues essential for triggering Avr2 induced

Cf-2-dependent HR are predominantly clustered on the β-sheet lobe in Rcr3 in closest proximity to the substrate binding groove (Kourelis et al., 2024). Gene duplication likely caused the functional divergence of *Rcr3* and *Pip1*, where *Cf-2* possibly coevolved to detect inhibitors that target Rcr3, but not the inhibitors that target Pip1. Absence of *Rcr3* in the absence of *Cf-2* does not affect susceptibility towards *C. fulvum* and *P. syringae*, but does increase susceptibility to *P. infestans* in tomato. By contrast, *Pip1* silencing increased susceptibility to all three pathogens, *C. fulvum*, *P. syringae* and *P. infestans*, demonstrating Pip1 plays a crucial role in broad range immunity (Ilyas et al., 2015). Recently, an EpiC2B-insensitive variant of Pip1 was engineered. Substitutions of two residues located outside the substrate binding groove of Pip1 were sufficient to render Pip1 insensitive to EpiC2B presumably without alterations in substrate specificity of Pip1 (Schuster et al., 2024). The role of Pip1 and C14 in Cf-2/Cf-like-mediated perception of various inhibitors remains to be further studied.

RLPs found in tomato species till date can be considered as a super-clade consisting several multigene families, where members sharing homology have been shown to function similarly or variably as they are widely distributed across taxonomic plant families. For instance, Ve1 is a Cf-like RLP that confers resistance against soil-borne vascular pathogen, *Verticillium dahlia* race 1 carrying Ave1 inhibitor (Fradin et al., 2011). Ve1 can recognise inhibitors from different fungal pathogens (de Jong et al., 2012) and characterisation of functional homologs across Solanaceae family indicated that Ve1 is an ancient immune receptor of land plants (Zhang et al., 2016). Further, LeEix1 and LeEix2 are members of *LeEix* receptor gene family in tomato that are homologs to *Ve* and *Cf* genes. While both *Le*Eix1 and *Le*Eix2 have the capacity to independently bind corresponding fungal elicitor EIX (Ethylene-inducing xylanase), only LeEix2 reportedly triggers HR after direct recognition of EIX. Receptor-mediated endocytosis is triggered by binding of EIX with *Le*Eix2, further allowing *Le*Eix2 to interact with cytoplasmic components and trigger HR

whereas *Le*Eix1 acts as a decoy receptor by attenuating HR signalling (Ron and Avni, 2004).

Brassinosteroid Insensitive 1-Associated Kinase1 (BAK1) in *Arabidopsis* and its ortholog Somatic Embryogenesis Receptor Kinase3 (SERK3) in tomato acts as regulatory LRR-RLK that typically associates with LRR-RLKs/LRR-RLPs in a ligand-dependent manner (Heese et al., 2007) to positively transduce inhibitor recognition signalling. Flagellin-Sensing 2 (FLS2) is a well-studied LRR-RLK example known to recognise bacterial flagellin flg22 resulting in trans-phosphorylation of the cytoplasmic kinase domain of BAK1 and FLS2 (Chinchilla et al., 2007, Sun et al., 2013). The examples of role of SERK3 in LRR-RLP-mediated inhibitor recognition includes Ve1 and *Le*Eix (Fradin et al., 2009, Bar et al., 2010). SERK3 has also been demonstrated to play a role in immunity against *P. syringae PstDC3000 hrcC* strain and root knot nematode, *Meloidogyne incognita* (Peng and Kaloshian, 2014).

Suppressor of BIR1-1(SOBIR1)/EVERSHED(EVR) has of late unfolded as another regulatory LRR-RLK in tomato that constitutively interacts with a broad range of plant immunity and growth related RLPs (Gao et al., 2009, Bi et al., 2014, Zhang et al., 2014, Domazakis et al., 2018) including Cf-9, Cf-4, Cf-2.2, *Le*Eix and Ve (Liebrand et al., 2013; Aranka et al., 2019, Huang et al., 2021, Huang et al., 2024). Cf-4 is a Cf-RLP that requires SOBIR1 (Liebrand et al., 2013) to confer specific perception of *C. fulvum* secreted Avr4 (Thomas et al., 1997). The ligand-independent complex association of Cf-4 and SOBIR1 further recruits SERK3/BAK1 to induce a downstream resistance signalling (Postma et al., 2016, DeFalco and Zipfel, 2021). The intrinsic kinase activity of SOBIR1 and SERK3/BAK1 directly trans-phosphorylate each other, initiating their full activation and elicitation of downstream cytoplasmic signal transduction. In tomato, AVR9/Cf-9-Induced Kinase1 (ACIK1) is a Receptor-like Cytoplasmic Kinase (RLCK) that also plays a role in downstream

of SOBIR1/BAK1-Cf-4 (Huang et al., 2024) and Cf-9 mediated perception of *C. fulvum* Avr9 (Jones at al., 1994; Rowland et al., 2005, Huang et al., 2021).

In Solanaceae, NRC proteins (NB-LRR Required for HR-associated Cell death), a subset of helper(H)-NLR (nucleotide binding (NB) leucine-rich repeat (LRR)) resistance genes are emerging as key players in sensor-NLR (s-NLR)-mediated disease resistance signalling (Wu et al., 2017, Jubic et al., 2019). Over evolutionary timescales, NLRs have functionally specialised as sensors or helpers in complex immune signalling (Adachi et al., 2019). Their role in immune signalling cascades initiated by cell surface receptors and NLRs is now becoming evident (Ngou et al., 2021, Yuan et al., 2021). H-NLRs interestingly also contribute to inhibitor perception signalling mediated by many LRR-containing receptors (Jubic et al., 2019, Li et al., 2019). For instance, silencing of tomato *NRC1* in *N. benthamiana* impacts HR-triggered by *Cf-4/Avr4* (Gabriels et al., 2006). Previous studies have reported the role of *NRC1* in *LeEix2- (*Gabriëls et al., 2007) and *Ve1*-mediated (Fradin et al., 2009) cell death response*.* over-expression of *SlNRC4a* was shown to enhances *LeEix2*-mediated defence while its silencing reduced the defence response (Leibman-Markus et al., 2018). With demonstrated potential of gain of function mutants in broad-spectrum resistance in tomato, H-NLR-SlNRC4a likely integrate diverse signals by RLPs and s-NLRs (Pizarro et al., 2020). Similar to RLPs like Cf-4 (Postma et al., 2016), the transduction of Cf-2 recognition signalling likely recruits SERK3/BAK1 that further activates NRC1 or its homolog, NRC3, and HR induction (Kourelis et al., 2022, Kourelis et al., 2024).

In Chapter 3, we showed that Avr2, EpiC1, EpiC2B and Cip1 are recognised in wild species of tomato and potato. Mutant Avr2, EpiCs and Cip1 inhibitors that cannot inhibit PLCP, triggered weak or no HR, indicating PLCPs are required for perception of these inhibitors. Distinct inhibitors are perceived by individuals of same and different populations. Our survey reported that Avr2 is the most frequently recognised inhibitor and recognition frequency variations exist across geographical regions. EpiCs were more frequently recognised in wild

potato species, the natural host of *P. infestans* as compared to tomato. Further, we did not observe any HR-triggered by the four inhibitors beyond potato clade in Solanaceae. In Chapter 4, we therefore identified that genotypic variation in *Cf-2*, *Cf-9*, *Hcr9-9DC* and number of *Hcr2* genes exist among individuals of same and different populations. *Cf-9* presence is more frequent than *Cf-2* in wild tomato populations, but *Cf-2-like* genes are present in wild potato and not all *Cf-2* positive plants recognise Avr2. We further identified that while *Rcr3* and *C14,* but not *Pip1* are diversifying within *S. pimpinellifolium*, *Rcr3* and *Pip1* are diversifying across wild tomato species. On the other hand, none of the three immune proteases is diversifying in wild potato. The evident lack of diversification of *Rcr3*, *Pip1* and *C14* in potato potentially indicate conserved role of these convergent host targets in distinct inhibitor recognitions. Polymorphism in *Cf* genes and cysteine proteases *Rcr3*, *Pip1* and *C14* is potentially important for long term adaptation to fluctuating pathogen pressures in local environments. While we reported the extent of existing variation in *Cf-2* and homologs in a small representative population pool in Chapter 4, the variation in their expression and their impact of recognition of unrelated inhibitors remains to be explored.

In this Chapter, we used *Tobacco rattle virus* (*TRV*)-based Virus-induced gene silencing (VIGS) to silence *Cf-2*, different clans of representative *Hcr2s*, *Rcr3*, *Pip1*, *C14* and *SOBIR1* in wild tomato *S. pimpinellifolium* and measure the effect on recognition of purified inhibitors Avr2, EpiC1, EpiC2B and Cip1. Due to its broad host range, TRV2-based VIGS has previously been used to silence genes in different Solanaceae species (Liu et al., 2002; Brigneti et al., 2004; Senthil-Kumar et al., 2007; Velásquez et al., 2009, Zhao et al., 2020). Therefore, we also show that genes from tomato effectively silence orthologs in diploid wild potato species, *S. infundibuliforme* and *S. bulbocastanum*. Silencing *Cf-2* reduces Avr2 recognition, but does not necessarily impact recognitions of other inhibitors, whereas silencing specific cysteine proteases reduced recognition of tested inhibitors to various extent. However, recognition of all four inhibitors clearly is reduced in *SOBIR1*-silenced plants.

We further took advantage of available comprehensive collection of genomics data and protein architecture prediction tools to identify Cf-like RLPs across the plant kingdom. We describe our HMMER-based approach that showed that Cf-like RLPs are restricted to Solanaceae. We manually annotated the LRRs, transmembrane domain and signal peptide in each candidate RLP and identified that Ve-RLP family is more ancient than Cf-like-RLPs, whereas EIX receptors have more recently evolved. Our work paves the way for characterising the potentially interconnected recognition signalling of extracellular inhibitors of unrelated pathogens. In the future, research attempts to pinpoint Cf-like receptor domains or functional variations in *Cf/Rcr3*-like systems that are capable of recognising a wide array of inhibitors from distantly related emerging pathogens can accelerate the engineering of broad spectrum resistance in Solanaceae crops.

5.2 Results

5.2.1 Silencing *Cf-2* compromises HR against Avr2, but does not affect recognition of Cip1 and EpiCs in *S. pimpinellifolium*

Our first aim was to ascertain if *Cf-2* and *Hcr2s* are required for recognition of EpiC1, EpiC2B, Cip1 and Avr2 in *S. pimpinellifolium*. A maximum-likelihood tree of 500 bootstrap replications was constructed using MEGA12 (Kumar et al., 2024) and used to guide the silencing of *Cf-2/Hcr2s* in tomato and in potato (**Figure 5.1 and supplementary 5.6**). Using SGN-VIGS tool (Fernandez-Pozo et al., 2015), we selected 300 bp fragments for clan-specific silencing based on available genomic data (Sol Genomics Genes-*S. pimpinellifolium* LA1589 and *S. tuberosum*) to target subsets of *Hcr2s* consisting highly homologs representative members. We cloned each fragment into pTRV2 and then transformed these binary vectors into *Agrobacterium tumefaciens* GV3101. Using agroinfiltration, we expressed *TRV*-carrying *Cf-2/Hcr2* silencing fragments in *S.*

pimpinellifolium LA0369 which recognises Avr2 and LA0753 which senses all four inhibitors. We used up to eight days-old clonal propagates of *Sp*LA0369(Plant 3) and *Sp*LA0753(Plant 3). RNA was isolated from three biological replicates to estimate relative transcript levels at four-weeks post agroinfiltration (**Figure 5.2**). In a $2^{-\Delta\Delta CT}$ method of transcript level quantification, endogenous *Actin* (Table 2.4, chapter 2) was used as a reference for normalisation. Based on non-parametric Student's *t*-test, the extent of silencing were estimated as statistically significant fold change compared to transcript levels in *TRV::GFP* control plants.

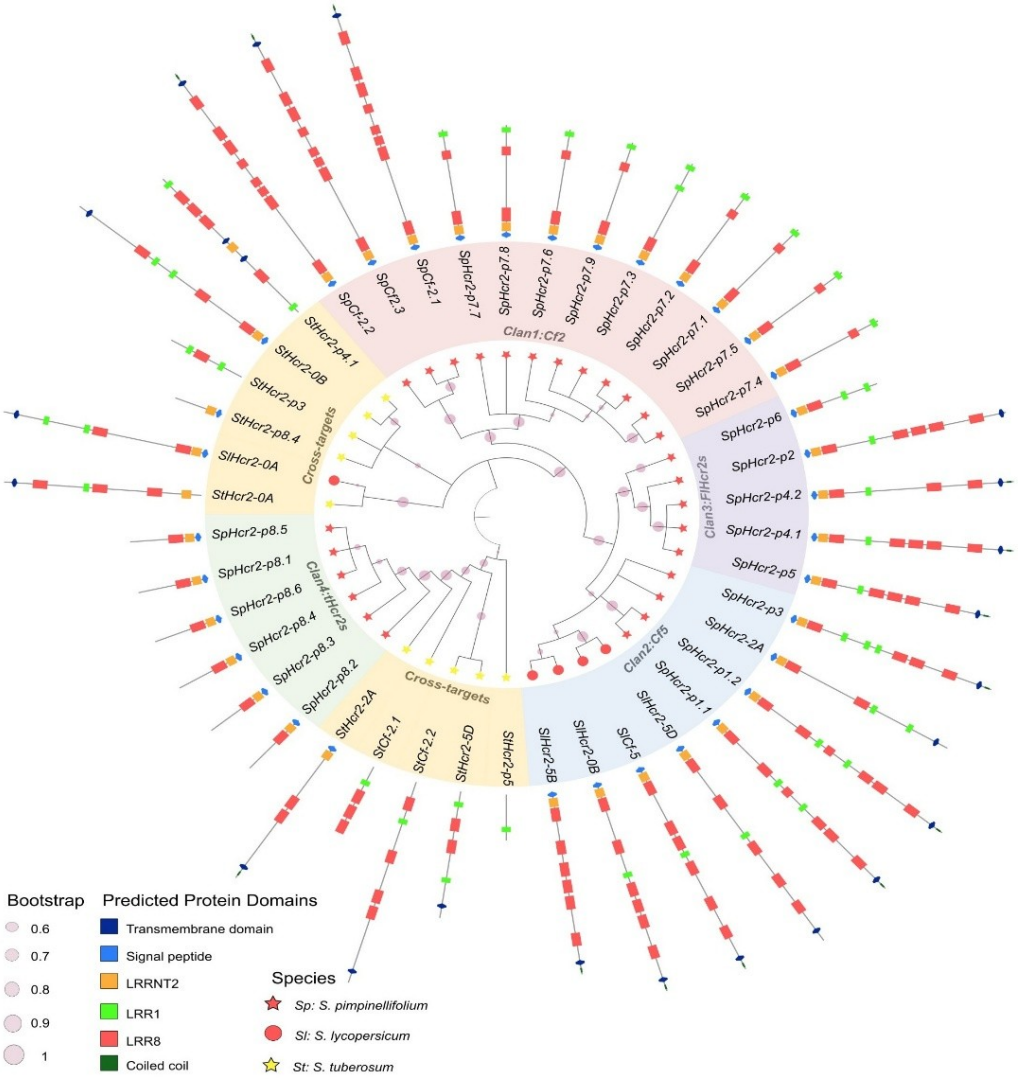


Figure 5.1 Phylogenetic relationships derived to guide silencing of *Cf-2* and *Hcr2* genes.
A maximum-likelihood DNA tree of already published *Cf-2*-homologs*(Hcr2s)*/orthologs in tomato and potato was generated using MUSCLE aligned fasta in MEGA12. The tree was rooted at midpoint and was used to design constructs for virus-induced gene silencing (VIGS) assays in wild tomato

and wild potato. Bootstrap values from 500 replicates, over 50% are indicated on branches. *Hcr2s* were classified into four main clans in this study, namely, *Cf-2* (clan 1), *Cf5* (clan 2), *Full-length Hcr2s* (clan 3) and *Truncated Hcr2s* (clan 4). Hence, four silencing vectors were constructed to knock-down various *Hcr2s*. Cross-targets that are potentially silenced are highlighted. Protein sequences were then used to predict structural features that are shown in detail next to each gene. VIGS sequences are shown in supplementary table 5.1(a) and silencing efficiency in different clans is shown in supplementary tables 5.1(b) to 5.1(f). *Phylogenetic tree raw files are attached as supplementary 5.6. Raw data files for supplementary tables are attached as supplementary file 5.7.

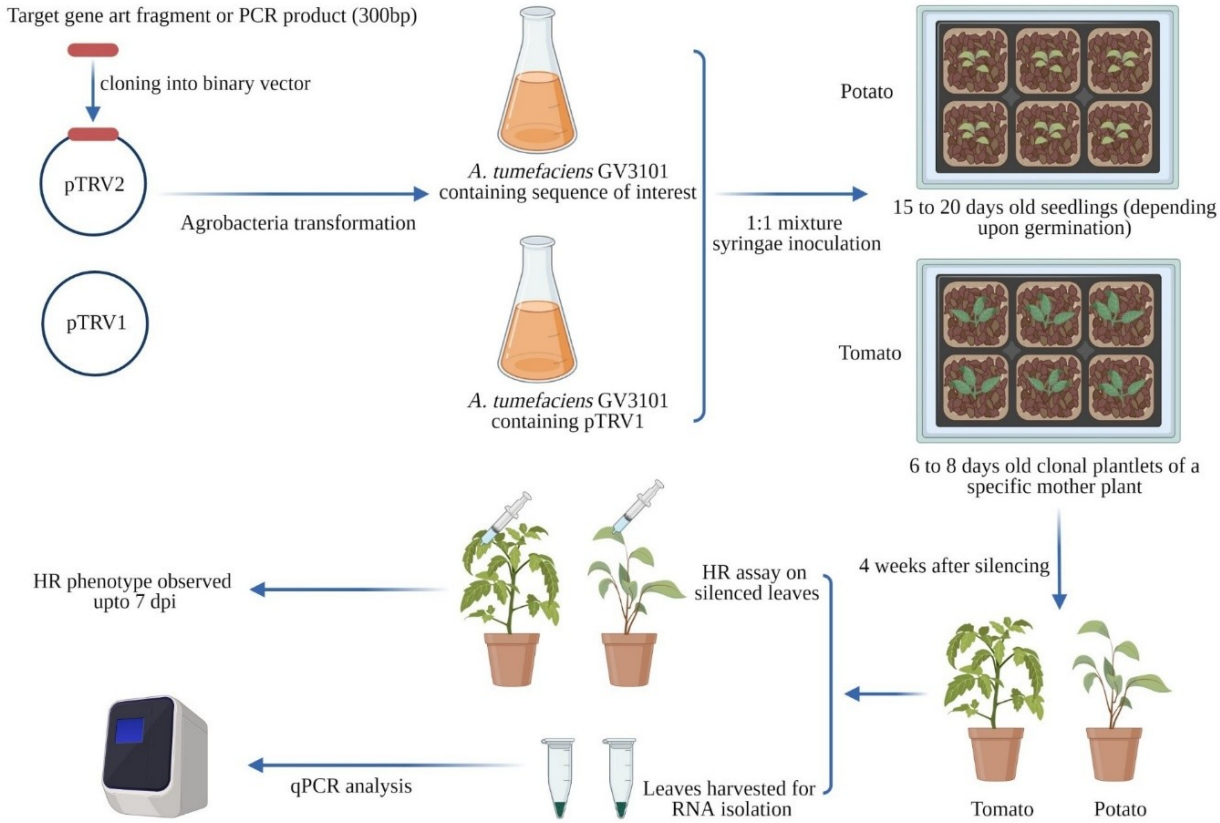


Figure 5.2 *TRV*-based virus-induced gene silencing (VIGS) assay in wild species of tomato and potato.

Illustration describing the procedure and analysis scheme used in this study, for silencing of various protein inhibitor recognition and defence components in wild species of tomato and potato. Fragments of interest (300 bp) were cloned into pTRV2, which were transformed into *Agrobacterium tumefaciens* GV3101. For silencing in wild tomato, up to eight days old clonal propagates were used, while 15 to 20 days old true seedlings were used for wild potato species. Four-weeks after initiating silencing, samples for RNA isolation were isolated and plants were then infiltrated for HR assay (described in figure 3.3). qPCR was performed to estimate changes at transcript levels.

Next, HR assay was performed (described in **Figure 3.3**, chapter 3), where purified Avr2, EpiCs, Cip1 and their corresponding mutant proteins were injected into leaves of silenced plant and HR responses were scored up to seven days post infiltration. In both *Sp*LA0369(P3) and *Sp*LA0753(P3), Avr2-triggered HR is reduced upon *Cf-2* (clan 1) silencing in comparison to *TRV::GFP* plants (**Figure 5.3(a) and Figure 5.4(a)**). Interestingly, qPCR transcript levels in *Cf-2/Hcr2* silenced plants were significantly reduced in *Sp*LA0753(P3) as compared to *Sp*LA0369(P3). Contrarily, we did not observe significant silencing of clan 2 and clan 3 subsets in *Sp*LA0369(P3), but there were variations in HR observed upon Avr2 infiltration. In *Sp*LA0369(P3), we observed that clan 2 and clan 4-specific silencing also reduced HR triggered by Avr2 (**Figure 5.3(b), (c) and (d)**).

While we initially hypothesised Cf-2-mediated recognition of other inhibitors in addition to Avr2 in *S. pimpinellifolium*, we observed that recognition of Cip1, EpiC1 and EpiC2B remained visibly unaffected in *Sp*LA0753(P3) plants silenced for *Cf-2* (**Figure 5.4(a)**). Efficient silencing of *Cf5*-clan members was noted in *Sp*LA0753(P3) which visibly reduced Avr2 recognition (**Figure 5.4(b)**), which was not observed in *Sp*LA0369(P3) counterpart. A difference in Avr2 and EpiC1-induced HR was also observed upon clan 3-silencing whereas silencing of truncated clan 4 seemingly affect EpiC1 but not EpiC2B (**Figure 5.4(c)**). *Sp*LA0369(P3) and *Sp*LA0753(P3) qPCR analysis did not directly reflect the relative fold changes in the transcript levels that would have been expected for silenced clan of interest.

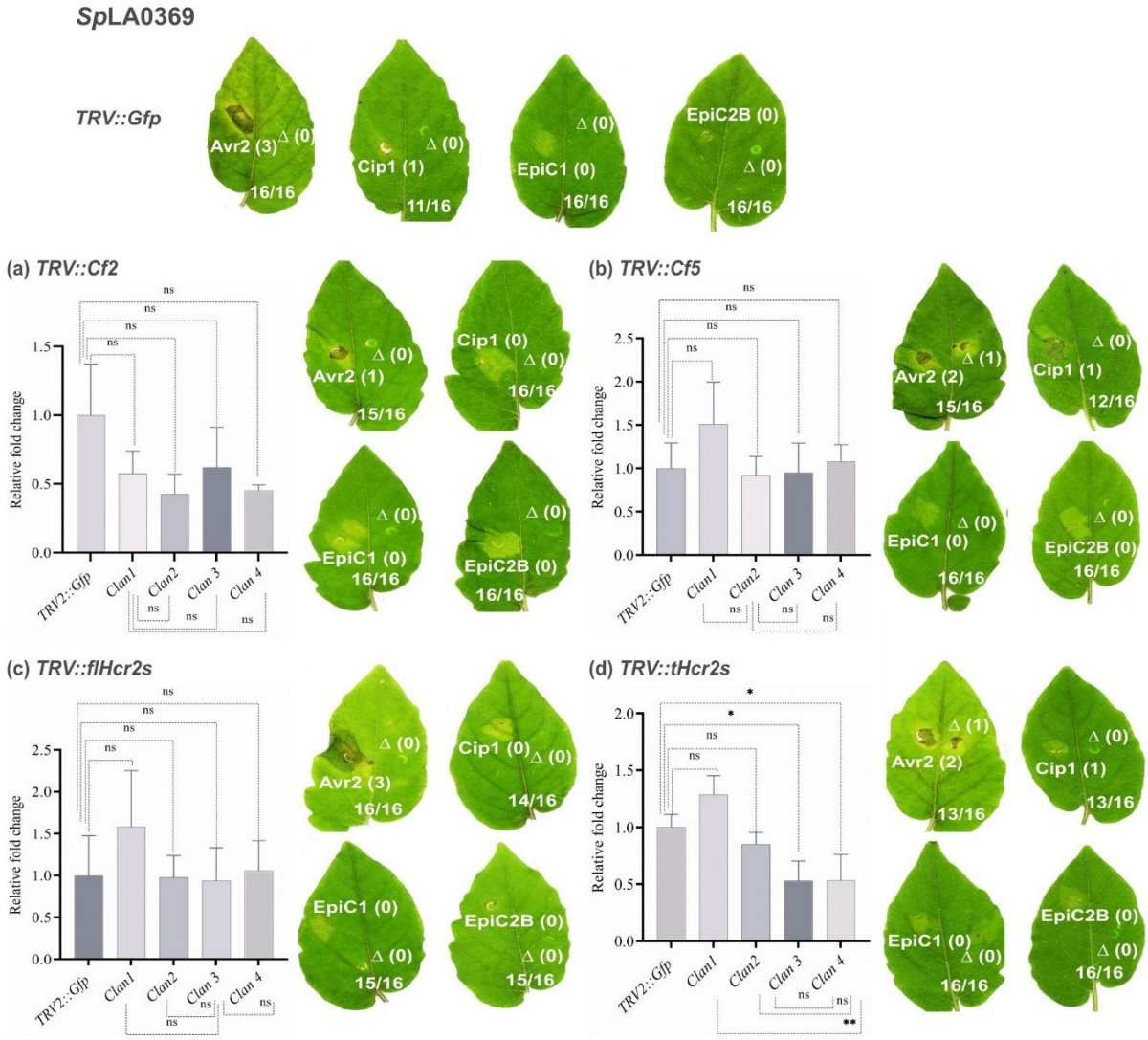


Figure 5.3 Silencing with *Cf-2* fragment reduce Avr2-induced HR in wild tomato *Sp*LA0369. *Sp*LA0369 was identified to respond against Avr2 in HR screening and thus selected for silencing of *Cf-2* and homologs using four different silencing vectors: **(a)** *TRV::Cf-2*, **(b)** *TRV::Cf5*, **(c)** *TRV::flHcr2s*, and **(d)** *TRV::tHcr2s*. Virus-induced gene silencing (VIGS) was performed as described in figure 5.2. *TRV::Gfp* treated plants represented control. Expression levels of different clans after VIGS treatment were quantified using qPCR analysis. Endogenous reference *Actin* was used for normalisation using $2^{-\Delta\Delta CT}$ method. Data of three biological replicates is represented as mean standard deviation (Std. Dev.). The extent of silencing as fold change is relative to transcript abundance in *TRV::Gfp* (set to 1). A non-parametric Student's *t*-test was performed to estimate statistical significance; asterisks indicate *p≤0.05, **p≤0.01, ns = non-significant. Silenced plants were treated with different inhibitors in an HR assay. Brackets show HR severity on a scale of 0-4 against each inhibitor treatment. Representative leaves were photographed at 7 dpi. Leaf counts indicate number of leaves with HR phenotype versus total number of leaves assayed. *VIGS fragment and specificity to targets/cross-targets are shown in supplementary 5.1 and 5.7, respectively.

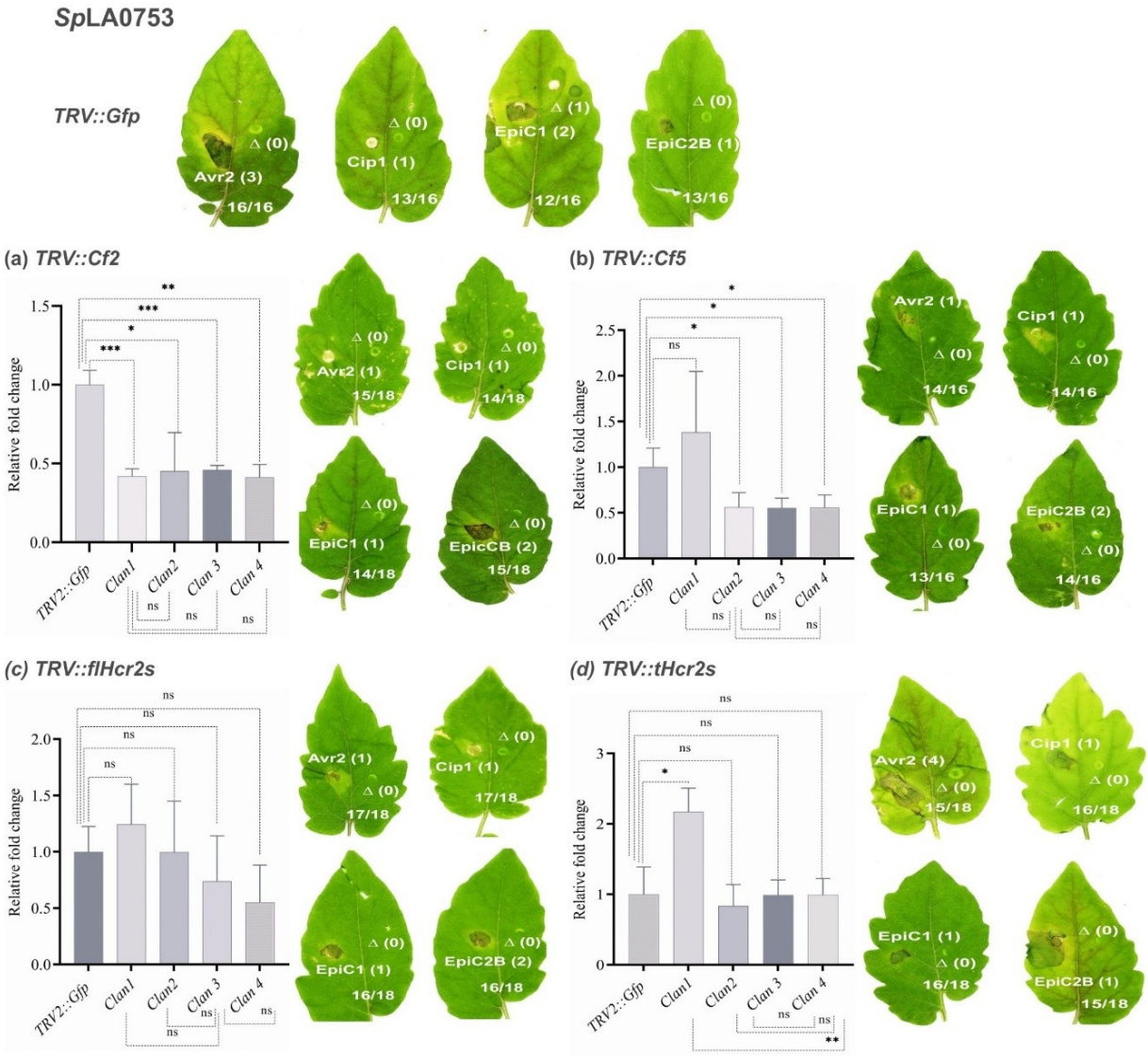


Figure 5.4 Avr2 recognition is reduced upon *Hcr2* silencing whilst EpiC1, EpiC2B and Cip1 recognition remains unaffected in wild tomato *Sp*LA0753.

*Sp*LA0753 individuals were silenced using **(a)** *TRV::Cf-2*, **(b)** *TRV::Cf5*, **(c)** *TRV::flHcr2s* and **(d)** *TRV::tHcr2s*. Silencing efficiency was estimated using qPCR, where relative expression of each *Cf-2/*homolog clan was normalised to endogenous *Actin* and calibrated to *TRV::Gfp* treated control (set to 1). Mean standard deviation was obtained from three biological replicates. A non-parametric Student's *t*-test derived significance as *p≤0.05, **p≤0.01, ***p≤0.001 and ns = non-significant. 7 dpi leaves from an HR assay on silenced plants are shown. Scores in brackets indicate HR scoring on a scale of 0-4 (figure 3.3) against each inhibitor treatment. Number of leaves with HR phenotype versus total number of leaves tested for HR are shown. *VIGS fragment and specificity to clan members and cross-targets are shown in supplementary 5.1 and 5.7.

Although we did not expect cross-silencing of genes outside the *Hcr2* family on the basis of SGN-VIGS predictions, we could expect cross-silencing within *Hcr2* family, given the presumed high number of *Hcr2s* in *S. pimpinellifolium* (**supplementary 5.6**) or within individual plants (**Figure 4.3**, chapter 4), sharing sequence homology with VIGS fragments (**supplementary 5.1 and 5.7**). While we were able to detect functional implications of four specific *Cf-2/Hcr2* clans in perception of Avr2, Cip1, EpiC1 and EpiC2B, results of our VIGS approach only give an indication of members that are capable of recognising distinct inhibitors. However, our results do suggest that (a) Cf-2 primarily recognises Avr2, but not EpiC2B in LA0369, (b) *Hcr2/Cf* gene may confer recognition of more than one if not all four inhibitors tested in LA0753.

5.2.2 Silencing of *Cf-2/Hcr2s* in wild potato do not influence EpiC2B perception

Since we observed extensive recognition of particularly EpiC2B, Avr2 and Cip1 in wild potato populations/species in chapter 3, we selected diploids, *S. infundibuliforme* CGN17720 and *S. bulbocastanum* CGN22732 as candidates for heterologously silencing *Cf-2/Hcr2* using the same *TRV* constructs as used in wild tomato *S. pimpinellifolium* (**supplementary 5.1 and 5.6**). *Si*CGN17720(P3) conferred recognition of EpiC2B and Avr2 or Cip1 and carries a *Cf-2-like* gene. *Sb*CGN22732(P3) recognised only EpiC2B and carries an *Hcr2*-gene (**Figure 4.7**, chapter 4). Hence, we hypothesised that similar to *S. pimpinellifolium*, Avr2 recognition is explained by the existence of a *Cf-2*-variant in wild potato whereas, diverse *Hcr2(s)* may act as primary receptor(s) to mediate recognition of EpiC2B and Cip1. We used 15 to 20 days old true seedlings of *Si*CGN17720(P3) and *Sb*22732(P3) to perform VIGS-based silencing. However, although we effectively silenced clan 1 and clan 4 (**Figure 5.5(a) and (d)**) specific plants of *Si*CGN17720(P3), we failed to detect response to Avr2 in control *TRV::GFP* plants (**Figure 5.5**).

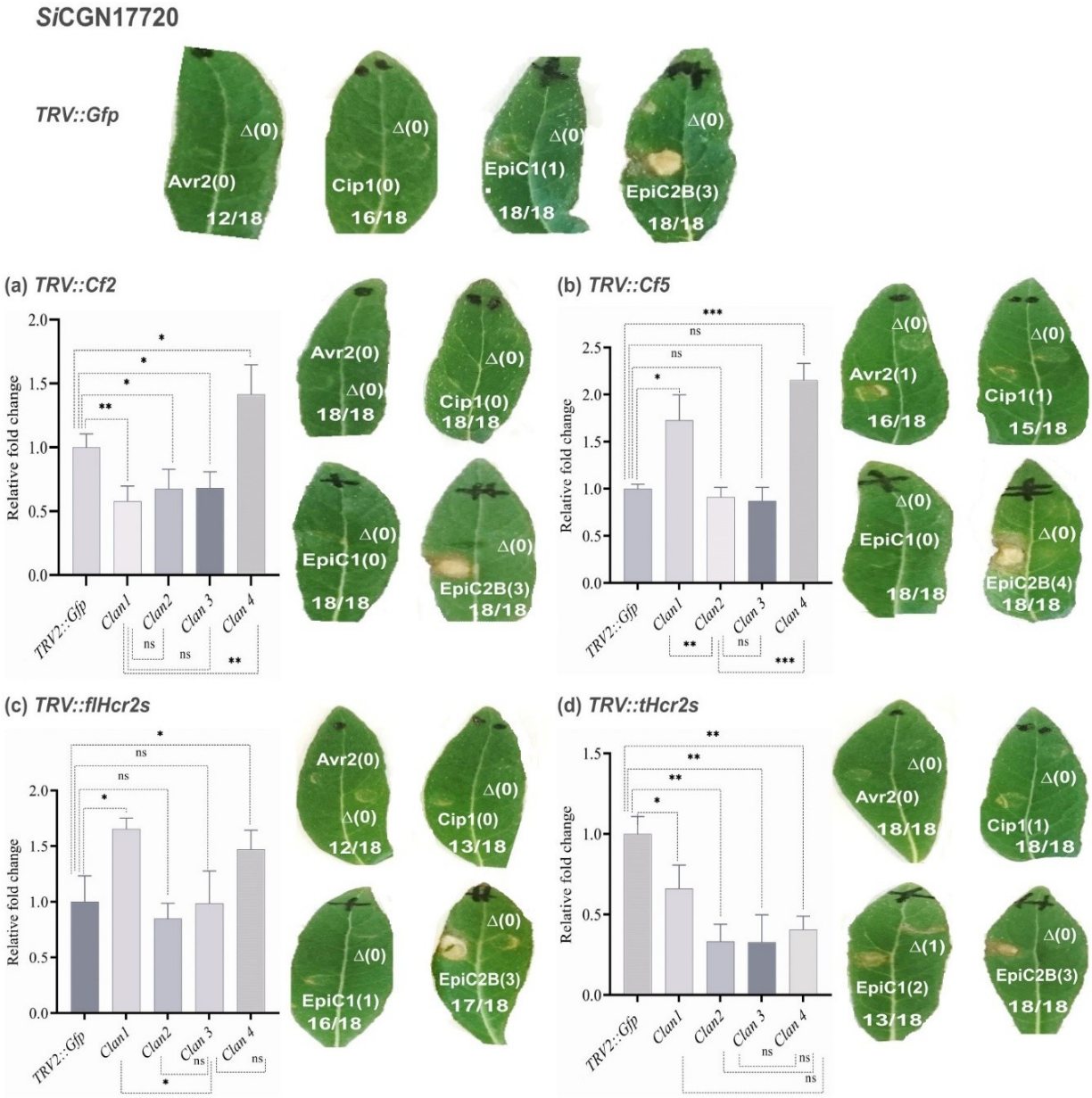


Figure 5.5 EpiC2B recognition is not affected in *Hcr2* silenced wild potato *Si*CGN17720.

*Si*CGN17720 was identified to recognise EpiC2B and at least one other inhibitor in absence of *Cf-2* gene-like PCR fragment. Silencing *Cf-2*/homolog clans was thus performed as detailed for wild tomato populations in figures 5.3 and 5.4. Data is represented as mean standard deviation estimated from three biological replicates. Significance from non-parametric Student's *t*-test is indicated as *p≤0.05, **p≤0.01, and ns = non-significant. Scores in brackets indicate HR intensity on a scale of 0-4 (figure 3.3) against each inhibitor treatment. Number of leaves with phenotype against inhibitor as compared to total number of leaves assayed are shown with representative leaves photographed at 7 dpi. *VIGS fragment and specificity to clan members and cross-targets are shown in supplementary 5.1 and 5.7.

Intriguingly, silencing of clan 2 and clan 4 did not result in alteration of transcript levels abundances, but reduced HR against Avr2 (**Figure 5.5(b)**) and EpiC1 (**Figure 5.5(d)**), respectively. Irrespective of silencing efficiency of heterologous sequences in *Si*GN17720, the severity of EpiC2B- induced HR remained unchanged in comparison to *TRV::GFP* plants (**Figure 5.5**). Similarly, rigorous HR was observed against EpiC2B when each of the four *Hcr2* clans was silenced in *Sb*CGN22732(P3) (**Figure 5.6**). However, we observed clans 2 and 4 were effectively silenced in *Sb*CGN22732(P3) as opposed to *Si*CGN17720(P3), which is likely due to absence of *Cf-2* in *Sb*CGN22732(P3). Our data suggest that while modulations in gene expression levels of *Hcr2s* is achieved using heterologous VIGS sequences of wild tomato, *Hcr2s* are probably not involved in mediating perception of EpiC(s), particularly EpiC2B.

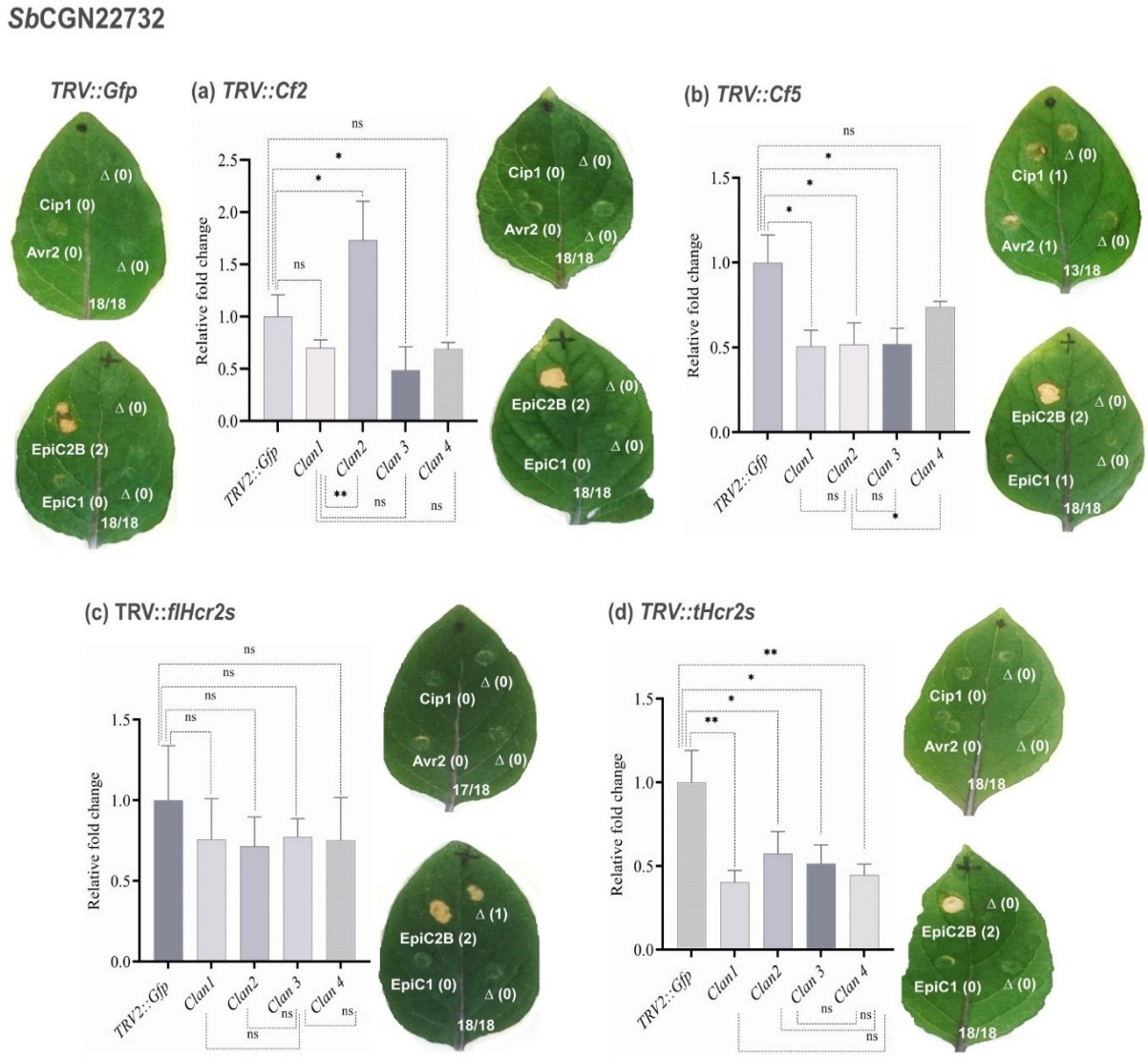


Figure 5.6 EpiC2B perception is not affected upon *Hcr2* silencing in wild potato *Sb*CGN22732. *Sb*CGN22732 specifically recognised EpiC2B in HR screening and do not consist *Cf-2*, but *full-length(fl)* or *truncated (t) Hcr2s*. *Cf-2/*homologs were silenced using four different vectors **(a)** *TRV::Cf-2*, **(b)** *TRV::Cf5*, **(c)** *TRV::flHcr2s* and **(d)** *TRV::tHcr2s*. Silencing efficiency was quantified using a qPCR approach described in figures 5.3 and 5.4. Experimental data is shown as standard mean deviation obtained from three biological controls. Statistical significance is derived from a non-parametric Student's *t*-test as: *p≤0.05, **p≤0.01, and ns = non-significant. HR assay was performed on silenced plants and symptoms were scored at 7 dpi. Scores in brackets indicate HR score on a scale of 0-4 (figure 3.3) against each inhibitor treatment. HR phenotype counts as number of leaves with HR symptoms against total number of leaves tested for HR are detailed. *VIGS fragment and specificity to clan members and cross-targets are shown in supplementary 5.1 and 5.7.

5.2.3 Silencing of *Rcr3*, *Pip1* and *C14* in *S. pimpinellifolium* differentially diminish HR induced by unrelated inhibitors

To investigate how *Rcr3*, *Pip1* and *C14* affect the recognition of Avr2, Cip1, EpiC1 and EpiC2B we performed VIGS in *Sp*LA0369(P3) and *Sp*LA0753(P3) as was described for *Cf-2/Hcr2s*. qPCR analysis revealed selective reduction of transcript levels of *Rcr3*, *Pip1* and *C14* in both *Sp*LA0369(P3) and *Sp*LA0753(P3) (**Figure 5.7(a) and (b)**). HR assays with purified Avr2, Cip1, EpiC1, EpiC2B and their corresponding mutant inhibitors on silenced plants revealed that *Pip1* plays a nearly equally important role in mediating recognition of all four inhibitors in *S. pimpinellifolium* (**Figure 5.7**). Remarkably, a similar reduction in HR against EpiCs and Cip1 was also observed in *C14*-silenced plants and against Avr2, EpiC2B and Cip1 in *Rcr3*-silenced plants. We found that *Rcr3* silencing also reduced Avr2 recognition in *Si*CGN17720(P3).

Silencing *Pip1* and *C14* affected Avr2 recognition similarly as *Rcr3*. Moreover, Cip1 recognition was significantly lowered in *Pip1* silenced plants whereas *C14* silencing caused diminished EpiC2B recognition the most in *Si*CGN17720(P3). *Rcr3* least affected EpiC2B recognition in wild potato. Based on shared homology of these cysteine proteases between tomato, distant wild relative tomato species and potato (**supplementary 5.3, 5.8, 5.9 and 5.10**), we did expect *S. pimpinellifolium* specific *TRV:*:Rcr3, *TRV*::Pip1 and *TRV*::C14 to successfully silence counterparts in wild potato without cross silencing between the three PLCPs. Our finding corroborates that while Rcr3, Pip1 and C14 are convergent immune protease targets of unrelated pathogen-derived inhibitors, they play different roles as co-receptors possibly by acting on distinct substrate preferences and thereby differentially co-mediating recognition and resistance against multiple pathogens. By contrast to Hcr2s, PLCPs appear to have increasingly convergent roles in inhibitor-induced host responses. Our findings indicate the signalling pathways of unrelated inhibitor perception is complex.

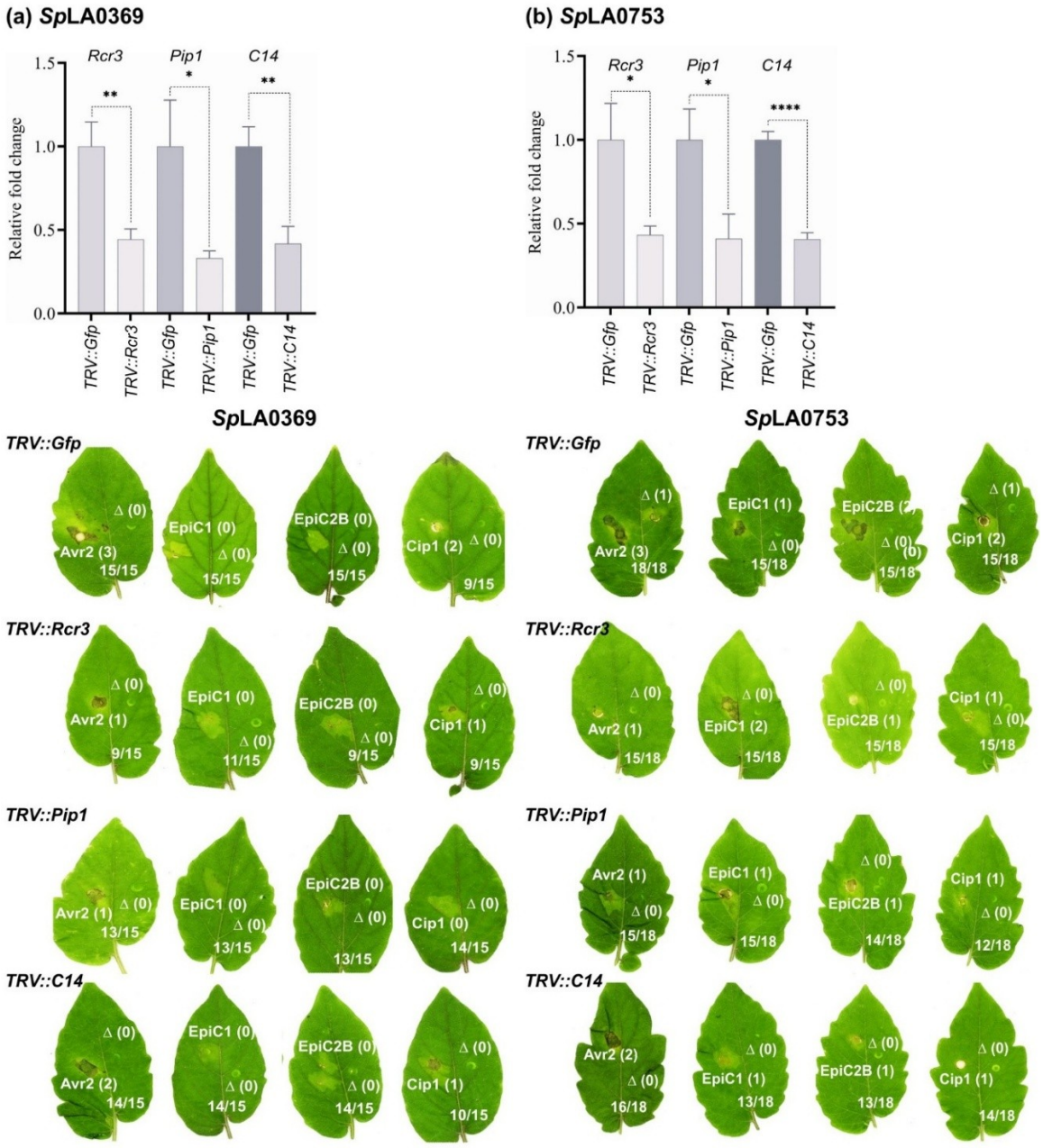


Figure 5.7 Silencing *Rcr3, Pip1* and C14 variably reduce recognition of inhibitors in *S. pimpinellifolium*.

Relative transcript levels were assayed using qPCR on RNA from leaf samples treated individually with *TRV*::Rcr3, *TRV*::Pip1 and *TRV*::C14 in **(a)** LA0369, and **(b)** LA0753. Endogenous *Actin* was used for normalisation in a $2^{-\Delta\Delta CT}$ method. The extent of silencing is represented as relative fold changes against transcript levels in *TRV::Gfp* control for each population (calibrated to 1). Data is shown as mean standard deviation from three biological replicates. Significant difference was analysed using a non-parametric Student's *t*-test as *p≤0.05, **p≤0.01, ***p≤0.001 and ****≤p0.0001. Leaves shown are from HR assay on silenced plants photographed at 7 dpi. Brackets indicate HR phenotype intensity on a scale of 0-4 towards inhibitor. Number of leaves showing HR symptom out of the total number of leaves evaluated for HR are also shown. *VIGS fragment/specificity to targets in Solanaceae species are shown in supplementary 5.3, 5.8, 5.9 and 5.10.

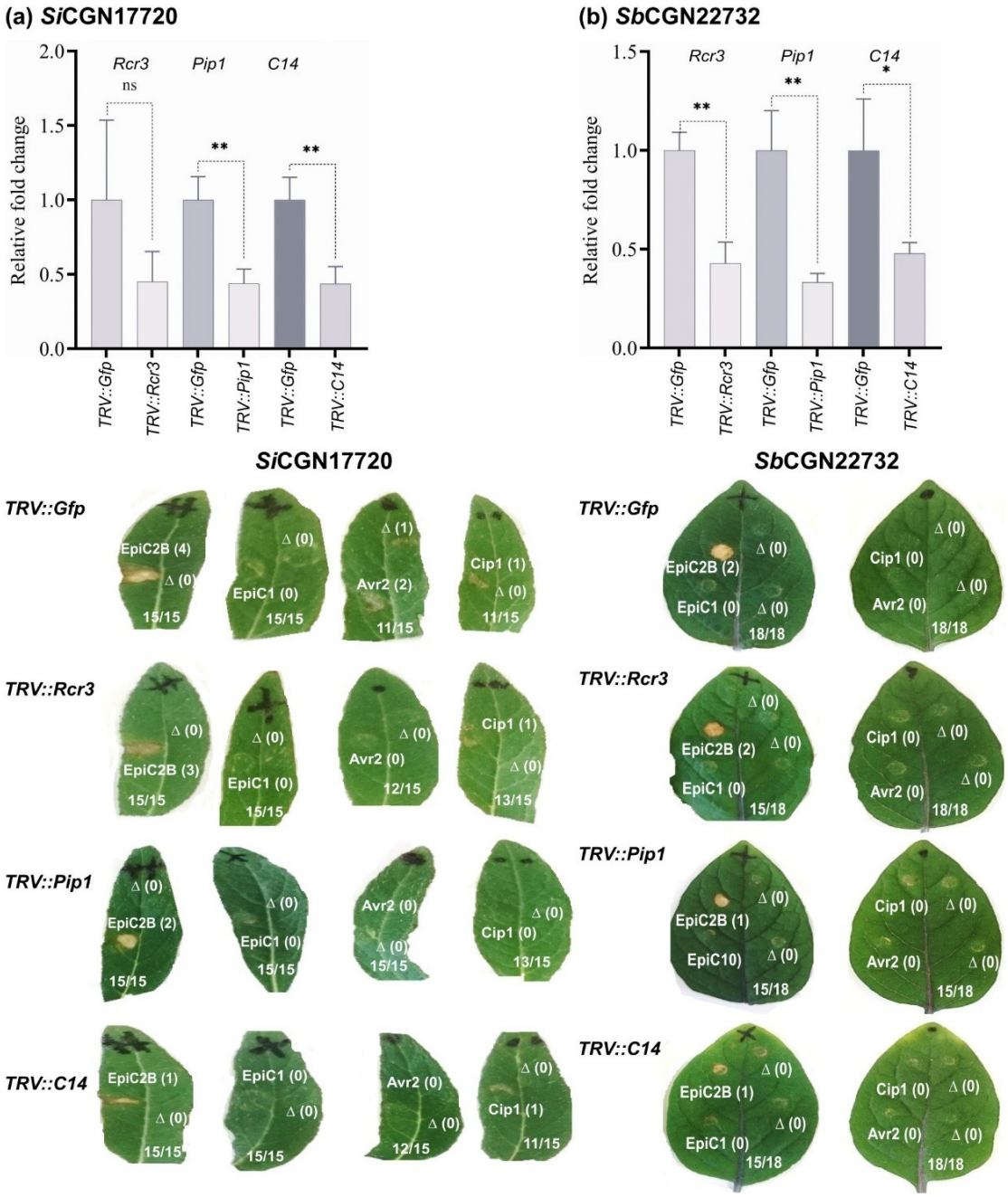


Figure 5.8 Effect of Rcr3, Pip1 and C14 silencing on HR-triggered by inhibitors in wild potato. *TRV::Rcr3*, *TRV::Pip1* and *TRV::C14* silencing in wild potato, **(a)** *Si*CGN17720, and **(b)** *Sb*CGN22732 show variation against inhibitor treatments. Performance of VIGS assay and the ability of silenced plants to trigger HR against inhibitors were assessed using qPCR and HR assay, respectively. The approach is similar to as described in figure 5.7. Significant relative fold changes estimated in a non-parametric Student's *t*-test are indicated as *p≤0.05, **p≤0.01, and ns = non-significant. Representative leaves from HR assay on silenced plants were photographed at 7 dpi. HR phenotype severity against each inhibitor is mentioned in brackets. Number of leaves with HR phenotype scored out of total number of leaves assayed for HR are also indicated. *VIGS fragment and specificity in closely and distantly related Solanaceae species are detailed in supplementary 5.3, 5.8, 5.9 and 5.10.

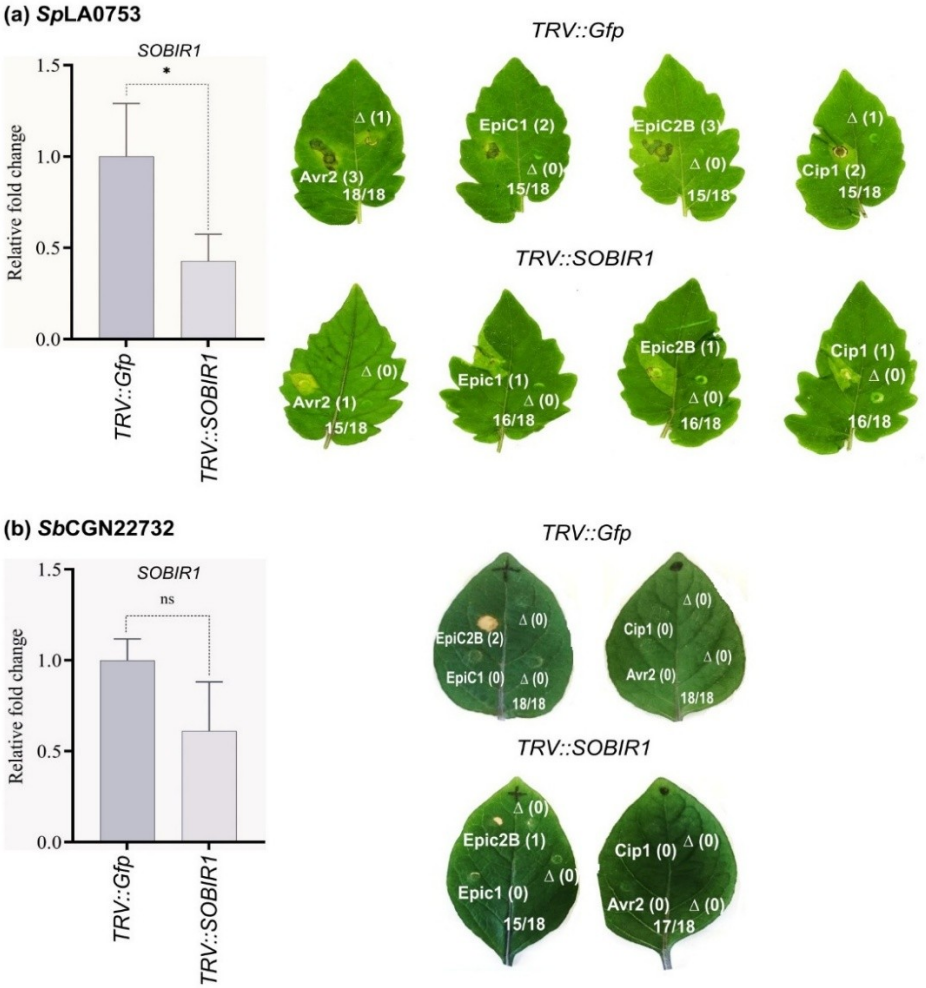


Figure 5.9 *SOBIR1* silencing reduces inhibitor recognition in wild tomato and wild potato.
To detect if *TRV::SOBIR1* plays a role in RLK-dependent resistance signalling of Avr2, EpiC1, EpiC2B and Cip1, *SOBIR1* was silenced (supplementary 5.3) in **(a)** *Sp*LA0753 and **(b)** *Sb*CGN22732. Efficiency of tomato *SOBIR1* VIGS fragment to silence *SOBIR1* from closely and distantly related species in Solanaceae is shown in supplementary 5.11. Effectiveness of *SOBIR1* silencing was determined using qPCR with normalisation of transcript levels to internal *Actin*. Data from biological replicates (n = 3) is shown as mean standard deviation. Statistical significance was obtained by a non-parametric Student's *t*-test as *p≤0.05. HR assays were performed on silenced plants and representative leaves photographed at 7 dpi are shown. Leaf counts represent number of leaves with HR phenotype versus total leaves tested in HR assay. Severity of HR symptoms is also indicated in brackets as scores 0-4. *TRV::Gfp* treatment represent silencing efficiency control and is same as represented for silencing of *Rcr3*, *Pip1* and *C14* in figures 5.7 and 5.8.

5.2.4 Recognition of unrelated inhibitors is dependent on SOBIR1 in wild tomato and potato

We finally addressed role of SOBIR1 in mediating recognition of Avr2, Cip1, EpiC1 and EpiC2B recognition by silencing *SOBIR1* in *Sp*LA0753(P3) and *Sb*CGN22732(P3). Over 90% homology shared between tomato and potato *spSOBIR1*-VIGS fragment was expected to silence *SOBIR1* in *Sb*CGN22732(P3) as well (**supplementary 5.3 and 5.11**). We consistently found that HR-triggered by Avr2, Cip1, EpiC1 and EpiC2B was diminished by silencing *SOBIR1* in *Sp*LA0753(P3) (**Figure 5.9(a)**). Distinguishing Cip1-induced HR in *SOBIR1*-silenced *Sp*LA0753(P3) plants from *TRV::GFP* control plants was visibly lower than other inhibitors. Further, EpiC2B-triggered HR in *Sb*CGN22732(P3) was visibly reduced in *SOBIR1* silenced plants (**Figure 5.9(b)**). Our results indicate that *SOBIR1* is required for recognition of Avr2, Cip1, EpiC1 and EpiC2B in wild tomato and potato.

5.2.5 Cf-like RLPs are widely distributed across Solanaceae and most abundantly in genus *Solanum*

In first section of this chapter, we had designed *Hcr2* VIGS assay based on limited number of representative genetic clades and it is possible that tomato and potato harbour a largely unexplored diversity of similar receptors. The finding that none of the four *Hcr2* silencing construct could be established to have a specific correlation with recognitions of EpiCs/Cip1 prompted us to conduct a phylogenetic study on diversity and number of Cf-like RLPs within Solanaceae and obtain a clearer landscape of species specialisation of the RLP repertoire which can help us to develop future approach to assess specific Hcr2s and their impact on diverse inhibitor recognition. To shed light on conservation of well-studied *Cf* genes, including *Cf-2* and closely related *Cf-9* outgroup within *Cf* superfamily as well as diversity and distribution of Cf-like RLPs, we leveraged an Hmmer-based *in-silico* mining approach

to search across Kingdom Viridiplantae (or green plants). A schematic illustration of our bioinformatics pipeline is detailed in **Figure 5.10**. Similar pipelines have previously been used to characterise domain evolution of NB-LRRs in Solanaceae (Seo E., et al 2016) and most recently for one of the extensive signalling peptides in angiosperms, stress-responsive Serine Rich Endogenous Peptides (SCOOPs) (Snoeck et al., 2024).

The Cf-2.2 protein sequence was used to scan over 300 proteomes present in EnsemblPlants v4.4 using PhMMERscan and high quality sequences passing a threshold e-value (detailed in Chapter 2) were found to be limited to Solanaceae. Representative proteins from genus-specific HMM-profiles obtained from HMMER alignments were then used to search NCBI-Protein and back-translated proteins to scan Sol Genomics protein/gff/cds genome datasets to detect Cf-like proteins that may have been missed from unavailable data in EnsemblPlants. A non-redundant set of manually curated 1456 sequences were retained after retrieval of Cf-like proteins. Sequences that shared over 90% identity in overall structure were considered duplicates and 970 unique sequences were further retained. We next performed a manual enrichment of Cf-related RLP sequences by scanning each of 970 sequences through Pfam, Phobius and SignalP. Certain sequences were identified to contain a kinase domain and were further removed in next step. A set of 549 proteins were retained as closely related to Cf-2, Cf-4 and Cf-9 as well as related RLPs, Ve (Kawchuk et al., 2001) and Eix (Ron and Avni, 2004). Next, we screened proteins for unusual domains (such as Malectin-like or Thaumatin-like) using IuPred3 and finally settled our search on 491 putative Cf-like RLPs. Although our search approach is biased by the availability and quality of available annotations, it still allowed us to acquire a general understanding of Cf-like RLPs within species and across Solanaceae.

S. tuberosum was found to contain the highest number of Cf-like RLPs (70), followed by *S. pimpinellifolium* (65) and *S. lycopersicum* (65) (**Figure 5.11**). Most Cf-like RLPs are encoded by genes that locate on chromosomes 0, 6 and 12. Surprisingly, we detected

significantly less Cf-like RLPs in wild tomato species *S. habrochaites* (4) and *S. peruvianum* (1) as compared to outgroup wild tomato relative, *S. lycopersicoides* (60) (**Figure 5.11(a)**). Overall, 300 of 491 RLPs were present in *Solanum*, followed by 50 in *Petunia*, 42 in *Nicotiana* and ten in genus *Capsicum* (**Figure 5.11(b)**). Regularity of LRRs is a striking feature of the Cf-2 and Cf-5 proteins, where A and B-type LRRs alternate with each other. A-type LRR has a consensus EEIXYLXSLXXLXLSENALNGSIP and the consensus ASLGNLNNLSXLXLYXNQLSGSIP forms B-type LRR (Dixon et al., 1996). Our results uncovered that only 21 of the 491 RLPs feature into this Cf-2 category (1081-1280 aa) with *S. pimpinellifolium* and *S. lycopersicum* containing four Hcr2 members each. Overall, RLPs ranged in lengths of 281 to 1680 aa classified into six primary architectural structure types (**Figure 5.11(c)**).

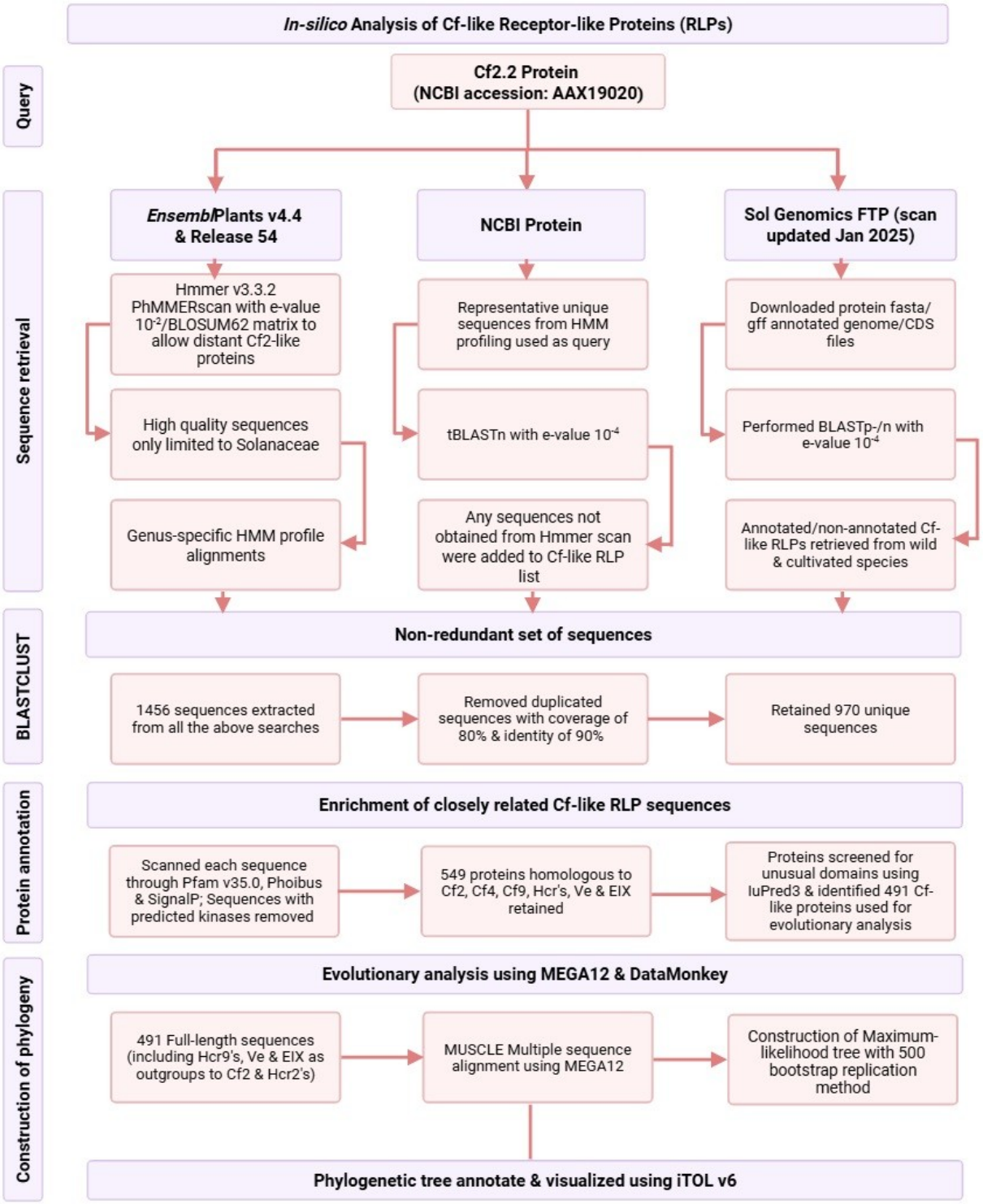


Figure 5.10: A detailed computational approach that identified Cf-like Receptor-like proteins (RLPs) in Solanaceae. Ve and EIX were included in this approach for outgroup clustering.

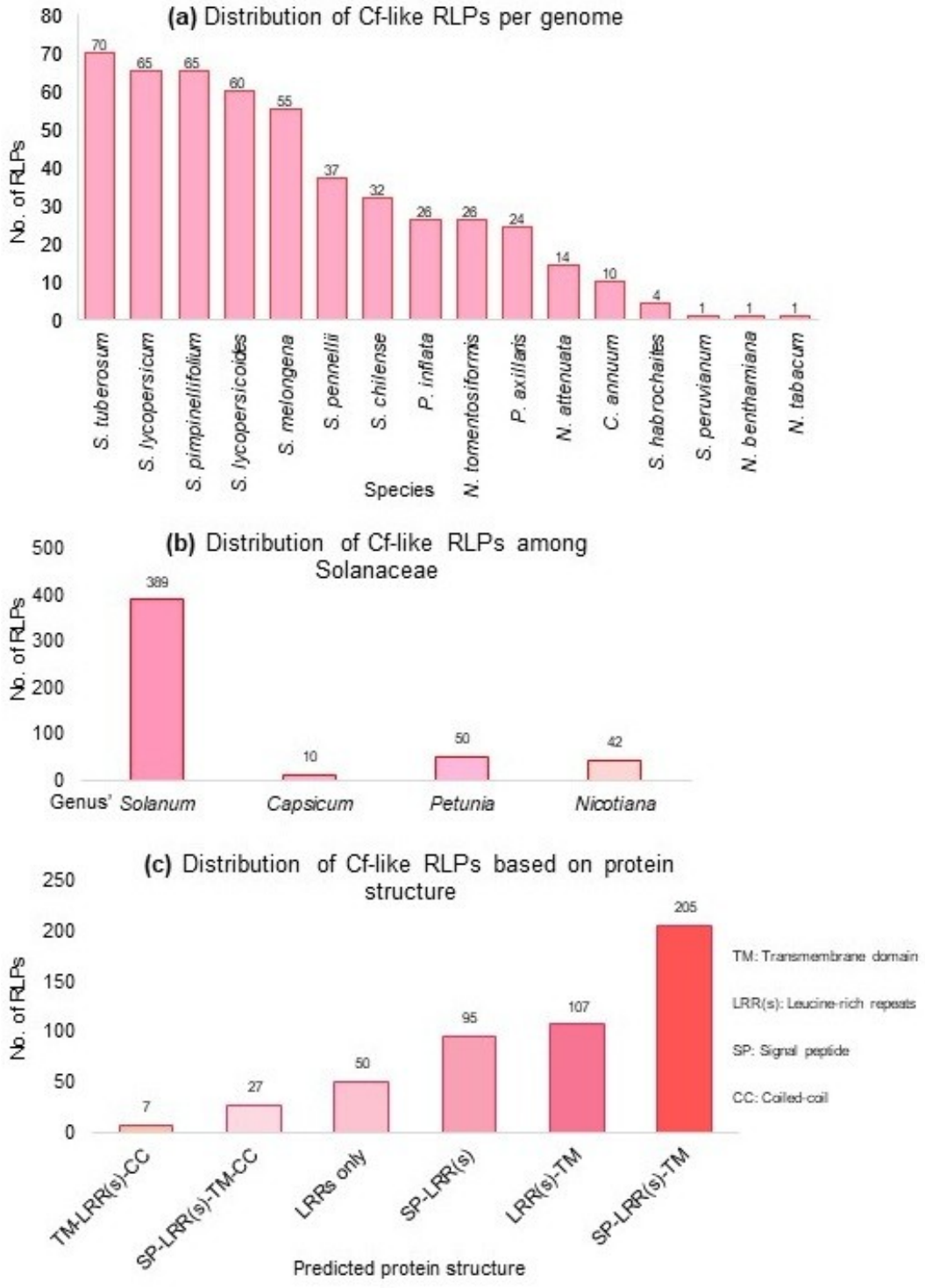


Figure 5.11 Distribution of Cf-like RLPs in Solanaceae.

Bar plots categorising Cf-like RLPs/Hcr's (explained in figure 5.10) mined from one genome per species show **(a)** number of RLPs retrieved from each species genome analysed, where *S. tuberosum* was found to have the most Hcr's. **(b)** Genus-wise distribution of species-specific RLPs indicate *Solanum* has the highest proportion. **(c)** Hcr's were classified into six categories based on predicted protein architecture; fractions of each type are detailed.

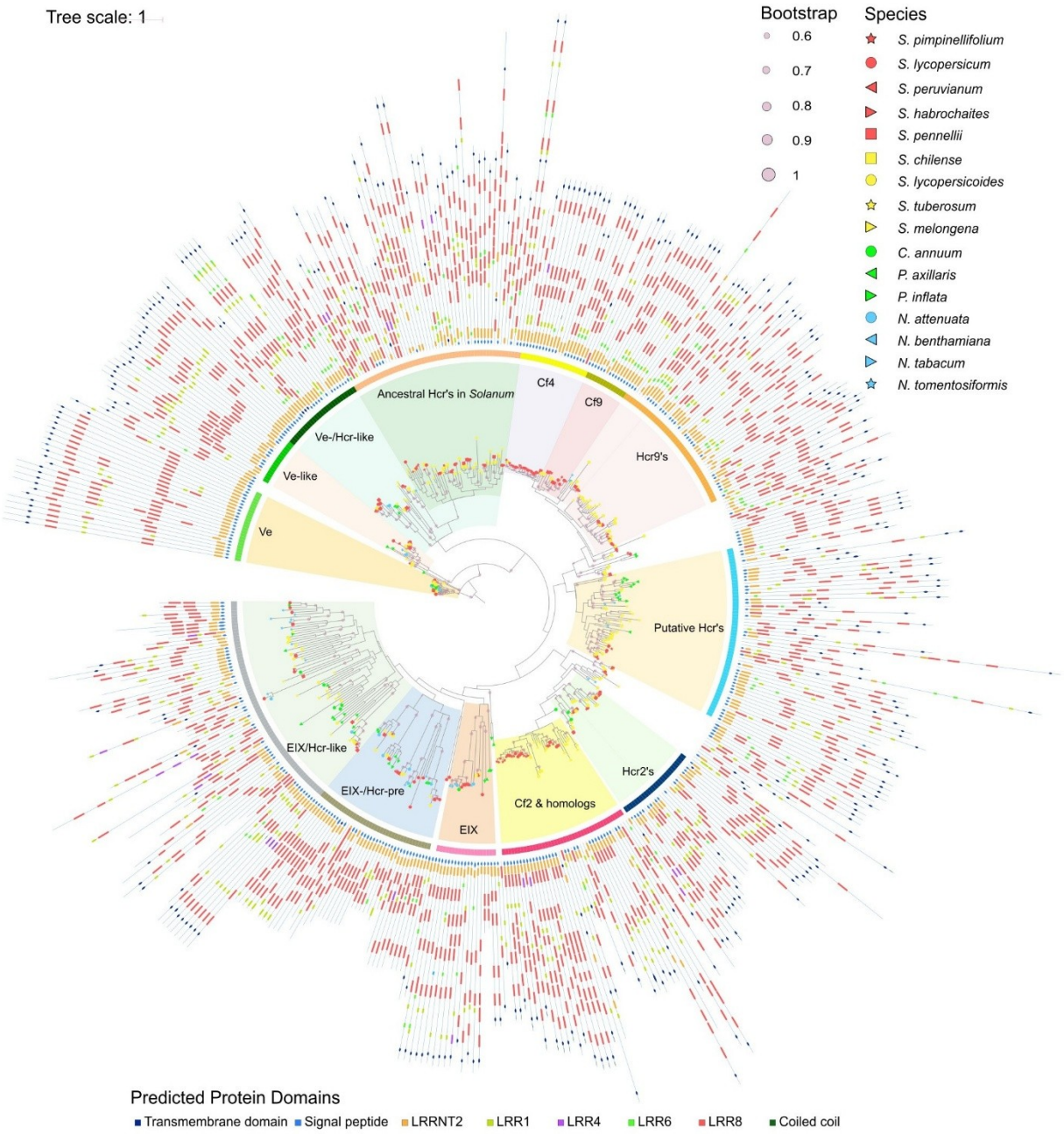


Figure 5.12 Hcr2s are most recently evolved Cf-like proteins.

491 Cf-like/Hcr RLPs having ≥ 90% similarity/query coverage ≥ 80% to Cf-2.2-RLP and lacking kinase/unusual domains were aligned using MUSCLE (extraction scheme shown in figure 5.10). Phylogenetic tree was constructed using a maximum-likelihood 500 bootstrap replication method in MEGA12. Cf-9, Ve and EIX were used as closely and distantly related outgroup proteins to Hcr2s. The tree is rooted at Ve clade. Source reference species for each protein is indicated at branch tip and bootstrap values over 50% are internally marked on each branch as grey circles. RLPs were distinguished into 13 clades based on sequence similarity and phylogenetic distance matrix. Each protein in the tree was further scanned using Pfam and Phobius for predicting protein domain architectures. Proteins are represented as grey bars indicating protein length with different domains. The tree was annotated using iTOL v6 and all raw files and annotation inputs are attached as supplementary file 5.12.

5.2.6 Phylogenetic analysis indicate that Cf-2/Hcr2s have recently evolved in Solanaceae

To understand and investigate the evolution of Cf-2/Hcr2-like RLPs across a lineage of closely related Cf-9/Hcr9 family in Solanaceae and distant outgroup receptors, Ve and Eix, we used our manually curated 491 Cf-like RLPs to build a MUSCLE protein alignment. We constructed a phylogenetic tree using a Maximum-likelihood method with 500 bootstrap replications using MEGA12 (Kumar et al., 2024). Although unrooted trees are often used to depict closely related gene/protein clusters (Kinene et al., 2016), we preferred to root our tree (**Figure 5.12**). Considering that Ve is an anciently evolved RLP in tomato (Fradin et al., 2011) and is a distant relative of Cf-2-RLP, we could use the outgroup method (Boykin et al., 2010) to root the tree (Williams, 2014) at Ve to derive relationships among RLPs and predict the direction of evolution of Cf-like RLPs. 451 of 491 RLPs were classified into 13 clades in the phylogenetic tree based on sequence similarity and distance matrix. We further used iTOL v6 to annotate the tree, including domain architectures/nomenclature of each protein in a cluster. LRR types were annotated as: LRR-N terminal plant-type-EEATALLKWKATFKNQNNSFLASWIPSSNACKDWYGVVC; LRR1 (degenerate)-VIALDLRCSQLQGKFHSNSSLFQL; LRR4 (degenerate)-SKLHVLRICDQYGLSLVPYNFELLLKN; LRR6-SHLTTLQLSGTELHGILPERVFHL and LRR8- ASLMTLYVDSVNIADRIPKSFSH.

Interestingly, when we rooted tree at tomato Ve, we found that the entire Ve clade clustered together, indicating ancient origin to all other clades of Cf-like RLPs (**Figure 5.12**). Further, Eix receptors are presumably younger relatives of Cf-RLPs with Eix-clade, Eix/Hcr-precursor clade and Eix/Hcr-like clades diverging after Cf-2/homolog clade in Solanaceae. However, Eix-RLPs are indeed present in anciently evolved species like *N. tomentosiformis* and *P. integrifolia* (**supplementary 5.12**). Among 13 clades, Eix/Hcr-like clade (70) has the

maximum number of RLPs while Cf-9-specific clade has the least members (14). We further conclude that Hcr2's clustered within and an adjacent clade (67, including Cf-2 and Cf5) are comparatively less abundant than Hcr9's (81, including Cf-9 and Cf-4) that are also consistently clustered in the tree. It is thus possible that intragenic recombination events in clades may have generated RLPs with novel specificities against e.g. EpiCs and Cip1 in tomato and potato that may cluster separately in evolutionary timescales in between. Our finding that Cf-like RLPs are unevenly dispersed in species and particular clades containing RLPs differing in length and structure is not unusual as this has previously been demonstrated for NB-LRR proteins in tomato (Meyers et al., 2003, Jupe et al., 2012). Cf-2 was previously predicted to be tomato specific, having evolved <6 mya (Kourelis et al., 2020). In this study, we discovered that Cf-2-speicific RLPs are only present in *S. pimpinellifolium*, *S. lycopersicum* and *S. pennellii,* which diverged ~2.1 mya (estimates based on **Figure 3.1**, chapter 3), confirming the recent evolution of Cf-2's function in the perception of *C. fulvum* producing Avr2. This further strengthens our proposition that a distinct ancient Hcr might mediate recognition of EpiCs and Cip1.

5.3 Discussion

Cell surface localised RLPs recognise small secreted proteins from distant microbial kingdoms to modulate an effective resistance response. Cf-2-RLP regulate perception by interaction with a co-receptor cysteine protease, Rcr3 associated with Avr2 of *C. fulvum*. The precise role of Hcr2s in mediating resistance against multiple yet specific inhibitors remains to be deciphered. Using the *TRV*-based VIGS approach, we show that *S. pimpinellifolium* is an efficient wild tomato species to study the involvement of various immunity components that may be involved in inhibitor recognition, particularly cysteine proteases, (*Rcr3*, *Pip1* and *C14*) and *SOBIR1*. We also silenced four different clans of the

Hcr2 family; *Cf-2* (clan 1), *Cf5* (clan 2), full-length *Hcr2s* (clan 3) and truncated *Hcr2s* (clan 4).

Many Solanaceae species have previously been shown to be amenable to TRV2-VIGS (Brigneti et al., 2004, Senthil-Kumar et al., 2007, Velásquez et al., 2011) and the use of a gene sequence from one species to silence orthologs in different species in Solanaceae is highly feasible. Rather than overall nucleotide homology, 100% similarity in stretches of 21 to 23 nucleotides between target gene and trigger VIGS sequence are more important (Thomas et al., 2001). In this study, 300 bp long specific *Hcr2* silencing sequence share over 90% nucleotide identity among members of the same clan within *S. pimpinellifolium* (with exception of one member of clan 3) (all nucleotide alignments are shown in **supplementary 5.7**). Further, there is extensive homology between members across *Hcr2* family, therefore, each clan-specific trigger sequence expectedly had a heightened potential of cross-silencing members of other clans.

S. pimpinellifolium LA0753 probably carries *Cf-2* and several *Hcr2*s (**Figure 4.4**-LA0753(P3), chapter 4) and shows HR upon Avr2, EpiCs and Cip1 infiltration (**Figure 3.4**, chapter 3). Silencing different clans of *Hcr2s* in LA0753 clearly reduced recognition of Avr2 but HR phenotypes towards EpiCs and Cip1 remained largely unaffected. *Cf-2*-silencing reduces Avr2 recognition in *S. pimpinellifolium* LA0369. However, the relative transcript abundance levels indicate that *Cf-2* and transcript levels of most *Hcr2*s were significantly reduced in LA0753 as compared to *Cf-2/Hcr2* carrying LA0369 (Plant 3, **Figure 4.4**, chapter 4). This indicates the presence of other more closely related *Hcr2*'s that were not separated on agarose gel (**Figure 4.4**, chapter 4) but were silenced due to their high homology to VIGS fragment and this may have impacted the HR severity towards different inhibitors in LA0753. Interestingly, we detected minor variation among variably responsive individuals of LA0753, but did not find any significant amino acid variation in sequenced *Rcr3* mature protease domain among LA0753(P3) and *S. pimpinellifolium* populations that responded

either to one or more inhibitors (**Figure 4.10**, chapter 4). Next, when *Rcr3*, *Pip1* and *C14* were individually silenced in *S. pimpinellifolium* LA0369 and LA0753, we noted reduced Avr2/Cip1-induced HR in *Rcr3*- and *Pip1*-silenced plants, whereas *C14*-silenced plants had reduced ability of recognising EpiCs.

When *Hcr2*s were silenced in wild potato, *S. infundibuliforme* CGN17720, which was shown to respond to Avr2, EpiCs and Cip1 (CGN17720(P3), **Figure 3.6**, chapter 3), no difference in response to EpiCs were noted. Moreover, in the *TRV::GFP* control plant of CGN17720, we did not detect HR against any other inhibitor except EpiCs, despite that this clonal lineage initially responded to Avr2. Similarly, when *Hcr2*s were silenced in another wild potato, *S. bulbocastanum* CGN22732 recognising EpiC2B (CGN22732(P3), **Figure 3.6**), no reduction in HR was found. The endogenous target *Hcr2s* however, were effectively silenced in *S. bulbocastanum* and *S. infundibuliforme*, as demonstrated by qRT-PCR. Interestingly, only one different *Hcr2* was detected in CGN17720(P3) and CGN22732(P3) (based on PCR produce lengths obtained in **Figure 4.8**, chapter 4).

C14 silencing reduced EpiC2B recognition in CGN17720 and CGN22732. *Pip1* silencing also affected EpiC2B recognition in wild potato while *Rcr3* silencing reduced Avr2 recognition which is already weak in wild potato. While protein sequences of Rcr3 from CGN17720(P3) and CGN22732(P3) are slightly different, which may explain a weak Avr2 recognition in CGN17720(P3) mediated by a *Cf-2*-like gene variant, existing variations in Pip1 and C14 may influence detection of EpiCs and Cip1 instead of Rcr3 in wild potato. SOBIR1 and BAK1 interact with multiple LRR-RLPs, including Cf-4 (Liebrand et al., 2013, Postma et al., 2016). Similar to several RLPs, *SOBIR1* silencing in LA0753 and heterologously in CGN22732, reduced HR towards all four inhibitors. This study provides the first initial evidence that recognition of EpiC1, EpiC2B and Cip1 in wild tomato and potato is mediated via a SOBIR1-dependent RLP.

The percentage identity between tomato and potato *Hcr2* nucleotides fluctuates between 60 to over 90% while among *Rcr3*, *Pip1*, *C14* and *SOBIR1* is over 90% (**supplementary 5.7 to 5.11**). Moreover, *S. bulbocastanum* reportedly consist several *R* genes against *P. infestans*, including *Rpi-blb2* on chromosome 6 (van der Vossen et al., 2005) and *Rpi-blb4* on chromosome 5 (Li et al., 2023). Given the LRR-RLP diversity in *S. bulbocastanum*, the presence of a distantly related *Hcr-like* gene conferring specific recognition of EpiC2B is very likely. Therefore, our study corroborates and adds to a growing list of the use of *TRV*-based heterologous gene silencing in a broad range of crop relatives for rapid and robust evaluation of resistance gene function. Considering that VIGS fragments despite specificities are capable of silencing partially complementary off-targets genes in wild species, the next steps in identifying the underpinning receptor gene could be use of revolutionary technologies like Oxford Nanopore for long-read sequencing (Jain et al., 2018, Wang et al., 2021) and modified dRenSeq (Armstrong and Hein, 2021) to identify *Hcr's* in *S. piminellifolium*, *S. bulbocastanum* and *S. infundibuliforme* that are different in comparison to a pool of non-responsive corresponding population of each species. Identifying candidate Cf-RLPs underlying recognition of EpiCs/Cip1 by generating de-novo assembly of populations of interest or by resistance gene enrichment sequencing (RENSeq) would reveal to us the structural differences in RLP-encoding genes between responsive populations.

Targeting highly conserved and short sequence variations among allelic *Hcr2*s with minimal off-targets can also be effective in achieving specific gene silencing and assessing impact on recognition of each inhibitor. Using CRISPR/Cas9 gene editing to knock-out highly homologous clades in *Hcr2* gene family also has challenges due to potential off-targets and multiplexing edits, because the high similarity may lead to targeting of the wrong *Hcr2* genes. The currently unknown redundant functionality of *Hcr2s* can make it even more difficult to observe HR phenotype variations upon inhibitor infiltrations even with multiple knock-out genes. Since studies in wild *Solanum* species are time consuming and

challenging, an alternative possible approach is to overexpress RLP candidates in *N. benthamiana* by agroinfiltration and testing them in combination with *Rcr3*, *Pip1* and *C14* variants identified in chapter 4.

The widespread analysis of *NB-LRR* genes in solanaceaous species have been well characterised in many studies (Xu et al, 2011, Jupe et al, 2012, Seo et al 2016). However, such studies to identify diversification and expansion of extracellular LRR-RLP gene families that are known to confer resistance to *C. fulvum*, *P. infestans* and *P. syringae* are limited. Here, we report a detailed analysis on the evolution of Cf-2-like RLPs in Solanaceae. To infer Cf-2 ancestry profile consistently with related RLPs Cf-9, Ve and EIX, we curated an HMMER-based approach and performed an *in-silico* phylogenetic analysis to search for diversity of Cf-like RLPs. We obtained 491 RLPs, including Hcr2s, Hcr9s and distant outgroup RLPs Eix and Ve and found that all these RLPs were limited to Solanaceae, with 389 RLPs within the genus *Solanum*. The differences in number and types of LRRs in each of thirteen clades despite shared homology, possibly confer divergence in function in different species. Moreover, we observed that Hcr9s are older than Hcr2s in Solanaceae, based on divergence of clades in RLP-tree rooted at tomato Ve-RLP (**Figure 5.12**). By contrast, Eix receptors diverged most recently evolved Cf-like RLPs in Solanaceae as seen in phylogenetic tree. Interestingly, only twenty-seven RLPs were found to be of Cf-2-type architecture, explaining the exclusivity of Cf-2 to tomato.

Based on divergence of *Rcr3* and *Pip1* homologs in Solanaceae, it was suggested that both evolved >50 mya. In contrast to *Rcr3* and *Pip1* evolution, *Cf-2/Hcr2s* were reported to be restricted only to *Solanum* species that evolved <6 mya (Ilyas et al., 2015, Kourelis et al., 2020). Our results indicate Hcr2s or broadly Cf-2-like receptors evolved ~33 mya (based on species evolutionary timescales, **Figure 3.1**, Chapter 3) as *in-silico* approach found Hcr-RLPs in the genomes of species that evolved anciently to lately in Solanaceae (**Figure 5.19**). It is possible that Hcr-RLPs consisting of only LRR motifs while lacking a

transmembrane domain may still play a role as PRR and confer recognition of inhibitor by associating with a membrane bound Hcr2-RLP and eventually interaction of this complex with an RLK to initiate a downstream signalling against EpiCs and Cip1. Truncated genes may lack a function of their own, but may serve as reservoirs for diversity in RLPs.

Although phylogeny derived from amino acid sequences has been a robust method to understand the evolution of a gene family, *in-silico* approach in this study underscores the importance of tracing proximal or tandem gene duplication, recombination events and selection pressures at the genetic levels underlying the diversity and evolution of these RLPs. Analysis of chromosomal locations of gene sequences and synteny may reveal a distinct yet relatively similar pattern of clades. Studies have shown that resistance genes in tomato are found in clusters (Andolfo et al., 2013) and such clusters are hypothesized to be driving rapid evolution and novel specificities of resistance genes (Hulbert et al., 2001, Friedman and Baker 2007). Therefore, further analysis of Cf-clades may hold crucial information to decipher the recognition of unrelated proteins.

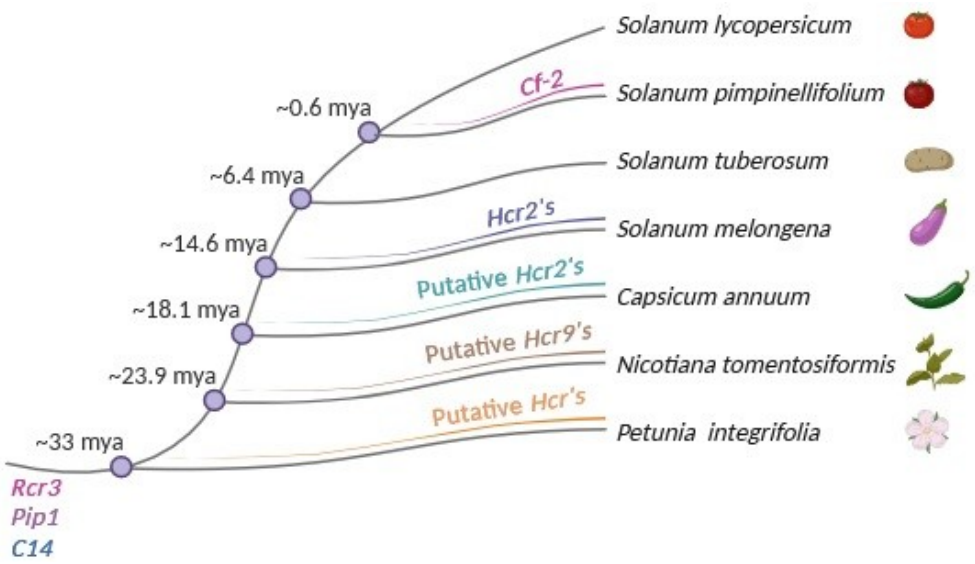


Figure 5.13 Summary of Cf-2/Hcr2 RLP evolution in Solanaceae.
Based on bioinformatics pipeline in this study, we found that Cf-2 evolved in *S. pimpinellifolium*, whereas, putative Hcr's are also present in species that are distant to cultivated tomato.

Extensive variations in homologs have recently been shown to confer a conserved detection of *Phytophthora* effectors in wild potato species (Witek et al, 2021). Elucidation of function of significantly closer homologs of *Cf* genes in this study, may thus provide further insights into the plant immunity networks that confer recognition of EpiCs and Cip1. SMRT-AgRenSeq-d, which was recently used to identify nine *NLR* candidates in *S. tuberosum* for cyst nematode *Globodera pallida* resistance (Wang et al., 2023) offer a method for rapid characterisation of a functional receptor for EpiCs and Cip1 recognition. In chapter 4, we discovered variations in *Rcr3*, *Pip1* and *C14* that exists in the limited pool of wild populations we screened. In this chapter, we identified the diversity of Cf-like RLPs that exist across Solanaceae. Therefore, as an obvious next step, it would be interesting to analyse the different species or clade-specific RLPs in combination with native variants of Rcr3, Pip1 and C14, in the presence of SERK3/BAK1, SOBIR1 or NRC3 and assess their impact on HR-triggered by Avr2, Cip1, EpiC1 or EpiC2B.

In conclusion, we present *TRV*-VIGS based molecular characterisation of Avr2 recognition requiring Cf-2 and Rcr3 in wild tomato and SOBIR1-dependent recognition of Avr2, EpiCs and Cip1 in wild tomato and potato. We further deduce silencing *C14* particularly affect recognitions of EpiCs in wild tomato and potato plants carrying or lacking *Cf-2*. Collectively, our results suggest that *Cf-2/Hcr2s* may not contribute to Epic1 and Epic2B recognition, but to Avr2 and Cip1. Our results further provide new insights into the evolution of Cf-2 in kingdom Viridae and more specifically into the phylogeny of Cf-like RLPs being limited to Solanaceae family. Our efforts of identification of Cf-like RLPs involved in the molecular perception of EpiCs and Cip1 have laid an early foundation for further research directions.

We propose the presence of different primary Hcr-RLPs that can detect distinct interactions among host cysteine proteases and pathogen-derived inhibitors. Hcr-RLPs are present that confer perception via similar downstream pathway when the interactions between Rcr3-EpiCs/Rcr3-Cip1, Pip1-EpiCs/Pip1-Cip1 and C14-EpiCs/C14-Cip1 are not sufficient to

trigger Cf-2-dependent recognition signalling. It is also likely that LRR domains of variants in Cf-2/Hcr2 are involved in differentially recognizing inhibitors from different pathogens. Bioengineering Hcr2's and associated co-receptor cysteine proteases and RLKs to widen perception of pathogen-derived inhibitors of convergent targets in host holds a sustainable potential of achieving crop resistance against multiple pathogens.

Supplementary 5.1(a) VIGS fragments to silence *Cf-2* and *Hcr2s* in wild tomato/potato

VIGS construct	**Fragment Sequence (300 bp)**
Cf-2 (clan 1) silencing	CAGATTTCAGGAACAATACCACCACAAATCGGTTTACTAGCCAAGCTTCA GATCATCCGCATATTTCACAATCAATTAAATGGATTTATTCCTAAAGAAATA GGTTACCTAAGGTCTCTTACTAAGCTATCTTTGGGTATCAACTTTCTTAGT GGTTCCATTCCTGCTTCAGTGGGGAATCTGAACAACTTGTCTTTTTTGTAT CTTTACAATAATCAGCTTTCTGGCTCTATTCCTGAAGAAATAAGTTACCTAA GATCTCTTACTGAGCTAGATTTGAGTGATAATGCTCTTAATGGC
Cf5 (clan 2) silencing	GGATATCCAGTTTCAAAAGGTTGTGGCAAAGATCCTGTGTCAGAGACAAA CTATACAGTGTCTGCGCTAGAAGATCAAGAAAGCAATTCTAAATTTTTCAA TGATTTTTGGAAAGCAGCTCTGATGGGCTATGGAAGTGGACTGTGTATTG GCATATCCATAATATATTTCTTGATCTCGACTGGAAATCTAAGATGGCTTG CAAGAATCATTGAAGAACTGGAACACAAAATTATTATGCAAAGGAGGAAG AAGCAGCGAGGTCAAAGAAATTACAGAAGAAGAAATAATCGCTTCTAG
Full-length Hcr2s (clan 3) silencing	CAACTCAACGACACATTTCCCATGTGGTTGGGAACTTTGCCAGAGCTGAG AGTTTTAAGGTTGACATCGAATAAATTGCATGGACCTATAAGATTATCAGG GGCTGAAATCATGTTTCCTGATCTTCGAATCATAGATCTCTCTCGCAATGC ATTCTTGCAAGACTTACCAACGAGTCTATTTGAACATTTGAAAGGGATGAG GACAGTTGATAAAACAATGGAGGAACCAAGTTATCATAGATATTACGATGA CTCGGTGGTAGTTGTGACAAAGGGATTGGAGCTTGAAATTGTGAGA
Truncated Hcr2s (clan 4) silencing	CTTTTCTCGAGAATCTTAATCTTAGCAACAACAATATCTCTGGCACCATTC CACCTGAGATTGGTAATCTCACAAATCTTGTCTATCTTGACTTGAACACCA ATCAGATTTCAGGAACAATTCCACCACAAATTGGTTCACTAGCCAAGCTTC AGATCATCTGCATATTTAACAATCATTTAAATGGCTTTATTCCTGAAGAAAT AGGTTACCTAAGGTCTCTTACTAAGCTATCTTTGAGTATCAACTTTCTTAGT GGTTCCATTCCTGCTTCATTGGGGAATCTGAACAACTTGTCTA

Nucleotide fragment sequences designed for assembly into pTRV2 vectors for virus-induced gene silencing of different clan-specific *Cf-2/Hcr2* genes in figure 5.1 are shown.

Supplementary 5.1(b) Target efficiency of four different VIGS fragments designed in this study to member genes of *Cf-2* clan.

Clan 1: *Cf-2* clan silencing		**Target efficiency based on % identity with four silencing fragments**			
S. No.	**Members**	**clan 1 fragment**	**clan 2 fragment**	**clan 3 fragment**	**clan 4 fragment**
1.	*SpCf-2.1*	100	97.3	98	93.7
2.	*SpCf-2.2*	100	98.3	98	93.7
3.	*SpCf-2.3*	100	97.7	98	93.7
4.	*SpHcr2p7.1*	98.7	75.3	65	93.7
5.	*SpHcr2p7.2*	98.7	75.3	65	93.7
6.	*SpHcr2p7.3*	98.7	76	65	93.7
7.	*SpHcr2p7.4*	98.7	75.3	65	93.7
8.	*SpHcr2p7.5*	98.7	75.3	65	93.7
9.	*SpHcr2p7.6*	98.7	75.3	65	93.7
10.	*SpHcr2p7.7*	98.3	75.3	65	93.7
11.	*SpHcr2p7.8*	98.7	75.3	65	93.7
12.	*SpHcr2p7.9*	98.7	75.3	65	93.7

Each VIGS fragment (300 bp) was aligned to *Cf-2*-clan member genes listed in this table (raw alignments are attached as supplementary 5.7). Pair-wise DNA sequence alignment was performed using EMBOSS Needle tool.

Supplementary 5.1(c) Target efficiency of four different VIGS fragments designed in this study to member genes of *Cf5* clan.

Clan 2: *Cf5* clan silencing		**Target efficiency based on % identity with four silencing fragments**			
S. No.	**Members**	**clan 1 fragment**	**clan 2 fragment**	**clan 3 fragment**	**clan 4 fragment**
1.	*SlCf5*	93.3	98	98	96.7
2.	*SlHcr2-5D*	90	98	98	96.7
3.	*SlHcr2-0B*	95.7	100	98.3	96.7
4.	*SlHcr2-5B*	95.3	99.3	96.3	96.7
5.	*SpHcr2p3*	91	100	98	95.3
6.	*SpHcr2p1.2*	92	98	96	96.7
7.	*SpHcr2p1.1*	92	98	96.3	96.7
8.	*SpHcr2-2A*	83.3	90	86.7	90.3

**Sp: Solanum pimpinellifolium; *Sl: Solanum lycopersicum*

Each VIGS fragment (300 bp) was aligned to *Cf5*-clan member genes listed in this table (raw alignments are attached as supplementary 5.7). Pair-wise DNA sequence alignment was performed using EMBOSS Needle tool.

Supplementary 5.1(d) Target efficiency of four different VIGS fragments designed in this study to member genes of *Full-length Hcr2s* clan.

Clan 3: *Full-length(Fl) Hcr2s* clan silencing		**Target efficiency based on % identity with four silencing fragments**			
S. No.	**Members**	**clan 1 fragment**	**clan 2 fragment**	**clan 3 fragment**	**clan 4 fragment**
1.	*SpHcr2p6*	91	68.3	66.3	95.7

2.	*SlHcr2p2*	93	65.7	100	95.3
3.	*SlHcr2p4.2*	91	100	100	96.3
4.	*SlHcr2p4.1*	91	100	100	96.3
5.	*SpHcr2p5*	90.7	100	99.7	96.3

**Sp: Solanum pimpinellifolium; *Sl: Solanum lycopersicum*

Each VIGS fragment (300 bp) was aligned to *Full-length(Fl) Hcr2s*-clan member genes listed in this table (raw alignments are attached as supplementary 5.7). Pair-wise DNA sequence alignment was performed using EMBOSS Needle tool.

Supplementary 5.1(e) Target efficiency of four different VIGS fragments designed in this study to member genes of *Truncated(t) Hcr2s* clan.

Clan 4: *Truncated (t) Hcr2s* clan silencing		**Target efficiency based on % identity with four silencing fragments**			
S. No.	**Members**	**clan 1 fragment**	**clan 2 fragment**	**clan 3 fragment**	**clan 4 fragment**
1.	*SpHcr2p8.1*	91.3	66.7	67.7	100
2.	*SpHcr2p8.2*	91.7	66.7	67.7	99.7
3.	*SpHcr2p8.3*	91.3	66.7	67.7	99.3
4.	*SpHcr2p8.4*	91.7	66.7	67.7	99.7
5.	*SpHcr2p8.5*	91.3	66.7	67.7	100
6.	*SpHcr2p8.6*	91.3	66.7	67.7	100

**Sp: Solanum pimpinellifolium*

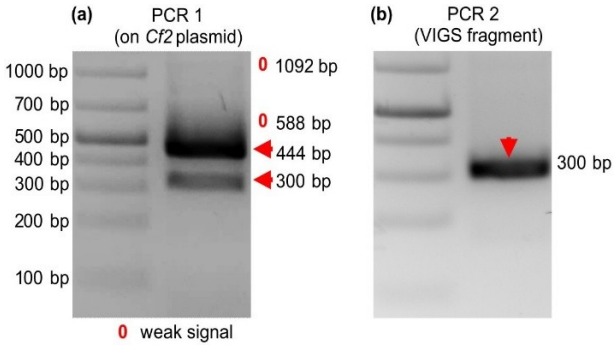
Each VIGS fragment (300 bp) was aligned to *Truncated(t) Hcr2s*-clan member genes listed in this table (raw alignments are attached as supplementary 5.7). Pair-wise DNA sequence alignment was performed using EMBOSS Needle tool.

Supplementary 5.1(f) Target efficiency of four different VIGS fragments designed in this study to cross-target *Hcr2s* in tomato and potato.

Cross-targets silencing		**Target efficiency based on % identity with four silencing fragments**			
S. No.	**Members**	**clan 1 fragment**	**clan 2 fragment**	**clan 3 fragment**	**clan 4 fragment**
1.	*StHcr2-2A*	87.7	90	89	89.7
2.	*StCf-2.1*	87.3	72.3	69.3	82
3.	*StCf-2.2*	72.7	93	88.3	75
4.	*StHcr2-5D*	49.7	87.3	88	57.3
5.	*StHcr2p5*	83	74.3	66	59.7
6.	*StHcr2p4.1*	79	82.3	77.7	84.7
7.	*StHcr2-0B*	78	77.7	79.3	84
8.	*StHcr2p3*	87.7	69.7	66.7	88.3
9.	*StHcr2p8.4*	62.7	69.3	70.7	90.3
10.	*StHcr2-0A*	83.7	78.7	86.7	87.7
11.	*SlHcr2-0A*	85.3	89	86.3	90.7

**St: Solanum tuberosum; Sl: Solanum lycopersicum*

Each VIGS fragment (300 bp) was aligned to cross-target *Hcr2* genes listed in this table (raw alignments are attached as supplementary 5.7). Pair-wise DNA sequence alignment was performed using EMBOSS Needle tool.



Supplementary 5.2 Agarose gel showing PCR of Cf-2 (clan 1) VIGS nucleotide fragment. **(a)** PCR1 was performed on *Cf-2::eGfp* plasmid (Table 2.8) using primer set SM_VIGS_Cf-2_Forward/Reverse (Table 2.6). Expected PCR products from PCR 1 are shown. **(b)** 300-bp product from PCR1 was used as template for PCR 2 to generate specific VIGS fragment for further assembly into pTRV2.

Supplementary 5.3 VIGS fragments used to silence cysteine proteases and *Receptor-like Kinase-SOBIR1* in wild tomato and potato.

VIGS construct	**Fragment Sequence (300 bp)**
Rcr3 silencing	ATGGCTATGAAAGTTGATTTGATGAATATTTTAATTACACTATTCTTTGTAA TTAGCATGTTCAACACTCAAACAAGAGGTCGCAGCCAGCCAAAACTGTCC GTGTCTGAGAGACACGAGCTGTGGATGTCACGTCATGGACGCGTTTACAA GGACGAAGTAGAAAAAGGAGAACGATTCATGATTTTCAAAGAAAACATGA AATTCATTGAGTCGGTCAATAAGGCAGGGAATCTGTCTTACAAGTTAGGG ATGAATGAATTTGCAGATATTACTTCACAAGAGTTTTTGGCTAAATTT
Pip1 silencing	ATGGCTTCCAATTTTTTCCTCAAGAATATTACTGTTGTTCTTCTTCTTTTTTC CATTCTTAGCCTATATCCCTTTATAGTAACTTCCCGCAACTTAAAAGAATTA TCCATGCTTGAAAGGCATGAAAATTGGATGGTTCATCATGGACGTGTATA CAAAGATGATATAGAAAAAGAACACCGCTTCAAAACATTCAAGGAAAACGT TGAGTTCATCGAATCTTTCAACAAGAACGGAACTCAACGTTATAAGCTAGC CATCAATAAATATGCTGATCTGACCACTGAGGAATTCACAACA
C14 silencing	ATGGCAGCTCACAGCTCAACTCTCACCATATCCATACTTCTCATGCTCATC TTCTCCACCTTATCCTCTGCTTCCGATATGTCAATTATTAGCTACGACGAG ACACATATTCACCGTCGTACCGACGATGAAGTCTCGGCGTTGTACGAGTC CTGGCTAATCGAGCACGGAAAATCGTACAACGCCTTAGGAGAAAAGGATA AGAGATTTCAGATCTTCAAGGATAACTTGAGATACATAGACGAACAGAACT CTGTTCCGAATCAGAGTTATAAGCTCGGATTGACGAAATTCGCCGAT
SOBIR1 silencing	ATGACTTCGAATATCCACTTTTTTCTTTTATACGTTGTGAGCCTTTTCCTTT TTGTTCAAGCAAGATTGAATCTTTATCCACCAGATCATGCTGCACTCTTGC TTGTACAAAAGGACTTAGGCATCATTTCTGTTAACAACCCGTGTACGCTCG CAGGAATATCGTGCGAGCGTAGACCGGGTAACACAACACAAGTTGTGAG AGTTACCCGTATTGTATTCAGATCCAACGGATTAAAGGGAACTTTGTCTTC TGCTATTGGCAAACTCACTGAGCTCAAAGAGCTTTCTCTTTCCGAC

Nucleotide fragment sequences used for pTRV2 virus-induced gene silencing of specific cysteine protease *Rcr3*, *Pip1* and *C14* (figures 5.7 and 5.8) are shown. VIGS fragment for silencing Receptor-like kinase *SOBIR1* (figure 5.9) is also shown.

Chapter 6

Thesis conclusion and future perspectives

Cladosporium fulvum-tomato, *Pseudomonas syringae*-tomato, *Phytophthora infestans*-tomato and *P. infestans*-potato are well-studied models for plant-pathogen interactions in Solanaceae family. However, pathogen pressures shaping the evolution of native host components consistently with proteins secreted by these unrelated pathogens are still relatively unexplored in genus/species-wide studies. In this work, we aimed to investigate natural variation in recognition frequency of purified inhibitors, Avr2 of *C. fulvum*, Cip1 of *P. syringae* and EpiC1 and EpiC2B of *P. infestans* across Solanaceae family. The *Cf-2* resistance gene was introgressed into *S. lycoperiscum* (Money Maker-*Cf-2*/*Rcr3*^{pim}) from the wild tomato relative *S. pimpinellifolium* and was shown to mediate indirect Avr2 recognition (Dixon et al., 2000, Kruger et al., 2002). Cf-2 reportedly has a dual function as an immune receptor as it was claimed to additionally confer recognition of venom allergen-like protein (Vap1), a protein secreted by the nematode pathogen, *Globodera rostochiensis* (Lozano-Torres et al., 2012). These data could, however, not be reproduced by our laboratory (Kourelis et al., 2020). Cf-2 specific inhibitor recognition is dependent on secreted tomato immune protease, Rcr3 (Rooney et al., 2005).

C14 and *Pip1* are two other immune protease genes that increase immunity against *C. fulvum*, *P. syringae* and *P. infestans* (Kaschani et al., 2010, Hoerger, 2011, Ilyas et al., 2015). *Pip1* is a paralog of *Rcr3*, but *C14* is unrelated. *Rcr3* and *Pip1* act contrastingly: whereas *Rcr3* does not contribute to *C. fulvum* resistance in the absence of *Cf-2*, *Pip1* acts in immunity against *C. fulvum*, so Rcr3 is a decoy of Pip1 (Ilyas et al., 2015). Rcr3 is weakly inhibited by EpiC1, EpiC2B and negligibly by Cip1 as compared to Avr2, however their infiltrations do not trigger HR in MM-*Cf-2*/*Rcr3*^{pim}. Interestingly, EpiCs and Cip1 have strong affinity towards C14 and also inhibit Pip1 effectively (Kaschani et al., 2010, Shindo et al.,

2016), implying the effective escape of Cf-2-mediated recognition by these stealthy inhibitors.

6.1 Recognition of unrelated inhibitors shows natural variation and is conserved in tomato and potato

In Chapter 3, our survey of 112 *S. pimpinellifolium* native populations revealed that Avr2, EpiC1, EpiC2B and Cip1 recognitions are heterogeneously distributed with variations in HR severity observed within same and different populations across geographical origin range. Collectively, we estimated Avr2 has the highest recognition frequency in *S. pimpinellifolium*. This is expected as tomato is a natural host of Avr2-producing *C. fulvum*. While EpiC2B is the second most recognised inhibitor in *S. pimpinellifolium*, EpiC1 is the least recognised of all four inhibitors and the difference in EpiC1 and EpiC2B recognitions could be due to the six amino acid variation that may affect PLCP inhibition strength. Our subsequent exploration of inhibitor recognition frequencies in wild relatives, distantly related to cultivated tomato *S. lycopersicum*, uncovered intra-specific and inter-specific differences in recognition of distinct inhibitors.

We found that infiltrated purified Avr2, EpiC1, EpiC2B or Cip1 proteins induced variable HR phenotypes in distantly related wild tomato species, but not in the outgroup wild tomato species, *S. ochranthum*, *S. sitiens* and *S. juglandifolium*. *S. lycopersicoides* LA2730 in Chile is the only outgroup tomato population that recognised Avr2. When we extended our survey of estimating inhibitor recognition pattern to wild potato species, a natural host of *P. infestans*, we observed that in a pool of 50 populations, EpiC2B frequently triggered a robust HR, whereas recognition of EpiC1, Avr2 and Cip1 appeared to be irregularly distributed. We further conclude that in the Centre origin region of *S. pimpinellifolium*, recognition frequency of all inhibitors is the highest and recognition of unrelated inhibitors is

independently distributed in wild tomato and wild potato. Collectively in *S. pimpinellifolium*, other wild tomato and potato, we noted that Avr2 recognition commonly occurs at lower altitudes. Contrastingly, the response frequencies of Cip1 and EpiCs are higher at increasing altitudes.

Surprisingly, we failed to observe any HR phenotype with infiltrations of any of the four tested inhibitors or their mutants in our screening of native populations representing different species of eggplant, pepper, tobacco and petunia. Therefore, our results suggest that recognition of Avr2, EpiC1, EpiC2B and Cip1 is conserved in *Solanum* species tomato and potato but does not occur in other species in Solanaceae. Absence of Avr2 recognition in eggplant, pepper, tobacco and petunia could be because they are not host of *C. fulvum*. However, *P. infestans* and *P. syringae* have a broader host range as compared to *C. fulvum*, yet EpiCs and Cip1 are not recognised broadly in our HR screening. Given this versatility in recognition of the same inhibitors among different populations and species, we next speculated the existence of underlying polymorphism in *Cf-2/Hcr2s* and *Rcr3*, *Pip1* and *C14*. Our PCR results from chapter 4 showed that *Cf-2* does not occur in all individuals of same population or in different species, whereas *Rcr3*, *Pip1* and *C14* are always present and have allelic intra-/inter-population variations. In nature, unrelated pathogens commonly infect the same or different host plants, therefore, selected genotypic variants may be available to promote polymorphism and eventually recognition specificities against same inhibitor in different host as well as against different inhibitors within same host.

6.2 *Cf-2* is present in wild relatives beyond *S. pimpinellifolium* and *Hcr2* number/type variations exist

A previous survey of *Cf-2/Hcr2* evolution in *S. pimpinellifolium* (Caicedo and Schaal, 2004) revealed that heterogeneous evolutionary processes are acting on the *Cf-2* gene family.

Nine categories, consisting of 26 *Hcr2s*, were identified in this survey. *C. fulvum* was suggested to have exerted pressure for maintenance and selection on functional *Cf* gene variants in wild tomato, allowing significant diversification of *Cf* genes and their expansion and conservation in wild tomato species (Krujit et al., 2005). In Chapter 4, our species- and genus-wide DNA PCR-based screen for presence of *Cf-2* and *Hcr2s*, our study is the first report of correlating prevalence of *Cf-2/Hcr2s* in association with Avr2 and distinct inhibitors, EpiC1, EpiC2B and Cip1 within *S. pimpinellifolium* and other wild relatives of tomato. We found that most Avr2 responsive plants contain a putative *Cf-2* typified by a large PCR product amplified using *Cf-2* primers. However, not all *Cf-2* containing plants were responsive to Avr2. Further, we did not observe a correlation between presence or absence of *Cf-2*, *Cf-9* and *9DC* and plant responses to EpiC1, EpiC2B and Cip1. Notably, *Cf-9* seems more abundant than *Cf-2* in *S. pimpinellifolium*.

A striking observation is the significant distinction between *Cf-2* frequency between Ecuador and South Peru in *S. pimpinellifolium*, where Avr2 response frequency was 9.5% and 31.6%, respectively but *Cf-2* frequency was 35% in Ecuador and 6.25% in South Peru. This indicates that either Avr2 recognition in *S. pimpinellifolium* does not always occur via Cf-2 or populations native to Ecuador and South Peru may have different *Cf-2* variants triggering distinct recognition profiles. In wild potato, *R* gene loci *Rpi-mcq1* and *R2* are known to have evolved separately in species from Mexican and Peruvian regions, but both recognise Avr2 of *P. infestans* (Aguilera-Galvez et al., 2018). Further, variation in number and types of *Hcr2s* was uncovered among plants of same species and from similar or different geographic regions. In other wild tomato plants genotyped beyond *S. pimpinellifolium*, *Hcr2s* and the *Cf-9* gene were consistently present in all selected species from different origin ranges, indicating *Cf-9* is more prevalent than *Cf-2* and *9DC* across the tomato clade.

We found *Hcr2s* to be present in other wild tomato species while revealing intra-population and inter-population variations in the number of LRRs, as shown by the different sizes of

the Hcr2 PCR fragments. PCR fragment, comparable to tomato, obtained using *Cf-2/*homolog primer pair show that *Cf-2-like* gene exist in diploid wild potato species. However, potato plants strongly responsive to EpiC2B clearly lacked a *Cf-2-like* gene, but carried another *Hcr2* gene with presumably less LRRs. Interestingly, we failed to detect *Cf-2* gene in non-responsive outgroup wild tomato species, *S. ochranthum*, but we amplified a *Hcr2* of similar size as *Cf-2* in non-responsive outgroup potato species, *S. palustre*. Moreover, a previous study from our group suggested that recombination events in the genus *Solanum* that diverged <6 Mya, lead to the evolution of *Cf-2* (Kourelis et al., 2020). This lead us to suggest that while *Cf-2* may have evolved at the shared timescales of wild tomato and potato (**Figure 3.1**), inhibitor recognition does not always occur in the presence of Cf-2.

6.3 *Rcr3*, *Pip1* and *C14* natural variation analysis revealed hotspots of positive selection in tomato and potato

In Chapter 4, our DNA sequencing of 86 natural variants of *Rcr3* from inhibitor responsive and non-responsive plants across different regions, we observed no amino acid substitutions in active site residues, but at sites comprising substrate binding groove in addition to novel mutations at a few other sites. However, most variant residues in *Rcr3* did not correlate with inhibitor recognition variations in the presence of *Cf-2/Hcr2s*. Our species-wide and gene-wide *in-silico* evolutionary analysis revealed that *Rcr3* is under positive selection within *S. pimpinellifolium* and across wild tomato species, which is consistent with a previous finding (Shabab et al., 2008). Our MEME based analysis identified that sites 111, 293, 294, 343 and 344 are under positive selection in *S. pimpinellifolium*, whereas only site 174 is positively selected in other wild tomato species. When we employed an alternative FUBAR based approach, we found that different sites 186, 196, 213 and 284 are also under diversifying selection within *S. pimpinellifolium* and site 222 and 330 in wild tomato species.

While we did not detect signatures of diversifying selection on *Rcr3* in wild potato, our results indicate that sites 161, 273 and 328 are positively selected. Similarly, when we sequenced 34 *Pip1* variants from wild tomato and potato in this study, we found active site residues were conserved. Our gene-wide analysis discovered that *Pip1* is under diversifying selection in other wild tomato species, but not in *S. pimpinellifolium* and wild potato clade. However, using MEME, we found that sites 228 and 310 are positively selected in *Pip1* in *S. pimpinellifolium*, but no specific sites that we tested are under positive selection in wild tomato and wild potato clade. Alternatively, in a FUBAR based analysis, sites 70, 72, 223 and 228 are also diversifying in *Pip1* in *S. pimpinellifolium*, sites 160, 228, 264, 285, 294, 324 and 339 in other wild tomato and sites 70, 77, 142, 186, 199, 228 and 264 in wild potato.

Our finding that *Rcr3* but not *Pip1* is diversifying within *S. pimpinellifolium* is consistent with previous indications that while *Pip1* exhibits increased amino acid variations as compared to similar proteases, the diversity in *Pip1* is reduced when compared to *Rcr3* (Shabab et al., 2008 and Ilyas et al., 2015). Our newly sequenced 34 variants of *C14* in this study show that C14 is under diversifying selection in *S. pimpinellifolium*, but not in wild tomato and wild potato (**Figure 4.14**), which is in contrast to a previous study that *C14* is positively selected in wild potato and not in wild tomato (Kaschani et al., 2010). Interestingly a MEME based approach identified only site 291 to be diversifying in *C14* in *S. pimpinellifolium*. However, FUBAR analysis revealed that sites 277, 291, 302 and 303 in C14 are also diversifying within *S. pimpinellifolium*. FUBAR also disclosed that sites 302 and 336 are positively selected in C14 in remaining wild tomato clade and sites 221 and 336 in C14 in wild potato.

Our findings that diversifying selection varies on an immune protease and a few different sites are under selection within *S. pimpinellifolium*, other wild tomato and wild potato as well as contrasting selection pressures on different immune protease within a same species clade suggest that although Rcr3, Pip1 and C14 may play a role in immunity against unrelated inhibitors, Avr2, EpiC1, EpiC2B and Cip1, based on their interaction affinities,

each of these immune protease primarily function in conferring a specific inhibitor recognition in association with a receptor. Further, the downstream signalling networks may still converge.

6.4 *Cf-2/Hcr2* silencing effectively compromise Avr2 recognition but not inevitably of EpiCs and Cip1

In Chapter 5, we used *TRV*-based VIGS to silence different clans of *Cf-2* and *Hcr2s* that are known to exist in *S. pimpinellifolium*. We selected Avr2-responsive LA0369(P3) and Avr2/EpiC1/EpiC2B/Cip1-responsive plant LA0753(P3) of *S. pimpinellifolium* to perform silencing on clonal propagates. We also selected Avr2/EpiC1/EpiC2B/Cip1-responsive wild potato *Si*CGN17720(P3) and EpiC2B-responsive wild potato *Sb*CGN22732(P3). Our qPCR analysis showed that *Cf-2/Hcr2* silencing was effective in *S. pimpinellifolium* and sufficiently achieved heterologously in wild potato. When we individually infiltrated each inhibitor, Avr2, EpiC1, EpiC2B, and Cip1, our HR observations indicated that, although *Cf-2* silencing primarily affects Avr2 recognition, it does not necessarily affect EpiCs and Cip1 perception. Rather, there is probably another *Hcr2* or a putative *Hcr* ancestor that could cause perception of EpiCs and Cip1. Besides *Cf-2*, the transcript levels of several *Hcr2s* were reduced in TRV2-based VIGS of different *Hcr2* clans. These candidate *Hcr2* genes are of particular interest in deciphering inhibitor recognition and variation between tomato and potato. It is also possible that more diverse *Hcr2* genes exist that may confer secondary and weakened perception response towards Avr2 and other inhibitors at different stages of plant growth similar to some *Hcr9* genes that reportedly confer recognition of *C. fulvum* derived Avr9 in older leaves and not in younger leaves (Parniske et al., 1997).

6.5 Silencing *Rcr3*, *Pip1*, *C14*, and *SOBIR1* reduces HR severity

When we used VIGS to silence *Rcr3*, *Pip1* and *C14* in *S. pimpinellifolium* LA0369(P3) and LA0753(P3) as well as in *S. infundibuliforme* CGN17720(P3) and *S. bulbocastanum* CGN22732(P3), we estimated an effective relative fold change in endogenous transcript abundance level of these immune proteases. Taken together, our results show that *Pip1* silencing reduces HR severity triggered by all four inhibitors nearly equally in *S. pimpinellifolium*, whereas *C14* silencing reduced recognition of EpiC2B and Cip1. Interestingly, a comparable impact on reduced recognition of Avr2, EpiC2B and Cip1 was observed when *Rcr3* was silenced in *S. pimpinellifolium*. *C14* silencing in wild potato reduced EpiC2B/EpiC1 recognition the most, whereas Cip1 recognition is reduced upon *Pip1* silencing. Our findings indicate that in contrast to *Hcr2s*, immune proteases *Rcr3*, *Pip1* and *C14*, play variable roles in inhibitor recognition in wild tomato and potato. This indicates that underlying molecular mechanisms of inhibitor recognition are complex. While the recognition may all involve proteases as co-receptors, inhibitor perception may be transduced via different Cf/Hc2-like receptors. However, when we silenced *SOBIR1*, recognition of all four inhibitors was reduced in plants of *S. pimpinellifolium* LA0753(P3) and *S. bulbocastanum* CGN22732(P3). This indicates that irrespective of *Cf-2* and *Hcr2* involved in recognition of Avr2, EpiCs and Cip1, *SOBIR1* is a convergent RLK that is required in mediating recognition of these inhibitors by similar or different Hcr2-RLPs.

6.6 *In-silico* analysis identified that Cf-2 originated in tomato, whereas Hcrs are distributed across Solanaceae

Chapter 5 revealed that Cf-2 is specific to tomato and does not occur in potato. This conclusion based on bioinformatics analysis of genomes sequenced from wild tomato and potato (Sol genomics). However, this contradicts of our results from PCR-based approach,

where a fragment analogous to *Cf-2* was amplified in potato. Sequencing to distinguish existing *Cf-2* polymorphism in wild tomato and potato species is thus important in future. Moreover, Hcr2s are found frequently in tomato and potato and scarcely in eggplant and pepper, and do not exist in other species in Solanaceae. The Hcr proteins are found to be limited to solanceae, where *S. pimpinellifolium* and *S. lycopersicum* have 65 Hcr's each and *S. tuberosum* has 70 Hcr's. It should be noted that our approach strictly excluded any Cf-like RLPs that contain a serine/threonine/tyrosine kinase domain or any other unusual domains. Our phylogenetic tree further described the direction of evolution, and our analysis suggest that Ve-like receptors are the most ancient, followed by Hcr9, Hcr2s and Eix-like receptor clades. *Hcr2s* are located mostly on chromosome 6 and 12 in tomato (Kourelis et al., 2020). Therefore, it is possible that multiple Hcr's with identical LRR domains confer recognition of a same inhibitor and are clustered at the same or various locus on chromosome 6 or 12. Alternatively, multiple Hcr's residing at the same locus have variations in the LRR domain that underpin functional distinctions in recognition of different inhibitors by different Hcr's.

6.7 Proposed molecular perception of Avr2, EpiCs and Cip1 in tomato and potato

Our findings lead us to propose two conclusions as illustrated in **Figure 6.1**: In our first interpretation (**Figure 6.1(A)**), C14 and a progenitor cysteine protease of Rcr3 and Pip1 functionally acquired inhibitor recognition capability early in Solanaceae and detected conserved secreted cysteine protease inhibitors from *Phytophthora* species. Cysteine protease inhibitors from different strains, for example of *P. parasitica*, are mostly conserved and trigger HR in various *Nicotiana* species (Zhang et al., 2020). Since *Phytophthora* sp. have broad host range across Solanaceae and their infections have been reported well over 160 years (Fry et al., 2015), it is likely that *P. infestans* derived EpiC2B and EpiC1 primarily

inhibited C14 and weakly inhibited diversified Rcr3 and Pip1 that have been present for ~50 mya in Solanaceae (Kourelis et al., 2020). As pathogen pressures of *P. syringae* and *C. fulvum* emerged in evolutionary time scales with a broader or species specific ability to infect hosts, C14, Pip1 and Rcr3 promoted host adaptation via differential affinities of interactions with distinct inhibitors. However, significant structural perturbations in immune proteases could only get triggered by strongly matching inhibitor and this complex occasionally interacts with a compatible Cf-2/Hcr2-like RLP and HR is induced. It is likely that these evolving pathogen-derived inhibitors and host immune protease convergent targets coevolved and further directed the evolution of functional cognate receptor in Solanaceae species, particularly within potato and tomato.

We found that although Cf-2 is limited to tomato, Hcr2s are also present in potato, eggplant and pepper (**Figure 5.12**). Further, we report that Cf-like RLPs diversified ~33 mya when *Petunia* sp evolved in Solanaceae, whereas Rcr3 and Pip1 were suggested to have evolved some ~36 to 50 mya (Ilyas et al., 2015, Kourelis et al., 2020). In our screening we failed to detect any response against Avr2, EpiCs and Cip1 in eggplant and pepper. Based on all these findings, our second conclusion (**Figure 6.1(B)**) is that anciently existing Hcr's evolved to constitutively interact with progenitor immune proteases of Rcr3, Pip1 and C14 in the apoplast. Concurrently, with multiple pathogen pressure and strong/weak association dynamics of cysteine inhibitors from different pathogens and host immune proteases, Hcr-receptors periodically co-evolved and developed novel recognition specificities towards distinct inhibitors. It is thus possible that distantly evolved Hcr RLPs instead of Cf-2 or Hcr2s, evolved independently in potato and in wild tomato species to mediate EpiC recognition.

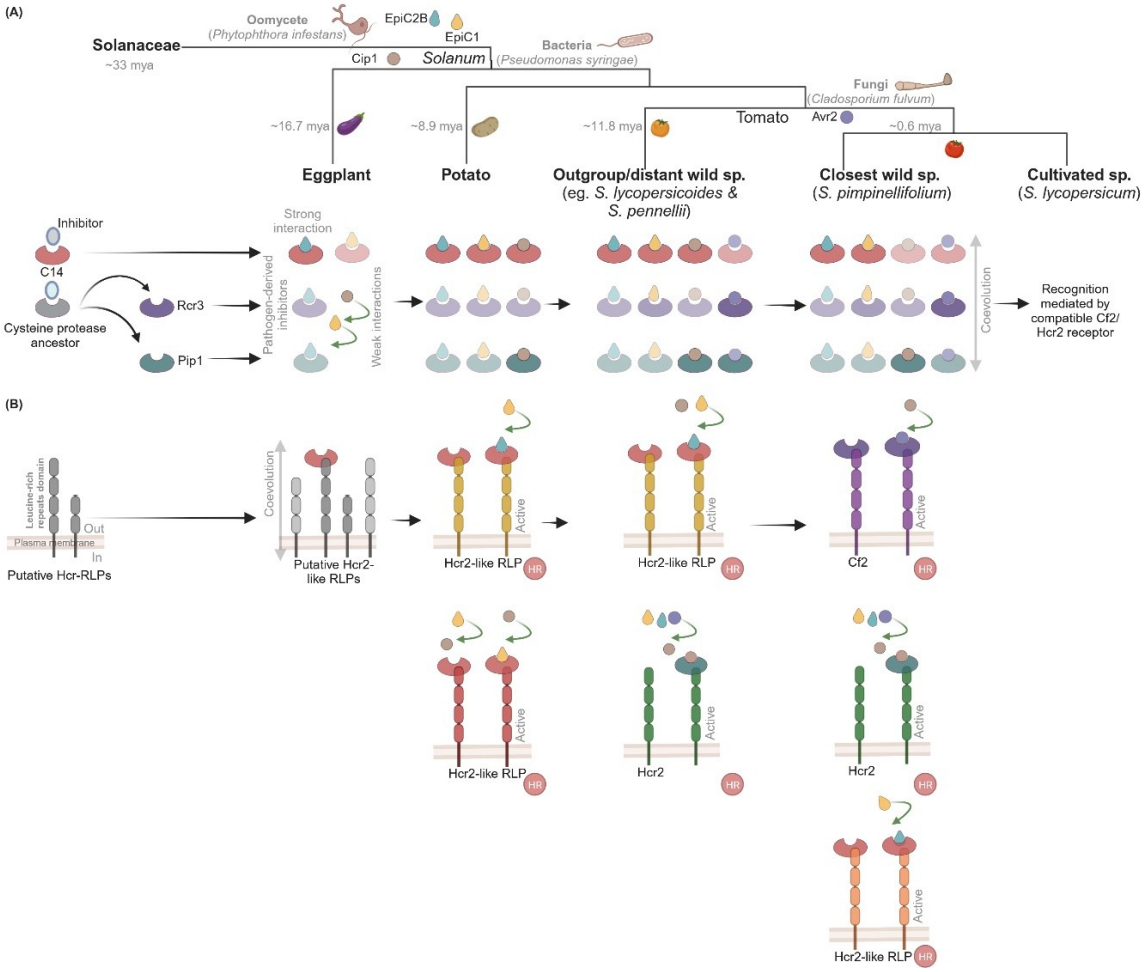


Figure 6.1 Proposed co-evolutionary dynamics of pathogen-derived inhibitors, Avr2, Cip1 and EpiC1s with host protease targets, Rcr3, Pip1 and C14 and recognition by Hcr2 receptors. **(A)** Given the broad host range of *P. infestans*, it is possible that C14 anciently has been interacting with inhibitors while Rcr3 and Pip1 diversification from an immune protease ancestor was triggered by unrelated pathogen-derived inhibitors, likely beyond genus *Solanum*. Distinct inhibitors interact strongly or weakly with Rcr3, Pip1 and C14. Driven by evolutionary arms race with pathogen over species evolution, these native host immune protease targets coevolved differential binding affinities with inhibitors, eventually shaping the repertoire of Hcr2-RLPs (as shown in B) leading to specific HR. **(B)** Alternatively, putative Hcr-RLPs existed beyond *Solanum* species, constitutively forming an inactive complex with ancient proteases. As pathogen pressure diversity intensified over evolutionary timescale, the interaction of cognate pathogen-derived inhibitor with host proteases associated with Hcr2-receptors induced conformational changes leading to protease-Hcr2 complex activation. This further directed the diversification of compatible Hcr2 receptors towards conferring successful recognition of multiple yet specific inhibitors within same host. Cf-2 likely evolved specifically in tomato to counter mounting specialised opposition of *C. fulvum* derived Avr2.

Recently, a study from our group identified residues in Rcr3 that potentially reside on Cf-interacting site and are critical in conferring *Cf-2*-dependent recognition signalling. Further

bioengineering of these residues in different *Rcr3* orthologs and paralog *Pip1* sufficiently enhanced their ability to trigger *Cf-2*-dependent HR against Avr2 (Kourelis et al., 2024). It was proposed that Rcr3, Cf-2 and SOBIR1 are constantly interacting in a complex in the absence of Avr2. Upon secretion of Avr2 by *C. fulvum* in the extracellular space, Avr2 binds Rcr3, which further initiates SERK3 recruitment into the Avr2-Rcr3-Cf-2-SOBIR1 complex and actively triggers HR (Kourelis et al., 2024). Similarly, we propose a perception model (**Figure 6.2**) of recognition of unrelated inhibitors by different or related Hcr2-like RLPs in association with a cysteine protease most likely to act as a co-receptor in mediating Avr2, EpiCs and Cip1 recognitions. The activated recognition signalling may further have overlapping downstream signalling components, such as, receptor-like cytoplasmic kinases (RLCKs), MAPKs and NRCs. RLCKs from various subfamilies reportedly contribute to SOBIR1 dependent immunity in *Nicotiana benthamiana* (Huang et al., 2024) and NRCs are widespread convergent network of immunity in Solanaceae (Huang et al., 2024) and their roles are emerging in different types of pathogen-derived inhibitor and plant resistance gene interactions in Solanaceae (Sugihara et al., 2025).

6.8 Future directions

In heterogeneous geographical landscapes, populations of same or different species are often fragmented. These meta-populations likely form intra-specific patches that share evolutionary signatures further benefiting host adaptations to multiple pathogens pressures. Considering the variation in local recognition frequency of distinct inhibitors Avr2, Cip1 and EpiCs within same and different species, naturally existing allelic variations in convergent immune protease pathogen targets, gene expression patterns in silencing experiments indicating cross-silencing of *Hcr2s* and diversity of Cf-like repertoire across Solanaceae, it is a challenge to identify a matching receptor that mediate recognition, most likely indirectly of EpiCs and Cip1.

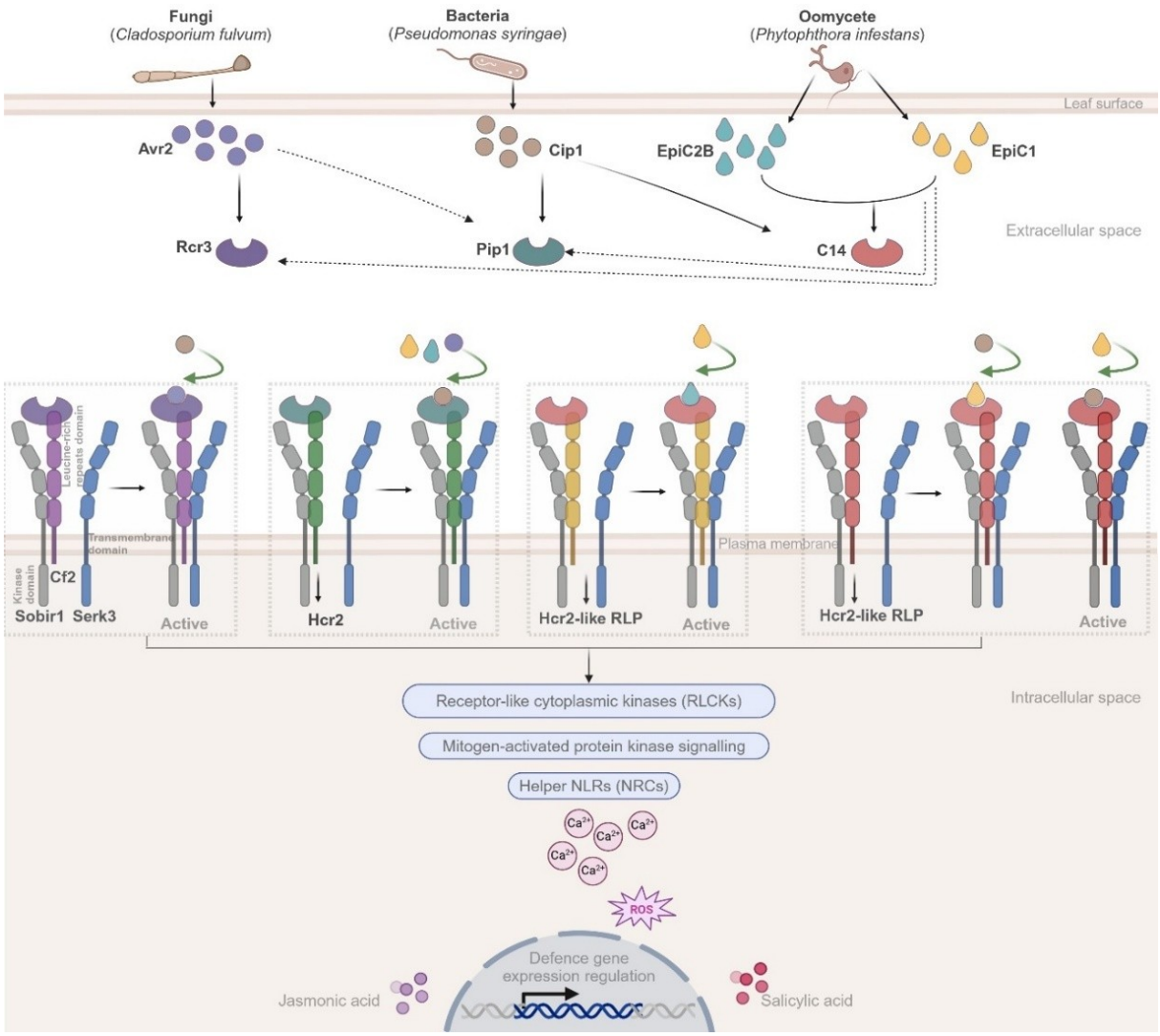


Figure 6.2 Perception model of unrelated pathogen-derived inhibitors Avr2, Cip1 and EpiCs. In the absence of pathogen infection, secreted host immune proteases, Rcr3, Pip1 and C14, RLPs, Hcr2s/Cf-2 having recognition specificities and RLK-Sobir1 are constitutively interacting in a complex. Upon pathogen invasion of host extracellular space, *C. fulvum* secreted Avr2, *P. syringae* secreted Cip1 and *P. infestans* secreted EpiCs bind differentially with Rcr3, Pip1 or C14, strongly or weakly. Specific inhibitor triggers a change in conformation of cognate Hcr2/Cf-2 receptor, which further catalyses RLK-Serk3 recruitment that leads to an active HR as inhibitor perception response. Despite specific Hcr2/Cf-2 mediating recognition of unrelated inhibitors at the cell surface, the downstream of all these recognitions probably overlap and trigger various intracellular changes that fine tune and transduce defence signalling. The overlapping processes may involve cytoplasmic interaction with localised RLCKs, MAPK signalling cascade phosphorylation and active recruitment of convergent network of NRCs. This may ultimately lead to secondary messenger outbursts of Ca^{2+} or $O2^{-}$. Differential gene regulation of defence related genes may underlie the relative expression level variations in SA/JA dependent signalling pathways, where SA is likely upregulated.

Functionally characterising natural variations in immune proteases in responsive plants and co-characterising functions of candidate RLP genes that have sequence and structural variations may provide indications of likely interactions that underlie inhibitor recognition variations. To mutually potentiate the defence response, Pattern-triggered immunity (PTI) and Effector-triggered immunity (ETI) have been demonstrated to work together (Yuan et al., 2021, Yuan et al., 2023). Further, SOBIR1, SERK3/BAK1 and EDS1 (Enhanced Disease Susceptibility) are PTI-associated convergent components of PTI and ETI playing key roles in response against different inhibitors (Tian et al., 2021). Therefore, it is important to analyse whether silencing these component in native species conferring inhibitor recognition regulates the recognition signalling.

Downstream cytosolic calcium influx trigger and activation of mitogen activated protein kinase and Ca^{2+} dependent protein kinases (CPKs) are early responses common before transcriptional activation that in turn regulate phytohormone accumulation in pathogen defence (Li et al., 2020, Guzmán-Benito et al., 2024). Salicylic acid and Jasmonic acid were recently suggested to play crucial roles in early stages of tomato defence response to *C. fulvum* infection, especially between 4 dpi to 8 dpi (Zhang et., 2020). Further RNA-Seq for transcriptome profiling of *Cf-16* mediated resistance in infected and non-infected tomato lines indicated over 1000 differentially expressed genes (DEGs), implying a common group of genes that contribute to various plant-pathogen interaction signal transduction pathways, are either positively or negatively regulated during *C. fulvum* infection (Zhang et al., 2020).

Specific upregulation of 12 *WRKYs* were also reported at early stages upon *C. fulvum* (Zhang et al., 2020) and they have also been shown to promote defence against bacteria, nematode and fungal pathogens (Tena et al., 2001). *WRKYs* in turn may regulate downstream resistance response pathways. Furthermore, *Cf-19* mediated resistance analysis revealed that silencing *EREB* transcription regulator, downregulates *WRKY80* abundance which further reduce *Cf-19* mediated resistance (Pei et al., 2024). Tomato has

83 *WRKY* genes (Karkute et al., 2018) and *WRKY80* is core to the cross-talk between MAPK signalling and plant-pathogen interaction pathway (Pei et al., 2024). Therefore, it would be interesting to investigate if these components play a role in Cf-2/Hcr2/Hcr-mediated indirect recognition of Avr2, EpiCs and Cip1.

It is likely that functional and perhaps redundant *Cf-like* RLP or *Hcr*-RLP genes are present in the wild tomato and potato populations that have been found to exhibit specific HR against four different inhibitors, Avr2, EpiC1, EpiC2B and Cip1. Based on knowledge of plant-pathogen-derived inhibitor interactions and evolution under various environmental conditions, the identification and analysis of functional Cf-like RLPs in these populations from different geographic origin centres and altitudes when exposed to Avr2, EpiCs or Cip1 can aid in the deployment of these RLP genes in subsequent breeding and bioengineering efforts. Generating CRISPR/Cas-mediated knockout lines for identified *Cf-like* RLP genes conferring recognition of EpiCs and Cip1 can predict the potential of using these RLPs in developing durable resistance. Further, pyramiding of functional *Cf-like* RLP genes with ability to recognise specific or multiple inhibitors could serve as an approach to achieve broad-spectrum resistance against *C. fulvum*, *P. infestans* and *P. syringae*, which are all devastating pathogens of economically important solananceae crops.

Bibliography

- Aguilera-Galvez C, Champouret N, Rietman H, Lin X, Wouters D, Chu Z, Jones JDG, Vossen JH, Visser RG, Wolters PJ, Vleeshouwers VGAA. Two different *R*-gene loci co-evolved with *Avr2* of *Phytophthora infestans* and confer distinct resistance specificities in potato. *Stud. Mycol*. **2018**: 89: 105–115. https://doi.org/10.1016/j.simyco.2018.01.002

- Albert I, Böhm H, Albert M, Feiler CE, Imkampe J, Wallmeroth N, Brancato C, Raaymakers TM, Oome S, Zhang H, Krol E, Grefen C, Gust AA, Chai J, Hedrich R, van den Ackerveken G, Nürnberger T. An RLP23-SOBIR1-BAK1 complex mediates NLP-triggered immunity. *Nat Plants*. **2015**: 5(1): 15140. https://doi.org/10.1038/nplants.2015.140

- Ali S, Tyagi A, Mir ZA. Plant immunity: at the crossroads of pathogen perception and defence response. *Plants (Basel)*. **2024**: 13(11): 1434. https://doi.org/10.3390/plants13111434

- Andolfo G, Sanseverino W, Rombauts S, van de Peer Y, Bradeen JM, Carputo D, Frusciante L, Ercolano MR. Overview of tomato (*Solanum lycopersicum*) candidate pathogen recognition genes reveals important *Solanum R* locus dynamics. *New Phytol*. **2013**: 197(1): 223-237. https://doi.org/10.1111/j.1469-8137.2012.04380.x

- Arafa RA, Moussa OM, Soliman NEK, Shirasawa K, Kamel SM, Rakha MT. Resistance to *Phytophthora infestans* in tomato wild relatives. *Afr. J. Agric. Res*. **2017**: 12: 2188–2196. http://dx.doi.org/10.5897/AJAR2017.12422

- Arafa RA, Rakha MT, Soliman NEK, Moussa OM, Kamel SM, Shirasawa K. Rapid identification of candidate genes for resistance to tomato late blight disease using next-generation sequencing technologies. *PLoS ONE*. **2017**: 12(12): e0189951. https://doi.org/10.1371/journal.pone.0189951

- Armstrong M, Hein I. Identification of Resistance Genes Using Diagnostic R-Gene Enrichment Sequencing (dRenSeq). *Methods Mol Biol*. **2021**: 2354: 213-219. https://doi.org/10.1007/978-1-0716-1609-3_10

- Aubriot X, Knapp S, Syfert MM, Poczai P, Buerki S. Shedding new light on the origin and spread of the brinjal eggplant (*Solanum melongena* L.) and its wild relatives. *Am J Bot*. **2018**: 105(7): 1175-1187. https://doi.org/10.1002/ajb2.1133

- Bai, S, Wang X, Guo M, Cheng G, Khan A, Yao W, Gao Y, Li J. Selection and evaluation of reference genes for quantitative real-time PCR in tomato (*Solanum lycopersicum* L.) inoculated with *Oidium neolycopersici*. *Agronomy*. **2022**: 12*:* 3171. https://doi.org/10.3390/agronomy12123171

- Balint-Kurti P. The plant hypersensitive response: concepts, control and consequences. *Mol Plant Pathol*. **2019**: 20(8): 1163-1178. https://doi.org/10.1111/mpp.12821

- Bar M, Sharfman M, Ron M, Avni A. BAK1 is required for the attenuation of ethylene-inducing xylanase (Eix)-induced defense responses by the decoy receptor *Le*Eix1. *Plant J*. **2010**: 63(5): 791-800. https://doi.org/10.1111/j.1365-313X.2010.04282.x

- Becker RA, Wilks AR (original code developers), Brownrigg R (R version), Minka P, Deckmyn A (enhancements and maintainer). Maps: draw geographical maps. *CRAN-R package*. **2024**. https://cran.r-project.org/package=maps

- Bentham AR, De la Concepcion JC, Mukhi N, Zdrzałek R, Draeger M, Gorenkin D, Hughes RK, Banfield MJ. A molecular roadmap to the plant immune system. *J Biol Chem*. **2020**: 295(44): 14916-14935. https://doi.org/10.1074/jbc.rev120.010852

- Bernal-Cabrera A, Martínez-Coca B, Herrera-Isla L, Ynfante-Martínez D, Peteira-Delgado B, Portal O, Leiva-Mora M, & De Wit PJ. The first report on the occurrence race 9 of the tomato leaf mould pathogen *Cladosporium fulvum* (syn. *Passalora fulva*) in Cuba. *Eur J Plant Pathol*. **2021**: 160: 731 - 736. https://doi.org/10.1007/s10658-021-02261-4

- Bi G, Liebrand TW, Cordewener JH, America AH, Xu X, Joosten MH. *Arabidopsis thaliana* receptor-like protein AtRLP23 associates with the receptor-like kinase AtSOBIR1. *Plant Signal Behav*. **2014**: 9(2): e27937. https://doi.org/10.4161/psb.27937

- Bi G, Liebrand TW, Bye RR, Postma J, van der Burgh AM, Robatzek S, Xu X, Joosten MH. SOBIR1 requires the GxxxG dimerization motif in its transmembrane domain to form constitutive complexes with receptor-like proteins. *Mol Plant Pathol*. **2016**: 17(1): 96-107. https://doi.org/10.1111/mpp.12266

- Böhm H, Albert I, Oome S, Raaymakers TM, van den Ackerveken G, Nürnberger T. A conserved peptide pattern from a widespread microbial virulence factor triggers pattern-induced immunity in Arabidopsis. *PLoS Pathog*. **2014**: 10(11): e1004491. https://doi.org/10.1371/journal.ppat.1004491

- Bolger A, Scossa F, Bolger ME, Lanz C, Maumus F, Tohge T, Quesneville H, Alseekh S, Sørensen I, Lichtenstein G, Fich EA, Conte M, Keller H, Schneeberger K, Schwacke R, Ofner I, Vrebalov J, Xu Y, Osorio S, Aflitos SA, Schijlen E, Jiménez-Goméz JM, Ryngajllo M, Kimura S, Kumar R, Koenig D, Headland LR, Maloof JN, Sinha N, van Ham RC, Lankhorst RK, Mao L, Vogel A, Arsova B, Panstruga R, Fei Z, Rose JK, Zamir D, Carrari F, Giovannoni JJ, Weigel D, Usadel B, Fernie AR. The genome of the stress-tolerant wild tomato species *Solanum pennellii*. *Nat Genet*. **2014**: 46(9): 1034-8. https://doi.org/10.1038/ng.3046

- Bombarely A, Moser M, Amrad A, Bao M, Bapaume L, Barry CS, Bliek M, Boersma MR, Borghi L, Bruggmann R, Bucher M, D'Agostino N, Davies K, Druege U, Dudareva N, Egea-Cortines M, Delledonne M, Fernandez-Pozo N, Franken P, Grandont L, Heslop-Harrison JS, Hintzsche J, Johns M, Koes R, Lv X, Lyons E, Malla D, Martinoia E, Mattson NS, Morel P, Mueller LA, Muhlemann J, Nouri E, Passeri V, Pezzotti M, Qi Q, Reinhardt D, Rich M, Richert-Pöggeler KR, Robbins TP, Schatz MC, Schranz ME, Schuurink RC, Schwarzacher T, Spelt K, Tang H, Urbanus SL, Vandenbussche M, Vijverberg K, Villarino GH, Warner RM, Weiss J, Yue Z, Zethof J, Quattrocchio F, Sims TL, Kuhlemeier C. Insight into the evolution of the Solanaceae from the parental genomes of *Petunia hybrida*. *Nat Plants*. **2016**: 2(6): 16074. https://doi.org/10.1038/nplants.2016.74

- Boutrot F, Zipfel C. Function, Discovery, and Exploitation of Plant Pattern Recognition Receptors for Broad-Spectrum Disease Resistance. *Annu Rev Phytopathol*. **2017**: 55: 257-286. https://doi.org/10.1146/annurev-phyto-080614-120106

- Boykin LM, Kubatko LS, Lowrey TK. Comparison of methods for rooting phylogenetic trees: a case study using Orcuttieae (Poaceae: Chloridoideae). *Mol Phylogenet Evol*. **2010**: 54(3): 687-700. https://doi.org/10.1016/j.ympev.2009.11.016

- Bozkurt TO, Schornack S, Win J, Shindo T, Ilyas M, Oliva R, Cano LM, Jones AM, Huitema E, van der Hoorn RA, Kamoun S. Phytophthora infestans effector AVRblb2 prevents secretion of a plant immune protease at the haustorial interface. *Proc Natl Acad Sci U S A*. **2011**: 108(51): 20832-7. https://doi.org/10.1073/pnas.1112708109

- Brading PA, Hammond-Kosack KE, Parr A, Jones JD. Salicylic acid is not required for *Cf-2*- and *Cf-9*-dependent resistance of tomato to *Cladosporium fulvum*. *Plant J.* **2000**: 23(3): 305-18. https://doi.org/10.1046/j.1365-313x.2000.00778.x

- Brigneti G, Martín-Hernández AM, Jin H, Chen J, Baulcombe DC, Baker B, Jones JD. Virus-induced gene silencing in *Solanum* species. *Plant J*. **2004**: 39(2): 264-72. https://doi.org/10.1111/j.1365-313x.2004.02122.x

- Brownrigg, Ray. Maps: Draw Geographical Maps. *CRAN: Package mapdata*. **2022**. https://cran.r-project.org/package=mapdata

- Bundalovic-Torma C, Lonjon F, Desveaux D, Guttman DS. Diversity, Evolution, and Function of *Pseudomonas syringae* Effectoromes. *Annu Rev Phytopathol*. **2022**: 60: 211-236. https://doi.org/10.1146/annurev-phyto-021621-121935

- Cai D, Rodríguez F, Teng Y, Ané C, Bonierbale M, Mueller LA, Spooner DM. Single copy nuclear gene analysis of polyploidy in wild potatoes (*Solanum* section Petota). *BMC Evol Biol*. **2012**: 12:70. https://doi.org/10.1186/1471-2148-12-70

- Caldwell KS, Michelmore RW. *Arabidopsis thaliana* genes encoding defence signalling and recognition proteins exhibit contrasting evolutionary dynamics. *Genetics*. **2009**: 181(2): 671-84. https://doi.org/10.1534/genetics.108.097279

- Cammarano D, Jamshidi S, Hoogenboom G, Ruane AC, Niyogi D, Ronga D. Processing tomato production is expected to decrease by 2050 due to the projected increase in temperature. *Nat Food.* **2022**: 3(552). https://doi.org/10.1038/s43016-022-00521-y

- Castañeda-Álvarez NP, de Haan S, Juárez H, Khoury CK, Achicanoy HA, Sosa CC, Bernau V, Salas A, Heider B, Simon R, Maxted N, Spooner DM. Ex situ conservation priorities for the wild relatives of potato (*Solanum* L. Section petota). *PLoS One*. **2015**: 10(6): e0122599. https://doi.org/10.1371/journal.pone.0129873

- Catanzariti AM, Lim GTT, Jones DA. The tomato *I-3* gene: a novel gene for resistance to *Fusarium* wilt disease. *New Phytol*. **2015**: 207(1): 106-118. https://doi.org/10.1111/nph.13348

- Chen J, Peng P, Tian J, He Y, Zhang L, Liu Z, Yin D, Zhang Z. *Pike*, a rice blast resistance allele consisting of two adjacent *NBS–LRR* genes, was identified as a novel allele at the *Pik* locus. *Mol Breeding*. **2015**: 35: 117. https://doi.org/10.1007/s00438-021-01795-w

- Chen JY, Xiao HL, Gui YJ, Zhang DD, Li L, Bao YM, Dai XF. Characterisation of the *Verticillium dahliae* Exoproteome Involved in Pathogenicity from Cotton-Containing Medium. *Front Microbiol*. **2016**: 7:1709. https://doi.org/10.3389/fmicb.2016.01709

- Chen T, Kan J, Yang Y, Ling X, Chang Y, Zhang B. A *Ve* homologs gene from *Gossypium barbadense*, *Gbvdr3*, enhances the defence response against *Verticillium dahliae*. *Plant Physiol Biochem*. **2016**: 98: 101-11. https://doi.org/10.1016/j.plaphy.2015.11.015

- Chinchilla D, Zipfel C, Robatzek S, Kemmerling B, Nürnberger T, Jones JD, Felix G, Boller T. A flagellin-induced complex of the receptor FLS2 and BAK1 initiates plant defence. *Nature*. **2007**: 448(7152): 497-500. https://doi.org/10.1038/nature05999

- Coomber A, Saville A, Ristaino JB. Evolution of *Phytophthora infestans* on its potato host since the Irish potato famine. *Nat Commun*. **2024**: 15(1):6488. https://doi.org/10.1038/s41467-024-50749-4

- Couto D, Zipfel C. Regulation of pattern recognition receptor signalling in plants. *Nat Rev Immunol*. **2016**: 16(9): 537-52. https://doi.org/10.1038/nri.2016.77

- Dangl JL, Jones JD. Plant pathogens and integrated defence responses to infection. *Nature*. **2001**: 411(6838): 826-33. https://doi.org/10.1038/35081161

- de Jonge R, van Esse HP, Maruthachalam K, Bolton MD, Santhanam P, Saber MK, Zhang Z, Usami T, Lievens B, Subbarao KV, Thomma BP. Tomato immune receptor Ve1 recognises effector of multiple fungal pathogens uncovered by genome and RNA sequencing. *Proc Natl Acad Sci U S A*. **2012**: 109(13): 5110-5. https://doi.org/10.1073/pnas.1119623109

- de Kock MJ, Iskandar HM, Brandwagt BF, Laugé R, de Wit PJ, Lindhout P. Recognition of *Cladosporium fulvum* Ecp2 elicitor by non-host *Nicotiana* spp. is mediated by a single dominant gene that is not homologs to known *Cf*-genes. *Mol Plant Pathol*. **2004**: 5(5): 397-408. https://doi.org/10.1111/j.1364-3703.2004.00239.x

- De Wit PJGM. The tomato crop. *Agrios' Plant Pathology*. **2024**. https://doi.org/10.1016/B978-0-12-822429-8.00038-8

- DeFalco TA, Zipfel C. Molecular mechanisms of early plant pattern-triggered immune signalling. *Mol Cell*. **2021**: 81(17): 3449-3467. https://doi.org/10.1016/j.molcel.2021.07.029

- Derivnina L, Petre B, Kellner R, Dagdas YF, Sarowar MN, Giannakopoulou A, De la Concepcion JC, Chaparro-Garcia A, Pennington HG, van West P, Kamoun S. Emerging oomycete threats to plants and animals. *Philos Trans R Soc Lond B Biol Sci*. **2016**: 371(1709): 20150459. https://doi.org/10.1098/rstb.2015.0459

- Derivnina L, Contreras MP, Adachi H, Upson J, Vergara Cruces A, Xie R, Skłenar J, Menke FLH, Mugford ST, MacLean D, Ma W, Hogenhout SA, Goverse A, Maqbool A, Wu CH, Kamoun S. Plant pathogens convergently evolved to counteract redundant nodes of an NLR immune receptor network. *PLoS Biol*. **2021**: 19(8): e3001136. https://doi.org/10.1371/journal.pbio.3001136

- Dickinson MJ, Jones DA, Jones JD. Close linkage between the *Cf-2/Cf-5* and *Mi* resistance loci in tomato. *Mol Plant Microbe Interact*. **1993**: 6(3): 341-7. https://doi.org/10.1094/mpmi-6-341

- Dixon MS, Jones DA, Hatzixanthis K, Ganal MW, Tanksley SD, Jones JD. High-resolution mapping of the physical location of the tomato *Cf-2* gene. *Mol Plant Microbe Interact*. **1995**: 8(2): 200-6. https://doi.org/10.1094/mpmi-8-0200

- Dixon MS, Jones DA, Keddie JS, Thomas CM, Harrison K, Jones JD. The tomato *Cf-2* disease resistance locus comprises two functional genes encoding leucine-rich repeat proteins. *Cell*. **1996**: 84(3): 451-9. https://doi.org/10.1016/s0092-8674(00)81290-8

- Dixon MS, Hatzixanthis K, Jones DA, Harrison K, Jones JD. The tomato *Cf-5* disease resistance gene and six homologs show pronounced allelic variation in leucine-rich repeat copy number. *Plant Cell*. **1998**: 10(11): 1915-25. https://doi.org/10.1105/tpc.10.11.1915

- Dixon MS, Golstein C, Thomas CM, van Der Biezen EA, Jones JD. Genetic complexity of pathogen perception by plants: the example of *Rcr3*, a tomato gene required specifically by *Cf-2*. *Proc Natl Acad Sci U S A*. **2000**: 97(16): 8807-14. https://doi.org/10.1073/pnas.97.16.8807

- Domazakis E, Wouters D, Visser RGF, Kamoun S, Joosten MHAJ, Vleeshouwers VGAA. The ELR-SOBIR1 Complex Functions as a Two-Component Receptor-Like Kinase to Mount Defense Against *Phytophthora infestans*. *Mol Plant Microbe Interact*. **2018**: 8: 795-802. https://doi.org/10.1094/mpmi-09-17-0217-r

- Dong SM, Zhou SQ. Potato late blight caused by *Phytophthora infestans*: From molecular interactions to integrated management strategies. *J Integr Agric*. **2022**: 21(12): 3456-3466. https://doi.org/10.1016/j.jia.2022.08.060

- Dong S, Stam R, Cano LM, Song J, Sklenar J, Yoshida K, Bozkurt TO, Oliva R, Liu Z, Tian M, Win J, Banfield MJ, Jones AM, van der Hoorn RA, Kamoun S. Effector specialization in a lineage of the Irish potato famine pathogen. *Science*. **2014**:343(6170): 552-5. https://doi.org/10.1126/science.1246300

- Dong S, Raffaele S, Kamoun S. The two-speed genomes of filamentous pathogens: waltz with plants. *Curr Opin Genet Dev*. **2015**: 35: 57-65. https://doi.org/10.1016/j.gde.2015.09.001

- Dongus JA, Parker JE. EDS1 signalling: At the nexus of intracellular and surface receptor immunity. *Curr Opin Plant Biol*. **2021**: 62: 102039. https://doi.org/10.1016/j.pbi.2021.102039

- Du Y, Chen X, Guo Y, Zhang X, Zhang H, Li F, Huang G, Meng Y, Shan W. *Phytophthora infestans* RXLR effector PITG20303 targets a potato MKK1 protein to suppress plant immunity. *New Phytol*. **2021**: 229(1): 501-515. https://doi.org/10.1111/nph.16861

- Engler C, Youles M, Gruetzner R, Ehnert TM, Werner S, Jones JD, Patron NJ, Marillonnet S. A golden gate modular cloning toolbox for plants. *ACS Synth Biol*. **2014**: 3(11): 839-43. https://doi.org/10.1021/sb4001504

- Erickson JL, Schuster M. Extracellular proteases from microbial plant pathogens as virulence factors. *Curr Opin Plant Biol*. **2024**: 82: 102621. https://doi.org/10.1016/j.pbi.2024.102621

- FAO, IFAD, UNICEF, WFP and WHO. The State of Food Security and Nutrition in the World 2023: Urbanization, agrifood systems transformation and healthy diets across the rural–urban continuum. *FAO*. **2023**. https://doi.org/10.4060/cc3017en

- Feehan JM, Castel B, Bentham AR, Jones JD. Plant NLRs get by with a little help from their friends. *Curr Opin Plant Biol*. **2020**:6: 99-108. https://doi.org/10.1016/j.pbi.2020.04.006

- Felix G, Duran JD, Volko S, Boller T. Plants have a sensitive perception system for the most conserved domain of bacterial flagellin. *Plant J*. 1999: 18(3):265-76. https://doi.org/10.1046/j.1365-313X.1999.00265.x

- Fernandez-Pozo N, Menda N, Edwards JD, Saha S, Tecle IY, Strickler SR, Bombarely A, Fisher-York T, Pujar A, Foerster H, Yan A, Mueller LA. The Sol Genomics Network (SGN)--from genotype to phenotype to breeding. *Nucleic Acids Res*. **2015**: 43(Database issue): D1036-41. https://doi.org/10.1093/nar/gku1195

- Fischer I, Diévart A, Droc G, Dufayard JF, Chantret N. Evolutionary Dynamics of the Leucine-Rich Repeat Receptor-Like Kinase (LRR-RLK) Subfamily in Angiosperms. *Plant Physiol*. **2016**: 170(3):1595-610. https://doi.org/10.1104/pp.15.01470

- Flor H H. Genetics of pathogenicity in *Melampsora lini*. *J. Agric. Res*. **1946**: 73: 337–357. https://eurekamag.com/research/013/721/013721372.php?srsltid=AfmBOoo3TGBVEPZmGnLaO4OgITNFohcEZfxGBmLstBBtmBsSEjtSIERT

- Flor HH. The complementary genic systems in Flax and Flax-rust. *Adv Genet*. **1956**: 8: 29-54. https://doi.org/10.1016/S0065-2660(08)60498-8

- Fradin EF, Abd-El-Haliem A, Masini L, van den Berg GC, Joosten MH, Thomma BP. Interfamily transfer of tomato *Ve1* mediates *Verticillium* resistance in *Arabidopsis*. *Plant Physiol*. **2011**: 156(4): 2255-65. https://doi.org/10.1104/pp.111.180067

- Fradin EF, Zhang Z, Juarez Ayala JC, Castroverde CD, Nazar RN, Robb J, Liu CM, Thomma BP. Genetic dissection of *Verticillium* wilt resistance mediated by tomato *Ve1*. *Plant Physiol*. **2009**: 150(1): 320-32. https://doi.org/10.1104/pp.109.136762

- Friedman AR, Baker BJ. The evolution of resistance genes in multi-protein plant resistance systems. *Curr Opin Genet Dev*. **2007**: 6: 493-9. https://doi.org/10.1016/j.gde.2007.08.014

- Friesen TL, Faris JD. Characterisation of the wheat-Stagonospora nodorum disease system: what is the molecular basis of this quantitative necrotrophic disease interaction? *Can J Plant Pathol*. **2010**: 32(1): 20-28. https://doi.org/10.1080/07060661003620896

- Friesen TL, Faris JD. Characterisation of effector-target interactions in necrotrophic pathosystems reveals trends and variation in host manipulation. *Annu Rev*

Phytopathol. **2021**: 59: 77-98. https://doi.org/10.1146/annurev-phyto-120320-012807

- Fry WE, Birch PR, Judelson HS, Grünwald NJ, Danies G, Everts KL, Gevens AJ, Gugino BK, Johnson DA, Johnson SB, McGrath MT, Myers KL, Ristaino JB, Roberts PD, Secor G, Smart CD. Five Reasons to Consider *Phytophthora infestans* a Re-emerging Pathogen. *Phytopathology*. **2015**: 105(7): 966-81.

- Gabriëls SH, Takken FL, Vossen JH, de Jong CF, Liu Q, Turk SC, Wachowski LK, Peters J, Witsenboer HM, de Wit PJ, Joosten MH. CDNA-AFLP combined with functional analysis reveals novel genes involved in the hypersensitive response. *Mol Plant Microbe Interact*. **2006**: 19(6): 567-76. https://doi.org/10.1094/mpmi-19-0567

- Gabriëls SH, Vossen JH, Ekengren SK, van Ooijen G, Abd-El-Haliem AM, van den Berg GC, Rainey DY, Martin GB, Takken FL, de Wit PJ, Joosten MH. An NB-LRR protein required for HR signalling mediated by both extra- and intracellular resistance proteins. *Plant J*. **2007**: 50(1): 14-28. https://doi.org/10.1111/j.1365-313x.2007.03027.x

- Gao M, Wang X, Wang D, Xu F, Ding X, Zhang Z, Bi D, Cheng YT, Chen S, Li X, Zhang Y. Regulation of cell death and innate immunity by two receptor-like kinases in *Arabidopsis*. *Cell Host Microbe*. **2009**: 6(1): 34-44. https://doi.org/10.1016/j.chom.2009.05.019
- Carrizo García C, Barfuss MH, Sehr EM, Barboza GE, Samuel R, Moscone EA, Ehrendorfer F. Phylogenetic relationships, diversification and expansion of chili peppers (Capsicum, Solanaceae). *Ann Bot*. **2016**: 118(1): 35-51. https://doi.org/10.1093/aob/mcw079

- Garnier S, Ross N, Rudis R, Camargo AP, Sciaini M, Scherer C. Viridis - colourblind-Friendly colour Maps for R. *CRAN-R package version 0.6.4*. **2023**. https://cran.r-project.org/package=viridis

- Gerakari M, Katsileros A, Kleftogianni K, Tani E, Bebeli P, Papasotiropoulos V. Breeding of Solanaceous crops using AI: machine learning and deep learning approaches—a critical review. *Agronomy*. **2025**: 15(757). https://doi.org/10.3390/agronomy15030757

- Gerritsen H. Mapplots: data visualisation on maps. *CRAN-R package*. **2018**: https://cran.r-project.org/package=mapplots

- Gijzen M, Nürnberger T. Nep1-like proteins from plant pathogens: recruitment and diversification of the NPP1 domain across taxa. *Phytochemistry*. **2006**: 67(16): 1800-7. https://doi.org/10.1016/j.phytochem.2005.12.008

- Greenbaum D, Baruch A, Hayrapetian L, Darula Z, Burlingame A, Medzihradszky KF, Bogyo M. Chemical approaches for functionally probing the proteome. *Mol Cell Proteomics*. **2002**: 1(1): 60-8. https://doi.org/10.1074/mcp.t100003-mcp200

- Gu Z, Gu L, Eils R, Schlesner M, Brors B. circlize Implements and enhances circular visualization in R. *Bioinformatics*. **2014**: 19: 2811-2.

- Gu Z. Complex heatmap visualization. *Imeta*. **2022**: 1(3): e43. https://doi.org/10.1002/imt2.43

- Güzman-Benito I, Robinson C, Hua C, Sede AR, Elvira-Gonzalez L, Punzon I, Heinlein M, Nürnberger T, Llave C. The receptor-like kinase BIR1 inhibits elicitor-induced plasmodesmata callose deposition and PTI gene expression and requires EDS1 and SOBIR1 to cause dose-dependent cell-death in *Arabidopsis*. *BioRxiv*. 2024. https://doi.org/10.1101/2023.06.23.546234

- Halim VA, Hunger A, Macioszek V, Landgraf P, Nürnberger T, Scheel D, Rosahl S. The oligopeptide elicitor pep-13 induces salicylic acid-dependent and -independent defence reactions in potato. *Physiol. Mol. Plant Pathol*. **2004**: 64: 311–318. https://doi.org/10.1016/j.pmpp.2004.10.003

- Hassan JA, Diplock N, Chau-Ly IJ, Calma J, Boville E, Yee S, Harris TM, Lewis JD. *Solanum pimpinellifolium* exhibits complex genetic resistance to *Pseudomonas syringae* pv. *tomato*. *Front Plant Sci*. **2024**: 15: 1416078. https://doi.org/10.3389/fpls.2024.1416078

- Hijmans RJ, Spooner DM. Geographic distribution of wild potato species. *Am J Bot*. **2001**: 88(11): 2101-12. https://doi.org/10.2307/3558435

- Hijmans RJ, van Etten J, Sumner M, Cheng J, Baston D, Bevan A, Bivand R, Busetto L, Canty M, Fasoli B, Forrest D, Ghosh A, Golicher D, Gray J, Greenberg JA, Hiemstra P, Hingee K, Ilich A, Institute for Mathematics Applied Geosciences, Karney C, Mattiuzzi M, Mosher S, Naimi B, Nowosad J, Pebesma E, Lamigueiro OP, Racine EB, Rowlingson B, Shortridge A, Venables B, Wueest R. *CRAN-R package*. **2023 (2025 updated)**. https://cran.r-project.org/package=raster

- Holdsworth M, Liu H, Castellana S, Abbas M, Liu J, Perata P. Geography, altitude, agriculture and hypoxia. *Plant Physiol*. **2025**: 197(1). https://doi.org/10.1093/plphys/kiae535

- Homma F, Huang J, van der Hoorn RAL. AlphaFold-Multimer predicts cross-kingdom interactions at the plant-pathogen interface. *Nat Commun*. **2023**: 14(1): 6040. https://doi.org/10.1038/s41467-023-41721-9

- Hörger AC, Ilyas M, Stephan W, Tellier A, van der Hoorn RA, Rose LE. Balancing selection at the tomato RCR3 Guardee gene family maintains variation in strength of pathogen defence. *PLoS Genet*. **2012**: 8(7): e1002813. https://doi.org/10.1371/journal.pgen.1002813

- Hörger A. Evolution of disease resistant genes in wild tomato species. *der Ludwig-Maximilians-Universität München.* **2011**. https://edoc.ub.uni-muenchen.de/13107/1/Hoerger_Anja.pdf

- Hu G, deHart AK, Li Y, Ustach C, Handley V, Navarre R, Hwang CF, Aegerter BJ, Williamson VM, Baker B. EDS1 in tomato is required for resistance mediated by TIR-class *R* genes and the receptor-like *R* gene *Ve*. *Plant J*. **2005**: 42(3): 376-91. https://doi.org/10.1111/j.1365-313x.2005.02380.x
- Huang WRH, Joosten MHAJ. Immune signalling: receptor-like proteins make the difference. *Trends Plant Sci.* **2025**: 1: 54-68. https://doi.org/10.1016/j.tplants.2024.03.012

- Huang WRH, Schol C, Villanueva SL, Heidstra R, Joosten MHAJ. Knocking out *SOBIR1* in *Nicotiana benthamiana* abolishes functionality of transgenic receptor-like

protein Cf-4. *Plant Physiol*. **2021**: 185(2): 290-294. https://doi.org/10.1093/plphys/kiaa047

- Huang CY, Huang YS, Sugihara Y, Wang HY, Huang LT, Lopez-Agudelo JC, Chen YF, Lin KY, Chiang BJ, Toghani A, Kourelis J, Wang CH, Derevnina L, Wu CH. Subfunctionalization of *NRC3* altered the genetic structure of the *Nicotiana NRC* network. *PLoS Genet*. **2024**: 20(9): e1011402. https://doi.org/10.1371/journal.pgen.1011402

- Huang WRH, Braam C, Kretschmer C, Villanueva SL, Liu H, Ferik F, van der Burgh AM, Boeren S, Wu J, Zhang L, Nürnberger T, Wang Y, Seidl MF, Evangelisti E, Stuttmann J, Joosten MHAJ. Receptor-like cytoplasmic kinases of different subfamilies differentially regulate SOBIR1/BAK1-mediated immune responses in *Nicotiana benthamiana*. *Nat Commun*. 2024: 15(1): 4339. https://doi.org/10.1038/s41467-024-48313-1

- Hulbert SH, Webb CA, Smith SM, Sun Q. Resistance gene complexes: evolution and utilization. *Annu Rev Phytopathol*. 2001: 39: 285-312. https://doi.org/10.1146/annurev.phyto.39.1.285

- Ilyas M. The role of papain-like cysteine proteases of tomato in pathogen defence. der Universität zu Köln. 2014. https://www.academia.edu/95537596/The_role_of_papain_like_cysteine_proteases_of_tomato_in_pathogen_defense
- Ilyas M, Hörger AC, Bozkurt TO, van den Burg HA, Kaschani F, Kaiser M, Belhaj K, Smoker M, Joosten MH, Kamoun S, van der Hoorn RA. Functional Divergence of Two Secreted Immune Proteases of Tomato. *Curr Biol*. **2015**: 25(17): 2300-6. https://doi.org/10.1016/j.cub.2015.07.030

- Jain M, Koren S, Miga KH, Quick J, Rand AC, Sasani TA, Tyson JR, Beggs AD, Dilthey AT, Fiddes IT, Malla S, Marriott H, Nieto T, O'Grady J, Olsen HE, Pedersen BS, Rhie A, Richardson H, Quinlan AR, Snutch TP, Tee L, Paten B, Phillippy AM, Simpson JT, Loman NJ, Loose M. Nanopore sequencing and assembly of a human genome with ultra-long reads. *Nat Biotechnol*. **2018**: 36(4): 338-345. https://doi.org/10.1038/nbt.4060

- Jiang X, Li Y, Li R, Gao Y, Liu Z, Yang H, Li J, Jiang J, Zhao T, Xu X. Transcriptome Analysis of the *Cf-13*-Mediated Hypersensitive Response of Tomato to *Cladosporium fulvum* Infection. *Int J Mol Sci*. **2022**: 23(9): 4844. https://doi.org/10.3390/ijms23094844

- Jonathan ML, Anderson J. RPMG: Graphical user interface (GUI) for interactive R analysis. *CRAN: R package*. **2019** (updates 2023). https://cran.r-project.org/package=RPMG

- Jones JD, Dangl JL. The plant immune system. *Nature*. **2006**: 444(7117): 323-9. https://doi.org/10.1038/nature05286

- Jones DA, Thomas CM, Hammond-Kosack KE, Balint-Kurti PJ, Jones JD. Isolation of the tomato *Cf-9* gene for resistance to *Cladosporium fulvum* by transposon tagging. Science. **1994**: 266(5186): 789-93. https://doi.org/10.1126/science.7973631

- Joosten MH, Cozijnsen TJ, De Wit PJ. Host resistance to a fungal tomato pathogen lost by a single base-pair change in an *avirulence* gene. *Nature*. **1994**: 367(6461): 384-6. https://doi.org/10.1038/367384a0

- Joosten M, de Wit P. THE TOMATO-*CLADOSPORIUM FULVUM* INTERACTION: A Versatile Experimental System to Study Plant-Pathogen Interactions. *Annu Rev Phytopathol*. **1999**: 37: 335-367. https://doi.org/10.1146/annurev.phyto.37.1.335

- Joosten MH. Isolation of apoplastic fluid from leaf tissue by the vacuum infiltration-centrifugation technique. Methods *Mol Biol*. **2012**: 835: 603-10. https://doi.org/10.1007/978-1-61779-501-5_38

- Jubic LM, Saile S, Furzer OJ, El Kasmi F, Dangl JL. Help wanted: helper NLRs and plant immune responses. *Curr Opin Plant Biol*. **2019**: 50: 82-94. https://doi.org/10.1016/j.pbi.2019.03.013

- Jupe F, Pritchard L, Etherington GJ, Mackenzie K, Cock PJ, Wright F, Sharma SK, Bolser D, Bryan GJ, Jones JD, Hein I. Identification and localisation of the NB-LRR gene family within the potato genome. *BMC Genomics*. **2012**: 13: 75. https://doi.org/10.1186/1471-2164-13-75

- Kahlon PS, Seta SM, Zander G, Scheikl D, Hückelhoven R, Joosten MHAJ, Stam R. Population studies of the wild tomato species *Solanum chilense* reveal geographically structured major gene-mediated pathogen resistance. *Proc Biol Sci*. **2020**: 287(1941): 20202723. https://doi.org/10.1098/rspb.2020.2723
- Kamoun S, Furzer O, Jones JD, Judelson HS, Ali GS, Dalio RJ, Roy SG, Schena L, Zambounis A, Panabières F, Cahill D, Ruocco M, Figueiredo A, Chen XR, Hulvey J, Stam R, Lamour K, Gijzen M, Tyler BM, Grünwald NJ, Mukhtar MS, Tomé DF, Tör M, van Den Ackerveken G, McDowell J, Daayf F, Fry WE, Lindqvist-Kreuze H, Meijer HJ, Petre B, Ristaino J, Yoshida K, Birch PR, Govers F. The Top 10 oomycete pathogens in molecular plant pathology. *Mol Plant Pathol*. **2015**: 16(4): 413-34. https://doi.org/10.1111/mpp.12190

- Kanwar JS, Kerr EA, Harney PM. Linkage of *Cf-1* to *Cf-11* genes for resistance to tomato leaf mold, *Cladosporium fulvum* Cke. *TGC Report*. **1980**: 30: 20–21.

- Karkute SG, Gujjar RS, Rai A, Akhtar M, Singh M. Genome wide expression analysis of WRKY genes in tomato (*Solanum lycopersicum*) under drought stress. *Plant Gene.* **2018**: 13: 8–17. https://doi.org/10.1016/j.plgene.2017.11.002

- Kaschani F, Shabab M, Bozkurt T, Shindo T, Schornack S, Gu C, Ilyas M, Win J, Kamoun S, van der Hoorn RAL. An effector-targeted protease contributes to defense against *Phytophthora infestans* and is under diversifying selection in natural hosts. *Plant Physiol*. **2010**: 154(4): 1794-804. https://doi.org/10.1104/pp.110.158030

- Kawchuk LM, Hachey J, Lynch DR, Kulcsar F, van Rooijen G, Waterer DR, Robertson A, Kokko E, Byers R, Howard RJ, Fischer R, Prufer D. Tomato *Ve* disease resistance genes encode cell surface-like receptors. *Proc Natl Acad Sci U S A*. **2001**: 98(11): 6511-5. https://doi.org/10.1073/pnas.091114198

- Kerr EA, Patrick ZA, Bailey DL. Resistance in tomato species to new races of leaf mould (*Cladosporium fulvum* Cke). *Hortic. Res*. **1971**: 11: 84–92. https://www.webofscience.com/wos/woscc/full-record/WOS:A1971K996900003

- Kim SH, Qi D, Ashfield T, Helm M, Innes RW. Using decoys to expand the recognition specificity of a plant disease resistance protein. *Science*. **2016**: 351(6274): 684-7. https://doi.org/10.1126/science.aad3436

- Kinene T, Wainaina J, Maina S, Boykin LM. Rooting Trees, Methods for. *Encyclopedia of Evolutionary Biology*. **2016**: 489–93. https://doi.org/10.1016/B978-0-12-800049-6.00215-8

- Koenig D, Jiménez-Gómez JM, Kimura S, Fulop D, Chitwood DH, Headland LR, Kumar R, Covington MF, Devisetty UK, Tat AV, Tohge T, Bolger A, Schneeberger K, Ossowski S, Lanz C, Xiong G, Taylor-Teeples M, Brady SM, Pauly M, Weigel D, Usadel B, Fernie AR, Peng J, Sinha NR, Maloof JN. Comparative transcriptomics reveals patterns of selection in domesticated and wild tomato. *Proc Natl Acad Sci U S A*. **2013**: 110(28): E2655-62. https://doi.org/10.1073/pnas.1309606110

- Kosakovsky Pond SL, Frost SD. Not so different after all: a comparison of methods for detecting amino acid sites under selection. *Mol Biol Evol*. **2005**: 22(5): 1208-22. https://doi.org/10.1093/molbev/msi105

- Kosakovsky Pond SL, Poon AFY, Velazquez R, Weaver S, Hepler NL, Murrell B, Shank SD, Magalis BR, Bouvier D, Nekrutenko A, Wisotsky S, Spielman SJ, Frost SDW, Muse SV. HyPhy 2.5-A Customizable Platform for Evolutionary Hypothesis Testing Using Phylogenies. *Mol Biol Evol*. **2020**: 37(1): 295-299. https://doi.org/10.1093/molbev/msz197
- Kourelis J, Malik S, Mattinson O, Krauter S, Kahlon PS, Paulus JK, van der Hoorn RAL. Evolution of a guarded decoy protease and its receptor in solanaceous plants. *Nat Commun*. **2020**: 11(1): 4393. https://doi.org/10.1038/s41467-024-46611-2

- Kourelis J, Contreras MP, Harant A, Pai H, Lüdke D, Adachi H, Derevnina L, Wu CH, Kamoun S. The helper NLR immune protein NRC3 mediates the hypersensitive cell death caused by the cell-surface receptor Cf-4. *PLoS Genet*. **2022**: 18(9): e1010414. https://doi.org/10.1371/journal.pgen.1010414

- Kourelis J, Schuster M, Demir F, Mattinson O, Krauter S, Kahlon PS, O'Grady R, Royston S, Bravo-Cazar AL, Mooney BC, Huesgen PF, Kamoun S, van der Hoorn RAL. Bioengineering secreted proteases converts divergent *Rcr3* orthologs and paralogs into extracellular immune co-receptors. *Plant Cell*. **2024**: 36(9): 3260-3276. https://doi.org/10.1093/plcell/koae183

- Kourelis J. Interplay between cell-surface receptor and intracellular NLR-mediated immune responses. *New Phytol*. **2023**: 240(6): 2218-2226. https://doi.org/10.1111/nph.19212

- Kraus CM, Munkvold KR, Martin GB. Natural Variation in Tomato Reveals Differences in the Recognition of AvrPto and AvrPtoB Effectors from *Pseudomonas syringae*. *Mol Plant*. **2016**: 9(5): 639-649. https://doi.org/10.1016/j.molp.2016.03.001

- Krüger J, Thomas CM, Golstein C, Dixon MS, Smoker M, Tang S, Mulder L, Jones JD. A tomato cysteine protease required for Cf-2-dependent disease resistance and suppression of auto-necrosis. *Science*. **2002**: 296(5568): 744-7. https://doi.org/10.1126/science.1069288

- Kruijt M, Kip DJ, Joosten MH, Brandwagt BF, de Wit PJ. The *Cf-4* and *Cf-9* resistance genes against *Cladosporium fulvum* are conserved in wild tomato species. *Mol Plant Microbe Interact*. **2005**: 18(9): 1011-21. https://doi.org/10.1094/mpmi-18-1011

- Krujit M. Molecular evolution of *Cladosporium fulvum* disease resistance genes in wild tomato. *Thesis Wageningen University*, *The Netherlands*. **2004**. https://doi.org/10.18174/121591

- Kumar S, Suleski M, Craig JM, Kasprowicz AE, Sanderford M, Li M, Stecher G, Hedges SB. TimeTree 5: An Expanded Resource for Species Divergence Times. *Mol Biol Evol*. **2022**: 39(8): msac174. https://doi.org/10.1093/molbev/msac174

- Kumar S, Stecher G, Suleski M, Sanderford M, Sharma S, Tamura K. MEGA12: Molecular Evolutionary Genetic Analysis Version 12 for Adaptive and Green Computing. *Mol Biol Evol*. **2024**: 41(12): msae263. https://doi.org/10.1093/molbev/msae263

- Lacombe S, Rougon-Cardoso A, Sherwood E, Peeters N, Dahlbeck D, van Esse HP, Smoker M, Rallapalli G, Thomma BP, Staskawicz B, Jones JD, Zipfel C. Interfamily transfer of a plant pattern-recognition receptor confers broad-spectrum bacterial resistance. *Nat Biotechnol*. **2010**: 28(4): 365-9. https://doi.org/10.1038/nbt.1613

- Laflamme B. Recreating or Rcr3ating? Bioengineering homologs of the Rcr3 protease to activate plant immunity. *Plant Cell*. **2024**: 36(9): 2982-2983. https://doi.org/10.1093/plcell/koae187

- Lakovidis M, Soumpourou E, Anderson E, Etherington G, Yourstone S, Thomas C. Genes Encoding Recognition of the *Cladosporium fulvum* Effector Protein Ecp5 Are Encoded at Several Loci in the Tomato Genome. *G3 (Bethesda)*. **2020**: 10(5): 1753-1763. https://doi.org/10.1534/g3.120.401119

- Langford AN. The parasitism of *Cladosporium fulvum* Cooke and the genetics of resistance to it. *Can J Res C*. **1937**: 15: 108–128. https://doi.org/10.1139/cjr37c-008

- Latorre B, Lolas M. First report of bacterial speck caused by *Pseudomonas syringae* in Chile. **Cienc. Investig. Agrar.** 1988: 15: 151.

- Lauge R, Goodwin PH, De Wit PJGM, Joosten MHAJ. Specific HR-associated recognition of secreted proteins from *Cladosporium fulvum* occurs in both host and non-host plants. *The Plant J*. **2000**: 23(6): 735-45. http://dx.doi.org/10.1046/j.1365-313x.2000.00843.x

- Leibman-Markus M, Pizarro L, Schuster S, Lin ZJD, Gershony O, Bar M, Coaker G, Avni A. The intracellular nucleotide-binding leucine-rich repeat receptor (SlNRC4a) enhances immune signalling elicited by extracellular perception. *Plant Cell Environ*. **2018**: 41(10):2313-2327. https://doi.org/10.1111/pce.13347

- Li JB, Sun YD, Liu H, Wang YY, Jia YL, Xu MH. Natural variation of rice blast resistance gene Pi-d2. *Genet Mol Res*. **2015**: 14(1): 1235-49. https://doi.org/10.4238/2015.february.13.2

- Li J, Huang H, Zhu M, Huang S, Zhang W, Dinesh-Kumar SP, Tao X. A Plant Immune Receptor Adopts a Two-Step Recognition Mechanism to Enhance Viral Effector Perception. *Mol Plant*. **2019**: 12(2): 248-262. https://doi.org/10.1016/j.molp.2019.01.005

- Li L, Habring A, Wang K, Weigel D. Atypical Resistance Protein RPW8/HR Triggers Oligomerization of the NLR Immune Receptor RPP7 and Autoimmunity. *Cell Host Microbe*. **2020**: 27(3): 405-417.e6. https://doi.org/10.1016/j.chom.2020.01.012

- Li J, Kaur A, Harrower B, Armstrong M, Dou D, Wang X, Hein I. Identification and mapping of *Rpi-blb4* in diploid wild potato species *Solanum bulbocastanum*. *Crop J*. **2023**: 11(6): 1828–1835. https://doi.org/10.1016/j.cj.2023.08.005

- Liebrand TW, van den Berg GC, Zhang Z, Smit P, Cordewener JH, America AH, Sklenar J, Jones AM, Tameling WI, Robatzek S, Thomma BP, Joosten MH. Receptor-like kinase SOBIR1/EVR interacts with receptor-like proteins in plant immunity against fungal infection. *Proc Natl Acad Sci U S A*. **2013**: 110(24): 10010-5. https://doi.org/10.1073/pnas.1220015110

- Liu Y, Schiff M, Dinesh-Kumar SP. Virus-induced gene silencing in tomato. *Plant J*. **2002**: 31(6): 777-86. https://doi.org/10.1046/j.1365-313x.2002.01394.x

- Liu Y, Schiff M, Marathe R, Dinesh-Kumar SP. Tobacco *Rar1*, *EDS1* and *NPR1/NIM1* like genes are required for *N*-mediated resistance to *tobacco mosaic virus*. *Plant J*. **2002**: 4: 415-29. https://doi.org/10.1046/j.1365-313x.2002.01297.x

- Liu G, Zhao T, You X, Jiang J, Li J, Xu X. Molecular mapping of the *Cf-10* gene by combining SNP/InDel-index and linkage analysis in tomato (*Solanum lycopersicum*). *BMC Plant Biol*. **2019**: 19(1): 15. https://doi.org/10.1186/s12870-018-1616-7

- Liu Y, Zhang X, Yuan G, Wang D, Zheng Y, Ma M, Guo L, Bhadauria V, Peng YL, Liu J. A designer rice NLR immune receptor confers resistance to the rice blast fungus carrying non-corresponding avirulence effectors. *Proc Natl Acad Sci U S A*. **2021**: 118(44): e2110751118. https://doi.org/10.1073/pnas.2110751118

- Lozano-Torres JL, Wilbers RH, Gawronski P, Boshoven JC, Finkers-Tomczak A, Cordewener JH, America AH, Overmars HA, Van 't Klooster JW, Baranowski L, Sobczak M, Ilyas M, van der Hoorn RA, Schots A, de Wit PJ, Bakker J, Goverse A, Smant G. Dual disease resistance mediated by the immune receptor Cf-2 in tomato requires a common virulence target of a fungus and a nematode. *Proc Natl Acad Sci U S A*. **2012**: 109(25): 10119-24. https://doi.org/10.1073/pnas.1202867109

- Lu Y, Tsuda K. Intimate Association of PRR- and NLR-Mediated Signaling in Plant Immunity. *Mol Plant Microbe Interact*. **2021**: 34(1): 3-14. https://doi.org/10.1094/mpmi-08-20-0239-ia

- Luderer R, Takken FLW, De Wit PJGM, Joosten MHAJ. *Cladosporium fulvum* overcomes Cf-2-mediated resistance by producing truncated Avr2 elicitor proteins. *Mol Microbiol*. **2002**: 45(3): 875-84. https://doi.org/10.1046/j.1365-2958.2002.03060.x

- Maidment JHR, Shimizu M, Bentham AR, Vera S, Franceschetti M, Longya A, Stevenson CEM, De la Concepcion JC, Białas A, Kamoun S, Terauchi R, Banfield MJ. Effector target-guided engineering of an integrated domain expands the disease

resistance profile of a rice NLR immune receptor. *Elife*. **2023**: 12: e81123. https://doi.org/10.7554/elife.81123

- Mesarich CH, Okmen Bilal, Rovenich Hanna, Griffiths SA, Wang C, Jashni MK, Mihajlovski A, Collemare J, Hunziker L, Deng CH, van der Burgt A, Beenen HG, Templeton MD, Bradshaw RE, De Wit PJGM. Specific hypersensitive response-associated recognition of new apoplastic effectors from *Cladosporium fulvum* in wild tomato. *Mol Plant Microbe Interact*. **2018**: 31(1): 145-162. https://doi.org/10.1094/MPMI-05-17-0114-FI

- Meyers BC, Kozik A, Griego A, Kuang H, Michelmore RW. Genome-wide analysis of NBS-LRR-encoding genes in *Arabidopsis*. *Plant Cell*. **2003**: 15(4): 809-34. https://doi.org/10.1105/tpc.009308

- Monaghan J, Zipfel C. Plant pattern recognition receptor complexes at the plasma membrane. *Curr Opin Plant Biol*. **2012**: 15(4): 349-57. https://doi.org/10.1016/j.pbi.2012.05.006

- Montesinos-Navarro A, Wig J, Pico FX, Tonsor SJ. Arabidopsis thaliana populations show clinal variation in a climatic gradient associated with altitude. *New Phytol*. **2011**: 189(1): 282-94. https://doi.org/10.1111/j.1469-8137.2010.03479.x

- Mooney BC, van der Hoorn RAL. Novel structural insights at the extracellular plant-pathogen interface. *Curr Opin Plant Biol*. **2024**: 82: 102629. https://doi.org/10.1016/j.pbi.2024.102629

- Murrell B, Wertheim JO, Moola S, Weighill T, Scheffler K, Kosakovsky Pond SL. Detecting individual sites subject to episodic diversifying selection. *PLoS Genet*. **2012**: 8(7): e1002764. https://doi.org/10.1371/journal.pgen.1002764

- Murrell B, Moola S, Mabona A, Weighill T, Sheward D, Kosakovsky Pond SL, Scheffler K. FUBAR: a fast, unconstrained bayesian approximation for inferring selection. *Mol Biol Evol*. **2013**: 30(5): 1196-205. https://doi.org/10.1093/molbev/mst030

- Murrell B, Weaver S, Smith MD, Wertheim JO, Murrell S, Aylward A, Eren K, Pollner T, Martin DP, Smith DM, Scheffler K, Kosakovsky Pond SL. Gene-wide identification of episodic selection. *Mol Biol Evol.* **2015**: 32(5): 1365-71. https://doi.org/10.1093/molbev/msv035

- Neuwirth E. RColorBrewer: ColorBrewer Palettes. *CRAN-R package v 1.1-3*. **2022**. https://cran.r-project.org/package=RColorBrewer

- Ngou BPM, Ahn HK, Ding P, Jones JDG. Mutual potentiation of plant immunity by cell-surface and intracellular receptors. *Nature*. **2021**: 592(7852): 110-115. https://doi.org/10.1038/s41586-021-03315-7

- Ngou BPM, Jones JDG, Ding P. Plant immune networks. *Trends Plant Sci*. **2022**: 27(3): 255-273. https://doi.org/10.1016/j.tplants.2021.08.012

- Nürnberger T, Nennstiel D, Jabs T, Sacks WR, Hahlbrock K, Scheel D. High affinity binding of a fungal oligopeptide elicitor to parsley plasma membranes triggers multiple defence responses. *Cell*. **1994**: 78(3): 449-60. https://doi.org/10.1016/0092-8674(94)90423-5

- Panter SN, Hammond-Kosack KE, Harrison K, Jones JD, Jones DA. Developmental control of promoter activity is not responsible for mature onset of *Cf-9B*-mediated resistance to leaf mould in tomato. *Mol Plant Microbe Interact*. **2002**: 15(11): 1099-107. https://doi.org/10.1094/mpmi.2002.15.11.1099

- Parniske M, Hammond-Kosack KE, Golstein C, Thomas CM, Jones DA, Harrison K, Wulff BB, Jones JD. Novel disease resistance specificities result from sequence exchange between tandemly repeated genes at the *Cf-4/9* locus of tomato. *Cell*. **1997**: 91(6): 821-32. https://doi.org/10.1016/s0092-8674(00)80470-5

- Parniske M, Wulff BB, Bonnema G, Thomas CM, Jones DA, Jones JD. *Homologs of the Cf-9 disease resistance gene* (*Hcr9*s) are present at multiple loci on the short arm of tomato chromosome 1. *Mol Plant Microbe Interact*. **1999**: 12(2): 93-102. https://doi.org/10.1094/mpmi.1999.12.2.93

- Paulus JK, Kourelis J, Ramasubramanian S, Homma F, Godson A, Hörger AC, Hong TN, Krahn D, Ossorio Carballo L, Wang S, Win J, Smoker M, Kamoun S, Dong S, van der Hoorn RAL. Extracellular proteolytic cascade in tomato activates immune protease Rcr3. *Proc Natl Acad Sci U S A*. **2020**: 117(29): 17409-17417. https://doi.org/10.1073/pnas.1921101117

- Pebesma EJ, Bivand RS. Classes and methods for spatial data in R. *CRAN-R packages*. **2005**. https://cran.r-project.org/package=sp

- Pedley KF, Martin GB. Molecular basis of Pto-mediated resistance to bacterial speck disease in tomato. *Annu Rev Phytopathol*. **2003**: 41: 215-43. https://doi.org/10.1146/annurev.phyto.41.121602.143032

- Pei T, Ge S, Wang Z, Wang Y. Transcription factor analysis of the Cf-19-mediated resistance response in tomato infected by Cladosporium fulvum. *Sci Hortic*. **2024**: 325: 112681. http://dx.doi.org/10.1016/j.scienta.2023.112681

- Peng HC, Kaloshian I. The tomato leucine-rich repeat receptor-like kinases SlSERK3A and SlSERK3B have overlapping functions in bacterial and nematode innate immunity. *PLoS One*. **2014**: 9(3): e93302. https://doi.org/10.1371/journal.pone.0093302

- Peralta IE, Spooner DM, Knapp S. Taxonomy of wild tomatoes and their relatives (*Solanum* sect. *Lycopersicoides*, sect. *Juglandifolia*, sect. *Lycopersicon*; *Solanaceae*). *Am. Soc. Plant Taxonomists*. **2008**: 84: 151-160. https://www.cabidigitallibrary.org/doi/full/10.5555/20103064022

- Pizarro L, Leibman-Markus M, Gupta R, Kovetz N, Shtein I, Bar E, Davidovich-Rikanati R, Zarivach R, Lewinsohn E, Avni A, Bar M. A gain of function mutation in SlNRC4a enhances basal immunity resulting in broad-spectrum disease resistance. *Commun Biol*. **2020**: 3(1): 404. https://doi.org/10.1038/s42003-020-01130-w

- Postma J, Liebrand TW, Bi G, Evrard A, Bye RR, Mbengue M, Kuhn H, Joosten MH, Robatzek S. Avr4 promotes Cf-4 receptor-like protein association with the BAK1/SERK3 receptor-like kinase to initiate receptor endocytosis and plant immunity. *New Phytol*. **2016**: 210(2): 627-42. https://doi.org/10.1111/nph.13802

- Qi Y, Tsuda K, Glazebrook J, Katagiri F. Physical association of pattern-triggered immunity (PTI) and effector-triggered immunity (ETI) immune receptors in

Arabidopsis. *Mol Plant Pathol*. **2011**: 12(7): 702-8. https://doi.org/10.1111/j.1364-3703.2010.00704.x

- Richau KH, Kaschani F, Verdoes M, Pansuriya TC, Niessen S, Stüber K, Colby T, Overkleeft HS, Bogyo M, van der Hoorn RA. Subclassification and biochemical analysis of plant papain-like cysteine proteases displays subfamily-specific characteristics. *Plant Physiol*. **2012**: 158(4): 1583-99. https://doi.org/10.1104/pp.112.194001

- Roberts R, Mainiero S, Powell AF, Liu AE, Shi K, Hind SR, Strickler SR, Collmer A, Martin GB. Natural variation for unusual host responses and flagellin-mediated immunity against *Pseudomonas syringae* in genetically diverse tomato accessions. *New Phytol*. **2019**: 223(1): 447-461. https://doi.org/10.1111/nph.15788

- Rodriguez F, Wu F, Ané C, Tanksley S, Spooner DM. Do potatoes and tomatoes have a single evolutionary history, and what proportion of the genome supports this history? *BMC Evol Biol*. **2009**: 9: 191. https://doi.org/10.1186/1471-2148-9-191

- Ron M, Avni A. The receptor for the fungal elicitor ethylene-inducing xylanase is a member of a resistance-like gene family in tomato. *Plant Cell*. **2004**: 6(6): 1604-15. https://doi.org/10.1105/tpc.022475
- Rooney HC, Van't Klooster JW, van der Hoorn RA, Joosten MH, Jones JD, de Wit PJ. *Cladosporium* Avr2 inhibits tomato Rcr3 protease required for Cf-2-dependent disease resistance. *Science*. **2005**: 308(5729): 1783-6. https://doi.org/10.1126/science.1111404

- Schornack S, van Damme M, Bozkurt TO, Cano LM, Smoker M, Thines M, Gaulin E, Kamoun S, Huitema E. Ancient class of translocated oomycete effectors targets the host nucleus. *Proc Natl Acad Sci U S A*. **2010**: 107(40): 17421-6. https://doi.org/10.1073/pnas.1008491107

- Schuster M, Eisele S, Armas-Egas L, Kessenbrock T, Kourelis J, Kaiser M, van der Hoorn RAL. Enhanced late blight resistance by engineering an EpiC2B-insensitive immune protease. *Plant Biotechnol J*. **2024**: 22(2): 284-286. https://doi.org/10.1111/pbi.14209

- Schwessinger B, Roux M, Kadota Y, Ntoukakis V, Sklenar J, Jones A, Zipfel C. Phosphorylation-dependent differential regulation of plant growth, cell death, and innate immunity by the regulatory receptor-like kinase BAK1. *PLoS Genet*. **2011**: 7(4): e1002046. https://doi.org/10.1371/journal.pgen.1002046

- Schwessinger B, Bahar O, Thomas N, Holton N, Nekrasov V, Ruan D, Canlas PE, Daudi A, Petzold CJ, Singan VR, Kuo R, Chovatia M, Daum C, Heazlewood JL, Zipfel C, Ronald PC. Transgenic expression of the dicotyledonous pattern recognition receptor EFR in rice leads to ligand-dependent activation of defence responses. *PLoS Pathog*. **2015**: 11(3): e1004809. https://doi.org/10.1371/journal.ppat.1004809

- Seear PJ, Dixon MS. Variable leucine-rich repeats of tomato disease resistance genes Cf-2 and Cf-5 determine specificity. *Mol Plant Pathol*. **2003**: 4(3): 199-202. https://doi.org/10.1046/j.1364-3703.2003.00162.x
- Senthil-Kumar M, Mysore KS. Virus-induced gene silencing can persist for more than 2 years and also be transmitted to progeny seedlings in *Nicotiana benthamiana*

and tomato. *Plant Biotechnol J*. **2011**: 9(7): 797-806. https://doi.org/10.1111/j.1467-7652.2011.00589.x

- Senthil-Kumar M, Hema R, Anand A, Kang L, Udayakumar M, Mysore KS. A systematic study to determine the extent of gene silencing in *Nicotiana benthamiana* and other Solanaceae species when heterologous gene sequences are used for virus-induced gene silencing. *New Phytol*. **2007**: 176(4): 782-791. https://doi.org/10.1111/j.1469-8137.2007.02225.x

- Seo E, Kim S, Yeom SI, Choi D. Genome-Wide Comparative Analyses Reveal the Dynamic Evolution of Nucleotide-Binding Leucine-Rich Repeat Gene Family among Solanaceae Plants. *Front Plant Sci*. **2016**: 7: 1205. https://doi.org/10.3389/fpls.2016.01205

- Shabab M, Shindo T, Gu C, Kaschani F, Pansuriya T, Chintha R, Harzen A, Colby T, Kamoun S, van der Hoorn RA. Fungal effector protein AVR2 targets diversifying defense-related cys proteases of tomato. *Plant Cell*. **2008**: 20(4): 1169-83. https://doi.org/10.1105/tpc.107.056325

- Shen LL, Waheed A, Wang YP, Nkurikiyimfura O, Wang ZH, Yang LN, Zhan J. Multiple Mechanisms Drive the Evolutionary Adaptation of *Phytophthora infestans* Effector Avr1 to Host Resistance. *J Fungi (Basel)*. **2021**: 7(10): 789. https://doi.org/10.3390/jof7100789

- Shindo T, van der Hoorn RA. Papain-like cysteine proteases: key players at molecular battlefields employed by both plants and their invaders. *Mol Plant Pathol*. **2008**: 9(1): 119-25. https://doi.org/10.1111/j.1364-3703.2007.00439.x

- Shindo T, Misas-Villamil JC, Hörger AC, Song J, van der Hoorn RA. A role in immunity for Arabidopsis cysteine protease RD21, the ortholog of the tomato immune protease C14. *PLoS One*. **2012**: 7(1): e29317. https://doi.org/10.1371/journal.pone.0029317

- Shindo T, Kaschani F, Yang F, Kovács J, Tian F, Kourelis J, Hong TN, Colby T, Shabab M, Chawla R, Kumari S, Ilyas M, Hörger AC, Alfano JR, van der Hoorn RA. Screen of Non-annotated Small Secreted Proteins of *Pseudomonas syringae* Reveals a Virulence Factor That Inhibits Tomato Immune Proteases. *PLoS Pathog*. **2016**: 12(9): e1005874. https://doi.org/10.1371/journal.ppat.1005874

- Simko I, Haynes KG, Ewing EE, Costanzo S, Christ BJ, Jones RW. Mapping genes for resistance to *Verticillium albo-atrum* in tetraploid and diploid potato populations using haplotype association tests and genetic linkage analysis. *Mol Genet Genomics*. **2004**: 271(5): 522-31. https://doi.org/10.1007/s00438-004-1010-z

- Snoeck S, Lee HK, Schmid MW, Bender KW, Neeracher MJ, Fernández-Fernández AD, Santiago J, Zipfel C. Leveraging coevolutionary insights and AI-based structural modeling to unravel receptor-peptide ligand-binding mechanisms. *Proc Natl Acad Sci U S A*. **2024**: 121(33): e2400862121. https://doi.org/10.1073/pnas.2400862121

- Song WY, Wang GL, Chen LL, Kim HS, Pi LY, Holsten T, Gardner J, Wang B, Zhai WX, Zhu LH, Fauquet C, Ronald P. A receptor kinase-like protein encoded by the rice disease resistance gene, Xa21. *Science*. **1995**: 270(5243): 1804-6. https://doi.org/10.1126/science.270.5243.1804

- Song J, Win J, Tian M, Schornack S, Kaschani F, Ilyas M, van der Hoorn RA, Kamoun S. Apoplastic effectors secreted by two unrelated eukaryotic plant pathogens target the tomato defense protease Rcr3. *Proc Natl Acad Sci U S A*. **2009**: 106(5): 1654-9. https://doi.org/10.1073/pnas.0809201106

- Song Y, Liu L, Wang Y, Valkenburg DJ, Zhang X, Zhu L, Thomma BPHJ. Transfer of tomato immune receptor Ve1 confers Ave1-dependent *Verticillium* resistance in tobacco and cotton. *Plant Biotechnol J.* **2018**: 16(2): 638-648. https://doi.org/10.1111/pbi.12804

- Sugihara Y, Kourelis J, Contreras MP, Pai H, Harant A, Selvaraj M, Toghani A, Martínez-Anaya C, Kamoun S. Helper NLR immune protein NRC3 evolved to evade inhibition by a cyst nematode virulence effector. *PLoS Genet*. **2025**: 21(4): e1011653. https://doi.org/10.1371/journal.pgen.1011653

- Sun Y, Li L, Macho AP, Han Z, Hu Z, Zipfel C, Zhou JM, Chai J. Structural basis for flg22-induced activation of the *Arabidopsis* FLS2-BAK1 immune complex. *Science*. **2013**: 342(6158): 624-8. https://doi.org/10.1126/science.1243825

- Tang J, Lin J, Yang Y, Chen T, Ling X, Zhang B, Chang Y. Ectopic expression of a *Ve* homolog *VvVe* gene from *Vitis vinifera* enhances defense response to *Verticillium dahliae* infection in tobacco. *Gene*. **2016**: 576(1 Pt 3): 492-8. https://doi.org/10.1016/j.gene.2015.10.068

- Tena G, Asai T, Chiu WL, Sheen J. Plant mitogen-activated protein kinase signalling cascades. *Curr Opin Plant Biol*. **2001**: 4(5): 392-400. https://doi.org/10.1016/s1369-5266(00)00191-6

- Thomas CM, Jones DA, Parniske M, Harrison K, Balint-Kurti PJ, Hatzixanthis K, Jones JD. Characterisation of the tomato *Cf-4* gene for resistance to *Cladosporium fulvum* identifies sequences that determine recognitional specificity in Cf-4 and Cf-9. *Plant Cell*. **1997**: 9(12): 2209-24. https://doi.org/10.1105/tpc.9.12.2209

- Thomas CM, Dixon MS, Parniske M, Golstein C, Jones JD. Genetic and molecular analysis of tomato *Cf* genes for resistance to *Cladosporium fulvum*. *Philos Trans R Soc Lond B Biol Sci*. **1998**: 353(1374): 1413-24. https://doi.org/10.1098/rstb.1998.0296

- Thomas CL, Jones L, Baulcombe DC, Maule AJ. Size constraints for targeting post-transcriptional gene silencing and for RNA-directed methylation in *Nicotiana benthamiana* using a potato virus X vector. *Plant J*. **2001**: 25(4): 417-25. https://doi.org/10.1046/j.1365-313x.2001.00976.x

- Thomma BP, van Esse HP, Crous PW, DE Wit PJ. *Cladosporium fulvum* (syn. *Passalora fulva*), a highly specialized plant pathogen as a model for functional studies on plant pathogenic *Mycosphaerellaceae*. *Mol Plant Pathol*. **2005**: 6(4): 379-93. https://doi.org/10.1111/j.1364-3703.2005.00292.x

- Thomma BP, Nürnberger T, Joosten MH. Of PAMPs and effectors: the blurred PTI-ETI dichotomy. *Plant Cell*. **2011**: 23(1): 4-15. https://doi.org/10.1105/tpc.110.082602

- Tian M, Benedetti B, Kamoun S. A Second Kazal-like protease inhibitor from *Phytophthora infestans* inhibits and interacts with the apoplastic pathogenesis-

related protease P69B of tomato. *Plant Physiol*. **2005**: 138(3): 1785-93. https://doi.org/10.1104/pp.105.061226

- Tian M, Win J, Song J, van der Hoorn R, van der Knaap E, Kamoun S. A *Phytophthora infestans* cystatin-like protein targets a novel tomato papain-like apoplastic protease. *Plant Physiol*. **2007**: 143(1): 364-77. https://doi.org/10.1104/pp.106.090050

- Tian H, Wu Z, Chen S, Ao K, Huang W, Yaghmaiean H, Sun T, Xu F, Zhang Y, Wang S, Li X, Zhang Y. Activation of TIR signalling boosts pattern-triggered immunity. *Nature*. **2021**: 598(7881): 500-503. https://doi.org/10.1038/s41586-021-03987-1

- Torres Ascurra YC, Zhang L, Toghani A, Hua C, Rangegowda NJ, Posbeyikian A, Pai H, Lin X, Wolters PJ, Wouters D, de Blok R, Steigenga N, Paillart MJM, Visser RGF, Kamoun S, Nürnberger T, Vleeshouwers VGAA. Functional diversification of a wild potato immune receptor at its centre of origin. *Science*. **2023**: 381(6660): 891-897. https://doi.org/10.1126/science.adg5261

- Torres Ascurra YC, Wouters D, Visser RGF, Nüernberger T, Vlesshouwers VGAA. Stacking of PRRs in potato to achieve enhanced resistance against *Phytophthora infestans*. *Biorxiv*. **2023**. http://dx.doi.org/10.1101/2023.09.07.556738
- Untergasser A, Cutcutache I, Koressaar T, Ye J, Faircloth BC, Remm M, Rozen SG. Primer3--new capabilities and interfaces. *Nucleic Acids Res*. **2012**: 40(15): e115. https://doi.org/10.1093/nar/gks596

- van den Ackerveken GFJM, Vossen JPMJ, De Wit PJGM. The AVR9 race-specific elicitor of *Cladosporium fulvum* is processed by endogenous and plant proteases. *Plant Physiol*. **1993**: 103: 91–96. https://doi.org/10.1104/pp.103.1.91

- van der Biezen EA, Jones JD. Plant disease-resistance proteins and the gene-for-gene concept. *Trends Biochem Sci*. **1998**: 23(12): 454-6. https://doi.org/10.1016/s0968-0004(98)01311-5

- van der Burgh AM, Joosten MHAJ. Plant Immunity: Thinking Outside and Inside the Box. *Trends Plant Sci.* **2019**: 24(7): 587-601. https://doi.org/10.1016/j.tplants.2019.04.009

- van der Burgh AM, Postma J, Robatzek S, Joosten MHAJ. Kinase activity of SOBIR1 and BAK1 is required for immune signalling. *Mol Plant Pathol*. **2019**: 20(3): 410-422. https://doi.org/10.1111/mpp.12767

- van der Hoorn RA, Kamoun S. From Guard to Decoy: a new model for perception of plant pathogen effectors. *Plant Cell*. **2008**: 20(8): 2009-17. https://doi.org/10.1105/tpc.108.060194

- van der Hoorn RA, Laurent F, Roth R, De Wit PJ. Agroinfiltration is a versatile tool that facilitates comparative analyses of *Avr9/Cf-9*-induced and *Avr4/Cf-4*-induced necrosis. *Mol Plant Microbe Interact*. **2000**: 13(4): 439-46. https://doi.org/10.1094/mpmi.2000.13.4.439

- van der Hoorn RA, Kruijt M, Roth R, Brandwagt BF, Joosten MH, De Wit PJ. Intragenic recombination generated two distinct *Cf* genes that mediate *AVR9*

recognition in the natural population of *Lycopersicon pimpinellifolium*. *Proc Natl Acad Sci U S A*. **2001**: 98(18): 10493-8. https://doi.org/10.1073/pnas.181241798

- van der Hoorn RA, Roth R, De Wit PJ. Identification of distinct specificity determinants in resistance protein Cf-4 allows construction of a Cf-9 mutant that confers recognition of avirulence protein Avr4. *Plant Cell*. **2001**: 13(2): 273-85. https://doi.org/10.1105/tpc.13.2.273

- van der Vossen EA, Gros J, Sikkema A, Muskens M, Wouters D, Wolters P, Pereira A, Allefs S. The *Rpi-blb2* gene from *Solanum bulbocastanum* is an *Mi-1* gene homolog conferring broad-spectrum late blight resistance in potato. *Plant J*. **2005**: 44(2): 208-22. https://doi.org/10.1111/j.1365-313x.2005.02527.x

- van Esse HP, Van't Klooster JW, Bolton MD, Yadeta KA, van Baarlen P, Boeren S, Vervoort J, de Wit PJ, Thomma BP. The *Cladosporium fulvum* virulence protein Avr2 inhibits host proteases required for basal defence. *Plant Cell*. **2008**: 20(7): 1948-63. https://doi.org/10.1105/tpc.108.059394

- van Treuren R, Magda A, Hoekstra R, Van Hintum TJL. Genetic and economic aspects of marker-assisted reduction of redundancy from a wild potato germplasm collection. *Genet. Resour. Crop Evol.* **2004**: 51: 277–290. 10.1023/B:GRES.0000024013.27067.ac

- Van't Klooster JW, Van der Kamp MW, Vervoort J, Beekwilder J, Boeren S, Joosten MH, Thomma BP, De Wit PJ. Affinity of Avr2 for tomato cysteine protease Rcr3 correlates with the Avr2-triggered Cf-2-mediated hypersensitive response. *Mol Plant Pathol*. **2011**: 12(1): 21-30. https://doi.org/10.1111/j.1364-3703.2010.00647.x

- Varshney RK, Tuberosa R. Translational genomics in crop breeding for biotic stress resistance: an introduction. *Transl. Genomics Crop Breed.: Biot. Stress.* **2013***:* 1: 1–9. https://oar.icrisat.org/7590/7/ch1.pdf

- Velásquez AC, Chakravarthy S, Martin GB. Virus-induced gene silencing (VIGS) in *Nicotiana benthamiana* and tomato. *J Vis Exp*. **2009**: 28: 1292. https://doi.org/10.3791/1292

- Videira S, Groenewald J, Nakashima C, Braun U, Barreto RW, De Wit PJGM, Crous PW. Mycosphaerellaceae – chaos or clarity? *Stud. Mycol.* **2017**: 87: 257–421. https://doi.org/10.1016/j.simyco.2017.09.003

- Vincent H, Wiersema J, Kell S, Fielder H, Dobbie S, Castañeda-Álvarez NP, Guarino L, Eastwood R, LeÖn B. A prioritized crop wild relative inventory to help underpin global food security. *Biol. Conserv*. **2013**: 167: 265–275. https://doi.org/10.1016/j.biocon.2013.08.011

- Vleeshouwers VGAA, van Dooijeweert W, Govers F, Kamoun S, Colon LT. Does basal PR gene expression in *Solanum* species contribute to non-specific resistance to *Phytophthora infestans*? *Physiol and Mol Plant Pathol*. **2000**: 57(1): 35-42. https://doi.org/10.1006/pmpp.2000.0278

- Vinatzer BA, Patocchi A, Gianfranceschi L, Tartarini S, Zhang HB, Gessler C, Sansavini S. Apple contains receptor-like genes homologs to the *Cladosporium fulvum* resistance gene family of tomato with a cluster of genes cosegregating with

Vf apple scab resistance. *Mol Plant Microbe Interact*. **2001**: 14(4): 508-15. https://doi.org/10.1094/mpmi.2001.14.4.508

- Wang G, Fiers M, Ellendorff U, Wang Z, de Wit PJ, Angenent GC, Thomma BPHJ. The diverse roles of extracellular leucine-rich repeat-containing receptor-like proteins in plants. *Crit. Rev. Plant Sci*. **2010**: 29: 285–299. https://doi.org/10.1080/07352689.2010.502082

- Wang Y, Xu Y, Sun Y, Wang H, Qi J, Wan B, Ye W, Lin Y, Shao Y, Dong S, Tyler BM, Wang Y. Leucine-rich repeat receptor-like gene screen reveals that *Nicotiana* RXEG1 regulates glycoside hydrolase 12 MAMP detection. *Nat Commun*. **2018**: 9(1): 594. https://doi.org/10.1038/s41467-018-03010-8

- Wang Y, Zhao Y, Bollas A, Wang Y, Au KF. Nanopore sequencing technology, bioinformatics and applications. *Nat Biotechnol*. **2021**: 39(11): 1348-1365. https://doi.org/10.1038/s41587-021-01108-x

- Wang S, Xing R, Wang Y, Shu H, Fu S, Huang J, Paulus JK, Schuster M, Saunders DGO, Win J, Vleeshouwers V, Wang Y, Zheng X, van der Hoorn RAL, Dong S. Cleavage of a pathogen apoplastic protein by plant subtilases activates host immunity. *New Phytol*. **2021**: 229(6): 3424-3439. https://doi.org/10.1111/nph.17120

- Wang Y, Brown LH, Adams TM, Cheung YW, Li J, Young V, Todd DT, Armstrong MR, Neugebauer K, Kaur A, Harrower B, Oome S, Wang X, Bayer M, Hein I. SMRT-AgRenSeq-d in potato (*Solanum tuberosum*) as a method to identify candidates for the nematode resistance Gpa5. *Hortic Res*. **2023**: 10(11): uhad211. https://doi.org/10.1093/hr/uhad211

- Wang H, Zhao D, Wei J, Xiong Y, Chen S, Liu J, Liu Z, Du J, Li C. A *Phytophthora infestans* RXLR effector PiAVR3b suppresses plant immunity by perturbing jasmonic acid biosynthesis. *Sci Hortic*. **2024**: 331: 113122. https://doi.org/10.1016/j.scienta.2024.113122

- Wawra S, Trusch F, Matena A, Apostolakis K, Linne U, Zhukov I, Stanek J, Koźmiński W, Davidson I, Secombes CJ, Bayer P, van West P. The RxLR Motif of the Host Targeting Effector AVR3a of *Phytophthora infestans* Is Cleaved before Secretion. *Plant Cell*. **2017**: 29(6): 1184-1195. https://doi.org/10.1105/tpc.16.00552

- Weaver S, Shank SD, Spielman SJ, Li M, Muse SV, Kosakovsky Pond SL. Datamonkey 2.0: A Modern Web Application for Characterizing Selective and Other Evolutionary Processes. *Mol Biol Evol*. **2018**: 35(3): 773-777. https://doi.org/10.1093/molbev/msx335

- Weber E, Engler C, Gruetzner R, Werner S, Marillonnet S. A modular cloning system for standardized assembly of multigene constructs. PLoS One. 2011 Feb 18;6(2): e16765. https://doi.org/10.1371/journal.pone.0016765

- Wickham H, François R, Henry L, Müller K, Vaughan D. dplyr: A grammar of data manipulation. *CRAN-R packages*. **2023**. https://CRAN.R-project.org/package=dplyr

- Wickham H. ggplot2: Elegant Graphics for Data Analysis. *Springer-Verlag NY*. **2016**. https://doi.org/10.1007/978-3-319-24277-4_9

- Williams TA. Evolution: rooting the eukaryotic tree of life. *Curr Biol*. **2014**: 24(4): R151-2. https://doi.org/10.1016/j.cub.2014.01.026

- Witek K, Lin X, Karki HS, Jupe F, Witek AI, Steuernagel B, Stam R, van Oosterhout C, Fairhead S, Heal R, Cocker JM, Bhanvadia S, Barrett W, Wu CH, Adachi H, Song T, Kamoun S, Vleeshouwers VGAA, Tomlinson L, Wulff BBH, Jones JDG. A complex resistance locus in *Solanum americanum* recognises a conserved *Phytophthora* effector. *Nat Plants*. **2021**: 7(2): 198-208. https://doi.org/10.1038/s41477-021-00854-9

- Wu CH, Abd-El-Haliem A, Bozkurt TO, Belhaj K, Terauchi R, Vossen JH, Kamoun S. NLR network mediates immunity to diverse plant pathogens. *Proc Natl Acad Sci U S A*. **2017**: 114(30): 8113-8118. https://doi.org/10.1073/pnas.1702041114

- Wu Z, Li M, Dong OX, Xia S, Liang W, Bao Y, Wasteneys G, Li X. Differential regulation of TNL-mediated immune signalling by redundant helper CNLs. *New Phytol*. **2019**: 222(2): 938-953. https://doi.org/10.1111/nph.15665

- Wulff BB, Thomas CM, Smoker M, Grant M, Jones JD. Domain swapping and gene shuffling identify sequences required for induction of an Avr-dependent hypersensitive response by the tomato Cf-4 and Cf-9 proteins. *Plant Cell*. **2001**: 13(2): 255-72. https://doi.org/10.1105/tpc.13.2.255

- Xu X, Pan S, Cheng S, Zhang B, Mu D, Ni P, Zhang G, Yang S, Li R, Wang J, Orjeda G, Guzman F, Torres M, Lozano R, Ponce O, Martinez D, De la Cruz G, Chakrabarti SK, Patil VU, Skryabin KG, Kuznetsov BB, Ravin NV, Kolganova TV, Beletsky AV, Mardanov AV, Di Genova A, Bolser DM, Martin DM, Li G, Yang Y, Kuang H, Hu Q, Xiong X, Bishop GJ, Sagredo B, Mejía N, Zagorski W, Gromadka R, Gawor J, Szczesny P, Huang S, Zhang Z, Liang C, He J, Li Y, He Y, Xu J, Zhang Y, Xie B, Du Y, Qu D, Bonierbale M, Ghislain M, Herrera Mdel R, Giuliano G, Pietrella M, Perrotta G, Facella P, O'Brien K, Feingold SE, Barreiro LE, Massa GA, Diambra L, Whitty BR, Vaillancourt B, Lin H, Massa AN, Geoffroy M, Lundback S, DellaPenna D, Buell CR, Sharma SK, Marshall DF, Waugh R, Bryan GJ, Destefanis M, Nagy I, Milbourne D, Thomson SJ, Fiers M, Jacobs JM, Nielsen KL, Sønderkær M, Iovene M, Torres GA, Jiang J, Veilleux RE, Bachem CW, de Boer J, Borm T, Kloosterman B, van Eck H, Datema E, Hekkert Bt, Goverse A, van Ham RC, Visser RG. Genome sequence and analysis of the tuber crop potato. *Nature*. **2011**: 475(7355): 189-95. https://doi.org/10.1038/nature10158

- Yang L, McLellan H, Naqvi S, He Q, Boevink PC, Armstrong M, Giuliani LM, Zhang W, Tian Z, Zhan J, Gilroy EM, Birch PR. Potato NPH3/RPT2-Like Protein StNRL1, Targeted by a *Phytophthora infestans* RXLR Effector, Is a Susceptibility Factor. *Plant Physiol*. **2016**: 171(1): 645-57. https://doi.org/10.1104/pp.16.00178

- Yang L, Ouyang HB, Fang ZG, Zhu W, Wu EJ, Luo GH, Shang LP, Zhan J. Evidence for intragenic recombination and selective sweep in an effector gene of *Phytophthora infestans*. *Evol Appl*. **2018**: 11(8): 1342-1353. https://doi.org/10.1111/eva.12629

- Yang LN, Liu H, Duan GH, Huang YM, Liu S, Fang ZG, Wu EJ, Shang L, Zhan J. The *Phytophthora infestans* AVR2 Effector Escapes R2 Recognition Through Effector Disordering. *Mol Plant Microbe Interact*. **2020**: 33(7): 921-931. https://doi.org/10.1094/mpmi-07-19-0179-r

- Yang LN, Ouyang H, Nkurikiyimfura O, Fang H, Waheed A, Li W, Wang YP, Zhan J. Genetic variation along an altitudinal gradient in the *Phytophthora infestans* effector gene *Pi02860*. *Front Microbiol*. **2022**: 13: 972928. https://doi.org/10.3389/fmicb.2022.972928

- Yuan M, Jiang Z, Bi G, Nomura K, Liu M, Wang Y, Cai B, Zhou JM, He SY, Xin XF. Pattern-recognition receptors are required for NLR-mediated plant immunity. *Nature*. **2021**: 592(7852): 105-109. https://doi.org/10.1038/s41586-021-03316-6

- Yuan M, Cai B, Xin XF. Plant immune receptor pathways as a united front against pathogens. *PLoS Pathog*. **2023**: 19(2): e1011106. https://doi.org/10.1371/journal.ppat.1011106

- Zaborowska J, Łabiszak B, Perry A, Cavers S, Wachowiak W. Candidate Genes for the High-Altitude Adaptations of Two Mountain Pine Taxa. *Int J Mol Sci*. **2021**: 22(7): 3477. https://doi.org/10.3390/ijms22073477

- Zdrzałek R, Xi Y, Langner T, Bentham AR, Petit-Houdenot Y, De la Concepcion JC, Harant A, Shimizu M, Were V, Talbot NJ, Terauchi R, Kamoun S, Banfield MJ. Bioengineering a plant NLR immune receptor with a robust binding interface toward a conserved fungal pathogen effector. *Proc Natl Acad Sci U S A*. **2024**: 121(28): e2402872121. https://doi.org/10.1073/pnas.2402872121

- Zhang D, Li H, Liu G, Xie L, Feng G, Xu X. Mapping of the *Cladosporium fulvum* resistance gene *Cf-16*, a major gene involved in leaf mold disease in tomato. *Front Genet*. **2023**: 14: 1219898. https://doi.org/10.3389/fgene.2023.1219898

- Zhang N, Gan J, Carneal L, González-Tobón J, Filiatrault M, Martin GB. Helper NLRs Nrc2 and Nrc3 act codependently with Prf/Pto and activate MAPK signaling to induce immunity in tomato. *Plant J*. **2024**: 117(1): 7-22. https://doi.org/10.1111/tpj.16502

- Zhang L, Kars I, Essenstam B, Liebrand TW, Wagemakers L, Elberse J, Tagkalaki P, Tjoitang D, van den Ackerveken G, van Kan JA. Fungal endopolygalacturonases are recognised as microbe-associated molecular patterns by the arabidopsis receptor-like protein RESPONSIVENESS TO BOTRYTIS POLYGALACTURONASES1. *Plant Physiol*. **2014**: 164(1): 352-64. https://doi.org/10.1104/pp.113.230698

- Zhang T, Jin Y, Zhao JH, Gao F, Zhou BJ, Fang YY, Guo HS. Host-Induced Gene Silencing of the Target Gene in Fungal Cells Confers Effective Resistance to the Cotton Wilt Disease Pathogen Verticillium dahliae. *Mol Plant*. **2016**: 9(6): 939-42. https://doi.org/10.1016/j.molp.2016.02.008

- Zhang W, Planas-Marquès M, Mazier M, Šimkovicová M, Rocafort M, Mantz M, Huesgen PF, Takken FLW, Stintzi A, Schaller A, Coll NS, Valls M. The tomato P69 subtilase family is involved in resistance to bacterial wilt. *Plant J*. **2024**: 118(2): 388-404. https://doi.org/10.1111/tpj.16613

- Zhao T, Jiang J, Liu G, He S, Zhang H, Chen X, Li J, Xu X. Mapping and candidate gene screening of tomato *Cladosporium fulvum*-resistant gene *Cf-19*, based on high-throughput sequencing technology. *BMC Plant Biol*. **2016**: 16: 51. https://doi.org/10.1186/s12870-016-0737-0

- Zhao T, Liu W, Zhao Z, Yang H, Bao Y, Zhang D, Wang Z, Jiang J, Xu Y, Zhang H, Li J, Chen Q, Xu X. Transcriptome profiling reveals the response process of tomato carrying *Cf-19* and *Cladosporium fulvum* interaction. *BMC Plant Biol*. **2019**: 19(1): 572. https://doi.org/10.1186/s12870-019-2150-y

- Zhao T, Pei T, Jiang J, Yang H, Zhang H, Li J, Xu X. Understanding the mechanisms of resistance to tomato leaf mold: a review. *HPJ*. **2022**: 8(6): 667-675. https://doi.org/10.1016/j.hpj.2022.04.008

- Zhao J, Jiang H, Wang G, Wang Z, Dong J, Song J. Virus-Induced Gene Silencing in Diploid and Tetraploid Potato Species. *Methods Mol Biol*. **2020**: 2172: 39-50. https://doi.org/10.1007/978-1-0716-0751-0_4

- Zönnchen J, Gantner J, Lapin D, Barthel K, Eschen-Lippold L, Erickson JL, Villanueva SL, Zantop S, Kretschmer C, Joosten MHAJ, Parker JE, Guerois R, Stuttmann J. EDS1 complexes are not required for PRR responses and execute TNL-ETI from the nucleus in *Nicotiana benthamiana*. *New Phytol*. **2022**: 236(6):2249-2264. https://doi.org/10.1111/nph.18511

DPhil publications

1. Kourelis, J., Malik, S., Mattinson, O., Krauter, S., Kahlon, P.S., Paulus, J.K., and van der Hoorn, R.A.L. Evolution of a guarded decoy protease and its receptor in solanaceous plants. *Nat Commun.* **11**, 4393 (2020).
2. Malik, S., and van der Hoorn, R.A.L. Inspirational decoys: a new hunt for effector targets. *New Phytolo.* **210**, 371-373 (2016).

Conference presentations/abstracts submitted

1. Malik, S., Kourelis, J., Paulus, J.K., and van der Hoorn, R.A.L. Understanding extracellular perception of pathogens in solanaceae: from natural variation to evolution. *59th Annual International Conference of Association of Microbiologists of India and International Symposium on Host Pathogen Interactions, Hyderabad, India*. (2018). [Won the Best Research Poster Presentation Award]
2. Malik, S., Kourelis, J., Paulus, J.K., Sueldo, D.J., and van der Hoorn, R.A.L. Understanding *Cf-2/Rcr3* pathogen perception system: from natural variation to evolution in solanaceae. *5th International Conference on Biotic-Plant Interactions, Xiamen, China*. (2017).
3. Malik, S., and van der Hoorn, R.A.L. *Cf-2/Rcr3* pathogen perception mechanism: its natural variation and evolution in solanaceae family. *Molecular Biology of Plant Pathogens Conference, British Society of Plant Pathology, Durham, UK*. (2017).
4. Malik, S., Kourelis, J., Paulus, J.K., and van der Hoorn, R.A.L. Natural variation and evolution of *Cf-2/Rcr3* pathogen perception mechanism in solanaceae family. *Gordon Research Conference on Cellular and Molecular Fungal Biology, New Hampshire, USA*. (2016).

Participation Only

5. Plant and Animal Genome Conference (PAG-Asia Chapter), *The Westin Gurgaon, India*. (18th to 20th March 2025).
6. First Vaishwik Bharatiya Vaigyanik (VAIBHAV) Virtual Summit, *Ministry of Science and Technology-Government of India*. (3rd Oct to 2nd Nov 2020).
7. Local Ambassador Day, *Biochemical Society of the UK*, Manchester, UK. (2019).
8. 3rd Agriscience Chemical Biology Postgraduate Symposium, *RSC-BMCS & AGRI-net, Imperial College London, South Kensington Campus, UK*. (2017).

9. A Complex Recipe, *Oxford-India Centre for Sustainable Development (OICSD), Blavatnik School, University of Oxford, UK*. (2016).
10. Plant Protease Meeting, *Plant Chemetics Lab, Somerville College, Oxford, UK*. (2016).

DPhil induction courses/trainings/other workshops attended at the University of Oxford

1. Scientific reading, Writing and Speaking, Michaelmas Term 2015, Department of Plant Sciences (now Biology), South Parks Road, Oxford. Organiser: Prof Nick J Kruger.
2. Plant Diversity, Michaelmas Term 2015, Oxford Botanic Garden and Arboretum, Rose Lane, Oxford. Organiser: Prof Stephen Harris.
3. Getting Public Excited About Science, Michaelmas Term 2015, Oxford Botanic Garden and Arboretum, Rose Lane, Oxford. Organise: Department of Plant Sciences (now Biology).
4. Scientific Writing: Core Skills, 10th November 2015, St. Anne's College, Woodstock Road, Oxford. Facilitator: John Dixon.
5. The Idea Generator: Creativity and Evaluation for Research and Technology Transfer, 12th November 2015, Department of Earth Sciences, South Parks Road, Oxford. Facilitator: Anne Miller.
6. Biological Safety & Genetic Modification Training course, 8th December 2015, Nuffield Department of Medicine-Research Building, Old Road Campus, Roosevelt Drive. Organiser: University Safety Office.
7. Biological Sciences Graduate Teacher Training Course, 27th September 2016, Department of Plant Sciences (now Biology), South Parks Road, Oxford. Organiser: Departments of Plant Sciences and Zoology (now Biology).
8. OICSD Workshop designed to stimulate multi-disciplinary thinking and personal development to enhance productivity at work, 19th November 2016, Cassington, Oxfordshire. Organiser: Oxford-India Centre for Sustainable Development, Somerville College.
9. R for Biologists: 2nd February 2017 to 22nd March 2017 (weekly sessions), DTP Teaching Room, Department of Zoology/University Science Area, Mansfield Road, Oxford. Facilitator: Chris Terry.
10. Scientific Writing Workshop, 5th July 2018, Department of Plant Sciences, South Parks Road. Organiser: Prof Renier A.L. van der Hoorn.
11. MPLS Workshop on Communicating Your Research to Wider Audiences, 4th June 2025, Department of Engineering, Banbury Road, Oxford. Facilitator: Kirsty Heber-Smith.

Academic assessments at the Department of biology, University of Oxford

- Transfer of DPhil Status, Report and Oral Presentation [Passed on 12th Jul 2016; Expected by 13th Jan 2017].
- Confirmation of DPhil Status, Report and Oral Poster Presentation, [Passed on 6th Nov 2017; Expected by 5th Oct 2018].

Academic activities related to my research, University of Oxford

- Graduate Laboratory Demonstrator: Gene for Gene Interaction (plant adaptations course for second year), MT 2016 and HT 2018. Organised by Prof Renier van der Hoorn, Department of Biology (Plant Sciences).
- Graduate Laboratory Demonstrator: Tree of Life (evolutionary biology course for first year), TT 2017 and TT 2018. Organised by Prof Sebastian Shimeld and Dr Melissa Jansen van Rensburg, Department of Biology (Zoology).

Public Outreach Activities of My Research at University of Oxford

- Science Outreach to Political Leaders in India, March to May 2025. Wrote a featured blog on initiative, Department of Biology, University of Oxford. “Taking advantage of crop’s wild relatives to bioengineer climate-resilient agriculture, achieve food security, and environmental sustainability.” https://bit.ly/4kAlHmn
- Poster Presentation to Public under the category “Climate Resilient Agriculture” for BioE3 Policy Awareness Campaign Competition organised by the Department of Biotechnology, Ministry of Science & Technology, India, 2024. [Had the highest views/outreach among entries on X/Twitter]
- Oral Presentation and Experimental Demonstration of transient assays using *Nicotiana benthamiana* to >120 A-Level students at Science Day Fair, Oxford University Museum of Natural History, Parks Road, Oxford, 2016 and 2018.
- Oral Presentation and Experimental Demonstration of protein purification using Ni-NTA affinity chromatography and mock agroinfiltration in *Nicotiana benthamiana* to a large audience at Plant Fascination Day Fair, Harcourt Arboretum, Oxford, 2016.

Other activities, University of Oxford

- President, University of Oxford-India Society, Jun 2018-Mar 2019.
- First Student Representative Member, Interim Strategic Board of the University, India-Oxford Initiative, 2019.
- Policy Blog Editor, University of Oxford-India Society, Nov 2017-Feb 2019.
- Ambassador at Oxford, Biochemical Society of the UK, Nov 2017-Jun 2019.
- Education & Women Representative MCR, Somerville College, Nov 2017-Jun 2019.
- General Secretary, University of Oxford-India Society, Nov 2017-May 2018.
- Academic Advisor, Karta Initiative UK, Jul 2016-Sep 2019.